

INVESTIGATING THE EFFECTS OF ASYMMETRIC DIMETHYLARGININE IN THE MICROCIRCULATION

Yu Yeung Hanson Ng

Keble College

University of Oxford

A thesis submitted for the degree of

Doctor of Philosophy

Hilary 2024

For my parents, grandparents, and auntie.

ABSTRACT

Coronary resistance arteries develop spontaneous myogenic tone in response to intraluminal pressure, this autoregulation helps to couple blood flow to match metabolic demands of the myocardium. Endothelial dysfunction, involving the loss of nitric oxide (NO) and endothelium-dependent hyperpolarization (EDH), is an early hallmark of cardiovascular disease. This compromises the autoregulation and is associated with reduced vasodilation and abnormal vasoconstriction (vasospasm). Endogenous methylarginines, such as asymmetric dimethylarginine (ADMA), reduce NO bioavailability by inhibiting endothelial NO synthase (NOS), and elevated plasma ADMA concentration is a strong predictor of cardiovascular disease and mortality. Despite the clinical importance, our understanding of the roles of ADMA and EDH in coronary microvascular dysfunction (CMD) is still rudimentary. This thesis aimed to investigate the effects of ADMA and EDH in the coronary and mesenteric microcirculation using wire and pressure myography, immunohistochemistry and Ca^{2+} imaging. The significant findings of this thesis are: i) ADMA exerts greater inhibition on NOS in the coronary microcirculation compared to mesenteric arteries, abolishing NO-dependent vasodilation; ii) the expression of the ADMA-metabolising enzyme, dimethylarginine dimethylaminohydrolase 1 (DDAH1), is greater in the endothelium of mesenteric arteries compared to coronary arteries; iii) intermediate conductance Ca^{2+}-activated K^+ (IK_{Ca}) channels alone underpins EDH vasodilation in coronary arteries; iv) L-arginine is effective in reversing endothelial dysfunction; and v) ADMA enhances vascular smooth muscle cell and endothelial cell Ca^{2+} events. In summary, this thesis demonstrates the ability of ADMA to cause endothelial dysfunction, which has previously been questioned. This results in the inhibition of NO-dependent vasodilation and vasospasm. The expression of endothelial DDAH1 protects NOS activity and the lower expression in coronary arteries may predispose them to a greater

susceptibility to endothelial dysfunction. Therefore, in addition to L-arginine, strategies to enhance DDAH1 expression and/or activity may be beneficial in CMD.

ACKNOWLEDGEMENTS

I am extremely grateful to my supervisors Professor Kim Dora and Professor Christopher Garland for their generosity since my master's in 2018. Without their encouragement, I would not have embarked on this journey. Thank you for their patience and brilliance, and for believing in me. I can certainly say I would not have completed my doctorate without their unwavering support, particularly during the last months of my DPhil and moments of doubt.

I would like to thank my previous and current lab members: Dr Katie Banecki, Dr Lucy Donovan, Lily Wallis, Dr Lauren Phillips, Dr JinHeng Lin, Dr Will Stockdale, Dr Lludmyla Borysova and Dr Hamish Lemmey. Their presence, guidance, and laughter made even the difficult times enjoyable. They inspire me to be better and I have learned so much from them. I will treasure our connections and experience forever.

To all my family – *thank you.* A special thank you to my parents, brother and grandparents for their care and giving me the freedom to pursue my passion from a young age. I am forever indebted to them and the sacrifices they have made for my (and my brother's) education. *I hope I have made you proud.* A special mention and thank you to my auntie for her kindness and support. *I wish you were here to share this moment with me.*

I feel immensely lucky to be surrounded by amazing group of friends – particularly Alex, Alison (also for proofreading), Katie, Paljana, Kylie, Karolina, and Vicky. I cannot thank them enough for their positivity, laughter and always being by my side, especially during the difficult times.

Finally, I would like to express my gratitude to the British Heart Foundation for funding my studentship. This has truly been an opportunity of a lifetime.

PUBLICATIONS

Borysova, L., **Ng, Y. Y. H.,** Wragg, E. S., Wallis, L. E., Fay, E., Ascione, R. & Dora, K. A. 2021. High spatial and temporal resolution Ca^{2+} imaging of myocardial strips from human, pig and rat. *Nat Protoc,* 16**,** 4650-4675.

Data from this thesis (Chapters 3 – 6):

Ng, Y. Y. H., Dora, K. A., Lemmey, H. A. L., Lin, J., Alden, J., Wallis, L., Donovan, L., Shorthose, O., Leiper, F. C., Leiper, J. & Garland, C. J. 2024. Asymmetric dimethylarginine enables depolarizing spikes and vasospasm in mesenteric and coronary resistance arteries. *Hypertension,* 81**,** 764-775.

CONFERENCE COMMUNICATIONS

Ng, Y. Y. H., Leiper, F., Leiper, J., Dora, K. A., Garland, C.J., DDAH1 prevents eNOS inhibition by ADMA in rat small mesenteric arteries. Poster presentation at *Europhysiology 2022*; 16 –18 September 2022, Copenhagen, Denmark.

Ng, Y.Y.H., Dora, K. A., Garland, C. J., Asymmetric dimethylarginine augments myogenic tone and inhibits vasodilation in rat coronary arteries. Selected for poster presentation at *American Physiology Summit*; 20 – 23 April 2023; Long Beach, CA, USA.

Ng, Y.Y.H., Dora, K. A., Garland, C. J., Asymmetric dimethylarginine augments myogenic tone and inhibits vasodilation in rat coronary arteries. Oral presentation at *European Society for Microcirculation Conference 2023*; 24 – 27 April 2023, Aarhus, Denmark.

CONTENTS

CHAPTER ONE

INTRODUCTION 1

1.1 MORPHOLOGY OF RESISTANCE ARTERIES.....2

1.1.1 The structure of resistance arteries.....2

1.1.2 Myoendothelial (gap) junctions.....3

1.2 REGULATION OF MICROVASCULAR TONE 5

1.2.1 Neurohumoral vasoconstriction.....5

1.2.2 Myogenic tone.....7

1.2.3 Endothelial nitric oxide-dependent vasodilation.....8

1.2.4 Endothelium-dependent hyperpolarization vasodilation.....10

1.2.5 Myoendothelial feedback.....12

1.2.6 Coronary microvascular dysfunction.....13

1.3 ENDOGENOUS METHYLARGININES.....14

1.3.1 Biosynthesis and clearance of methylarginines.....14

1.3.2 Clinical relevance of ADMA.....17

1.4 THESIS AIMS AND OBJECTIVES 21

CHAPTER TWO

MATERIALS AND METHODS.....22

2.1 ANIMALS AND TISSUE PREPARATION.....23

2.1.1 Preparation of rat mesenteric resistance arteries 23

2.1.2 Preparation of rat intra-septal coronary arteries 23

2.2 WIRE MYOGRAPHY 25

2.2.1 Mounting of arteries in a wire myograph 25

2.2.2 Studying rat mesenteric arteries under isometric tension 31

2.2.3 Analysis of mesenteric artery isometric tension recordings 31

2.2.4 Studying rat intra-septal coronary arteries under isometric tension 32

2.2.5 Analysis of coronary artery isometric tension recordings 32

2.2.6 Measuring VSM intracellular Ca^{2+} in coronary arteries under isometric tension 33

2.2.7 Analysis of intracellular Ca^{2+} events 33

2.3 PRESSURE MYOGRAPHY 35

2.3.1 Artery cannulation and pressurisation 35

2.3.2 Studying pressurised rat mesenteric arteries 39

2.3.3 Analysis of mesenteric artery diameter recordings 40

2.3.4 Studying pressurised rat intra-septal coronary arteries 40

2.3.5 Analysis of coronary artery diameter recordings 42

2.3.6 Measuring endothelial cell intracellular Ca^{2+} in pressurised coronary arteries 43

2.3.7 Analysis of intracellular Ca^{2+} events 43

2.4 IMMUNOHISTOCHEMISTRY 45

2.4.1 Immunolabelling in arteries under isometric tension 45

2.4.2 Imaging immunohistochemistry 45

2.4.3 Analysis of immunofluorescence images 46

2.5 WESTERN BLOTS 48

2.5.1 Tissue homogenisation 48

2.5.2 Western blotting *48*

2.6 SOLUTIONS, DRUGS AND ANTIBODIES **50**

2.6.1 Solutions *50*

2.6.2 Drugs and compounds *50*

2.6.3 Antibodies *52*

2.6.4 Fluorescent Indicators *52*

2.7 STATISTICAL ANALYSES **55**

CHAPTER THREE

CHARACTERISING THE EFFECTS OF DIMETHYLARGININES ON THE FUNCTION OF MESENTERIC RESISTANCE ARTERIES 56

3.1 INTRODUCTION **57**

3.1.1 Aims and hypotheses *60*

3.2 MATERIALS AND METHODS **61**

3.2.1 Wire myography *61*

3.2.2 Pressure myography *61*

3.2.3 Inhibitors *61*

3.3 RESULTS **62**

3.3.1 ADMA enhances PE-induced vasoconstriction and attenuates NO-dependent vasorelaxation in mesenteric arteries under isometric tension *62*

3.3.2 SDMA has no effects on vasoconstriction and vasorelaxation in mesenteric arteries under isometric tension *65*

3.3.3 ADMA attenuates NO-dependent vasodilation in pressurised mesenteric arteries 68

3.4 DISCUSSION 70

3.5 CONCLUSION 76

CHAPTER FOUR

CHARACTERISING THE EFFECTS OF ADMA AND ENDOTHELIUM-DEPENDENT HYPERPOLARIZATION INHIBITION IN THE CORONARY MICROVASCULATURE 78

4.1 INTRODUCTION 79

4.1.1 Aims and hypotheses 82

4.2 MATERIALS AND METHODS 83

4.2.1 Wire myography 83

4.2.2 Pressure myography 83

4.2.3 Inhibitors 83

4.3 RESULTS 84

4.3.1 ADMA augments myogenic tone in intra-septal coronary arteries 84

4.3.2 Inhibition of nitric oxide synthase and IK_{Ca} channels abolishes vasorelaxation to acetylcholine in intra-septal coronary arteries 90

4.3.3 ADMA abolishes nitric oxide-dependent vasodilation to acetylcholine in pressurised intra-septal coronary arteries 93

4.4 DISCUSSION 96

4.5 CONCLUSION 105

CHAPTER FIVE

INVESTIGATING THE ROLE OF DIMETHYLARGININE DIMETHYLHYDROLASE 1 IN THE MESENTRIC AND CORONARY MICROCIRCULATION 107

5.1 INTRODUCTION 108

5.1.1 Aims and hypotheses 111

5.2 MATERIALS AND METHODS 112

5.2.1 Wire myography 112

5.2.2 Pressure myography 112

5.2.3 Immunohistochemistry and imaging 112

5.2.4 Western blotting 113

5.2.5 Inhibitors 113

5.3 RESULTS 114

5.3.1 DDAH1 prevents endothelial nitric oxide synthase inhibition by ADMA in mesenteric arteries 114

5.3.2 DDAH1 inhibition augments myogenic tone in intra-septal coronary arteries under isometric tension 119

5.3.3 DDAH1 expression is greater in the endothelium of mesenteric arteries compared to intra-septal coronary arteries 121

5.4 DISCUSSION 125

5.5 CONCLUSION 135

CHAPTER SIX

INVESTIGATING THE EFFECTS OF L-ARGININE SUPPLEMENATION IN ADMA-MEDIATED ENDOTHELIAL DYSFUNCTION.....137

6.1 INTRODUCTION 138

6.1.1 Aims and hypotheses 140

6.2 MATERIALS AND METHODS 141

6.2.1 Wire myography 141

6.2.2 Pressure myography.....141

6.2.3 Drugs and inhibitors 141

6.3 RESULTS.....142

6.3.1 L-arginine, but not D-arginine, rescues vasorelaxation and vasodilation in mesenteric arteries.....142

6.3.2 L-arginine reverses ADMA-induced myogenic tone to basal levels in intra-septal coronary arteries 149

6.3.3 L-arginine rescues vasodilation in pressurised intra-septal coronary arteries in the presence of ADMA 152

6.4 DISCUSSION 154

6.5 CONCLUSION 166

CHAPTER SEVEN

INVESTIGATING THE EFFECTS OF ADMA ON INTRACELLULAR Ca^{2+} IN THE CORONARY MICROCIRCULATION.....168

7.1 INTRODUCTION 169

7.1.1 Aims and hypotheses 170

7.2 MATERIALS AND METHODS 171

7.2.1 Wire myography 171

7.2.2 Wire myography calcium imaging 171

7.2.3 Pressure myography 171

7.2.4 Pressure myography calcium imaging 171

7.2.5 Inhibitors 172

7.3 RESULTS 173

7.3.1 Augmented myogenic tone with ADMA in intra-septal coronary arteries is associated with an increase in VSMC Ca^{2+} flashes 173

7.3.2 ADMA increases EC Ca^{2+} events in pressurised intra-septal coronary arteries 175

7.4 DISCUSSION 177

7.5 CONCLUSION 183

CHAPTER EIGHT

SUMMARY AND FUTURE DIRECTIONS 185

CHAPTER NINE

REFERENCES 195

LIST OF FIGURES

Figure 1.1.1 The structure of resistance arteries. 4

Figure 1.2.1 Signalling pathway for vascular smooth muscle cell contraction. 6

Figure 1.2.2 Signalling pathway endothelium-dependent vascular smooth muscle cell relaxation. 11

Figure 1.3.1 Overview of the synthesis and clearance pathways of methylarginines. 16

Figure 2.2.1 Excised mesenteric arcade and isolated mesenteric artery mounted in a wire myograph. 27

Figure 2.2.2 Wire myograph set-up for isometric tension recordings. 28

Figure 2.2.3 Excised heart and intra-septal coronary artery mounted in a confocal wire myograph chamber. 29

Figure 2.2.4 Confocal wire myograph set-up for simultaneous recording of isometric tension and intracellular Ca^{2+}. 30

Figure 2.2.5 Analysis of intracellular Ca^{2+} events in VSM of coronary arteries under isometric tension. 34

Figure 2.3.1 Pressure myography set-up for diameter recordings using DMT chamber. 37

Figure 2.3.2 Pressure myography set-up for intracellular calcium recordings using the confocal chamber. 38

Figure 2.3.3 Intra-septal coronary artery pressurised to 80 mmHg. 41

Figure 2.3.4 Analysis of intracellular Ca^{2+} events in endothelial cells of pressurised coronary artery. 44

Figure 2.4.1 Analysis of immunofluorescence images. 47

Figure 3.3.1 Asymmetric dimethylarginine (ADMA) markedly increases vasoconstriction to α_1-adrenoreceptor agonist, phenylephrine (PE) in mesenteric arteries. 63

Figure 3.3.2 Endothelium-dependent vasorelaxation to acetylcholine (ACh) persists in the presence of asymmetric dimethylarginine (ADMA) during the block of endothelium-dependent hyperpolarization (EDH) in mesenteric arteries under isometric tension. 64

Figure 3.3.3 Symmetric dimethylarginine (SDMA) has no effects on vasoconstriction to the α_1-adrenoreceptor agonist phenylephrine (PE) in mesenteric arteries. 66

Figure 3.3.4 Symmetric dimethylarginine (SDMA) has no effects on endothelium-dependent vasorelaxation to acetylcholine (ACh) in mesenteric arteries during endothelium-dependent hyperpolarization (EDH) blockade. 67

Figure 3.3.5 Endothelium-dependent vasodilation to acetylcholine (ACh) persists in the presence of asymmetric dimethylarginine (ADMA) during endothelium-dependent hyperpolarization (EDH) blockade in pressurised mesenteric arteries. 69

Figure 3.5.1 Summary of Chapter 3 – Endogenous nitric oxide synthase inhibitor, asymmetric dimethylarginine (ADMA), increases vasoreactivity of rat mesenteric resistance arteries. 77

Figure 4.3.1 Asymmetric dimethylarginine (ADMA) increases myogenic tone, comparable to the synthetic nitric oxide synthase inhibitor L-NAME, in intra-septal coronary arteries under isometric tension. 86

Figure 4.3.2 Endothelium-dependent hyperpolarization (EDH) is not involved in the modulation of myogenic tone in intra-septal coronary arteries. 87

Figure 4.3.3 Asymmetric dimethylarginine (ADMA) increases myogenic tone in pressurised intra-septal coronary arteries. 88
Figure 4.3.4 Endothelium-dependent hyperpolarization (EDH) blockade does not affect myogenic tone in pressurised intra-septal coronary arteries. 89
Figure 4.3.5 Nitric oxide synthase and IK_{Ca} blockade abolishes acetylcholine (ACh) vasorelaxation in intra-septal coronary arteries. 92
Figure 4.3.6 Asymmetric dimethylarginine (ADMA) attenuates vasodilation to acetylcholine (ACh) in pressurised intra-septal coronary arteries by inhibiting nitric oxide production. 94
Figure 4.3.7 Nitric oxide synthase and endothelium-dependent hyperpolarization (EDH) blockade prevents vasodilation in pressurised intra-septal coronary arteries..... 95
Figure 4.5.1 Summary of Chapter 4 – Nitric oxide (NO) and intermediate conductance Ca^{2+}-activated K^+ (IK_{Ca}) channel modulates the vasoreactivity of intra-septal coronary arteries. 106
Figure 5.3.1 Inhibition of dimethylarginine dimethylaminohydrolase 1 (DDAH1) by L-257 further attenuates persistent acetylcholine (ACh) vasorelaxation in mesenteric arteries in the presence of asymmetric dimethylarginine (ADMA) and endothelium-dependent hyperpolarization (EDH) blockade. 116
Figure 5.3.2 Time-dependent effects of dimethylarginine dimethylaminohydrolase 1 (DDAH1) selective inhibitor, L-257, incubation on percentage of maximum vasorelaxation (E_{max}). 117
Figure 5.3.3 Dimethylarginine dimethylaminohydrolase 1 (DDAH1) inhibition by L-257 further suppresses vasodilation to acetylcholine (ACh) in pressurised mesenteric arteries in the presence of asymmetric dimethylarginine (ADMA) and endothelium-dependent hyperpolarization (EDH) blockade. 118

Figure 5.3.4 Inhibition of dimethylarginine dimethylaminohydrolase 1 (DDAH1) by L-257 increases myogenic tone in intra-septal coronary artery under isometric tension. 120
Figure 5.3.5 Expression of dimethylarginine dimethylaminohydrolase 1 (DDAH1) is greater in mesenteric compared to intra-septal coronary artery endothelium. 122
Figure 5.3.6 Expression of dimethylarginine dimethylaminohydrolase 1 (DDAH1) in rat kidney and liver. 123
Figure 5.3.7 Primary antibody negative control images. 124
Figure 5.5.1 Summary of Chapter 5 – Dimethylarginine dimethylaminohydrolases 1 (DDAH1) expression is greater in mesenteric versus coronary resistance arteries and prevents endothelial nitric oxide (NO) synthase (eNOS) inhibition by asymmetric dimethylarginine (ADMA). 136
Figure 6.3.1 L-arginine (L-Arg) restores acetylcholine (ACh) vasorelaxation in the presence of asymmetric dimethylarginine (ADMA), endothelium-dependent hyperpolarization and dimethylarginine dimethylaminohydrolase 1 (DDAH1) inhibition in mesenteric arteries. 144
Figure 6.3.2 D-arginine is unable to restore vasorelaxation to acetylcholine (ACh) in the presence of asymmetric dimethylarginine (ADMA) and endothelium-dependent hyperpolarization blockade in mesenteric arteries. 145
Figure 6.3.3 L-arginine rescues vasodilation to acetylcholine (ACh) in pressurised mesenteric arteries in the presence of asymmetric dimethylarginine (ADMA) and endothelium-dependent hyperpolarization blockade. 147

Figure 6.3.4 L-arginine rescues vasodilation to acetylcholine (ACh) in pressurised mesenteric arteries even during dimethylarginine dimethylaminohydrolase 1 (DDAH1), nitric oxide synthase and endothelium-dependent hyperpolarization blockade. 148

Figure 6.3.5 L-Arginine (1 mM) reverses asymmetric dimethylarginine (ADMA)-induced myogenic tone but not control myogenic tone in intra-septal coronary arteries under isometric tension. 150

Figure 6.3.6 L-Arginine reverses asymmetric dimethylarginine (ADMA)-induced vasoconstriction in pressurised intra-septal coronary arteries. 151

Figure 6.3.7 L-arginine (1 mM) rescued vasodilation to acetylcholine (ACh) in pressurised intra-septal coronary arteries in the presence of asymmetric dimethylarginine (ADMA). 153

Figure 6.5.1 Summary of Chapter 6 – L-arginine (L-Arg) supplementation reverses the endothelial nitric oxide (NO) synthase (eNOS) inhibition by asymmetric dimethylarginine (ADMA). 167

Figure 7.3.1 Asymmetric dimethylarginine (ADMA) increases the frequency of vascular smooth muscle cell (VSMC) Ca^{2+} flashes and myogenic tone (MT) in intra-septal coronary arteries. 174

Figure 7.3.2 Asymmetric dimethylarginine (ADMA) increases endothelial cell (EC) Ca^{2+} events in pressurised intra-septal coronary arteries. 176

Figure 7.5.1 Summary findings of Chapter 7 – Asymmetric dimethylarginine (ADMA) increases intracellular Ca^{2+} events in vascular smooth muscle (VSM) and endothelial cells (EC) of coronary resistance arteries. 184

Figure 8.1 Summary of thesis findings. 194

LIST OF TABLES

Table 1.3.1 Summary of the mentioned studies in Chapter 3.1 that reported elevated plasma concentration of ADMA. 20

Table 2.6.1 List of drugs and compounds used in this thesis. 51

Table 2.6.2 List of antibodies used in this thesis. 53

Table 2.6.3 List of fluorescent indicators used in this thesis. 54

Table 3.1.1 Summary table of the mentioned studies in Chapter 3.1 that examined the effects of NOS inhibition by exogenous ADMA. 59

Table 6.4.1 Summary table of the mentioned studies in Chapter 6.4 that examined the effects of L-arginine supplementation in patients with cardiovascular disease. 163

ABBREVIATIONS

4124W	S-2-amino-4(3methylguanidino)butanoic acid
ACh	Acetylcholine
ADMA	N^G,N^G-dimethylarginine; Asymmetric dimethylarginine
AGTX2	Alanine-glyoxylate aminotransferase 2
α_1-AR	α_1–adrenoceptor
ANOCA	Angina with non-obstructive coronary artery disease
Ap	Apamin
AS	Atherosclerosis
BEC	(S)-(2-boronoethyl)-l-Cysteine-HCl
BK_{Ca}	Large-conductance Ca^{2+}-activated K^+ channel
CAD	Coronary artery disease
CalB	CalBryte 520 AM
CaM	Calmodulin
CAT	Cation amino acid transporter
CFR	Coronary flow reserve
cGMP	Cyclic guanosine monophosphate
CMD	Coronary microvascular dysfunction
CNP	C-type natriuretic peptide
CV	Cardiovascular
D-Arg	D-arginine
DAG	Diacylglycerol
DDAH1/DDAH2	Dimethylarginine dimethylaminohydrolase 1/2

EC Ca^{2+}	Endothelial cell Ca^{2+}
EDH	Endothelium dependent hyperpolarization
EDHF	EDH factor
EET	Epoxyeicosatrienoic acids
eNOS	Endothelial nitric oxide synthase
ER	Endoplasmic reticulum
FXR	Farnesoid X receptor
GTP	Guanosine-5'-triphosphate
HC	Hypercholesterolaemia
HF	Heart failure
HTN	Hypertension
IEL	Internal elastic lamina
IK_{Ca}	Intermediate-conductance Ca^{2+}-activated K^+ channel
IP_3	Inositol 1,4,5-trisphosphate
IP_3R	IP_3 receptors
K_{IR}	Inwardly rectifying K^+ channel
L-257	N^G-(2-methoxyethyl) arginine
L-Arg	L-arginine
L-NAME	N_ω-Nitro-L-arginine methyl ester
L-NIO	N-iminoethyl-L-ornithine
L-NMMA	N^G-monomethyl-L-arginine
L-NNA	L-N^G-nitro arginine
L-type VDCC	L-type voltage-dependent Ca^{2+} channel
M_3R	M_3 muscarinic receptor
MEGJ	Myoendothelial gap junction

MEJ	Myoendothelial junction
MLCK	Myosin light chain kinase
MLCP	Myosin light chain phosphatase
MT	Myogenic tone
MVA	Microvascular angina
NEM	*N*-ethylmaleimide
Nif	Nifedipine
NNC	NNC 55-0396
NO	Nitric oxide
NOS	Nitric oxide synthase
NS	NS 6180
OGB-1	Oregon green 488 BAPTA-1 AM
PAD	Peripheral artery disease
PE	Phenylephrine
PIP_2	Phosphatidylinositol
PKC	Protein kinase C
PKG	Protein kinase G
PLC	Phospholipase C
PRMT1/PRMT2	Protein-arginine methyltransferase 1/2
PGI_2	Prostacyclin
Rho K	Rho-associated protein kinase
RhoA	Ras homolog family member A
ROC	Receptor-operated channels
SAH	S-adenosylhomocysteine
SAM	S-adenosylmethionine

SDMA	N^G,$N^{G'}$-dimethylarginine; Symmetric dimethylarginine
SERCA	Sarcoendoplasmic reticulum Ca^{2+}-ATPase
sGC	Soluble guanylyl cyclase
SHR	Spontaneous hypertensive rat
SK_{Ca}	Small-conductance Ca^{2+}-activated K^+ channel
SNAP	*S*-Nitroso-*N*-acetyl-DL-penicillamine
SNOG	*S*-nitrosoglutathione
SR	Sarcoplasmic reticulum
T-type VDCC	T-type voltage-dependent Ca^{2+} channels
T2DM	Type 2 diabetes mellitus
TR	TRAM 34
TRP	Transient receptor potential channel
UDCA	Ursodeoxycholic acid
VSMC	Vascular smooth muscle cell

CHAPTER ONE

INTRODUCTION

1.1 MORPHOLOGY OF RESISTANCE ARTERIES

The cardiovascular system consists of the heart, the macrocirculation and microcirculation; together are responsible for the delivery of oxygenated blood and nutrients and removal of waste products from organs and tissues. Due to its location and elastic nature, the macrocirculation, modulates the pulsatile pressure and blood flow from the heart. This pulsatile blood flow is converted to near-steady flow as it travels through the vascular tree. The microcirculation, the focus on this thesis, consists of resistance arteries and arterioles (diameter <500 μm) and is the site with the most significant changes in blood pressure and vascular resistance (Mulvany and Aalkjaer, 1990). These resistance arteries play a vital role in the regulation of blood flow to tissues and organs. Therefore, they can dynamically modulate vascular resistance, through extrinsic and intrinsic factors, to ensure blood flow matches the metabolic demands of the tissues they supply. As such, disturbances in the microcirculation can result in the development of cardiovascular diseases, and consequently the microvascular signalling pathways are of research interests.

1.1.1 The structure of resistance arteries

The structure of resistance arteries (**Figure 1.1.1**) is histologically similar to all blood vessels, comprising of 3 layers: *tunica intima*, *tunica media*, *tunica adventitia* (Mulvany and Aalkjaer, 1990). The innermost layer, *tunica intima*, is made up of a single squamous layer of endothelial cells that lines the artery lumen. The internal elastic lamina is a fenestrated sheet of elastin which acts as a boundary between the intimal and medial layer. *Tunic media* is comprised of layers of vascular smooth muscle cells (VSMCs) arranged in a circumferential arrangement. In resistance arteries, endothelial cells project through the fenestrations in the internal elastic lamina and make physical contact with nearby VSMCs in the medial layer, forming

myoendothelial junctions. Finally, *tunica adventitia* is the outermost layer and is composed of connective tissues (e.g. elastin and collagen), fibroblasts and perivascular nerves.

1.1.2 Myoendothelial (gap) junctions

Myoendothelial junctions (MEJs; **Figure 1.1.1 inset**) were first described in 1957 by Moore and Ruska where they observed frequent protrusions from endothelial cells through fenestrations in the internal elastic lamina and contact with VSMCs (Moore and Ruska, 1957). Similar observations were reported in subsequent studies in rabbit medial thigh muscles, and it was hypothesised that myoendothelial junctions may serve as conductive domains for transcytosis and heterocellular communications (Rhodin, 1967). Since their discovery, myoendothelial junctions have been reported in the microvasculature in various species and vascular beds, including rodents, pigs and humans (Aydin et al., 1991, Beny and Pacicca, 1994, Sandow and Hill, 2000, Mather et al., 2005). Subsequent studies have shown the presence of myoendothelial gap junctions (MEGJs) in these projections and their involvement in the bidirectional transmission of electrochemical signals and modulation of vascular tone (Beny and Pacicca, 1994, Dora et al., 1997, Mather et al., 2005). Moreover, the prevalence of these protrusions increases as diameter of mesenteric arteries decreases (Sandow and Hill, 2000). Therefore, this myoendothelial coupling is considered to play an important role in maintaining microvascular homeostasis. Despite the significant progress in understanding MEGJs using transmission electron microscopy, examining the presence and function of MEGJs remains to be difficult due to the small and delicate structures.

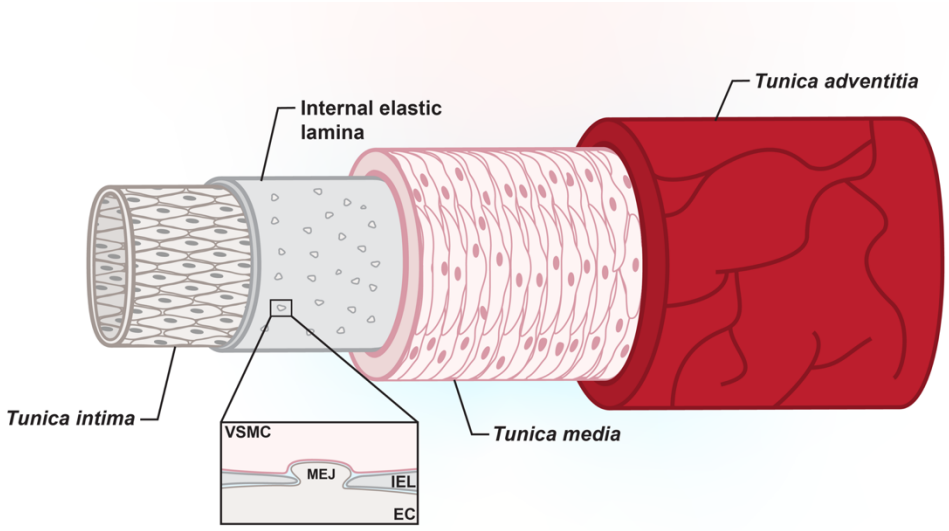


Figure 1.1.1 The structure of resistance arteries. Diagram representation of the structure of resistance arteries. The *tunica intima* is the innermost layer consisting of a monolayer of endothelial cells (ECs). The *tunica media* is comprised of multiple layers of vascular smooth muscle cells (VSMCs) and is responsible for vasoconstriction. The internal elastic lamina (IEL) is located between the *tunica intima* and *tunica media* and is a fenestrated sheet of elastin. The endothelium can protrude through these fenestrations and make contact with neighbouring VSMCs, forming myoendothelial junctions (MEJs; Inset). The outermost layer, the *tunica adventitia*, is primarily made up of connective tissue (elastin and collagen), fibroblasts and perivascular nerves.

1.2 REGULATION OF MICROVASCULAR TONE

As mentioned, the microcirculation is crucial in regulating the delivery of blood to tissues and organs. Therefore, to ensure blood flow matches metabolic demands, resistance arteries and arterioles tightly modulate vascular tone and resistance through vasoconstriction and vasodilation, which are governed by various neurohumoral, myogenic and endothelium-dependent mechanisms.

1.2.1 Neurohumoral vasoconstriction

The plasma membrane of VSMCs expresses various channels and receptors that can modulate vascular reactivity through VSMC contraction (**Figure 1.2.1**). Stimulation of G_q α-subunit-coupled metabotropic receptors in VSMCs, such as α_1-adrenoreceptors via the release of norepinephrine from sympathetic nerves and adrenal medulla, leads to the production of diacylglycerol (DAG) and inositol 1,4,5-trisphosphate (IP_3) via the activation of phospholipase C (PLC) (Brozovich et al., 2016). This drives the initial increase in intracellular Ca^{2+} concentration as IP_3 stimulates Ca^{2+} release from intracellular store (e.g. sarcoplasmic reticulum) by acting on IP_3 receptors, and DAG activates receptor-operated channels (e.g. transient receptor potential (TRP) channels) resulting in Ca^{2+} influx from extracellular space. The rise in intracellular Ca^{2+} depolarises VSMC and increases membrane potential, resulting in the activation of L-type voltage-dependent Ca^{2+} channels (L-type VDCC). The L-type VDCC mediated Ca^{2+} influx represents the main mechanism for the rise in intracellular Ca^{2+} and sustaining VSMC contraction. Intracellular Ca^{2+} forms a complex with calmodulin which activates myosin light chain kinase (MLCK), leading to the phosphorylation of myosin light chain and crossbridge formation between myosin and actin, resulting in VMC contraction. (Brozovich et al., 2016).

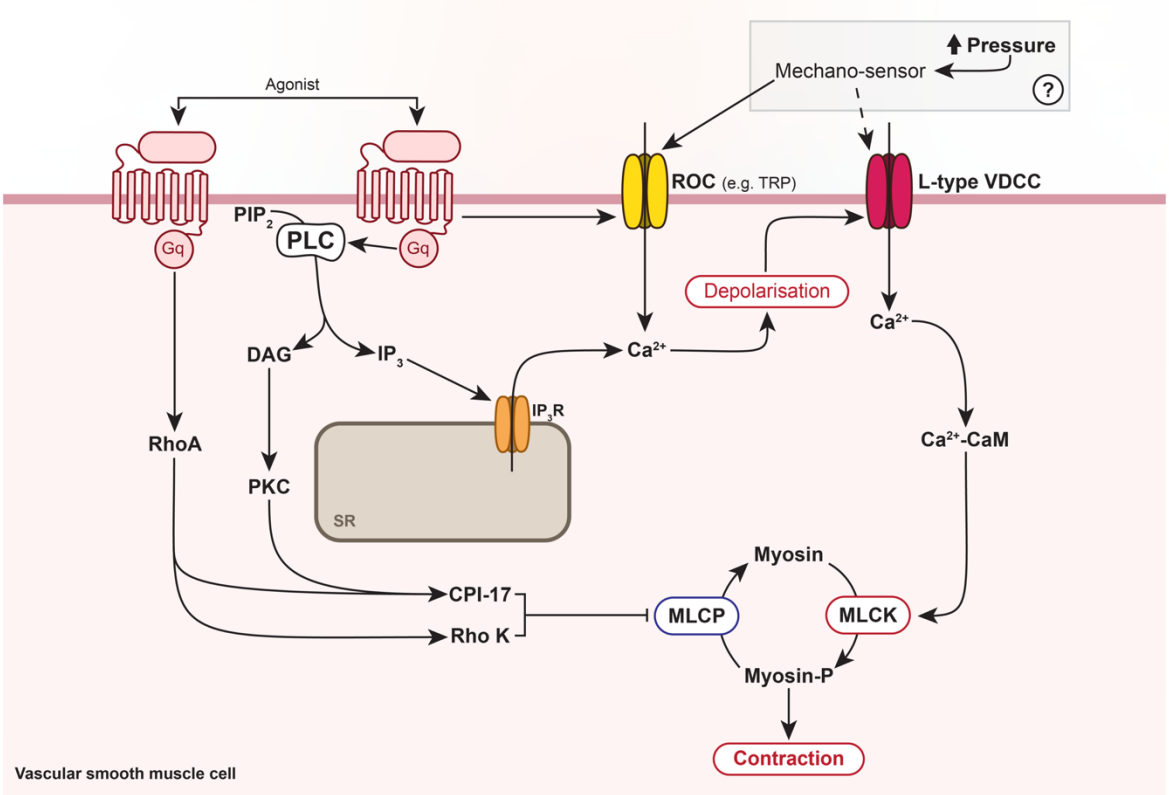


Figure 1.2.1 Signalling pathway for vascular smooth muscle cell contraction. Dashed arrows indicate simplified pathway. CaM = Calmodulin; DAG = Diacylglycerol; IP_3(R)= Inositol 1,4,5-trisphosphate (receptor); L-type VDCC = L-type voltage-dependent Ca^{2+} channels; MLCK = Myosin light chain kinase; MLCP = Myosin light chain phosphatase; PIP_2 = Phosphatidylinositol; PKC = protein kinase C; PLC = Phospholipase C; Myosin-P = Phosphorylated myosin; ROC = Receptor-operated channels; RhoA = Ras homolog family member A; Rho K = Rho-associated protein kinase; SR = Sarcoplasmic reticulum; TRP = Transient receptor potential channel.

Metabotropic receptors coupled to $G_{12/13}$ protein (e.g. angiotensin 1 receptors) can sensitise VSMCs to Ca^{2+} and promote VSMC contraction by activating Rho-associated protein kinase via RhoA, leading to the phosphorylation (inhibition) of myosin light chain phosphatase (MLCP). Additionally, both Rho A and DAG activate CPI-17, the latter indirectly via protein kinase C, leading to inhibition of MLCP (Kanaide et al., 2003).

The clearance of intracellular Ca^{2+} during repolarisation and hyperpolarization plays a crucial role in vascular and intracellular Ca^{2+} homeostasis. The main mechanisms of Ca^{2+} removal and thus termination of VSMC contraction are: i and ii) extrusion via Na^{+}/Ca^{2+} exchanger and Ca^{2+}-ATPase; iii) sequestration by sarcoplasmic reticular Ca^{2+}-ATPase; and iv) uptake by mitochondria (Oloizia and Paul, 2008). Furthermore, activation of VSMC store-operated Ca^{2+} channels upon Ca^{2+} depletion also contributes to the refilling of intracellular Ca^{2+} stores for subsequent contraction (Brozovich et al., 2016).

1.2.2 Myogenic tone

In addition to agonist-induced vasoconstriction, resistance arteries, such as the coronary microcirculation, exhibit basal level of vasoconstriction (myogenic tone) in response to a given intraluminal pressure. First described by Bayliss (1902), the myogenic response is defined as the intrinsic pressure-sensitive vasoconstriction or vasodilation of resistance arteries in response to changes in intraluminal pressure. While neurohumoral and endothelial inputs can modulate myogenic tone, the development of this basal vasoconstriction is independent of either input (Kuo et al., 1990). Interestingly, the presence and magnitude of the myogenic response varies across vascular beds. For example, although rat mesenteric resistance arteries develop myogenic tone, this myogenic response is weaker compared to cerebral and coronary arteries of similar diameter (Landry et al., 2006). Furthermore, within the same vascular bed,

the response to changes in intraluminal pressure and the modulation on myogenic tone can differ between arteries and arterioles (Morse et al., 2022).

While the precise pressure sensing mechanism remains to be elucidated, evidence points to the downstream involvement of various TRP channels and cation channels in myogenic response, suggesting the complexity in the development of myogenic tone and across vascular beds. It is widely established that this basal vasoconstriction is dependent on VSMC depolarisation (**Figure 1.2.1**). Knot and Nelson (1998) observed a pressure-induced depolarisation and increase in VSMC Ca^{2+} in myogenically active cerebral arteries. The removal of extracellular Ca^{2+} or the addition of L-type VDCC inhibitors abolished myogenic tone and the rise in VSMC Ca^{2+}, suggesting the dependence on VDCC activation and Ca^{2+} influx. Therefore, comparable to agonist-induced stimulation, pressure-induced VSMC depolarisation results in the stimulation of L-Type VDCC, leading to the activation of the VSMC contractile machinery previous mentioned and generation of myogenic tone.

1.2.3 Endothelial nitric oxide-dependent vasodilation

Once thought to be acting as an inert barrier, the endothelium is now known for participating in a host of modulatory activities, including the regulation of vascular tone. The seminal work by Furchgott and Zawadzki (1980) in rabbit thoracic aorta strips, which later was honoured with a Nobel Prize, revealed that mechanical or enzymatic removal of the endothelium abolishes relaxation to the muscarinic M_3 receptor agonist, acetylcholine (ACh). Thus, for the first time, indicating the endothelial modulation on vascular smooth muscle contraction. It is now known that the endothelium governs vascular tone through the synthesis and release of nitric oxide (NO) and prostacyclin (PGI_2), and endothelium-dependent hyperpolarization (EDH), with NO and EDH being the major vasodilatory pathways. The contribution of these

endothelium-dependent vasodilatory factors varies across species, vascular beds, vessel diameter and agonist stimulation (Nagao et al., 1992, Garland and McPherson, 1992).

Initially known as endothelium-derived relaxing factor by Furchgott and Zawadzki, NO is synthesised by endothelial cells upon agonist stimulation, such as ACh and bradykinin, and subsequent increase in intracellular Ca^{2+} (**Figure 1.2.2**). Similar to the described activation of VSMC α_1-adrenoreceptors, ACh activates the G_q α-subunit-coupled endothelial muscarinic M_3 receptors, resulting in the production of IP_3 and DAG through PLC activation and subsequent IP_3-induced mobilisation of Ca^{2+} from intracellular stores (e.g. endoplasmic reticulum). The rise in intracellular Ca^{2+} forms a complex with calmodulin, which activates endothelial nitric oxide synthase (eNOS), resulting in the conversion of L-arginine into NO (Palmer et al., 1988a, Palmer et al., 1988b). A reduction in intracellular Ca^{2+} causes the dissociation of the Ca^{2+}-calmodulin complex from eNOS, leading to its inactivation. Similarly, the depletion of intracellular stores stimulating the opening of store-operated channels, and store Ca^{2+} is refilled by extracellular Ca^{2+} (Sandoo et al., 2010). Alternatively, eNOS can also be activated by direct phosphorylation by protein kinases independent of Ca^{2+}, such as serine/threonine protein kinase Akt (Fulton et al., 1999).

Once synthesised, NO diffuses to neighbouring VSMCs, activating soluble guanylyl cyclase (sGC) and the conversion of guanosine-5'-triphosphate (GTP) to cyclic guanosine monophosphate (cGMP) (Arnold et al., 1977). The generation of cGMP stimulates protein kinase G (PKG), leading to the phosphorylation of various targets to decrease VSMC Ca^{2+} sensitivity, including MLCP (Sandoo et al., 2010). The activation of MLCP and reduction in VSMC Ca^{2+} sensitivity promotes VSMC relaxation, thus resulting in vasodilation. In addition to its role on sGC, NO can directly activate large-conductance Ca^{2+}-activated K^+ (BK_{Ca})

channels in VSMCs, assisting K^+ efflux and hyperpolarization, thus VSMC relaxation (Mistry and Garland, 1998).

1.2.4 Endothelium-dependent hyperpolarization vasodilation

In contrast to conduit arteries, NO-dependent vasodilation only represents a portion of the response to vasodilators in resistance arteries. Inhibition of eNOS with N_ω-Nitro-L-arginine methyl ester (L-NAME) significantly attenuates or abolishes ACh vasorelaxation in rat aortic and pulmonary arterial segments, but only partially inhibits vasorelaxation in mesenteric and femoral arteries (Nagao et al., 1992), indicating other factors are at play.

Bolton et al. (1984) first reported endothelium-dependent VSMC hyperpolarization upon muscarinic receptor stimulation with carbachol in guinea pig mesenteric arteries was abolished following removal of the endothelium. Since then, endothelium-dependent hyperpolarization (EDH) has been observed in various species and vascular beds, including the mesenteric and coronary resistance arteries (Feletou and Vanhoutte, 1988, Chen et al., 1988, Garland and McPherson, 1992, Waldron and Garland, 1994b, Liu et al., 2015). Subsequent studies revealed that endothelial small- and intermediate-conductance Ca^{2+}-activated K^+ (SK_{Ca} and IK_{Ca} respectively) channels underpin the endothelium-dependent EDH (Waldron and Garland, 1994a). Therefore, in resistance arteries, in addition to stimulating NO synthesis, the rise in intracellular Ca^{2+} activates IK_{Ca} and SK_{Ca} channels resulting in K^+ efflux from endothelial cells into the myoendothelial junction (**Figure 1.2.2**). This subsequently hyperpolarizes vascular smooth muscle via the activation of inwardly rectifying K^+ (K_{IR}) channels and Na^+/K^+-ATPase on VSMCs (Edwards et al., 1998). Other EDH factors (EDHFs), such as epoxyeicosatrienoic acids (EETs), C-type natriuretic peptide (CNP), H_2O_2 have also been proposed to be involved in modulating VSMC contraction (Garland et al., 2011, Scotland et al., 2005).

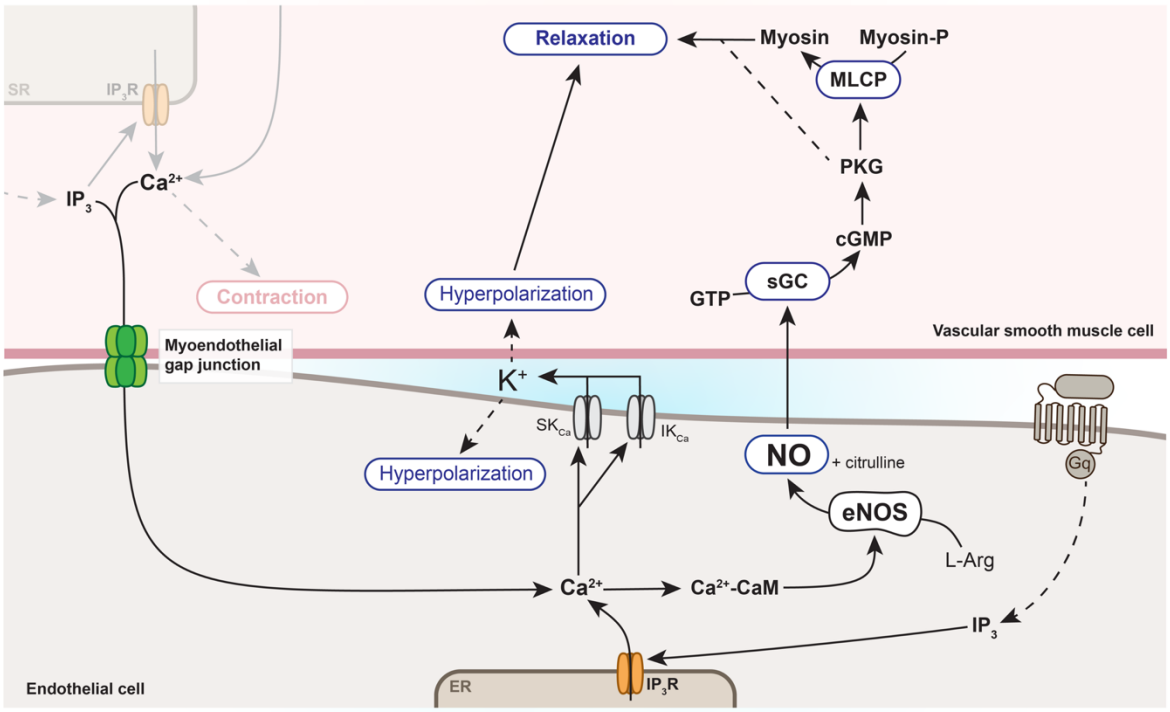


Figure 1.2.2 Signalling pathway for endothelium-dependent vascular smooth muscle cell relaxation. Dashed arrows indicate simplified pathway. CaM = Calmodulin; cGMP = Cyclic guanosine monophosphate; eNOS = endothelial nitric oxide (NO) synthase; ER = Endoplasmic reticulum; GTP = Guanosine triphosphate; IK_{Ca} = Intermediate-conductance Ca^{2+}-activated K^+ channel; $IP_3(R)$= Inositol 1,4,5-trisphosphate (receptor); L-Arg = L-arginine; MLCP = Myosin light chain phosphatase; PKG = protein kinase G; Myosin-P = Phosphorylated myosin; sGC = Soluble guanylyl cyclase; SK_{Ca} = small-conductance Ca^{2+}-activated K^+ channel.

Moreover, MEGJs are likely to play a crucial role in EDH as blocking gap junctions prevented ACh-induced VSMC hyperpolarization in guinea pig mesenteric arterioles (Yamamoto et al., 1999). Comparable observations using the gap junction mimetic blocker, Gap 27, in rat mesenteric resistance arteries showed that ACh-induced hyperpolarization was significantly attenuated in VSMC but not in endothelial cells (Sandow et al., 2002). Therefore, an association with MEGJs may explain the greater contribution of EDH recorded in resistance arteries compared to larger conduit arteries.

1.2.5 Myoendothelial feedback

In addition to agonist-induced (endothelium-dependent) vasodilation, the tight coupling between the endothelium and vascular smooth muscle allows the endothelium to modulate VSMC contraction in the absence of direct agonist stimulation. Rees et al. (1990) reported that NOS inhibition with L-NAME produced a concentration-dependent augmentation in PE vasoconstriction in rabbit aortic rings. The L-NAME augmented tone was lost upon endothelium removal (Adeagbo and Triggle, 1993), suggesting the release of NO from the endothelium upon vasoconstrictor stimulation. Similarly in myogenically active pressurised coronary resistance arteries, Garcia and Bund (1998) were the first to report that NOS inhibition or endothelium denudation enhanced coronary myogenic tone, supporting the role of the endothelium and the release of NO in modulating myogenic tone under basal conditions. In pressurised hamster cheek pouch arterioles, Dora et al. (1997) showed that the increase in VSMC Ca^{2+} by vasoconstrictors PE and high K^{+}, which do not stimulate endothelial cells, was followed by an increase in intracellular Ca^{2+} in endothelial cells. The possible direct effects of vasoconstrictors on endothelial cells were ruled out with intraluminal (endothelial cell specific) delivery of PE producing no effects on intracellular Ca^{2+} and arteriole diameter. Moreover, L-NAME potentiated PE- and K^{+}-induced vasoconstriction, indicating NO release. Therefore,

due to the central role of Ca^{2+} in vascular reactivity, it was hypothesised that VSMC Ca^{2+} may transfer to endothelial cells and may stimulate NO synthesis to modulate VSMC contraction (Dora et al., 1997). This intrinsic modulation on vascular tone is known as myoendothelial feedback.

1.2.6 Coronary microvascular dysfunction

Ischaemic heart disease as a result of coronary artery disease (CAD) remains one of the leading causes of global mortality. Much of the research into this disease has largely focused on understanding the process of atherosclerosis in the larger epicardial arteries and developing treatments for obstructive CAD. However, many patients presenting with myocardial ischaemia and angina-like symptoms often have angiographically normal, non-obstructive coronary artery disease (ANOCA). Patel et al. (2010) reported that ~60% of patients underwent cardiac catheterisation were classified as having normal, non-obstructed coronary arteries. Furthermore, approximately two-thirds of patients with ANOCA have some form of coronary microvascular dysfunction (CMD), characterised by reduced coronary flow reserve (CFR) in the absence of obstructed coronary arteries (Sara et al., 2015, Camici and Crea, 2007). Furthermore, a significant proportion (up to ~50%) of ANOCA patients present with microvascular angina, which was previously known as cardiac syndrome X, a subtype of CMD (Camici and Crea, 2007, Murthy et al., 2014). Despite the clinical importance, our understanding of CMD is still rudimentary, therefore, understanding the coronary microcirculation can provide insights into the underlying pathophysiology of CMD and help identify potential therapeutic targets. Recent studies observed elevated plasma concentration of asymmetric dimethylarginine (ADMA) in patients with microvascular angina, which suggests a possible role for this endogenous inhibition of NOS in the development of CMD (Chen et al., 2002, Lu et al., 2017).

1.3 ENDOGENOUS METHYLARGININES

As discussed, the endothelium plays a crucial role in maintaining vascular homeostasis through intrinsic and agonist-induced mechanisms. Therefore, disruptions to the endothelium, such as a reduction in NO synthesis, would reduce vasodilation and enhance vasoconstriction, predisposing individuals to cardiovascular disease. First reported by Vallance et al., N^G,N^G-dimethylarginine (asymmetric dimethylarginine; ADMA) is an endogenous inhibitor of NOS with the ability to disrupt endothelial function and NO synthesis *ex vivo* and *in vivo* (Vallance et al., 1992a). This has subsequently led to the emergence of ADMA as an independent cardiovascular risk factor.

1.3.1 Biosynthesis and clearance of methylarginines

Methylarginines are products of the proteolysis of proteins containing methylated L-arginine (**Figure 1.3.1A**). As part of post-translational protein modification, that is ubiquitous in almost all cells, protein-bound L-arginine residues can be monomethylated or dimethylated by protein-arginine methyltransferase (PRMT) enzymes, of which there are three classes: Type 1 (PRMT1), Type 2 (PRMT2) and Type 3 (PRMT3) (Anthony et al., 2005, Tewary et al., 2019). The three PRMT classes exhibit different catalytic activity, of which PRMT1 is responsible for the eventual formation of N^G-monomethyl-L-arginine (L-NMMA) and ADMA, whereas PRMT2 is responsible for L-NMMA and N^G,$N^{G'}$-dimethylarginine (symmetric dimethylarginine; SDMA) formation and PRMT3 is solely for L-NMMA formation (**Figure 1.3.1B**).

However, L-NMMA and ADMA, but not SDMA, are inhibitors of NOS (Vallance et al., 1992a). Therefore, the release of L-NMMA and ADMA from protein degradation allows free methylarginines to bind and inhibit eNOS. Despite that plasma ADMA concentration is 10-fold

higher than that reported for L-NMMA (Vallance et al., 1992a), much of the research has focused on L-NMMA as a possible pharmacological tool to probe the NO pathway.

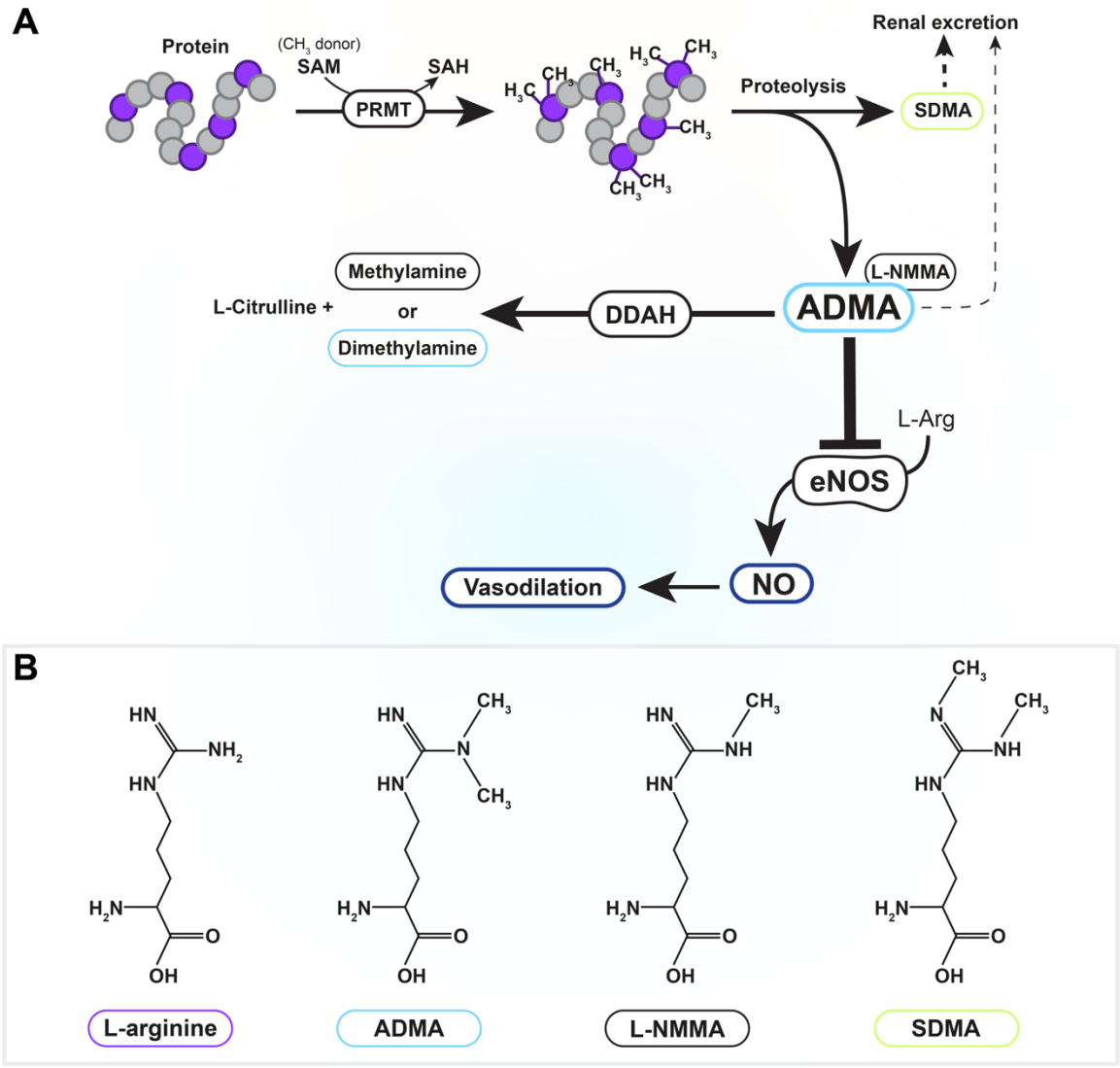


Figure 1.3.1 Overview of the synthesis and clearance pathways of methylarginines. A, Synthesis and clearance of N^G-monomethyl-L-arginine (L-NMMA), N^G,N^G-dimethylarginine (asymmetric dimethylarginine; ADMA) and N^G,$N^{G'}$-dimethylarginine (symmetric dimethylarginine; SDMA). Protein-bound L-arginine (L-Arg) depicted as purple circles. Dashed arrows indicate simplified pathway. **B,** The chemical structures of L-arginine, ADMA, L-NMMA and SDMA. DDAH = dimethylarginine dimethylaminohydrolase; eNOS = endothelial nitric oxide (NO) synthase; PRMT = protein-arginine methyltransferase; SAH = S-adenosylhomocysteine; SAM = S-adenosylmethionine; methyl (CH_3) donor.

The intracellular and plasma concentrations of methylarginines are modulated by renal excretion and enzymatic degradation (**Figure 1.3.1A**). Although elevated ADMA levels were first observed in patients with chronic renal failure (Vallance et al., 1992a, Kielstein et al., 1999), indicating the importance of renal excretion for methylarginine clearance, ADMA and L-NMMA clearance is dependent on enzymatic degradation. Both ADMA and L-NMMA are metabolised by dimethylarginine dimethylaminohydrolase (DDAH) into citrulline and methylamines, whereas SDMA is almost exclusively eliminated through urine excretion (Ogawa et al., 1987a, Ogawa et al., 1987b, Achan et al., 2003).

1.3.2 Clinical relevance of ADMA

The clinical importance of ADMA was first reported by Vallance et al. (1992a), where they observed an accumulation of ADMA in patients with chronic renal failure and hypertension. In these patients, dialysis normalised plasma ADMA concentration and improved vasodilation to ACh due to temporary reversal of NO production (Hand et al., 1998, Kielstein et al., 1999). The notion of ADMA serving as an endogenous inhibitor of NO synthesis was further supported by Böger et al. (2000), where they showed the capacity of endothelial cells to synthesise and release ADMA, and the ability of ADMA to inhibit NO synthesis.

Since then, numerous human (and animal) studies showed that elevated ADMA levels (0.60 – 8.7 μM; **Table 1.3.1**) are associated with cardiovascular risk factors and diseases (Vallance et al., 1992a, Böger et al., 1997, Surdacki et al., 1999, Abbasi et al., 2001, Sydow et al., 2003), including spontaneous hypertensive and insulin resistance obese rat models (Li et al., 2007, Li et al., 2011, Fan et al., 2013, El Assar et al., 2016). Antoniades et al. (2009) measured pre-operative serum ADMA concentrations in 201 patients undergoing coronary bypass surgery and investigated the vasodilation of saphenous vein and mammary arteries

ex vivo. They found that ADMA levels inversely associated with ACh and bradykinin vasodilation, and positively correlated with superoxide production, indicative of oxidative stress. Similarly, a study investigating the relationship between ADMA and hypertension revealed higher plasma ADMA levels and impaired endothelial function, indicated by blunted vasodilatory response to ACh, in hypertensive patients compared to controls (Perticone et al., 2005).

In a randomised study, Böger et al. (1998) compared plasma L-arginine and ADMA concentrations and flow-mediated vasodilation in hypercholesterolaemic and normo-cholesterolaemic subjects. Plasma ADMA levels were significantly elevated and the L-arginine/ADMA ratio decreased in people with hypercholesterolaemia, both of which were associated with impaired flow-mediated vasodilation in their forearm, signifying endothelial dysfunction.

The levels of plasma ADMA have also been implicated in ageing-associated vascular dysfunction and as an independent predictor of cardiovascular morbidity and mortality. In a prospective cohort study of 204 patients, plasma ADMA concentration increased with ageing, compared to baseline (Sverdlov et al., 2014). This finding is comparable to a larger longitudinal study of 1,025 people, where plasma ADMA was shown to increase with ageing and the small increase in plasma ADMA (~0.1 μM) was associated with a 26% higher risk for all-cause mortality (Pizzarelli et al., 2013). Moreover, a similar association between plasma ADMA levels and vascular dysfunction was reported in 2,096 healthy young individuals, where ADMA negatively correlated with vasodilation even after adjustment for known cardiovascular risk factors (Juonala et al., 2007). A separate prospective study investigated the relationship between ADMA and future cardiovascular events in almost 1,900 patients with coronary artery disease. The baseline ADMA concentration was higher in patients who experienced fatal and

non-fatal cardiovascular complications than those without adverse events (Schnabel et al., 2005). When baseline ADMA levels within this patient group were separated into subgroups, those with upper third highest ADMA levels exhibited a >2-fold increase in cardiovascular risk compared to those in the lowest third.

Despite the strong association of elevated plasma ADMA levels in cardiovascular disease, little is known about the effects of ADMA in the microcirculation, specifically in the heart. Therefore, further knowledge regarding the effects of ADMA in the coronary microcirculation, may help unravel the development of microvascular endothelial dysfunction.

Table 1.3.1 Summary of the mentioned studies in Chapter 3.1 that reported elevated plasma concentration of ADMA. SHR = Spontaneously hypertensive rat; PAD = Peripheral artery disease; T2D = Type 2 diabetes mellitus; CV = Cardiovascular; n/a = Not applicable.

Studies	Species	Plasma [ADMA] (µM)		*Notes
		Control	Pathological*	
Li et al. (2007)	Rat	0.66 ± 0.07	1.24 ± 0.18	Control vs SHR
Li et al. (2011)		~0.70	~1.20	
Fan et al. (2013)		1.14 ± 0.1	1.68	
El Assar et al. (2016)		~0.60	~0.85	Morbidly obese model
Vallance et al. (1992a)	Human	1.15 ± 0.13	8.7 ± 0.7	Control vs chronic renal failure patients
Böger et al. (1997)		1.0 ± 0.1	2.80 ± 0.22	Control vs PAD
Böger et al. (1998)		1.03 ± 0.09	2.17 ± 0.15	Normo- vs Hypercholesterolaemia
Surdacki et al. (1999)		1.1 ± 0.7	2.14 ± 1.1	Norm- vs Hypertensives
Abbasi et al. (2001)		0.69 ± 0.04	1.59 ± 0.22	Control vs T2DM
Sydow et al. (2003)		1.0 ± 0.1	3.8 ± 0.3	PAD and HC patients only
Perticone et al. (2005)		0.40 ± 0.09	0.59 ± 0.14	Norm- vs Hypertensives
Schnabel et al. (2005)		0.63	0.70	Patients without vs with CV events
Sverdlov et al. (2014)		0.52 ± 0.08	0.60 ± 0.09	Ageing in 4-year follow up study

1.4 THESIS AIMS AND OBJECTIVES

This thesis aims to investigate the effects of the endogenous dimethylarginine, ADMA, on the mesenteric and coronary microcirculation. Due to the current limitations in *in vivo* imaging techniques, this thesis uses *ex vivo* wire and pressure myograph techniques – for functional studies, coupled with immunohistochemistry and fluorescent imaging to elucidate protein expression and intracellular Ca^{2+} events in the microcirculation respectively.

Objectives are as follows:

i) To characterise the effects of ADMA on vasoreactivity and NO-dependent vasodilation in mesenteric resistance (**Chapter 3**) and intra-septal coronary arteries (**Chapter 4**).

ii) To investigate the modulatory role of DDAH1 on NOS inhibition with ADMA in mesenteric and coronary resistance arteries (**Chapter 5**).

iii) To determine whether L-arginine supplementation can reverse the endothelial dysfunction induced by ADMA (**Chapter 6**).

iv) To investigate the effects of ADMA on intracellular Ca^{2+} events in intra-septal coronary arteries (**Chapter 7**).

CHAPTER TWO

MATERIALS AND METHODS

2.1 ANIMALS AND TISSUE PREPARATION

All animal procedures were conducted in accordance with the University of Oxford local ethical guidelines, the ARRIVE guidelines and the UK Home Office Animal (Scientific Procedures) Act, 1986.

Male Wistar rats (7-8 weeks, 200 – 320 g; Charles River, UK) were used in this thesis. Animals were housed in individually ventilated cages in a temperature-controlled environment with a 24-hour light-dark cycle and water *ad libitum*. Animals were sacrificed in accordance with Schedule 1 Methods of the Animal (Scientific Procedures) Act, 1986, by rising CO_2 and subsequent cervical dislocation to confirm death. The mesenteric plexus and the heart were excised and immediately placed in ice-cold Krebs solution (**Chapter 2.6**).

2.1.1 Preparation of rat mesenteric resistance arteries

The mesenteric arcade was pinned down in a Sylgard-coated Petri dissecting dish containing fresh ice-cold Krebs solution (**Figure 2.2.1A**). A third-order mesenteric artery was dissected free of connective tissue and adipocytes (**Figure 2.2.1B and C**). A segment (circa 2 mm) with no visible side branches was removed and mounted in a Mulvany-Halpern multi-channel wire myograph (Models 610M or 700MO, Danish Myo Technology, Denmark) for isometric tension measurements (**Chapter 2.2; Figures 2.2.1** and **2.2.2**).

2.1.2 Preparation of rat intra-septal coronary arteries

The heart was pinned down in a Sylgard-coated Petri dissecting dish containing fresh ice-cold Krebs solutions (**Figure 2.2.3A**). The anterior wall of the right ventricles was cut open to reveal the intra-septal coronary artery (**Figure 2.2.3B; Arrowhead**). For wire myography experiments, an artery circa 2 mm long was dissected from surrounding cardiomyocytes and

connective tissues and mounted in a Mulvany-Halpern wire myograph for either isometric tension measurements (**Chapter 2.2; Figure 2.2.3**) and immunohistochemistry (**Chapter 2.4**) or for simultaneous isometric tension and intracellular Ca^{2+} event measurements in vascular smooth muscle (**Chapters 2.2.4 – 2.2.6**). For pressure myography experiments arteries free from visible side branches were mounted in either a 10 mL DMT pressure myograph for diameter measurements or in a 2 mL temperature-regulated confocal imaging chamber (RC-27, Warner Instruments, USA) for diameter and intracellular Ca^{2+} event measurements in the coronary endothelium (**Chapter 2.3**).

2.2 WIRE MYOGRAPHY

Developed by Mulvany and Halpern (1977), the Mulvany-Halpern wire myography is a widely used and reliable technique to study vascular function (e.g. vasoconstriction and vasorelaxation) of resistance arteries *ex vivo*. Furthermore, the development of the multi-channel wire myographs allows for the investigation of four different experimental conditions, particularly useful if paired comparisons are made in the same animal.

In summary, artery segments are held between the mounting jaws in a tissue chamber using two wires through the lumen (**Figures 2.2.1D** and **2.2.2**). One wire is mounted on a jaw connected to a force transducer, allowing for isometric tension recording. The other wire is mounted on a jaw attached to a micrometer to allow for distension (lateral stretching) during initial set up (normalisation). During the normalisation procedure, an exponential length-tension curve is generated from the recorded points to determine the optimum resting tension of arteries.

2.2.1 Mounting of arteries in a wire myograph

Circa 2 mm segments of mesenteric or intra-septal coronary arteries were mounted in using 25 µm gold-plated tungsten wires in a four-channel Mulvany-Halpern wire myograph (Models 610M or 700MO, Danish Myo Technology, Denmark) containing room temperature Krebs solution (**Chapter 2.6**). A subset of intra-septal coronary arteries was mounted in a confocal wire myograph chamber (Model 120CW, Danish Myo Technology, Denmark) for intracellular Ca^{2+} measurements in VSM. Arteries were subsequently warmed to 36.5 ± 0.5°C and allowed to equilibrate for 30 minutes before normalisation. Arteries were then normalised to a resting tension equivalent to that generated at 90% of the inner diameter of the vessel at 70 mmHg (mesenteric) and at 80 mmHg (for coronary). Changes in isometric tension were recorded at

10 Hz using a PowerLab/4SP data acquisition system (ADInstruments, New Zealand) and LabChart software (version 8, ADInstruments, New Zealand).

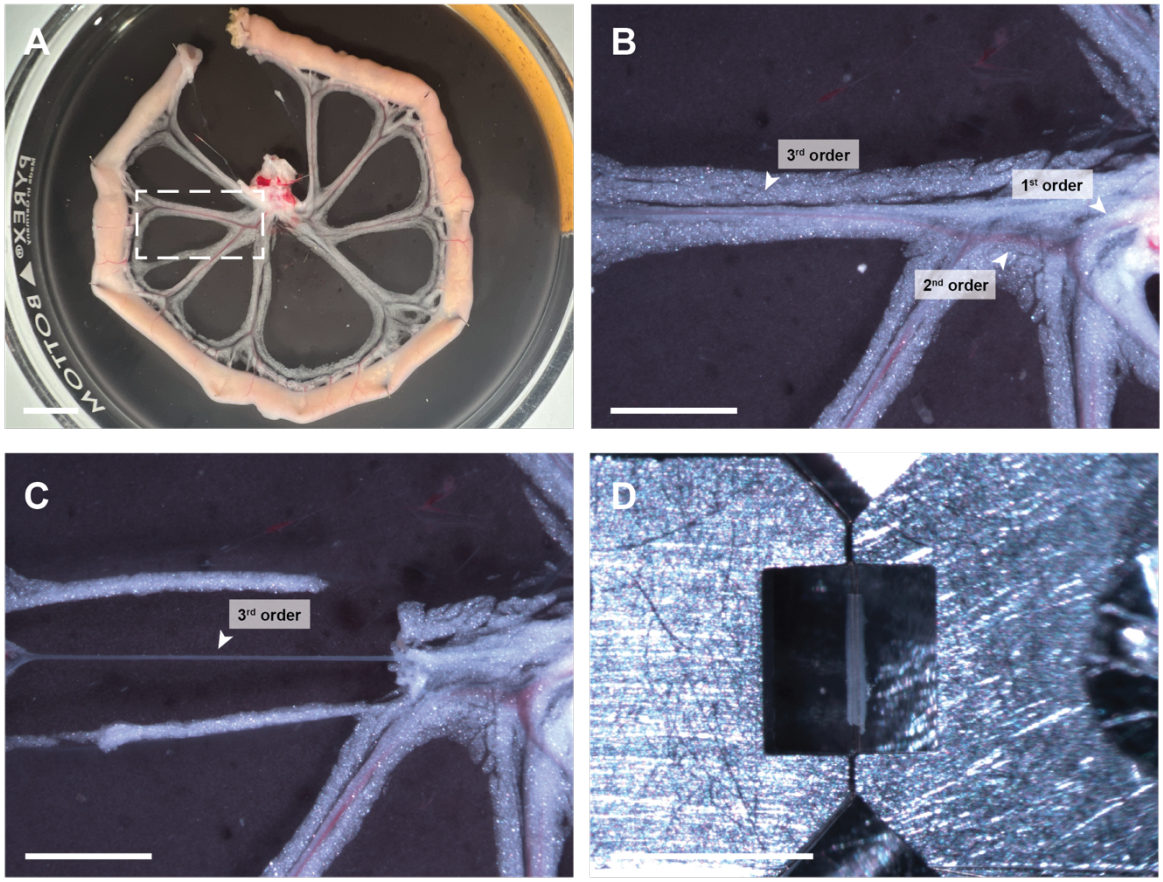


Figure 2.2.1 Excised mesenteric arcade and isolated mesenteric artery mounted in a wire myograph. A, Image of a pinned-out mesenteric arcade. Dashed box represents the region of magnification in (**B** and **C**). Scale bar = 10 mm. **B – C,** Magnified images of a section of the mesenteric arcade before (**B**) and after (**C**) the removal of the surrounding connective tissue and adipocytes. Arrowheads indicate the respective orders of arteries. Third-order mesenteric arteries were studied in all experiments. Scale bar = 5 mm. **D,** Image of an unstretched third-order mesenteric artery mounted in a wire myograph for isometric tension recording. The wires in the lumen are visible. Scale bar = 2 mm.

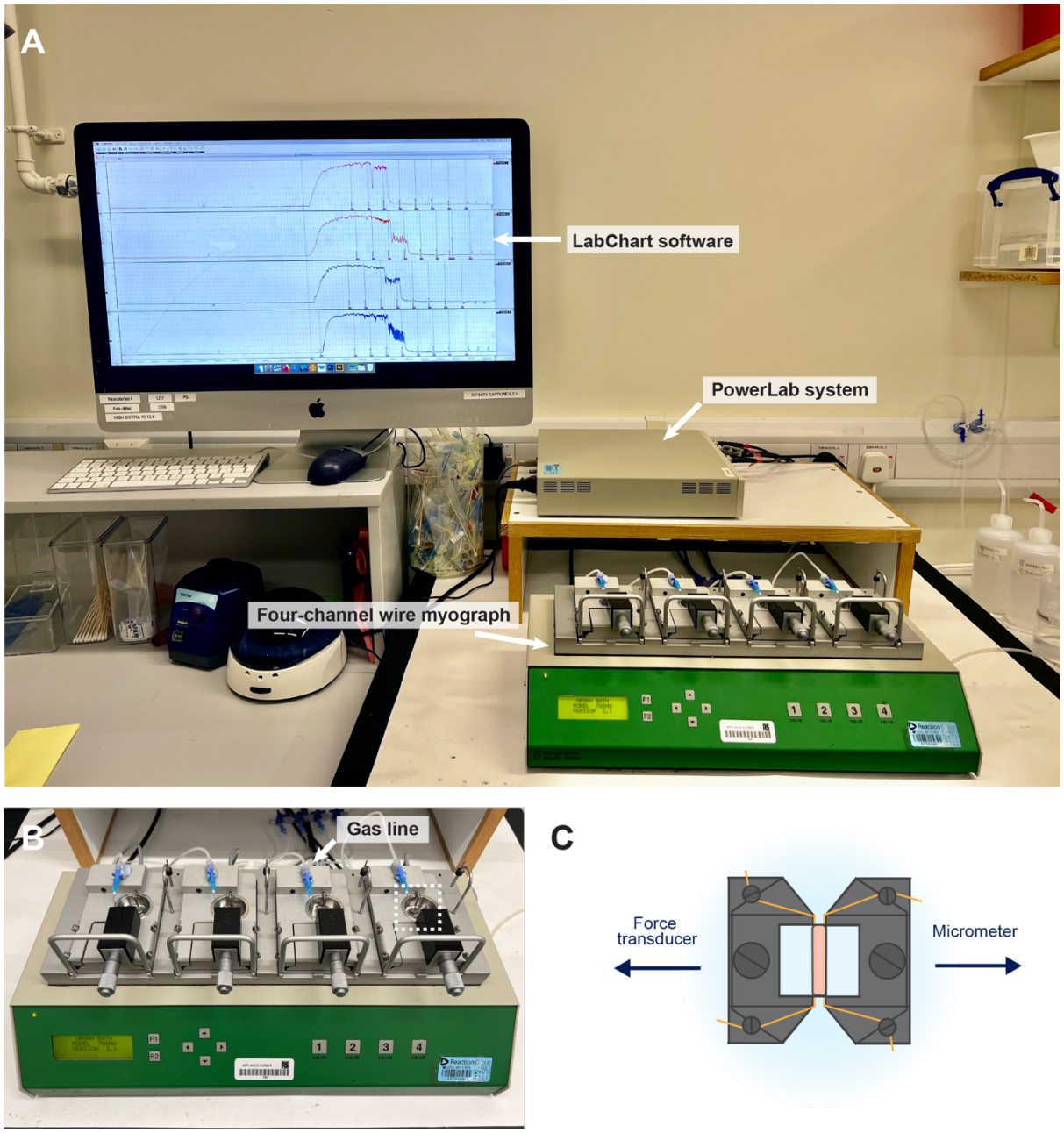


Figure 2.2.2 Wire myograph set-up for isometric tension recordings. A, Overview image of the wire myograph set-up used for the assessment of vasoreactivity, vasorelaxation and myogenic tone under isometric tension and immunohistochemistry. **B,** Image of the Mulvany-Halpern four-channel wire myograph. **C,** Diagram representation of the dashed box in (**B**) of an artery mounted between the jaws of a wire myograph chamber. Arrows indicate a force transducer attached to one jaw and a micrometer used for stretching the artery to the other.

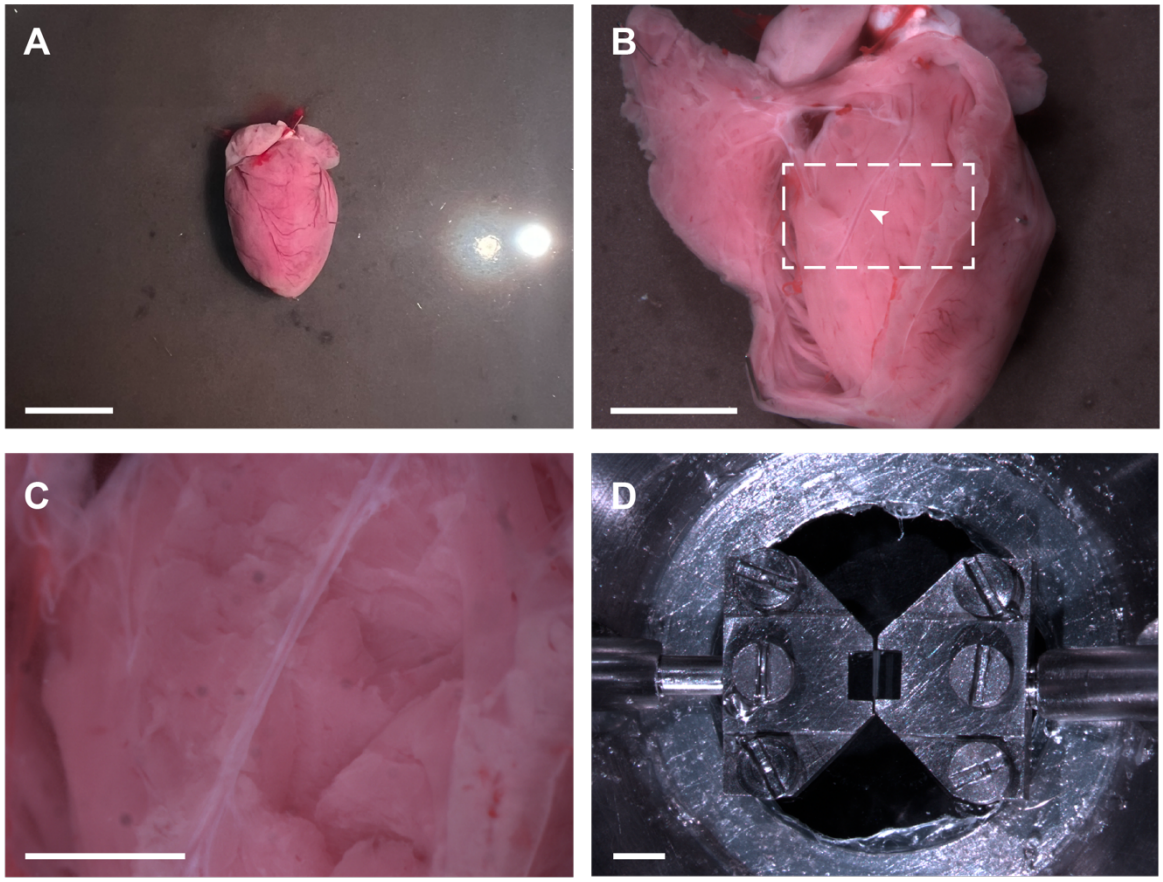


Figure 2.2.3 Excised heart and isolated intra-septal coronary artery mounted in a confocal wire myograph chamber. A, Image of a pinned-out heart. Scale bar = 10 mm. **B – C**, Images of the heart with the wall of the right ventricle cut open and the intra-septal coronary artery exposed before (**B**) and after (**C**) the removal of the surrounding connective tissue and cardiomyocytes. Arrowhead indicates the position of intra-septal coronary arteries studied in this thesis. **C,** Magnified region of the dashed box in (**B**). Scale bars (**B**) = 5 mm, (**C**) = 2 mm. **D,** Image of a circa 2 mm unstretched segment of coronary artery mounted in a confocal wire myograph chamber for simultaneous recording of isometric tension and vascular smooth muscle intracellular Ca^{2+}. Scale bar = 2 mm.

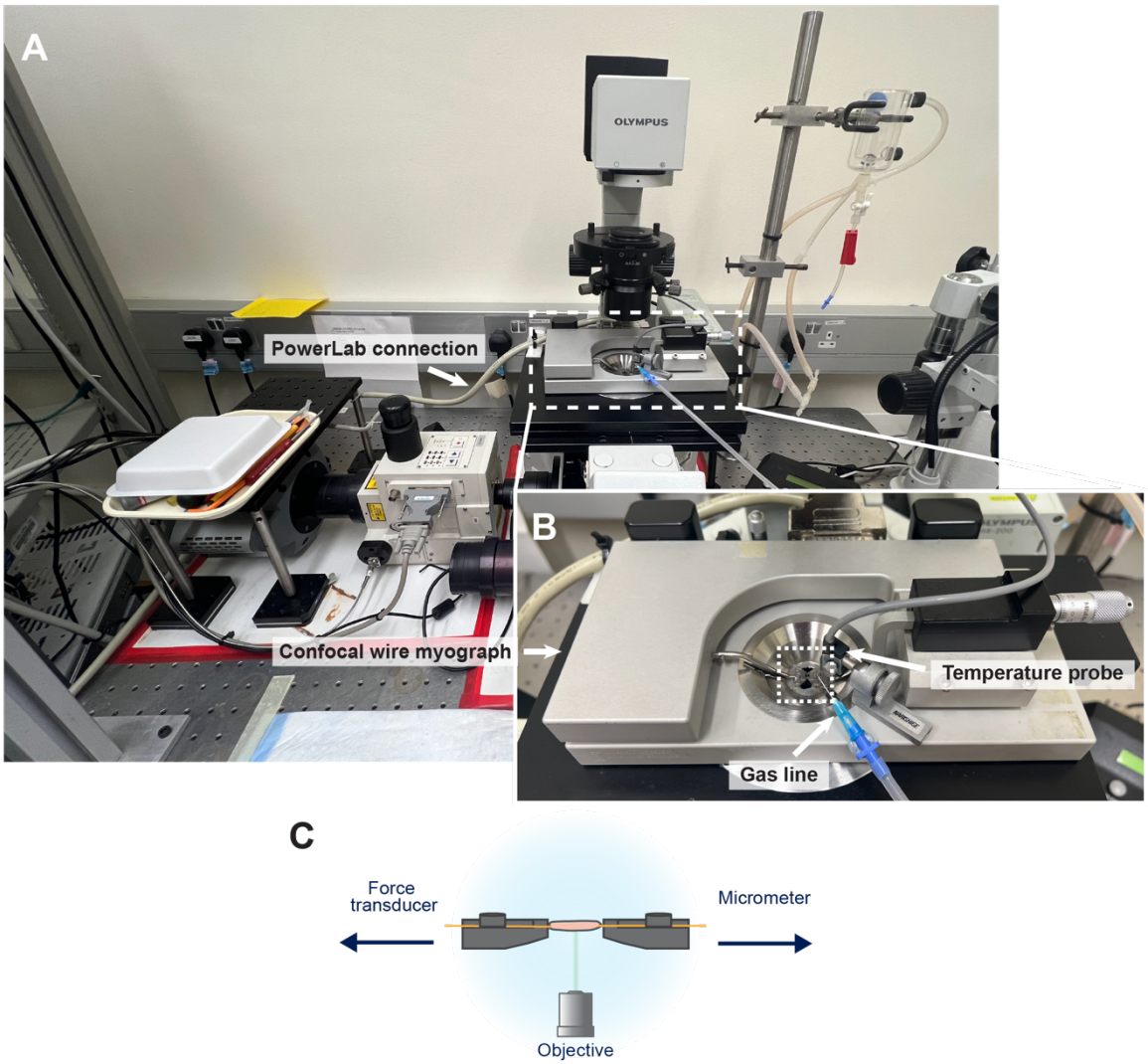


Figure 2.2.4 Confocal wire myograph set-up for simultaneous recording of isometric tension and intracellular Ca^{2+}. A, Overview image of the confocal wire myograph set-up used for measuring intracellular Ca^{2+} in coronary arteries. **B,** Image of the confocal wire myograph chamber (dashed region in (**A**). **C,** Diagram representation the dash box shown in (**B**) of an artery mounted between the jaws of a confocal wire myograph chamber for intracellular Ca^{2+} recordings. Arrows indicate the force transducer and micrometer for stretching during normalisation.

2.2.2 Studying rat mesenteric arteries under isometric tension

Vessel reactivity of mesenteric arteries (inner diameter: 150 – 320 μm) was assessed after an equilibration period (≥30 min) by pre-constriction to phenylephrine (PE; 0.5 – 3 μM) followed by endothelium-dependent vasorelaxation to acetylcholine (ACh; 0.001 – 1 μM). Only arteries that relaxed >95% were used for further experiments. For experiments investigating endothelium-dependent vasorelaxation, arteries were pre-constricted with PE after incubation with various inhibitors or compounds (**Chapter 2.6**), followed by cumulative addition of ACh (0.001 – 1 μM). Arteries were discarded if they exhibited an attenuation in PE-induced contraction over time (fade).

2.2.3 Analysis of mesenteric artery isometric tension recordings

Each tension data point represents the mean tension over a fifteen-second period. Contractility of mesenteric arteries is expressed as the isometric tension in millinewton (mN) over the length of artery in millimetre (mm). Mesenteric arteries did not usually develop myogenic tone, but if myogenic tone was present, the maximum vasorelaxation was used as the baseline tension.

$$Tension\ (mN/mm) = \frac{Tension\ induced\ by\ PE\ (mN)}{Artery\ length\ (mm)}$$

Vasorelaxation is expressed as a percentage of the baseline tension from tension during PE-induced vasoconstriction.

$$Vasorelaxation\ (\%) = \frac{(PE\ tension - Tension\ at\ peak\ response)}{(PE\ tension - Baseline\ tension)} \times 100$$

E_{max} was determined as the maximum vasorelaxation to the agonist.

2.2.4 Studying rat intra-septal coronary arteries under isometric tension

Coronary arteries (inner diameter: 170 – 330 μm) were left to equilibrate following normalisation and to develop myogenic tone, which we defined for experimental purposes as a minimum of 0.5 mN/mm above baseline tension. Endothelial cell function was assessed by cumulative addition of ACh (0.001 – 1 μM) from myogenic tone (in the absence of any vasoconstrictor). Only arteries with stable myogenic tone and relaxing >95% to ACh were used for further experiments. For experiments investigating myogenic tone, arteries were left for myogenic tone to re-develop before introducing inhibitors and compounds (**Chapter 2.6**). At the end of each experiment nifedipine (1 μM) was added to obtain maximal relaxation and to show the artery is functional.

2.2.5 Analysis of coronary artery isometric tension recordings

Each tension data point represents the mean tension over a fifteen-second period. Myogenic tone in intra-septal coronary is expressed as isometric tension (mN) over the length of artery (mm).

$$Myogenic\ Tone\ (mN/mm) = \frac{Tension\ \ (mN)}{Artery\ length\ (mm)}$$

Vasorelaxation is expressed as a percentage of the baseline tension from myogenic tone. Baseline tension is equivalent to 100% vasorelaxation.

$$Vasorelaxation\ (\%) = \frac{(Myogenic\ tone - Tension\ at\ peak\ response)}{(Myogenic\ tone - Baseline\ tension)} \times 100$$

E_{max} was determined as the maximum vasorelaxation to the agonist.

2.2.6 Measuring VSM intracellular Ca^{2+} in coronary arteries under isometric tension

Changes in VSM intracellular Ca^{2+} were imaged in a confocal wire myography chamber (**Figure 2.2.4**). Artery reactivity was assessed as described above. Viable arteries were loaded with calcium-sensitive fluorescent indicator CalBryte 520 AM (2550971, AA Bioquest, USA) (final concentration: 2.5 μM, 0.2% DMSO, 0.02% [w/v] Pluronic F-127 and Krebs buffer) at 30°C (**Chapter 2.6**) until a clear signal was detected (approximately 30 minutes). Arteries were subsequently incubated in Krebs buffer for 30 min at 36.5 ± 0.5°C to allow for de-esterification. Confocal images were obtained using a x40/1.15 NA water immersion objective (Olympus, Japan) and iXON 887 EMCCD camera (Andor Technology, UK) coupled to a Nipkow spinning disk confocal head (CSU22, Yokogawa, Japan) and inverted microscope (IX70, Olympus, Japan). Fluorescence intensity at 513 – 563 nm (excitation 488 nm) was acquired from the bottom surface of arteries at ~35 Hz (430 x 420 pixels) (Andor iQ v3.5, Andor Bioimaging Division, UK).

2.2.7 Analysis of intracellular Ca^{2+} events

Images were stored for offline analysis (iQ version 3.5, Andor Bioimaging Division and MetaMorph version 7.7.4.0, Molecular Devices, San Jose, USA). Data are expressed as relative fluorescence (F/F_0) from the full field of view following background subtraction and as frequency of Ca^{2+} events in Hz (**Figure 2.2.5**).

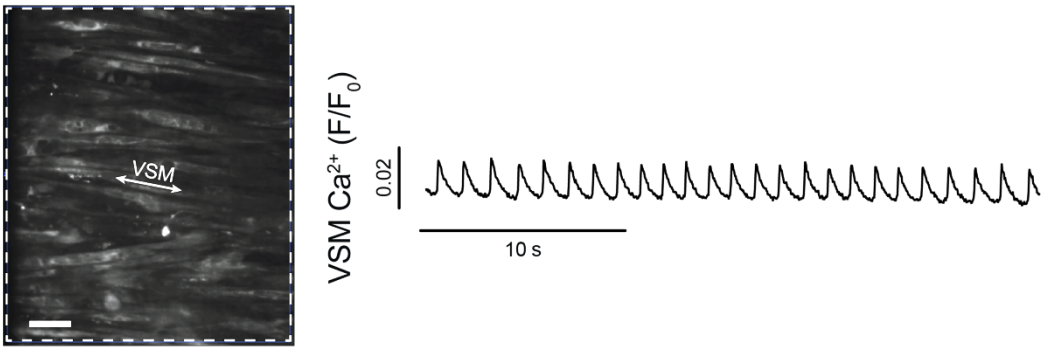


Figure 2.2.5 Analysis of intracellular Ca^{2+} events in vascular smooth muscle (VSM) of coronary arteries under isometric tension. Left panel, Image of vascular smooth muscle of coronary artery loaded with calcium-sensitive fluorescent indicator, CalBryte 520 AM. Dashed box indicates the region of interest use for analysis. Scale bar = 20 μm. **Right panel,** Example average fluorescence intensity time course (dashed region, left) which corresponds to simultaneous fluorescence changes in all the cells.

2.3 PRESSURE MYOGRAPHY

Established by Duling et al. (1981), pressure myography was developed by adapting existing techniques and apparatus for renal tubules introduced by Burg et al. (1966). Since its introduction, pressure myography has become indispensable in vascular research. This is of particular importance for coronary resistance arteries as: i) arteries can be studied in a tightly controlled environment and at physiologically relevant intraluminal pressures; and ii) current *in vivo* technologies do not allow for diameter measurements at this high resolution.

In summary, once each artery is excised from its vascular bed, the artery is cannulated between two glass micropipettes in a tissue chamber and is intra-luminally pressurised to its corresponding physiological pressure (**Figures 2.3.1** and **2.3.2**). Changes in vessel diameter can then be studied *ex vivo* in the presence of vasoactive agents.

Similar to wire myography, pressure myography can be coupled with other techniques such as fluorescence microscopy to record intracellular Ca^{2+} events, which would otherwise be impossible to conduct *in vivo*.

2.3.1 Artery cannulation and pressurisation

After the removal of surrounding tissues, mesenteric and intra-septal coronary arteries were cut into segments (circa 2 mm in length). In coronary arteries, the presence of unseen small side branches (<20 μm) resulted in re-cannulation of coronary artery segments until no leaks were detected, or they were discarded and replaced by a freshly isolated artery. Segments of arteries were subsequently transferred to a 10 mL DMT pressure myograph or a 2 mL confocal imaging chamber containing Krebs buffer (**Chapter 2.6**).

For the 10 mL DMT pressure myograph chamber (**Figure 2.3.1B**), the chamber was secured to a stage of an inverted microscope. The chamber was connected to a temperature heater and controller (Pressure Interface Model 110P, Danish Myo Technology, Denmark). Arteries were visualised using a 10x/0.3NA objective (Olympus, Japan) and images were recorded at similar frame rates as above. INFINITY LITE camera (Teledyne Lumenera, Canada) was attached to the inverted microscope and changes in artery inner diameter were recorded using INFINITY ANALYZE and CAPTURE (v7.0.2.930, Teledyne Lumenera, Canada).

For the 2 mL confocal imaging chamber (**Figure 2.3.2B**), the chamber was secured to a stage of an inverted microscope (FluoView1000, Olympus, Japan) with a heating element (PH-6, Warner Instruments, USA), which was connected to a temperature controller (TC-324C, Warner Instruments, USA). Arteries were visualised using a x10/0.3 NA objective (Olympus, Japan) and images were recorded at ~0.1 Hz during equilibration or the development of myogenic tone, or at ~1 Hz during experiments. Changes in artery inner diameter were recorded using FluoView FV10-ASM software (FV10-ASM v4.1, Olympus, Japan).

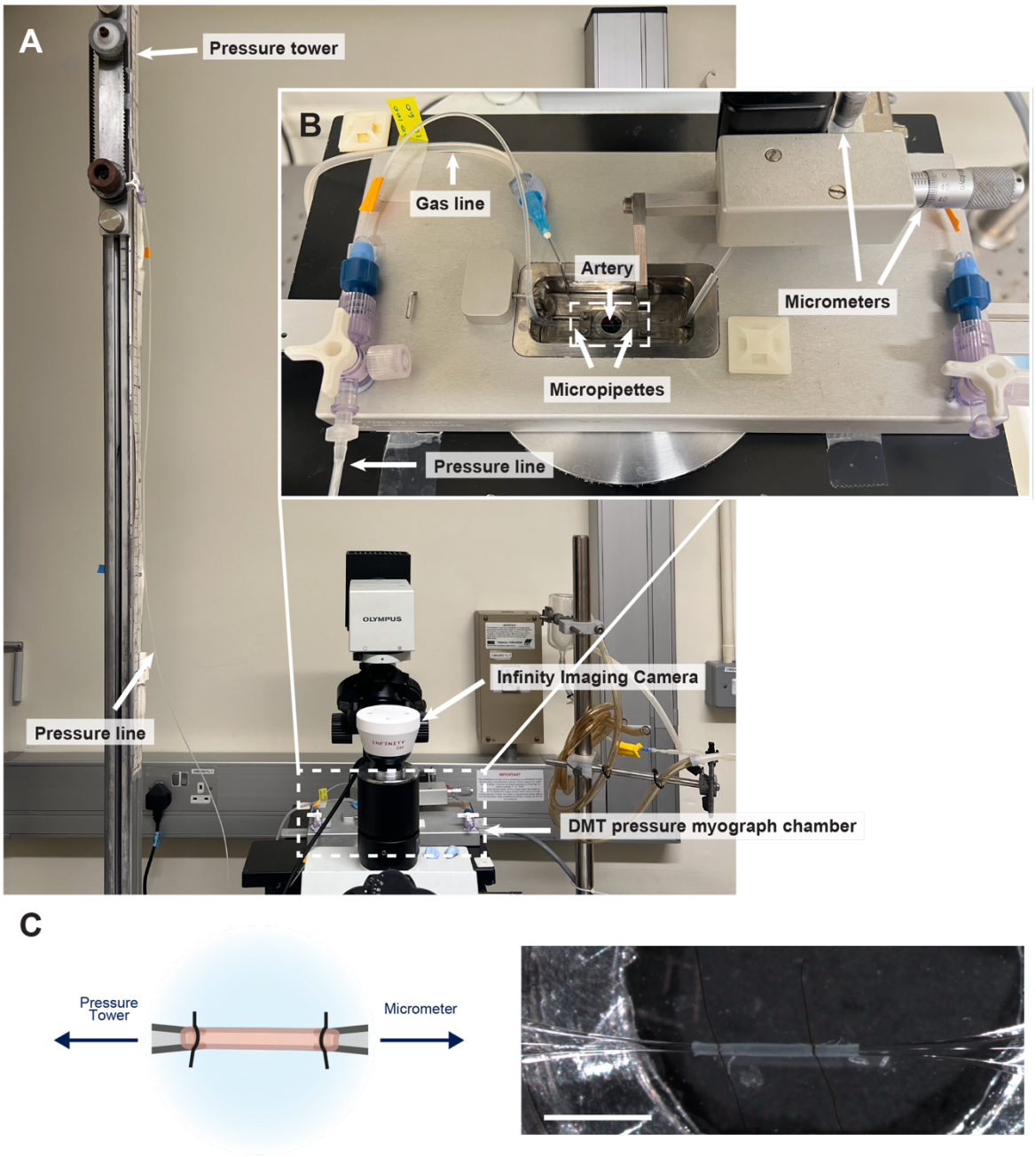


Figure 2.3.1 Pressure myography set-up for diameter recordings using DMT chamber. A, Image of a confocal microscope used for pressure myography experiments for diameter measurements. **B,** Image of the 10 mL DMT pressure myograph chamber with mounted artery of the dashed region in (**A**). **C,** Diagram representation of the pressure myography set-up (left panel) and magnified image of DMT pressure myograph chamber with artery mounted on to the micropipettes with sutures (right panel). Representation and magnified image of dashed region in (**B**). Scale bar = 2 mm.

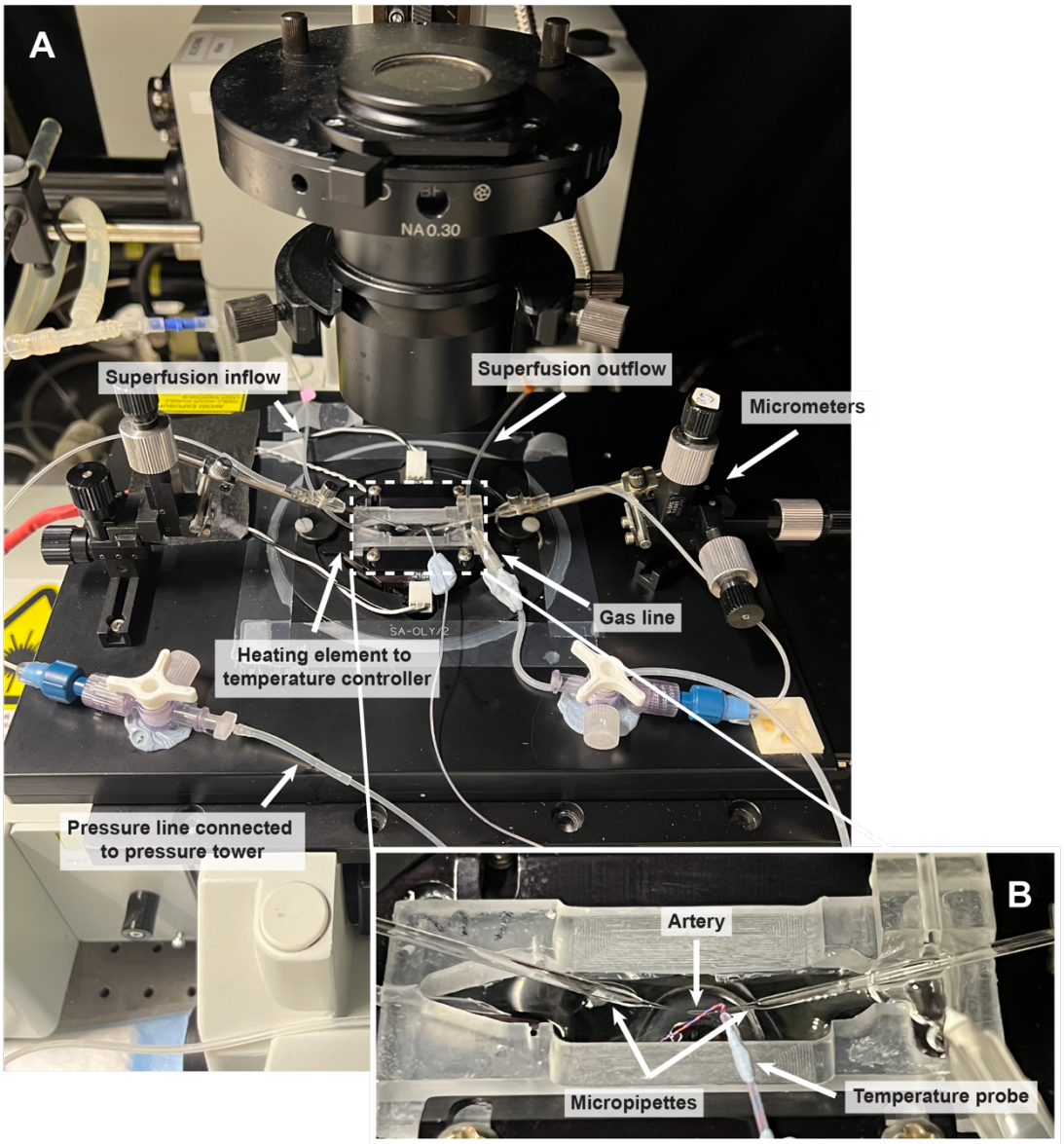


Figure 2.3.2 Pressure myography set-up for intracellular calcium recordings using the confocal chamber. A, Image of the 2 mL pressure myography confocal chamber mounted on a stage of a confocal microscope. **B,** Zoomed image of the 2 mL confocal chamber with a mounted artery, of the dashed region in (**A**).

Arteries were cannulated onto glass micropipettes (inner diameter: 80 μm; outer diameter: 140 μm) and secured using Ethilon nylon sutures (Ethicon, USA) (**Figures 2.3.1** and **2.3.2**). One micropipette was attached to a pressure line, which is connected to pressure tower. This allowed for the modulation of the intraluminal pressure of the artery by manually adjusting the pressure line. The Krebs solution in each chamber was gassed and heated to 36.5 ± 0.5°C. For the 10 ml DMT pressure myograph chamber, the Krebs solution in the bath was changed every 30 min. The 2 mL confocal imaging chamber was superfused with warmed and gassed Krebs solution at a flow rate of 2 mL/min. Care was taken to ensure the temperature was stable when the superfusion was switched off during concentration response curves. Once cannulated to the micropipettes, arteries were gradually pressurised and stretched longitudinally to avoid bowing of the artery. Leak tests at two intraluminal pressures were performed for each artery to ensure no side branches were present in the artery segment and to confirm the artery is securely held to the pipettes. If side branches were present, arteries were de-pressurised and re-cannulated when possible, and sutures were used to tie downstream of the side branches to obtain a side branch-free segment.

2.3.2 Studying pressurised rat mesenteric arteries

Mesenteric arteries (inner diameter: 150 – 320 μm) were pressurised to 70 mmHg and left to equilibrate for ≥60 min. Vessel reactivity was assessed using cumulative addition of ACh (0.001 – 1 μM) following pre-constriction with PE (0.5 – 1 μM). Arteries were only used for experiments if they displayed robust and maintained vasoconstriction to PE, and relaxed >95% to ACh. For experiments investigating vessel endothelium-dependent vasodilation, arteries were pre-constricted with PE after incubation with various inhibitors or compounds (**Chapter 2.6**), followed by cumulative addition of ACh (0.001 – 1 μM). Nifedipine (1 μM) was added to obtained maximal vasodilation.

2.3.3 Analysis of mesenteric artery diameter recordings

Inner diameter of mesenteric arteries was tracked using VasoTracker software (v1.1.0, VasoTracker, UK) (Lawton et al., 2019). Inner diameter was used for measurements, as also later used for coronary arteries, for consistency. Each data point represents the mean inner diameter over 30 s at the peak response.

Vasodilation is expressed as a percentage of the passive inner diameter from the inner diameter during PE pre-constriction:

$$Vasodilation\ (\%) = \frac{(Peak\ Response\ Diameter - PE\ Diameter)}{(Passive\ Diameter - PE\ Diameter)} \times 100$$

E_{max} was determined as the maximum vasodilation to the agonist.

2.3.4 Studying pressurised rat intra-septal coronary arteries

Coronary arteries (inner diameter: 170 – 330 μm) were pressurised to 80 mmHg. In contrast to mesenteric arteries, coronary artery was not pre-constricted with PE. Spontaneous myogenic tone was allowed to develop over a 60 – 70 min period at 36.5 ± 0.5°C. Vessel reactivity was assessed with cumulative ACh (0.001 – 1 μM) once myogenic tone was developed and stable (**Figure 2.3.3**). Only arteries with myogenic tone and dilated >95% to ACh were used for subsequent experiments. At the end of each experiment, nifedipine (1 μM) was added directly to the chamber to obtain the passive vessel diameter.

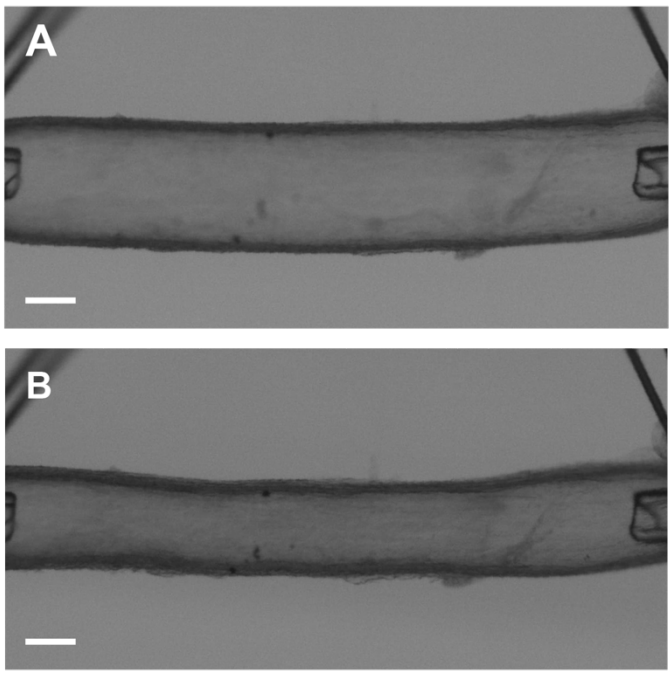


Figure 2.3.3 Intra-septal coronary artery pressurised to 80 mmHg. A – B. Bright-field images of a cannulated and pressurised coronary artery before (**A**) and after (**B**) the development of myogenic tone. Artery developed a stable myogenic tone (~42%) at 80 mmHg over 1 h. Scale bars = 100 µm.

2.3.5 Analysis of coronary artery diameter recordings

Inner diameter of coronary arteries was measured using VasoTracker software (v1.1.0, VasoTracker, UK) (Lawton et al., 2019). Outer diameter was not used for analysis due to the presence of residual cardiomyocytes and connective tissue on the outside of the artery, which would interfere with the detection of the outer artery wall. Each data point represents the mean diameter over 30 s at peak response.

Myogenic tone is expressed as a percentage of decrease from the passive inner diameter (without myogenic tone). One hundred percent (100%) myogenic tone corresponds to complete closure of artery lumen, where inner diameter = 0 μm.

$$Myogenic\ Tone\ (\%) = \frac{(Passive\ Diameter - Myogenic\ Tone\ Diameter)}{Passive\ Diameter} \times 100$$

Vasodilation is expressed as a percentage of the passive inner diameter from the inner diameter at myogenic tone:

$$Vasodilation\ (\%) = \frac{(Peak\ Response\ Diameter - Myogenic\ Tone\ Diameter)}{(Passive\ Diameter - Myogenic\ Tone\ Diameter)} \times 100$$

E_{max} was determined as the maximum vasodilation to the agonist.

2.3.6 Measuring endothelial cell intracellular Ca^{2+} in pressurised coronary arteries

Intracellular Ca^{2+} in endothelial cells of coronary arteries were measured in a 2 mL pressure myography confocal chamber (**Figure 2.3.2B**). Artery reactivity was assessed as described in **Chapter 2.3.4**. Viable arteries were de-pressurised to 10 mmHg and ECs were selectively loaded with the calcium-sensitive fluorescent indicator Oregon Green 488 BAPTA-1 AM (OGB-1; final concentration 10 μM, 0.7% DMSO, 0.05% [w/v] Pluronic F-127 and Krebs buffer) (**Chapter 2.6**) by intraluminal pumping through the lumen for a total of 30 min (pump on: 10 min; pump off: 20 min) at 30ºC. Krebs solution was subsequently pumped through the lumen for approximately 10 min to allow for de-esterification. Arteries were left to de-esterify for an additional 20 min with pumping off. Arteries were re-pressurised to 80 mmHg, warmed to 36.5 ± 0.5°C and left for tone to re-develop prior to experiments. Confocal images were obtained using a x40/1.15 NA water immersion objective (Olympus, Japan) and linescan confocal microscope (FV1000-MPE) based around an inverted microscope (IX81, Olympus, Japan). Fluorescence intensity at 513 – 563 nm (excitation 488 nm) was acquired at ~3 Hz (640 x 128 pixels) at 1x times digital zoom (FluoView Software, FV10-ASW v4.1, Olympus, Japan).

2.3.7 Analysis of intracellular Ca^{2+} events

Endothelial cell Ca^{2+} recordings were analysed offline using MetaMorph software (version 7.7.4.0, Molecular Devices, USA). Whole-cell regions were analysed and intracellular Ca^{2+} events were confirmed by eye and fluorescence intensity traces (**Figure 2.3.4**). The average of 9 – 10 endothelial cells were analysed per artery. Data are expressed as percentage of cells exhibited Ca^{2+} events and as frequency of Ca^{2+} events, expressed as events/cell/min.

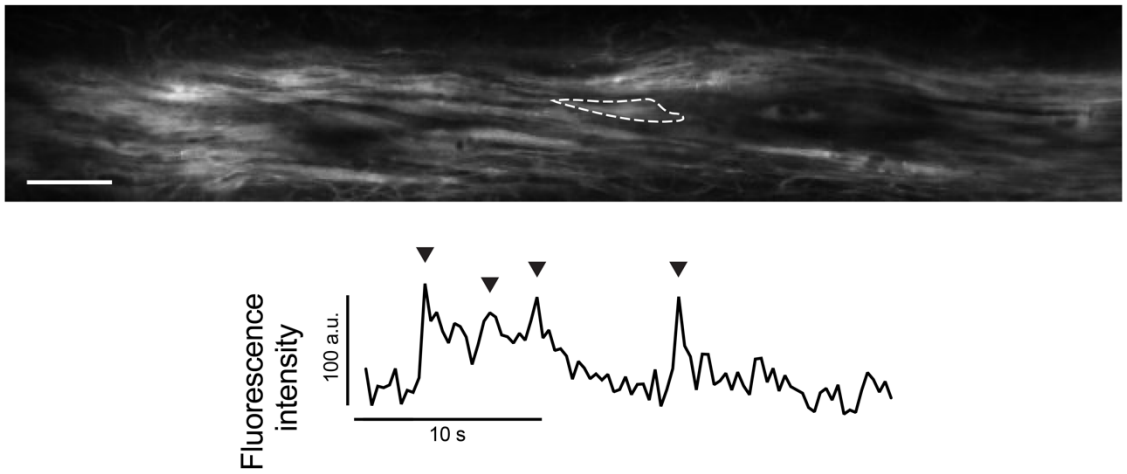


Figure 2.3.4 Analysis of intracellular Ca^{2+} events in endothelial cells of pressurised coronary artery. Top panel, Image of endothelial cells of coronary artery pressurised to 80 mmHg loaded with calcium-sensitive fluorescent indicator, Oregon Green 488 BAPTA-1 AM. Dashed region indicates the analysed cell. Endothelial cell indicated by dashed region. Scale bar = 50 μm. **Bottom panel,** Example fluorescence intensity trace of analysed cell (dashed region) in top panel. Arrowhead indicates a Ca^{2+} event.

2.4 IMMUNOHISTOCHEMISTRY

2.4.1 Immunolabelling in arteries under isometric tension

Once the viability of arteries was confirmed in the wire myograph, arteries were then fixed in 4% paraformaldehyde aqueous solution (157-4-100; Electron Microscopy Sciences) for one hour at room temperature, then washed for five minutes with phosphate buffer saline (PBS; 806552, Merck) three times. Arteries were sliced open longitudinally into 2 segments using a small scalpel and removed from the wire myograph. Arteries were incubated in blocking buffer (1% bovine serum albumin (BSA; A3059, Sigma), 0.5% Triton X-100 (T8532, Sigma), 0.05% Tween 20 (P2287, Sigma) in PBS) for 2 hours. Arteries were then incubated overnight at 4°C with primary antibodies (**Chapter 2.6**). On the following day, arteries were washed three times with PBS, then incubated with secondary antibodies and a nuclear dye (**Chapter 2.6**) for up to two hours at room temperature. Arteries were then washed with PBS before being placed in VECTORSHIELD anti-fade mounting medium (H-1000-10, 2BScientific, UK) on glass coverslips, with the endothelial cell layer faced flat on the coverslip.

2.4.2 Imaging immunohistochemistry

Immunolabelled arteries were excited at 405 and 488 nm with fluorescence intensity at 430 – 480 nm and 505 – 540 nm respectively acquired through a water immersion objective (40x, 1.15 NA, Olympus, Japan) using a laser scanning confocal microscope (FV1200, Olympus, Japan). Sequential z-stacks through the arteries were obtained at 0.5 µm increments, 1024 x 1024 pixels, 3.0x digital zoom, using Fluoview Software (FV10-ASW v4.1, Olympus, Japan) and reconstructed in Imaris Software (v7.7.1, Bitplane, USA).

2.4.3 Analysis of immunofluorescence images

Fluorescence intensity was analysed using Fiji Software (version 2.14.0). Mean fluorescence intensity was calculated by averaging the fluorescence intensity of five cells per artery (for the endothelial cell layer) or the full field of view (for VSM and nerves) (**Figure 2.4.1**).

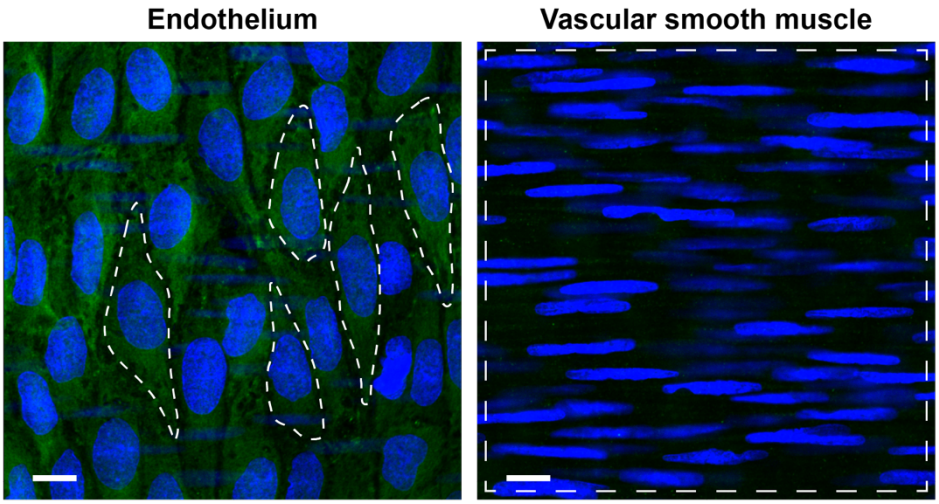


Figure 2.4.1 Analysis of immunofluorescence images. Five cells (for the endothelium – left panel) or full field of view (for vascular smooth muscle – right panel, and nerves) were analysed per artery. Mean fluorescence intensity was calculated by averaging the fluorescence intensity of the analysed regions. Dashed regions are examples of the analysed regions. Images taken a 3x digital zoom. Scale bar = 10 μm.

2.5 WESTERN BLOTS

2.5.1 Tissue homogenisation

Rat kidney and liver samples were excised, weighed, and immediately snap frozen in dry ice before storage at -80°C. Tissue was homogenised using Tissue Homogenising CKMix (P000918-LYSK0-A.0, Bertin Technologies, USA), containing CellLytic MT Cell Lysis Reagent (C3228-50ML, Sigma, UK) with protease inhibitor (10 µg/µl, P8430, Sigma, UK), and Minilys Personal Homogeniser (Bertin Technologies, USA). Samples were left on ice for 1 h. Homogenates were then centrifuged at 4°C for 20 min at 12,000 rpm.

Protein concentration was measured using the Bradford assay with albumin standards (0, 31.25, 65.5, 125, 500, 1,000, 2,000 µg/µl) containing protease inhibitors (10 µg/µl). Samples (0, 1:10 and 1:100 dilutions) and standards were incubated with Bradford reagent (B6916-500ML, Merck, Germany) for at least 5 minutes at toom temperature in the dark, before measuring the absorbance intensity using Li-Cor Odyssey M Imaging System (Li-Cor Biosciences, USA), with Empiria Studio Software (v2.2, Li-Cor Biosciences, USA).

2.5.2 Western blotting

Proteins at equal concentrations in loading buffer containing: Bolt LDS sample buffer, Bolt reducing agent and dH_2O, and protein ladder (Chameleon Duo Pre-stained Protein Ladder, LiCor Biosciences, US) were separated by (4 – 12%) Bolt-Tris Plus Mini Gel (NW04120BOX, Invitrogen, USA) in Bolt MOPS SDS running buffer by electrophoresis. Samples were subsequently electro-transferred onto an Immobilon-FL PVDF membrane (IPFL00005, Merck, Germany) in Bolt Transfer buffer (10% methanol and 0.001% Bolt antioxidant; BT005, Invitrogen, USA). Membrane was blocked in blocking buffer (5% milk and 0.001% Tween-20 in TBS buffer, 5% milk-TBST) for 1 h at room temperature, then incubated primary antibodies

(**Chapter 2.6**) in 5% milk-TBST overnight at 4°C. Following incubation membrane was washed with TBST buffer and blocked for 10 min in 5% milk-TBST before incubating with secondary antibodies (**Chapter 2.6**) in 5% milk-TBST for 1 h at room temperature. Western blots were imaged using Li-Cor Odyssey M Imaging System (Li-Cor Biosciences, US). Fluorescence intensity was analysed using Empiria Studio Software (v2.2, Li-Cor Biosciences, USA).

2.6 SOLUTIONS, DRUGS AND ANTIBODIES

2.6.1 Solutions

Tissue collection and experiments were performed in Krebs solution containing (in mM): 1.25 $CaCl_2$, 118.00 NaCl, 3.60 KCl, 1.20 $MgSO_4 \bullet 7H_2O$, 1.20 KH_2PO_4 11.00 glucose, and 25.00 $NaHCO_3$ (gassed with 5% CO_2, 21% O_2, balanced with N_2).

2.6.2 Drugs and compounds

All drugs and compounds used in this thesis are listed in **Table 2.6.1**. Phenylephrine (PE; P6126), acetylcholine (ACh; A6625), N_ω-Nitro-L-arginine methyl ester hydrochloride (L-NAME; N5751), N^G,N^G-Dimethylarginine dihydrochloride (ADMA; D4268), N^G,$N^{G\prime}$-Dimethyl-L-arginine dihydrochloride (SDMA; 311204), L-arginine monohydrochloride (L-Arg; A5131), D-arginine monohydrochloride (D-Arg; A6757), and nifedipine (Nif; N7634) were obtained from Sigma (UK). Apamin (Ap; 1652/1), NS6180 (NS; 4864) and TRAM 34 (TR; 2964) were obtained from Tocris (UK). Selective DDAH1 inhibitor L-257 (N^G-(2-methoxyethyl) arginine) was provided by Professor James Leiper from the University of Glasgow. All stock solutions were prepared using purifier (MilliQ) wate, except for NS6180 and TRAM 34 prepared in DMSO, and nifedipine prepared in 100% ethanol. All stocks solutions were prepared at 10^{-1} or 10^{-2} M, and subsequently diluted in Krebs buffer on the day of experiment, except for NS618 and TRAM 34 in DMSO to 10^{-3} M. Arteries were pre-incubated with inhibitors for at least 30 minutes before agonist application, except for apamin and L-257 for 1 hour. All drugs were added directly to the bath and mixed by gassing and manually with a pipette. For a subset of pressure myography experiments where superfusion was used, agonists were added directly to a static bath, and inhibitors were added to the superfusion, allowing for at least the same incubation time as used in a static bath.

Table 2.6.1 List of drugs and compounds used in this thesis.

Drug/Compound	Supplier (Product Code)	[Stock] (mM)	Solvent	[Bath] (mM)
Acetylcholine	Sigma (A6625)	10	Milli-Q	0.000001 – 0.001
Apamin	Tocris (1652/1)	0.1	Milli-Q	0.001
D-arginine monohydrochloride	Sigma (A6757) (Purity: ≥98%)	100	Milli-Q	1
L-arginine monohydrochloride	Sigma (A5131) (Purity: ≥98%)	100	Milli-Q	1, 10
N^G-(2-methoxyethyl) arginine (L-257)	-	100	Milli-Q	0.1
N^G,N^G-Dimethylarginine dihydrochloride (ADMA)	Sigma (D4268)	100	Milli-Q	0.3
N^G,$N^{G'}$-Dimethyl-L-arginine dihydrochloride (SDMA)	Sigma (311204)	100	Milli-Q	0.3
N_ω-Nitro-L-arginine methyl ester hydrochloride (L-NAME)	Sigma (N5751)	100	Milli-Q	0.1
Nifedipine	Sigma (N7634)	100	Ethanol	0.001
NS 6180	Tocris (4864)	100	DMSO	0.001
Phenylephrine	Sigma (P6126)	10	Milli-Q	0.0003 – 0.005
TRAM 34	Tocris (2946)	100	DMSO	0.001

2.6.3 Antibodies

All antibodies used in this thesis are listed in **Table 2.6.2**. Rabbit polyclonal anti-human DDAH1 IgG primary antibody (PA5-52278, Invitrogen, USA), goat polyclonal anti-rabbit IgG secondary antibody (A-11034, Invitrogen, USA) and nuclear dye Hoechst 33342 (H3570, Invitrogen, USA) were used for immunohistochemistry.

Rabbit polyclonal anti-human DDAH1 IgG primary antibody (PA5-52278, Invitrogen, USA), mouse monoclonal β-actin primary antibody (AC-15, ab6276, Abcam, UK), IRDye 800CW donkey anti-mouse (925-32212, Li-Cor Biosciences, USA) and IRDye 680RD donkey anti-rabbit (925-68073, Li-Cor Biosciences, USA) IgG secondary antibodies were used for western blotting.

2.6.4 Fluorescent Indicators

All fluorescent indicators used in this thesis are listed in **Table 2.6.3**. CalBryte 520 AM (2550971, AAT Bioquest, USA) and Oregon Green 488 BAPTA-1 AM (O6807, Invitrogen, USA) were used for studying intracellular Ca^{2+} events in coronary arteries.

Table 2.6.2 List of antibodies used in this thesis.

Antibodies	Supplier (Product code)	[Stock] (mg/mL)	Dilution
Rabbit polyclonal anti-human DDAH1 IgG primary antibody	Invitrogen (PA5-52278)	0.15	1:500
Peptide sequence: SKRTNQRGAEILADTFKDYAVSTVPVADGLHLKSFCSMAGPNLIAIGSSESAQKALKIMQQMSDHRYDKLTVPDDIAANCIYLNIPNKGHVLLHRTPEEYPESAKVYEKLKDHMLIPVSMSELEKVDGLLT			
Mouse monoclonal β-actin IgG primary antibody	Abcam (ab6276)	2.1	1:15,000
Goat polyclonal anti-rabbit IgG secondary antibody	Invitrogen (A-11034)	2	1:1,000
Hoechst 33342	Invitrogen (H3570)	10	1:10,000
IRDye 800CW donkey anti-mouse IgG secondary antibody	Li-Cor Biosciences (925-32212)	10	1:15,000
IRDye 680RD donkey anti-rabbit IgG secondary antibody	Li-Cor Biosciences (925-68073)	10	1:15,000

Table 2.6.3 List of fluorescent indicators used in this thesis.

Fluorescent indicators	Supplier (Product Code)	[Stock] (mM)	Solvent	[Final] (µM)
CalBryte 520 AM	AAT Bioquest (2550971)	2	DMSO	2.5
Oregon Green 488 BAPTA-1 AM	Invitrogen (O6807)	2	DMSO	10

2.7 STATISTICAL ANALYSES

All data analysis was completed post-hoc using Microsoft Excel (v16.77.1, Microsoft Corporation, USA) and GraphPad Prism software (v10.0.3, Molecular Devices, USA). Results are presented as mean ± SEM. Sample size (n) is indicative of the number of animals used per experiment. Sample size was determined using G*Power (version 3.1.9.6; Heinrich-Heine-Universität Düsseldorf, Düsseldorf, Germany) with α value = 0.05, β = 0.05 and 95% power. The effects of inhibitors on vasorelaxation or vasodilation to cumulative ACh was compared using the mean E_{max} ± SEM. Normality was assessed using Shapiro-Wilk test. For normally distributed data, statistical comparisons were made using paired or unpaired two-tailed t-tests, one-way ANOVA or mixed-effects analysis where appropriate. If statistically significant differences were detected Tukey's, Dunnett's or Sidak's multiple comparison post-test was used to compare the means between treatments. For non-normally distributed datasets, Kruskal-Wallis test followed by Dunn's multiple comparisons post-test were used. $P < 0.05$ is considered statistically significant.

CHAPTER THREE

CHARACTERISING THE EFFECTS OF DIMETHYLARGININES ON THE FUNCTION OF MESENTERIC RESISTANCE ARTERIES

3.1 INTRODUCTION

The endothelium plays an important role in the regulation of vascular tone via several mechanisms, one of which is the production of NO. The availability of NO is dependent on numerous factors, including the expression and activity of NOS. Therefore, disturbances to NOS specifically or the endothelium would disrupt NO synthesis and other endothelium-dependent vasodilatory pathways (e.g. endothelium-dependent hyperpolarization; EDH), compromising vascular function. Indeed, reduced NO bioavailability is a ubiquitous characteristic in many cardiovascular diseases and ageing. As aforementioned (**Chapter 1.3**), the *in vivo* activity of NOS is governed by methylarginines, such as ADMA. Methylarginines are produced via the proteolysis of protein L-arginine residues that have previously been methylated as part of their post-translational modification. For ADMA, protein-bound L-arginine residues are asymmetrically dimethylated by PRMT1. Once released, ADMA then competes with L-arginine for the active site of NOS, inhibiting NO synthesis.

As summarised in **Chapter 1.3**, Vallance et al. (1992a) first proposed the ability of ADMA acting as an endogenous modulator of NO synthesis as they observed an accumulation of ADMA in patients with chronic renal failure and hypertension. The elevated plasma ADMA concentration was normalised with dialysis and improved vasodilation to ACh (Hand et al., 1998, Kielstein et al., 1999). Since its discovery, studies (ranging from *in vitro* to *in vivo*) have directly examined the effects of ADMA on NO synthesis and vascular function.

Böger et al. (2000) reported the capacity of endothelial cells to synthesise and release ADMA, and the ability of ADMA to inhibit NO synthesis *in vitro*. Vallance et al. showed that ADMA extracted from patients inhibited NO synthesis in macrophages and enhanced contraction of pre-contracted rat aortic rings in a concentration-dependent manner (Vallance et al., 1992a,

Vallance et al., 1992b). Similarly, ADMA inhibited ACh-induced vasorelaxation in human renal arteries (Segarra et al., 2001) and abolished flow-induced vasodilation in skeletal muscle arterioles (Toth et al., 2007). These effects also translated to *in vivo* studies. Acute infusion (~ 5 min) of low-dose ADMA enhanced mean blood pressure and systemic vascular resistance in guinea pigs and rats, and in addition, reduced forearm blood flow in healthy subjects (Vallance et al., 1992a, Gardiner et al., 1993, Achan et al., 2003). Furthermore, longer term (14 days) ADMA infusion reduced plasma nitrite/nitrate levels, indicative of impaired NO production *in vivo*, and blunted vasorelaxation to ACh in rat aortic rings (De Gennaro Colonna et al., 2007). The protocols used in these *in vivo* animal and human studies are summarised in **Table 3.1.1**.

In summary, it is clear that ADMA i) is produced and released endogenously; ii) has the ability to modulate endothelial NO synthesis *ex vivo* and *in vivo*; iii) is strongly associated with a whole host of cardiovascular disease risk factor, like hypertension and ageing (**Table 1.3.1**); and iv) itself is an independent risk factor for cardiovascular morbidity and mortality. However, knowledge regarding the effects of ADMA on vasodilation in the microvasculature, such as mesenteric resistance arteries, is limited. Most cell and *ex vivo* studies either used synthetic NOS inhibitors, focused on the macrovasculature (e.g. aortic rings) or measured flow-mediated vasodilation in brachial arteries *in vivo*. Due to the importance of the microvasculature in regulating tissue perfusion and vascular resistance, it is imperative that we understand the effects of ADMA in different vascular beds, as this may help unravel the development of microvascular endothelial dysfunction. Using wire and pressure myography techniques, the current study investigated the functional impact of elevated ADMA, as observed in disease, on vasoconstriction and vasodilation in non-myogenically active mesenteric resistance arteries. In all experiments the NO-independent dilatory pathway in these arteries, EDH, was inhibited.

Table 3.1.1 Summary table of the *in vivo* studies mentioned in Chapter 3.1 that examined the effects of NOS inhibition by exogenous ADMA.

Studies	Species	Method	Dosage of ADMA (mg/kg)	Plasma [ADMA] (μM)	
				Before infusion	After infusion
Vallance et al. (1992a)	Guinea Pig	Infusion via jugular vein	1 – 30	~1.0	~9.8 (following 3 mg/kg)
Gardiner et al. (1993)	Rat	Bolus injection	1 – 100	3.0 – 4.0	1500 – 1800 (at 5 min) (Following 100 mg/kg)
Achan et al. (2003)	Human (healthy)	Intravenous injection	3	Not reported	2.6 ± 0.3 (30 min post-injection)
De Gennaro Colonna et al. (2007)	Rat	Osmotic minipump (14 days)	10	0.64 ± 0.04* (*Vehicle-treated)	1.25 ± 0.09

3.1.1 Aims and hypotheses

We hypothesised that ADMA would:

i) Increase vasoreactivity in isolated mesenteric arteries.

ii) Inhibit NO-dependent vasorelaxation and vasodilation to ACh in isolated mesenteric arteries during EDH blockade.

The aims of this chapter were to:

i) Characterise the effects of ADMA on the contractility to phenylephrine (PE) stimulation in isolated mesenteric arteries.

ii) Characterise the effects of EDH and ADMA on acetylcholine (ACh) vasorelaxation and vasodilation in isolated mesenteric arteries under isometric (wire myography) and isobaric (pressure myography) conditions during EDH blockade.

3.2 MATERIALS AND METHODS

3.2.1 Wire myography

Rat mesenteric resistance arteries were prepared for wire myography as described in **Chapters 2.1** and **2.2**. Arteries were normalised to a resting tension equivalent to that generated at 90% of the inner diameter of the vessel at 70 mmHg. Following equilibration, only arteries that exhibited robust and stable vasoconstriction to PE (absence of fade) and relaxed >95% to ACh (0.001 – 1 μM) were used for further experiments.

3.2.2 Pressure myography

Rat mesenteric resistance arteries were prepared for pressure myography as described in **Chapters 2.1** and **2.3**. Arteries were cannulated onto glass micropipettes and intra-luminally pressurised to 70 mmHg. Following equilibration, only arteries that displayed robust and stable vasoconstriction to PE and relaxed >95% to ACh (0.001 – 1 μM) were used for subsequent experiments.

3.2.3 Inhibitors

The following inhibitors were used to inhibit their respective targets: apamin (Ap; 100 nM) to inhibit SK_{Ca} channels, NS 6180 (NS; 1 μM) to inhibit IK_{Ca} channels, N^G,N^G-Dimethylarginine dihydrochloride (ADMA; 300 μM) to inhibit NOS, and inactive isomer N^G,$N^{G'}$-Dimethylarginine dihydrochloride (SDMA; 300 μM). See **Table 2.6.1** for more details.

3.3 RESULTS

3.3.1 ADMA enhances PE-induced vasoconstriction and attenuates NO-dependent vasorelaxation in mesenteric arteries under isometric tension

Representative traces of mesenteric arteries under isometric tension in the absence and during EDH and NOS inhibition are shown in **Figure 3.3.1A**. Mesenteric arteries were pre-constricted with sub-maximal concentrations of PE (0.3 – 5 μM). Inhibition of EDH with SK_{Ca} and IK_{Ca} channel inhibitors, apamin (Ap, 100 nM) and NS 6180 (NS, 1 μM) respectively, had no effect on vasoreactivity to PE (Log[PE]: Control: -5.60 ± 0.07 M; Ap, NS: -5.79 ± 0.09 M; $P > 0.05$ compared to Control; n =10 – 13; **Figure 3.3.1B**). Inhibition of NOS with ADMA (300 μM) during EDH inhibition lowered the concentration of PE used by ~3.72 fold (Log[PE]: Ap, NS, ADMA: -6.17 ± 0.06 M; n = 13; $P < 0.0001$ compared to Control, $P < 0.05$ compared to Ap, NS; **Figure 3.3.1B**) to evoke vasoconstriction of a similar magnitude to control (Tension: Control: 6.76 ± 0.27 mN/mm; Ap, NS: 5.93 ± 0.37 mN/mm; Ap, NS, ADMA: 6.60 ± 0.29 mN/mm; $P > 0.05$; n = 10 – 13; **Figure 3.3.1C**).

Cumulative ACh concentration-response curves were conducted in PE pre-constricted mesenteric arteries under isometric tension. ACh (0.001 – 1 μM) caused a concentration-dependent vasorelaxation (**Figure 3.3.2**). EDH blockade with apamin and NS 6180 attenuated the maximum of vasorelaxation (E_{max}) evoked by ACh compared to Control (Control: 99.8 ± 0.3%; Ap, NS: 95.4 ± 1.1%; n = 10; $P < 0.01$; Representative tension traces in **Figure 3.3.2A, C – D**). Unexpectedly, the further addition of ADMA did not abolish ACh-induced vasorelaxation, but only further attenuated the E_{max} evoked by ACh, with 70.4 ± 6.2% of vasorelaxation persisting during inhibition of both EDH and NOS (n = 10; $P < 0.01$ compared to Control and Ap, NS; **Figure 3.3.2B, C – D**).

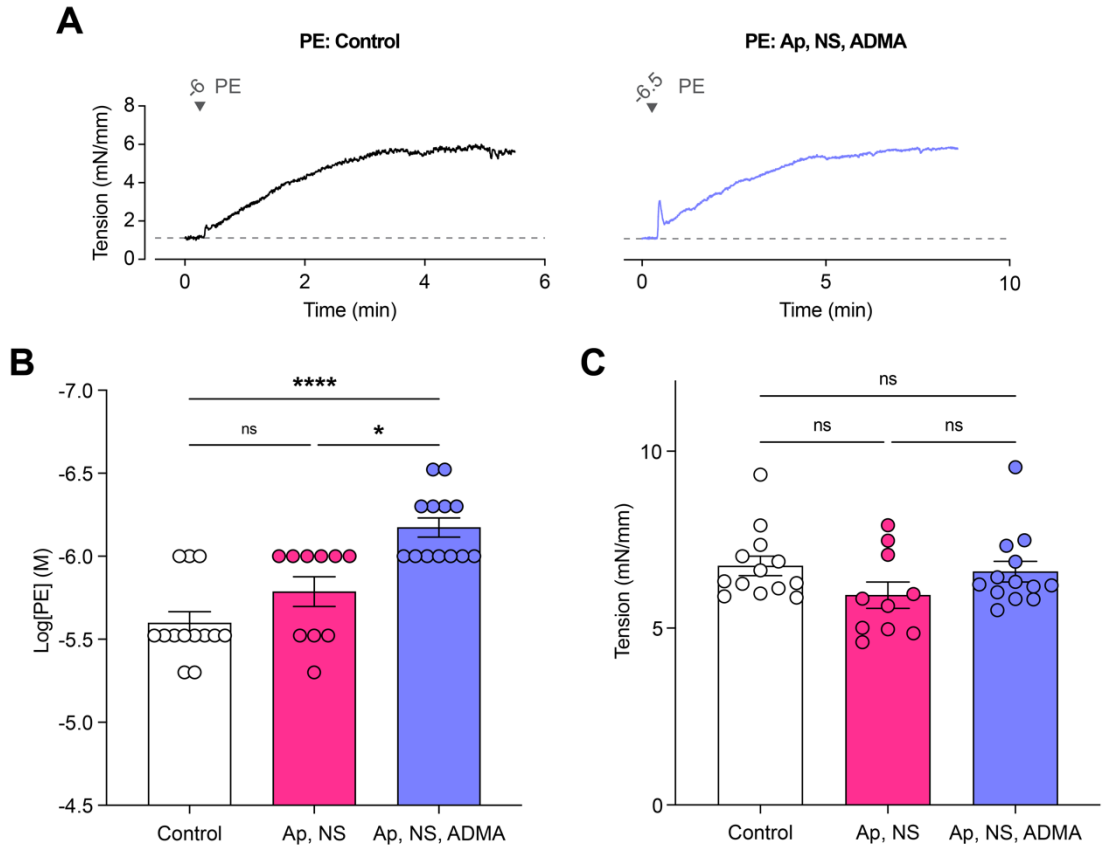


Figure 3.3.1 Asymmetric dimethylarginine (ADMA) markedly increases vasoconstriction to α_1-adrenoreceptor agonist, phenylephrine (PE) in mesenteric arteries. A, Representative tension traces for vasoconstriction to PE before (Control; Left panel) and after apamin (Ap; 100 nM), NS 6180 (NS; 1 μM), and ADMA (300 μM; Ap, NS, ADMA; Right panel). Dashed lines indicate baseline tension. **B – C,** Bar graphs summarising the concentrations of PE used to evoke vasoconstriction, expressed as Log[PE] in M (**B**) and PE-induced vasoconstriction expressed as tension in mN/mm (**C**) before and after Ap, NS ± ADMA. Data are means ± SEM; n = 10 – 13. ****$P < 0.0001$ compared to Control, *$P < 0.05$ compared to Ap, NS using Kruskal-Wallis test with Dunn's multiple comparisons test.

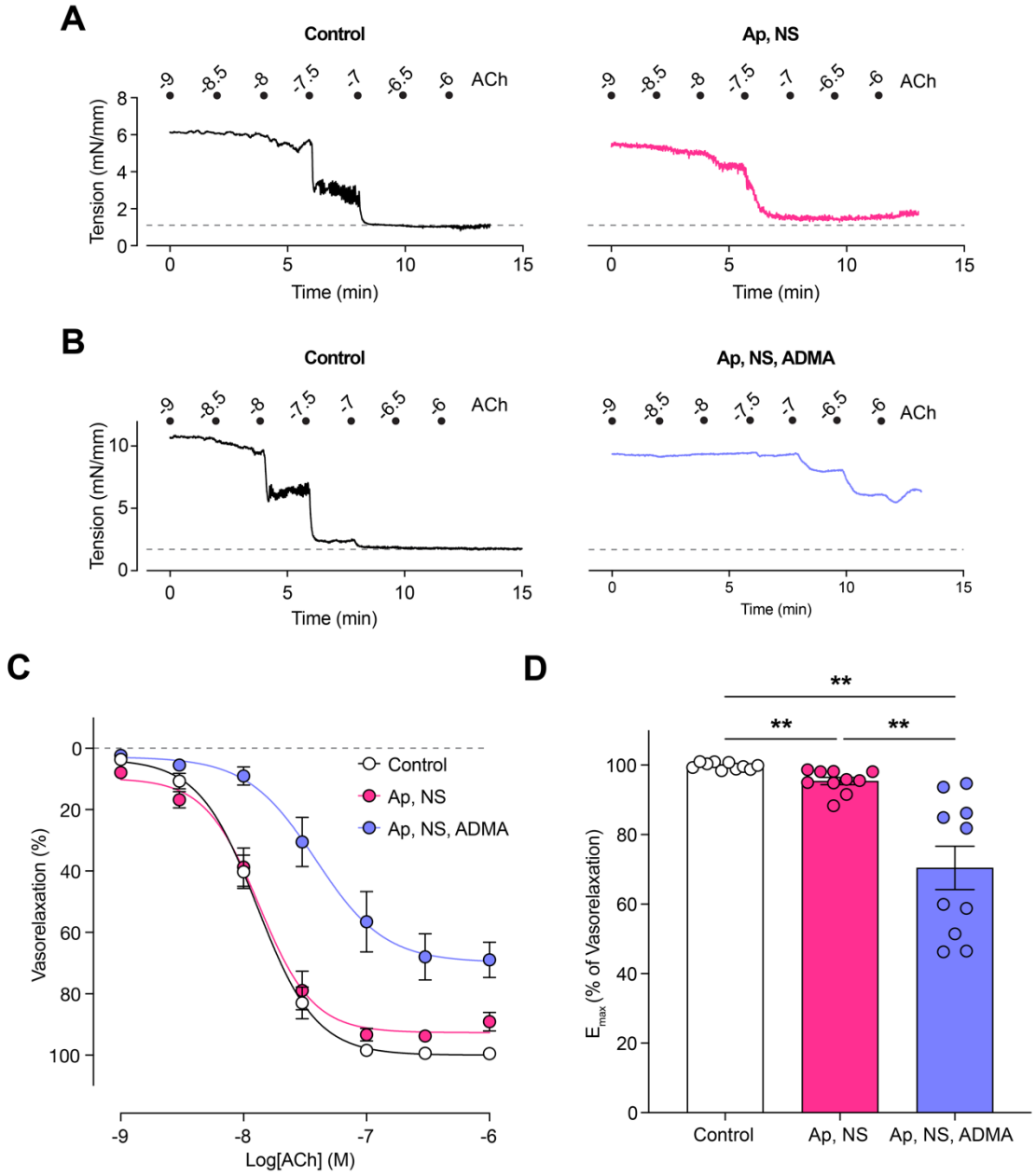


Figure 3.3.2 Endothelium-dependent vasorelaxation to acetylcholine (ACh) persists in the presence of asymmetric dimethylarginine (ADMA) during the block of endothelium-dependent hyperpolarization (EDH) in mesenteric arteries under isometric tension. A – B, Representative tension traces for vasorelaxation to cumulative ACh in phenylephrine (α_1-adrenoreceptor agonist) pre-constricted mesenteric arteries in the absence (Control) and presence of apamin (Ap; 100 nM) and NS 6180 (NS; 1 µM; **A**), and ADMA (300 µM; **B**). Dashed lines indicate baseline tension. **C,** ACh concentration-response curves summarising vasorelaxation in Ap, NS ± ADMA-treated arteries. **D,** Bar graph summarising E_{max} elicited by ACh in (**C**). Data are means ± SEM; n = 10. $^{**}P < 0.01$ compared to Control and Ap, NS using one-way ANOVA with Tukey's multiple comparisons test.

3.3.2 SDMA has no effects on vasoconstriction and vasorelaxation in mesenteric arteries under isometric tension

To confirm the effects on vasoconstriction and vasorelaxation observed were due to ADMA, ADMA was substituted with an inactive isomer, SDMA, which has no direct inhibitory effects on NOS (Vallance et al., 1992a). The presence of SDMA (300 μM) did not affect PE-induced vasoconstriction (Log[PE]: Control: -5.76 ± 0.11 M; Ap, NS: -5.86 ± 0.16 M; Ap, NS, SDMA: -5.86 ± 0.16 M; n = 6; $P > 0.05$; **Figure 3.3.3**).

Cumulative ACh concentration-response curves were conducted in PE pre-constricted mesenteric arteries under isometric tension. Similar to the previous experiments, EDH blockade with apamin and NS 6180 attenuated E_{max} evoked by ACh compared to Control (Control: 99.8 ± 0.3%; Ap, NS: 98.2 ± 0.1%; n = 6; $P < 0.01$; **Figure 3.3.4A, C – D**). However, the addition of SDMA (300 μM) during EDH blockade did not augment the inhibition on ACh-induced vasorelaxation (E_{max}; Ap, NS, SDMA: 97.5 ± 0.5%; n =6; $P > 0.05$ compared to Ap, NS; $P < 0.01$ compared to Control; Representative tension traces in **Figure 3.3.4B, C – D**).

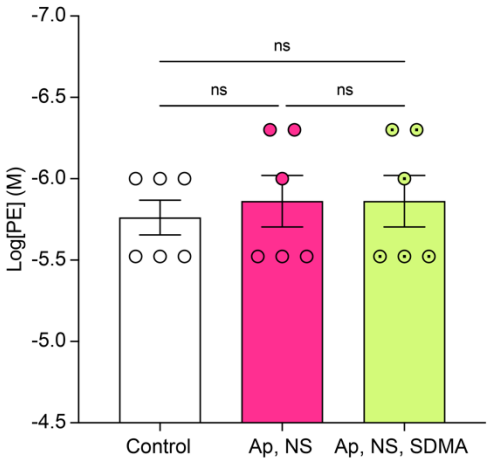


Figure 3.3.3 Symmetric dimethylarginine (SDMA) has no effects on vasoconstriction to the α_1-adrenoreceptor agonist phenylephrine (PE) in mesenteric arteries. Bar graph summarising the concentrations of PE, expressed as Log[PE] in (M), used to evoke vasoconstriction in mesenteric arteries before (Control) and after treatment with endothelium-dependent hyperpolarization blockers, apamin (Ap; 100 nM) and NS 6180 (NS; 1 μM), and inactive isomer SDMA (300 μM). Data are means ± SEM; n = 6. Using Kruskal-Wallis test with Dunn's multiple comparisons test.

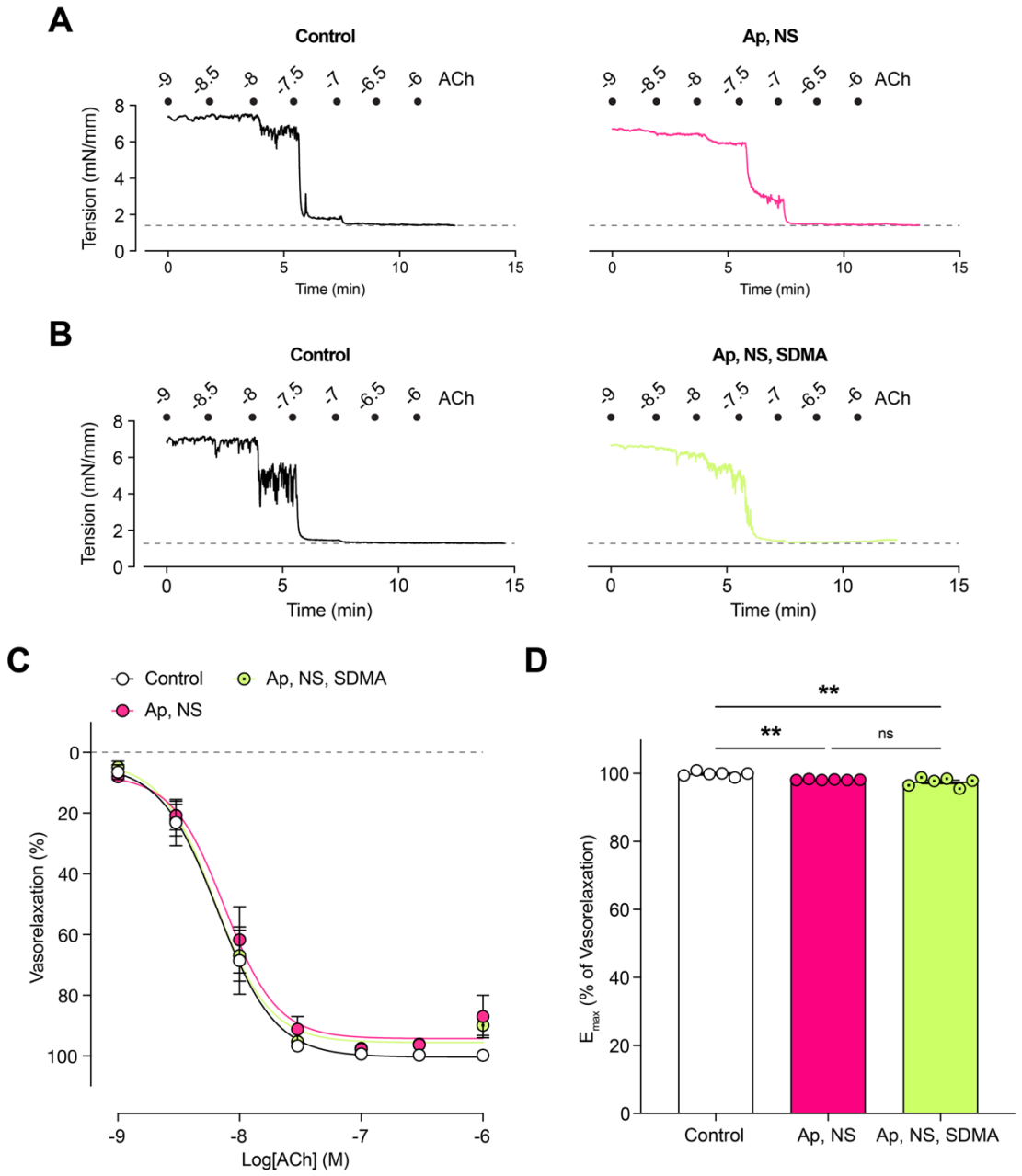


Figure 3.3.4 Symmetric dimethylarginine (SDMA) has no effects on endothelium-dependent vasorelaxation to acetylcholine (ACh) in mesenteric arteries during endothelium-dependent hyperpolarization (EDH) blockade. A – B, Representative tension traces for vasorelaxation to cumulative ACh in phenylephrine pre-constricted mesenteric arteries in the absence (Control) and presence of apamin (Ap; 100 nM) and NS 6180 (NS; 1 µM; **A**), and SDMA (300 µM; **B**) under isometric tension. Dashed lines indicate baseline tension. **C,** ACh concentration-response curves summarising vasorelaxation in Ap, NS ± SDMA-treated arteries. **D,** Bar graph summarising E_{max} elicited by ACh in (**C**). Data are means ± SEM; n = 10. $^{**}P < 0.01$ compared to Control and Ap, NS using one-way ANOVA with Tukey's multiple comparisons.

3.3.3 ADMA attenuates NO-dependent vasodilation in pressurised mesenteric arteries

Cumulative ACh (0.001 – 1 μM) concentration-response curves were also conducted in isolated mesenteric arteries cannulated on to micropipettes and pressurised in a pressure myograph. Mesenteric arteries were pre-constricted with sub-maximal concentrations of PE (0.3 – 1μM). EDH blockade, with apamin and NS 6180, had no effect on ACh-induced vasodilation (E_{max}; Control: 100 ± 0.0%; Ap, NS: 98.0 ± 3.0%; $P > 0.05$; n = 6 – 7; **Figure 3.3.5A left and middle panels, B – C**). Similar to arteries under isometric tension, the presence of ADMA (300 μM) during EDH blockade did not abolish but attenuated ACh-induced vasodilation in pressurised mesenteric arteries (E_{max}; 51.7 ± 8.7%; n = 6 – 7; $P < 0.01$ compared to Control and Ap, NS; **Figure 3.3.5**).

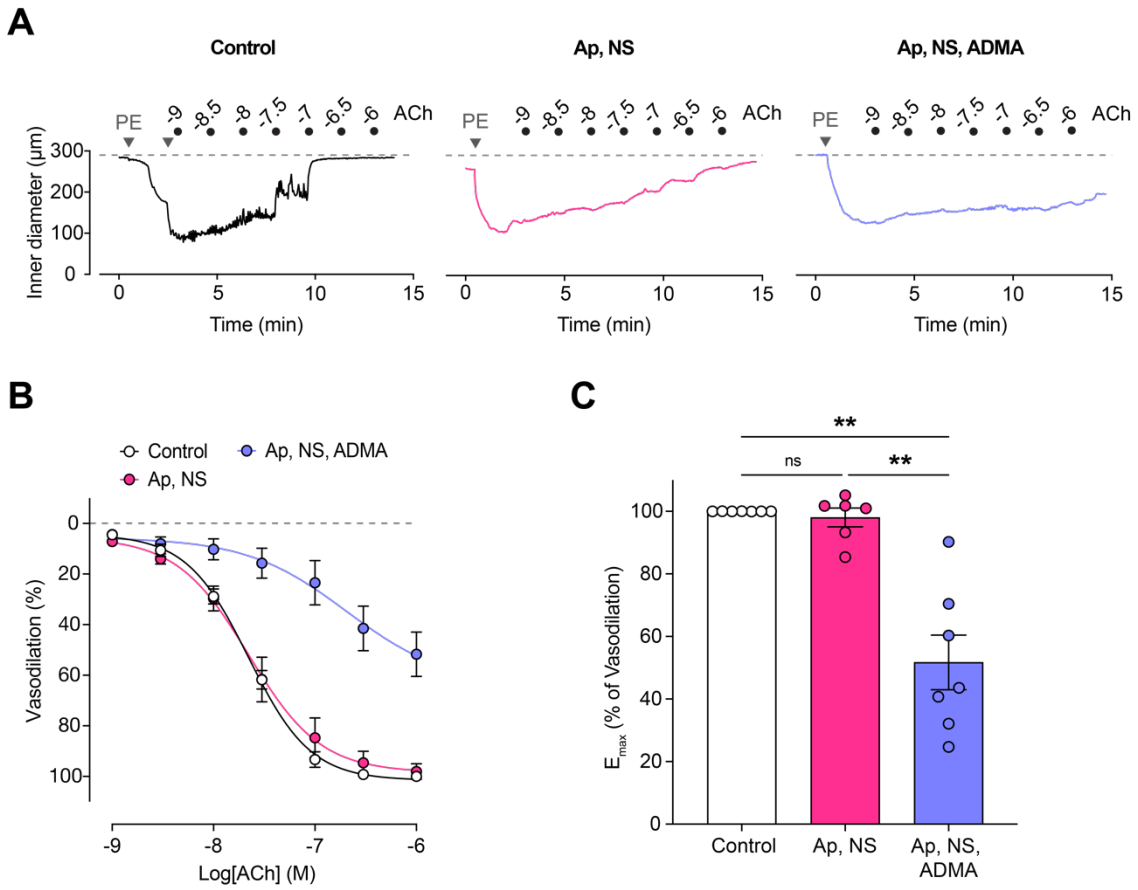


Figure 3.3.5 Endothelium-dependent vasodilation to acetylcholine (ACh) persists in the presence of asymmetric dimethylarginine (ADMA) during endothelium-dependent hyperpolarization (EDH) blockade in pressurised mesenteric arteries. A, Representative diameter traces for vasodilation to cumulative [ACh] before (Left panel) and after incubation with apamin (Ap; 100 nM), NS 6180 (NS; 1 µM) – EDH blockade (Middle panel), and the addition of ADMA (300 µM; Right panel) in phenylephrine (α_1-adrenoreceptor agonist; PE) pre-constricted pressurised mesenteric arteries. Dashed lines indicate passive inner diameter. **B,** Concentration-response curves summarising ACh-vasodilation in Ap, NS ± ADMA-treated pressurised mesenteric arteries. **C,** Bar graph summarising the E_{max} elicited by ACh in (**B**). Data are means ± SEM; n = 6 – 7. $^{**}P < 0.01$ compared to Control and Ap, NS using mixed-effects analysis with Tukey's multiple comparisons test.

3.4 DISCUSSION

This chapter aimed to characterise the effects of NOS inhibition by the endogenous dimethylarginine, ADMA, on vasoreactivity in isolated rat mesenteric arteries mounted under both isometric and isobaric conditions. The data presented here supports the hypothesis that ADMA increases vasoreactivity but only partially supports the hypothesis that ADMA inhibits NO-mediated vasodilation to ACh in the mesenteric vascular bed.

The present study examined the effects of 300 μM ADMA on vascular reactivity in mesenteric resistance arteries. This concentration of ADMA was chosen as it was previously reported to abolish NO synthesis, augment vasoconstriction in pre-constricted arteries and inhibit NO-dependent vasorelaxation/-dilation to vasodilators, such as ACh, in various vascular beds (Vallance et al., 1992a, Feng et al., 1998, Stankevicius et al., 2011, Rodriguez-Rodriguez et al., 2008). Furthermore, we examined the effects of the recently developed IK_{Ca} channel specific blocker, NS 6180, in the vasculature. Similar to the widely used IK_{Ca} channel blocker, TRAM 34, NS 6180 blocks channel activity by gaining access to the channel pore and binding to threonine 250 and valine 275 (Strobaek et al., 2013). In various cell models, NS 6180 (IC_{50}: ~13 nM) exhibited similar efficacy in inhibiting Ca^{2+}-activated K^+ conductance as TRAM 34 (IC_{50}: ~17 nM) (Strobaek et al., 2013).

Firstly, the dense innervation of tyrosine hydroxylase containing sympathetic nerves strongly supports an important role for VSM α-adrenergic receptors in regulating mesenteric vascular tone (Lin et al., 2023). Phenylephrine (PE), a selective α_1-adrenergic receptor agonist, was used to evoke vascular tone in our experiments. It was previously reported that SK_{Ca} channels, involved in EDH vasorelaxation, may regulate agonist-induced vasoconstriction. The inhibition by apamin or conditional knockout by doxycycline enhanced PE-induced tone of

mesenteric arteries in SK_{Ca} overexpression mouse model (Taylor et al., 2003). However, in the current study using wild type rats, simultaneous inhibition of SK_{Ca} and IK_{Ca} channels with apamin and NS 6180 respectively had no significant effects on PE-induced tone. In contrast, the additional block of NO synthesis with ADMA augmented vasoconstriction and sensitivity to PE, so that a lower concentration of PE was needed to elicit vasoconstriction of a similar magnitude in the absence of NOS inhibition. Unsurprisingly, this observation was absent when ADMA was substituted with the inactive endogenous isomer, SDMA.

The increased vascular reactivity to vasoconstrictors in the presence of ADMA is comparable to the effects reported in various vascular beds during inhibition of NO synthesis. The addition of endogenous methylarginine, L-NMMA, and synthetic L-arginine analogues, such as N-iminoethyl-L-ornithine (L-NIO) and L-NAME, at concentration used in this study enhanced vasoconstriction in rat and rabbit aortic rings (Rees et al., 1990, Rees et al., 1989, Adeagbo and Triggle, 1993). Similarly, incubation with L-N^G-nitro arginine (L-NNA), at similar concentrations, increased agonist-induced vasoconstriction in rabbit aortic segments (Moore et al., 1990) and in rabbit femoral arteries (Mulsch and Busse, 1990). Importantly, this effect is endothelium dependent as this augmentation in tone to vasoconstrictors was absent in denuded arteries, where the endothelium was removed (Adeagbo and Triggle, 1993, Rees et al., 1989).

Interestingly, the role of EDH appears to increase in the resistance arteries, including third-order mesenteric arteries studied here. It has been shown that block of K_{Ca} channels with apamin and TRAM 34 can increase vasoreactivity to PE (Smith et al., 2020). The findings in the current study support that: i) NO is involved in the regulation of PE-induced vasoconstriction and EDH plays a minimal role, and ii) elevated ADMA levels, as observed in

many cardiovascular diseases, enhance vasoreactivity (vasospasm) in mesenteric resistance arteries by inhibiting NO synthesis, contributing to microvascular dysfunction.

Moreover, using the synthetic NOS inhibitor, L-NAME, our group has shown this increase in vasoreactivity to PE during NOS inhibition is due to augmented electrical excitability in VSM, alongside reduced endothelium-dependent feedback responses. Upon PE stimulation, the increased electrical excitability enables previously quiescent VSM cells to generate Ca^{2+}-based depolarising spikes by recruiting T-type voltage-dependent Ca^{2+} channels (T-type VDCCs), leading to Ca^{2+} influx and vasoconstriction (Smith et al., 2020), ultimately resulting in vasospasm. In separate experiments from our group, 300 μM ADMA was able to increase VSM electrical excitability in mesenteric arteries (Ng et al., 2024), comparable to our previous observations with L-NAME. Therefore, the data presented here support the biological importance of ADMA in the modulation of vascular tone to vasoconstrictors.

Secondly, vasorelaxation in small resistance arteries is governed by concomitant NO release and hyperpolarization from the endothelium. Acetylcholine caused a concentration-dependent vasodilation in arteries via endothelial M_3 muscarinic receptors. As this study was interested in exploring the effects of NOS inhibition by ADMA, ADMA was added following EDH inhibition. Blocking SK_{Ca} and IK_{Ca} channels (EDH) with apamin and NS 6180 respectively caused a small reduction in ACh-induced vasorelaxation in mesenteric arteries under isometric tension.

The involvement of K^+ in EDH of rat resistance arteries was highlighted when the L-NNA-resistant vasorelaxation was prevented by the presence of high K^+ (Nagao et al., 1992). Subsequent studies with simultaneous microelectrode and tension recordings in rat mesenteric

arteries confirmed the importance of K^+ in EDH. The presence of high K^+ abolished agonist-induced hyperpolarization and prevented L-NAME resistant, EDH, vasorelaxation (Waldron and Garland, 1994b), thereby abolishing vasorelaxation to ACh. Similarly, high K^+ and the NO scavenger, haemoglobin, each attenuated ACh-induced vasorelaxation, but when combined, produced a greater inhibition on vasorelaxation in mesenteric arteries (Hwa et al., 1994). Later studies using various K^+ channels blockers have underpinned the importance of both SK_{Ca} and IK_{Ca} channels in EDH parallel to NO-dependent vasorelaxation/-dilation (Waldron and Garland, 1994a, Edwards et al., 1998). For example, the combination of apamin and the widely used IK_{Ca}-selective blockers, TRAM 34 or TRAM 39, during NOS inhibition prevented both vasorelaxation and hyperpolarization induced by ACh in rat mesenteric resistance arteries (Crane et al., 2003, Hinton and Langton, 2003, Xavier et al., 2014).

The effects of EDH blockade alone are limited as most studies investigated the contribution of EDH in vasorelaxation/-dilation following NO inhibition. Moreover, this is the first study to our knowledge that examined the functional effects of NS 6180 in the vasculature (Ng et al., 2024). The attenuation in vasorelaxation to ACh in the presence of apamin and either NS 6180 or TRAM 34 (**Figure 6.3.2**), at 1 μM, was comparable in this study, and support the notion that two blockers have similar potencies. Furthermore, the findings presented here are similar to the previous studies in rat mesenteric arteries with EDH block alone (Waldron and Garland, 1994b, Xavier et al., 2014).

The addition of ADMA during EDH block further suppressed vasodilation, with ~50% residual vasodilation remaining. Similar to the synthetic NOS inhibitors, ADMA is an analogue of L-arginine and competitively binds to NOS to inhibit NO synthesis, preventing NO-dependent vasodilation. Unlike its synthetic counterpart (see previous references), ADMA during EDH

block did not abolish vasodilation to ACh. We hypothesised that this could be due to differences in the entry into cells and/or endogenous modulation on the actions of ADMA. Whilst the former may explain this variation, the transport of L-NAME and ADMA into cells was not investigated in this thesis and warrants further investigation. Given their structural similarities to L-arginine, one could hypothesise that L-arginine analogues would utilise the same cation amino acid transporter (CAT) system to enter cells. Zharikov and Block (1998) reported that L-NAME exhibited weak inhibition (~12%) on L-arginine uptake compared to L-NMMA which almost abolished L-arginine transport into cells. In addition, the ester group in L-NAME creates a more lipophilic molecule which may aid passive diffusion through the cell membrane. Therefore, these findings may suggest an alternative route of entry for L-NAME that may explain the observed differences in this study using ADMA compared to the literature.

Subsequent studies overexpressing the human CAT-1 transporter investigated the uptake mechanism of ADMA and interaction with L-arginine entry. Strobel et al. (2012) confirmed the ability of ADMA and L-arginine to compete for CAT-1, with a higher affinity and transport capacity for ADMA. Similar observations were made in endothelial cells where intracellular ADMA concentration increased despite higher levels of extracellular L-arginine compared to ADMA, at a ratio of 10:1, demonstrating that ADMA has a higher affinity for endothelial cell entry compared to L-arginine (Cardounel et al., 2007). Therefore, in scenarios with elevated ADMA levels, such as cardiovascular diseases and in this study, ADMA can indirectly (by competing with L-arginine for entry) and directly (by competing with L-arginine for NOS binding) impact NO production. The L-arginine and intracellular ADMA concentrations, and CAT expressions were not measured in the present study, these should be further investigated as they may explain and correlate to the inhibitory effects observed.

Furthermore, unlike L-NAME, ADMA is subjected to metabolism by dimethylarginine dimethylaminohydrolase (DDAH). Therefore, once inside the cells, methylarginines, such as ADMA, are actively broken down into L-citrulline and dimethylamine (MacAllister et al., 1994). It is estimated that 80% and 90% of ADMA in humans and rats respectively are metabolised by this pathway (Achan et al., 2003). Therefore, DDAH acts as an endogenous mechanism that limits the accumulation of ADMA and inhibition of NOS at physiological condition. This further differentiates the inhibitory responses in the presence of ADMA and synthetic NOS inhibitors. The modulation of ADMA by DDAH is further investigated in **Chapter 5**.

These observations of ADMA in small resistance arteries are significant as they support the literature demonstrating that endogenous methylarginines are not as effects as synthetic NOS inhibitors. Interestingly, the plasma ADMA concentration is 10-fold higher than that reported for L-NMMA (Vallance et al., 1992a), and is raised in numerous cardiovascular diseases. Thus, although this suggests ADMA should be more relevant biologically compared to other endogenous methylarginines, there are likely to be other mechanisms involved that would contribute to this observed difference.

3.5 CONCLUSION

This chapter aimed to investigate the effects of NOS inhibition by endogenous dimethylarginine, ADMA, on vessel reactivity in isolated mesenteric resistance arteries using wire and pressure myography. The findings (**Figure 3.5.1**) support our hypotheses that ADMA increases vascular reactivity to vasoconstrictors, such as PE, and partially support the hypothesis that ADMA reduces NO-dependent vasodilation in response to the endothelial cell dependent vasodilator, ACh. In contrast to reports using synthetic NOS inhibitors, ADMA was unable to abolish vasodilation during EDH blockade with apamin and NS 6180 in mesenteric resistance arteries. We hypothesised this is due to i) differences in ADMA transport into cells, and ii) the modulatory action of ADMA by DDAH. The latter will be explored further in subsequent chapter (**Chapter 5**).

The observations made here offer valuable preliminary insights into the mechanisms by which elevated ADMA levels, as observed in numerous cardiovascular diseases, can cause vascular dysfunction (vasospasm and reduced vasodilatory capacity).

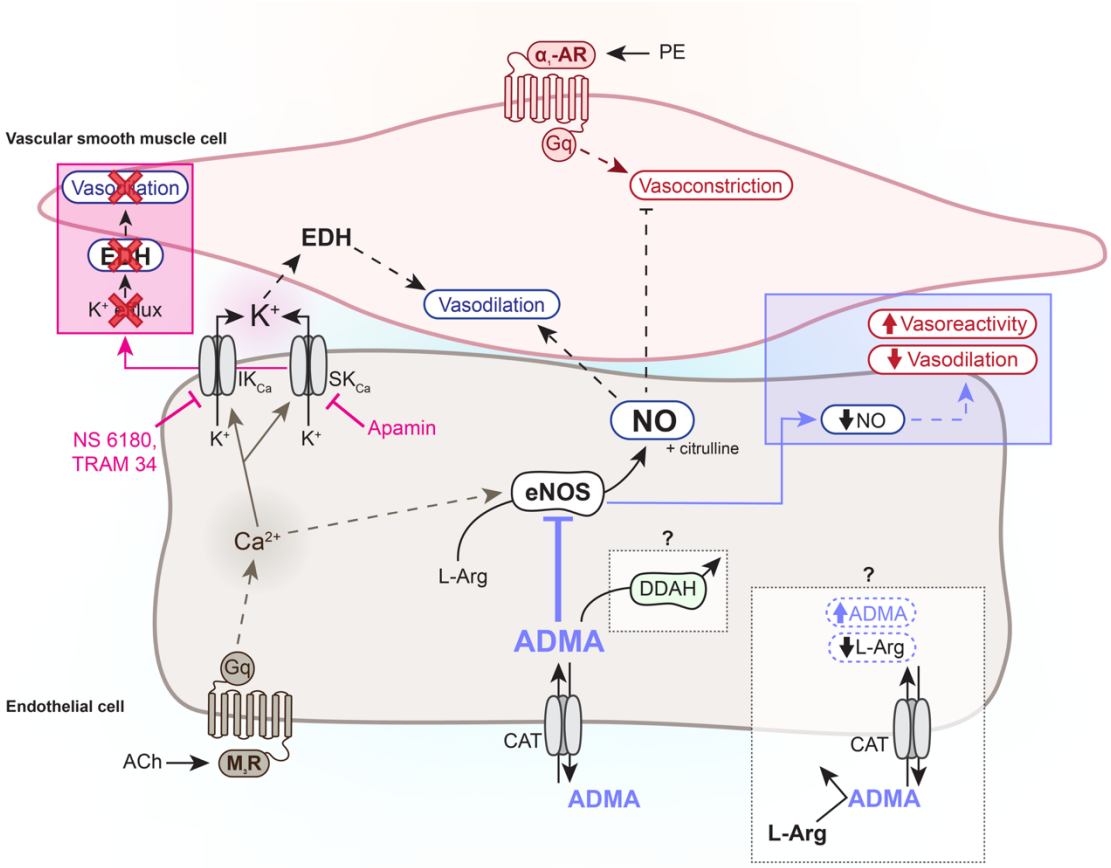


Figure 3.5.1 Summary of Chapter 3 – Endogenous nitric oxide synthase inhibitor, asymmetric dimethylarginine (ADMA), increases vasoreactivity of rat mesenteric resistance arteries. During endothelium-dependent hyperpolarization (EDH) inhibition with blockers of the small conductance (SK_{Ca}) and intermediate conductance (IK_{Ca}) Ca^{2+}-activated K^+ channels, apamin and either NS 6180 or TRAM 34 respectively, ADMA modulates vasoconstriction to vasoconstrictors such as the selective α_1-adrenergic receptor (α1-AR) agonist, phenylephrine (PE). Furthermore, ADMA attenuates NO-dependent vasodilation to the M_3 muscarinic receptor (M_3R) agonist, acetylcholine (ACh) by inhibiting endothelial nitric oxide synthase (eNOS). Unlike synthetic NOS inhibitors, residual vasodilation to ACh remains in the presence of ADMA, and we hypothesise (dotted boxes with question mark) this could be due to the: i) transport of ADMA into endothelial cell, as ADMA competes with L-arginine (L-Arg) for cationic amino acid transporter (CAT) system for cell entry, and ii) endogenous metabolism of ADMA by dimethylarginine dimethylaminohydrolase (DDAH). Dashed arrows represent simplified signalling pathways. Overall effects of ADMA (purple box) and apamin + NS 6180 (pink box).

CHAPTER FOUR

CHARACTERISING THE EFFECTS OF ADMA AND ENDOTHELIUM-DEPENDENT HYPERPOLARIZATION INHIBITION IN THE CORONARY MICROVASCULATURE

4.1 INTRODUCTION

In the heart, the coronary microcirculation (resistance arteries and arterioles) plays a crucial role in regulating vascular resistance and perfusion in order to match blood flow to metabolic demands. To accomplish this, coronary resistance arteries are highly adaptive and can finetune vascular tone according to intrinsic and extrinsic stimuli through numerous means, such as myogenic-dependent and endothelial-dependent mechanisms. As mentioned in **Chapter 1.2.2**, the myogenic response is defined as the inherent pressure-sensitive vasoconstriction or vasodilation in response to increases or decreases in intraluminal pressure respectively in resistance arteries. In the coronary microvasculature, the myogenic response is crucial in the generation of basal coronary vascular tone at a given pressure (myogenic tone). This myogenic tone creates a background tone by which vasoactive agents (constrictors and dilators) can act on. Therefore, disruptions to coronary myogenic tone and vasodilatory responses would predispose vascular dysfunction and cardiovascular diseases.

As aforementioned, the plasma levels of the endogenous NOS inhibitor ADMA are elevated in numerous cardiovascular disease risk factors and itself is an independent predictor of cardiovascular morbidity and mortality (**Table 1.3.1**). Focusing on the coronary microvasculature, ADMA has been linked to various types of anginas, such as microvascular angina, previously known as cardiac syndrome X, characterised by angina-like chest pains with near-to or normal coronary angiography. In these patients, the increase in coronary blood flow following intracoronary ACh infusion was reduced compared to controls, signifying endothelial dysfunction in microvascular angina (Egashira et al., 1993). Under physiological conditions, ACh released from parasympathetic nervous system predominantly acts on endothelial M_3 muscarinic receptors outweighing the contribution from vascular smooth muscle, resulting in endothelium-dependent vasodilation (Furchgott and Zawadzki, 1980).

However, in disease such as microvascular angina and hypertension (Treasure et al., 1992, Ong et al., 2012) and in experimental models of endothelial dysfunction (Furchgott and Zawadzki, 1980), ACh vasodilation is reduced and often evokes vasoconstriction as vascular smooth muscle overcomes the lack of endothelium-dependent vasodilatory input due to endothelial dysfunction. Therefore, intracoronary infusion of ACh has been routinely used when assessing coronary vascular function/vasospasm (Shimokawa et al., 2021) and has established itself as the gold-standard method for diagnosing microvascular angina due to its high sensitive and specificity (Kugiyama et al., 1996, Beltrame et al., 2016).

Supplementation of the precursor of NO, L-arginine, augmented coronary flow in response to ACh infusion in patients, suggesting that disrupted NO synthesis is involved in the blunted vasodilatory response of ACh observed in microvascular angina (Egashira et al., 1996, Lerman et al., 1998). Additionally, recent studies in patients with microvascular angina revealed elevated plasma levels of ADMA compared to controls and ADMA has been shown to be a strong predictor of morbidity and mortality in these patients (Chen et al., 2002, Lu et al., 2017). This indicates that ADMA, or at least disruptions to NO production, are the underlying pathophysiology in these patients.

Furthermore, in the absence of other obstructive coronary diseases, elevated plasma ADMA concentrations have also been observed in other coronary dysfunction, such as slow coronary flow syndrome and vasospastic angina. Patients with slow coronary blood flow exhibited higher plasma ADMA levels and reduced L-arginine/ADMA ratio (Selcuk et al., 2007). Similarly, plasma ADMA levels were raised in vasospastic angina, which associated with increase coronary tone, reduced NO levels, and lowered the concentration of vasoconstrictor

needed to provoke vasoconstriction/vasospasm (Hori et al., 2003). Therefore, these findings strongly implicate the involvement of NOS inhibition and ADMA in coronary vasospasm.

Despite the strong association of ADMA in non-obstructive coronary artery diseases, studies investigating the direct effects of ADMA in the coronary microcirculation are limited. The current literature mainly examined the functional impact of ADMA on myogenic responses in cerebral resistance arteries. Topical application of ADMA constricted basilar artery and cerebral arterioles from rodents and rabbits, attenuated ACh-induced vasodilation and blocked NO production in brain slices (Faraci et al., 1995). In human cerebral arteries mounted under isometric tension, the addition of ADMA caused concentration-dependent vasoconstriction and an attenuation in ACh vasorelaxation *ex vivo* (Segarra et al., 1999), and reduced cerebral blood flow in healthy subjects (Kielstein et al., 2006).

As mentioned in **Chapter 1.2**, in addition to NO, EDH plays a crucial role in vasodilation in the microvasculature. Despite this, limited studies have investigated the contribution of SK_{Ca} and IK_{Ca} channels in EDH vasodilation in the coronary microcirculation, particularly in the intra-septal coronary arteries. Therefore, due to the importance of the coronary microvasculature in regulating coronary perfusion, the strong indication for the involvement of ADMA in non-obstructive coronary artery diseases and cerebral microvasculature, and the limited data in EDH vasodilation in the coronary microcirculation. This chapter investigated the functional impact of endothelial dysfunction (elevated ADMA levels and EDH inhibition) on myogenic tone and ACh vasodilation in myogenically active intra-septal coronary arteries using wire and pressure myography techniques.

4.1.1 Aims and hypotheses

We hypothesised that:

i) ADMA would increase myogenic tone in active intra-septal coronary arteries.

ii) Similar to the observations made in mesenteric arteries (**Chapter 3**), ADMA would attenuate NO-dependent vasodilation to ACh in intra-septal coronary arteries.

iii) Both SK_{Ca} and IK_{Ca} channels would be involved in EDH in rat intra-septal coronary arteries.

The aims of this chapter were to:

i) Characterise the effects of ADMA on myogenic tone in isolated intra-septal coronary arteries under isometric (wire myograph) and isobaric (pressure myograph) conditions in the absence and presence of EDH blockade.

ii) Characterise the effects of ADMA on vasorelaxation (wire myograph) and vasodilation (pressure myograph) in isolated coronary arteries in the absence and presence of EDH blockade.

iii) Assess the involvement of SK_{Ca} and IK_{Ca} channels in EDH in the coronary microcirculation in the presence of ADMA.

4.2 MATERIALS AND METHODS

4.2.1 Wire myography

Rat intra-septal coronary arteries were prepared for wire myography as described in **Chapters 2.1** and **2.2**. Arteries were normalised to a resting tension equivalent to that generated at 90% of the inner diameter of the vessel at 80 mmHg. Following equilibration, coronary arteries were left to develop myogenic tone. Only arteries that developed stable myogenic tone and relaxed >95% to ACh (0.001 – 1 μM) were used for further experiments.

4.2.2 Pressure myography

Rat intra-septal coronary arteries were prepared for pressure myography as described in **Chapters 2.1** and **2.3**. Arteries were cannulated and secured on to glass micropipettes using nylon sutures, and intra-luminally pressurised to 80 mmHg. Following equilibration, coronary arteries were left to develop myogenic tone. Only arteries with stable myogenic tone and relaxed >95% to ACh (0.001 – 1μM) were used for subsequent experiments.

4.2.3 Inhibitors

The following inhibitors were used to inhibit their respective targets: apamin (Ap; 100 nM) to inhibit SK_{Ca} channels, NS 6180 (NS; 1 μM) to inhibit IK_{Ca} channels, and N^G,N^G-Dimethylarginine dihydrochloride (ADMA; 300 μM) and synthetic NOS inhibitor, N_ω-Nitro-L-arginine methyl ester hydrochloride (L-NAME; 100 μM) to inhibit NOS. See **Table 2.6.1** for more details.

4.3 RESULTS

4.3.1 ADMA augments myogenic tone in intra-septal coronary arteries

Intra-septal coronary arteries were mounted in either a wire myograph or pressure myograph to examine the effects of ADMA and EDH blockade on myogenic tone (MT) in intra-septal coronary arteries.

Under isometric tension, intra-septal coronary arteries spontaneously developed myogenic tone, increase in tension (No MT: 0.77 ± 0.10 mN/mm; Control: 2.05 ± 0.34 mN/mm; n = 7; $P < 0.05$; **Figure 4.3.1A left panel, and B**). The addition of 300 μM ADMA or 100 μM L-NAME markedly increased myogenic tone (ADMA: 3.29 ± 0.27 mN/mm; n = 7; $P < 0.01$ compared to Control; L-NAME: 3.17 ± 0.18 mN/mm; n = 7; $P < 0.05$ compared to Control; **Figure 4.3.1A middle and right panels, and B**). Furthermore, ADMA (300 μM) produced a comparable increase in myogenic tone to that of L-NAME (100 μM; $P = 0.8417$).

In separate experiments under isometric tension, the involvement of IK_{Ca} and SK_{Ca} channels (EDH pathway) in the modulation of myogenic tone was assessed during NOS blockade by ADMA (300 μM). To separate the possible contribution of IK_{Ca} and SK_{Ca} channels in myogenic tone regulation, the inhibitor for each channel: NS 6180 (1 μM) and apamin (100 nM) respectively, were added alone and in combination. Intra-septal coronary arteries spontaneously developed myogenic tone, which was augmented in the presence of ADMA (No MT: 0.83 ± 0.07 mN/mm; Control: 2.40 ± 0.33 mN/mm; ADMA: 4.54 ± 0.41 mN/mm; n = 12; $P < 0.001$ compared to Control; **Figure 4.3.2A left and middle panels, and B**). The addition of apamin, NS 6180 or in combination did not further increase myogenic tone (+ Ap: 4.97 ± 0.67 mN/mm; + NS: 4.16 ± 0.32 mN/mm; + Ap, NS: 4.33 ± 0.44 mN/mm; n = 5 – 7; $P > 0.05$ compared to ADMA; **Figure 4.3.2A right panel, and B**).

In coronary arteries pressurised at 80 mmHg, arteries developed myogenic tone (38.7 ± 2.0%; n = 12; **Figure 4.3.3A left panel, and B**). The addition of ADMA increased myogenic tone, expressed as maximum vasoconstriction (59.1 ± 2.4%; n = 12; $P < 0.0001$; **Figure 4.3.3A right panel, and B**).

In separate experiments, EDH blockade, with apamin and NS 6180, in addition to NOS inhibition with either ADMA or L-NAME did not further augment myogenic tone in pressurised intra-septal coronary arteries (Ap, NS, ADMA: 54.02 ± 4.97%; Ap, NS, L-NAME: 53.4 ± 4.6%; n = 6; $P > 0.9999$ compared to ADMA in **Figure 4.3.3**; **Figure 4.3.4**). Simultaneous inhibition of EDH and NOS, with either ADMA or L-NAME, increased myogenic tone compared to paired Control (Control: 38.3 ± 4.2%; $P < 0.001$ compared to Ap, NS ADMA and Ap, NS, L-NAME; **Figure 4.3.4**). Moreover, the endogenous inhibitor, ADMA, produced a comparable increase in myogenic tone to the synthetic inhibitor L-NAME ($P = 0.6982$; **Figure 4.3.4A middle and right panels, and B**).

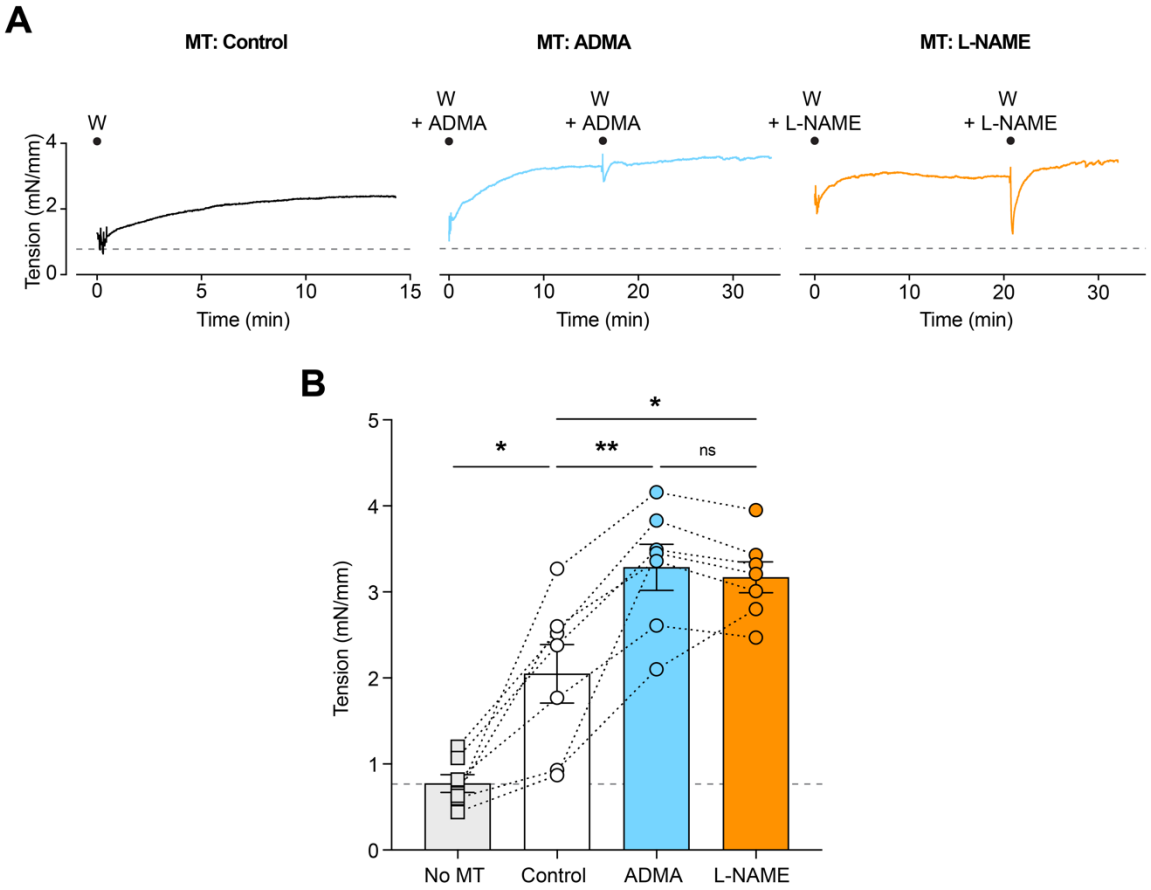


Figure 4.3.1 Asymmetric dimethylarginine (ADMA) increases myogenic tone, comparable to the synthetic nitric oxide synthase inhibitor L-NAME, in intra-septal coronary arteries under isometric tension. A, Representative tension traces of the myogenic tone (MT) in Control (Left panel), and in the presence of ADMA (300 µM; Middle panel) or L-NAME (100 µM; Right panel) of the same artery under isometric tension. W indicates wash. Dashed lines indicate the baseline tension. **B,** Bar graph summarising the tension before (no MT) and after the development of MT (Control) and in the presence of ADMA or L-NAME. Myogenic tone expressed as tension (mN/mm). Dashed line indicates mean baseline tension. Data are means ± SEM; n = 7. **P* < 0.05 and ***P* < 0.01 using one-way ANOVA with Tukey's multiple comparisons test.

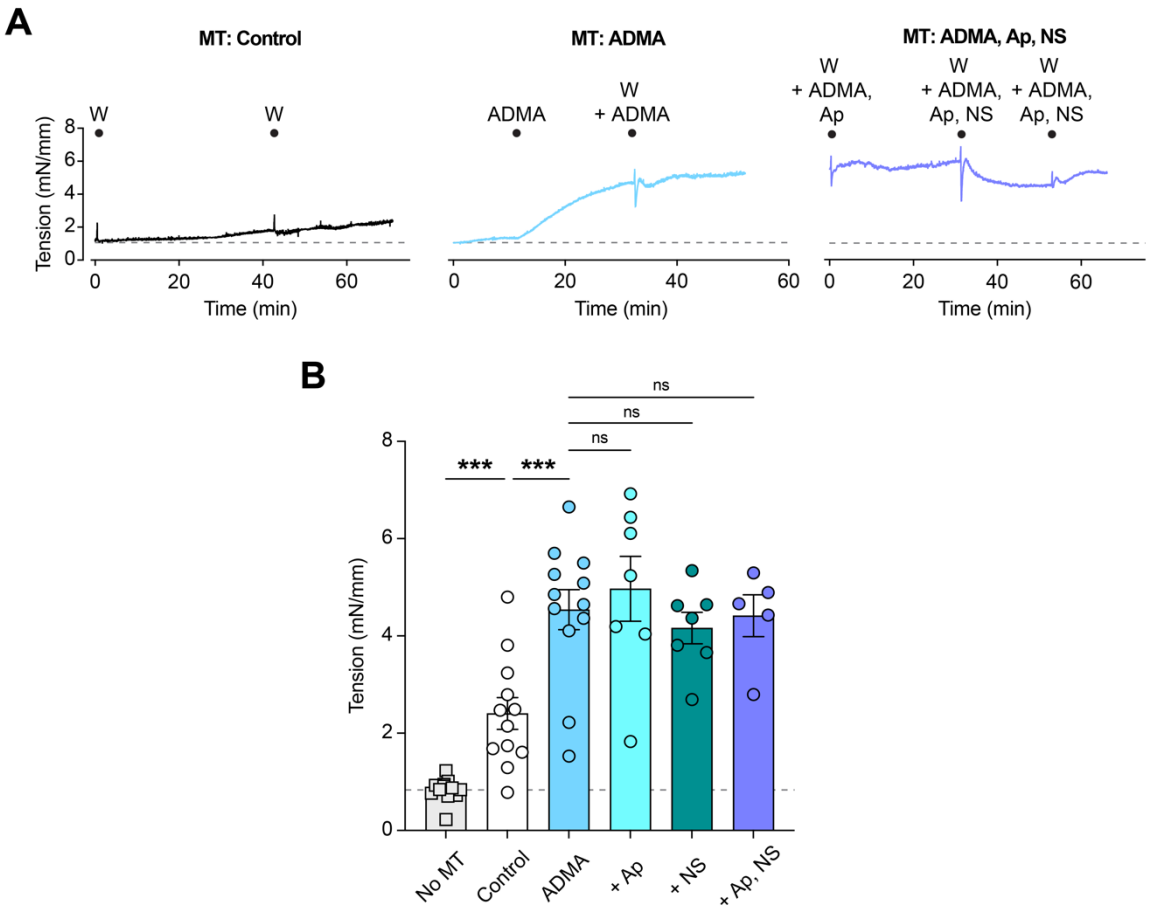


Figure 4.3.2 Endothelium-dependent hyperpolarization (EDH) is not involved in the modulation of myogenic tone in intra-septal coronary arteries. A, Representative tension traces for myogenic tone in Control (Left panel), in the presence of asymmetrical dimethylarginine (ADMA; 300 µM; Middle panel), and with the addition of apamin (Ap; 100 nM) and NS 6180 (NS; 1 µM; Right panel) in the same artery under isometric tension. W indicates wash. Dashed lines indicate the baseline tension. **B,** Bar graph summarising the tension before (no MT) and after the development of MT (Control) and in the presence of ADMA ± Ap ± NS. Myogenic tone expressed as tension (mN/mm). Dashed line indicates mean baseline tension. Data are means ± SEM; n = 5 – 12. ***$P < 0.001$ using mixed-effects analysis with Tukey's multiple comparisons test compared to Control, and mixed effects analysis with Dunnett's multiple comparisons test compared to ADMA.

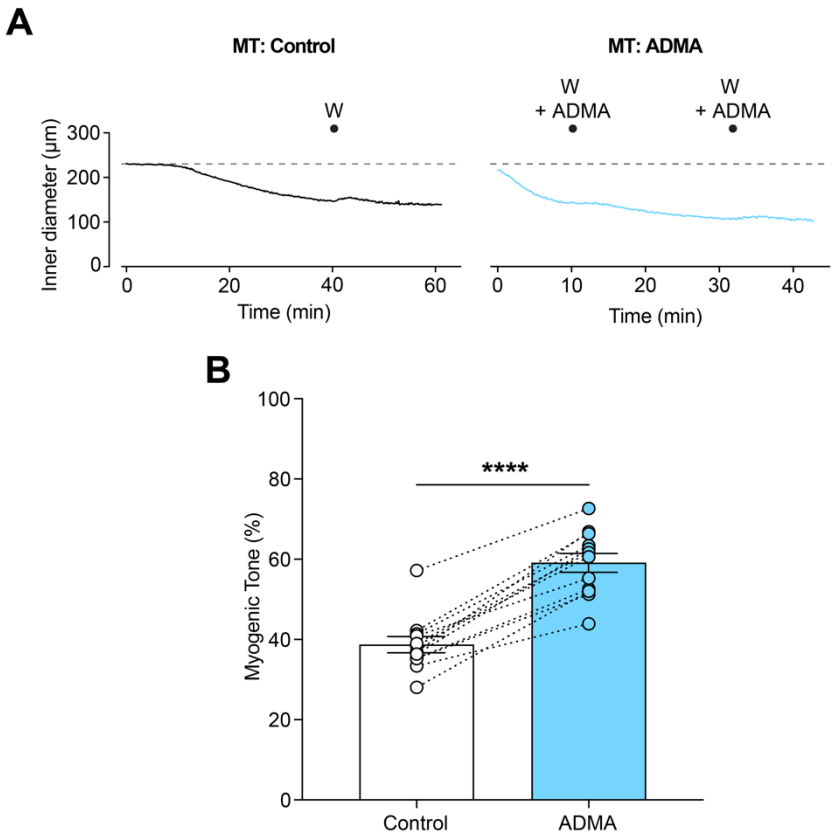


Figure 4.3.3 Asymmetric dimethylarginine (ADMA) increases myogenic tone in pressurised intra-septal coronary arteries. A, Representative diameter traces of the development of myogenic tone (MT) in Control (Left panel) and in the presence of ADMA (300 µM; Right panel) of the same pressurised artery. Wash is indicated by W. Dashed line indicates passive inner diameter. **B,** Bar graph summarising the percentage of myogenic tone in pressurised arteries before (Control) and after the addition of ADMA. Data are means ± SEM; n = 12. ****$P < 0.0001$ compared to Control using paired two-tailed t-test.

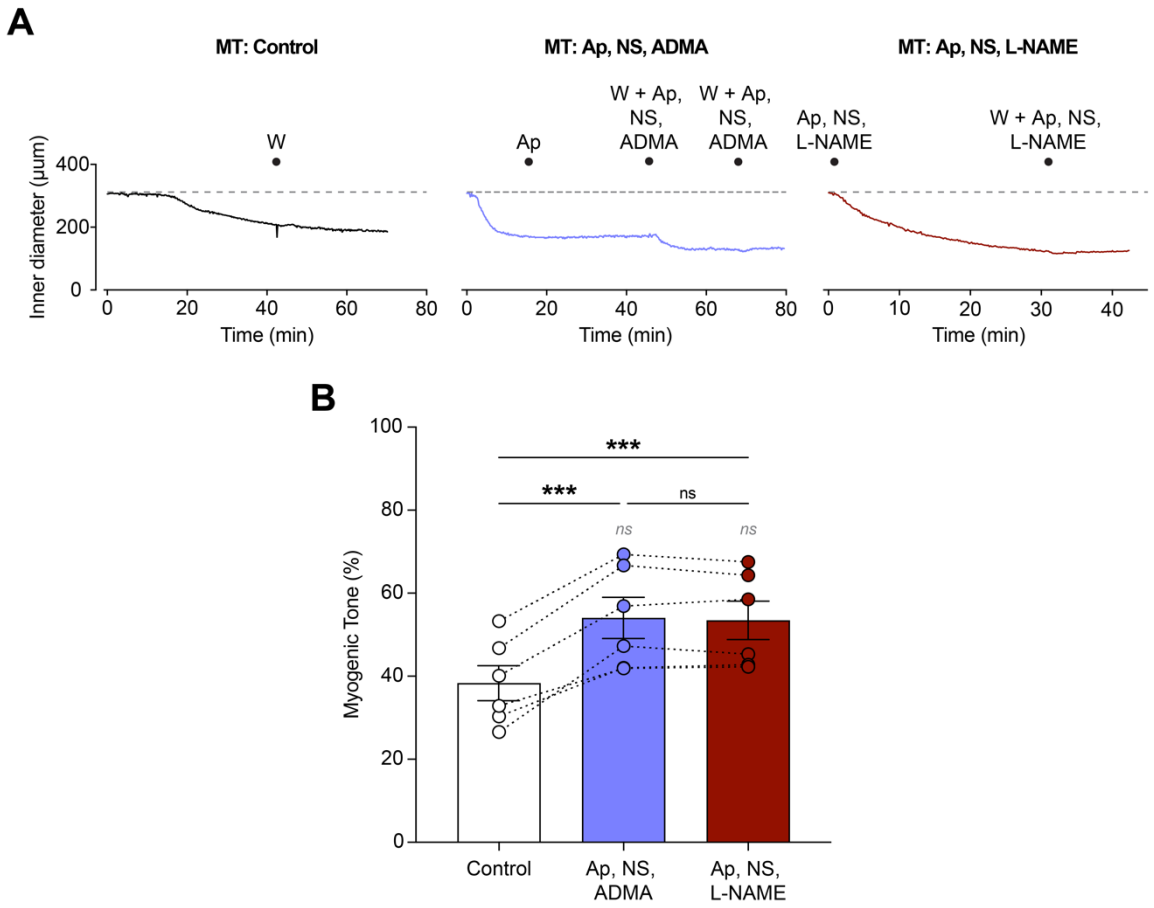


Figure 4.3.4 Endothelium-dependent hyperpolarization (EDH) blockade does not affect myogenic tone in pressurised intra-septal coronary arteries. A, Representative diameter traces of the development of myogenic tone (MT) in a pressurised artery in Control (Left panel) and in the presence of apamin (Ap; 100 nM), NS 6180 (NS; 1 µM) and asymmetric dimethylarginine ADMA (300 µM; Middle panel) or L-NAME (100 µM; Right panel). Dashed lines indicate passive inner diameter. W indicates wash. **B,** Bar graph summarising the percentage of myogenic tone in pressurised arteries before (Control) and after the addition of Ap, NS and ADMA or L-NAME. Data are means ± SEM; n = 6. ***$P < 0.001$ compared to Control using one-way ANOVA with Tukey's multiple comparisons test. *ns* compared to ADMA alone (n = 6 – 12, **Figure 4.3.3**) using mixed-effects analysis with Tukey's multiple comparisons test.

4.3.2 Inhibition of nitric oxide synthase and IK_{Ca} channels abolishes vasorelaxation to acetylcholine in intra-septal coronary arteries

To examine the contribution of NO and EDH in ACh-induced vasorelaxation in intra-septal coronary arteries, arteries were mounted in a wire myograph. Cumulative ACh concentration-responsive curves were constructed from myogenic tone before and during NOS and/or EDH blockade, by a combination of ADMA, apamin and NS 6180 treatments. Furthermore, to delineate the contribution of SK_{Ca} and IK_{Ca} channel in EDH vasorelaxation during NOS inhibition, apamin (SK_{Ca} channel inhibitor) and NS 6180 (IK_{Ca} channel inhibitor) was added either separately or combined in the presence of ADMA.

ACh caused a concentration-dependent vasorelaxation (**Figure 4.3.5A and B left panels, and C**). The addition of ADMA (300 μM) significantly attenuated vasorelaxation induced by ACh (E_{max}; Control: 100 ± 0.03%; ADMA: 36.6 ± 7.8%; n = 12; $P < 0.0001$ compared to Control; **Figure 4.3.5A and B middle panels, C and D**). The addition of IK_{Ca} channel inhibitor NS 6180 (NS; 1 μM) with ADMA completely abolished ACh-induced vasorelaxation, where the addition of cumulative ACh caused further vasoconstriction (E_{max}; ADMA, NS: -11.8 ± 1.7%; n = 7, $P < 0.01$ compared to ADMA alone; **Figure 4.3.5A right panel, C and D**). In contrast, vasorelaxation to cumulative ACh persisted in the presence of SK_{Ca} channel blocker, apamin (Ap; 100 nM) with ADMA (E_{max} ADMA, Ap: 42.5 ± 13.0%; n = 7; $P = 0.4803$ compared to ADMA alone; **Figure 4.3.5B right panel, C and D**). The magnitude of the inhibitory effects on ACh-induced vasorelaxation was similar between arteries incubated with ADMA and NS 6180 (ADMA, NS) and the combined blockade of NOS, SK_{Ca} and IK_{Ca} channels (E_{max}; ADMA, Ap, NS: -10.7 ± 3.3%; n = 5, $P > 0.9999$; **Figure 4.3.5C and D**).

Moreover, comparable inhibitory effects on vasorelaxation to cumulative ACh was observed when ADMA (300 μM) was substituted with L-NAME (100 μM) in the presence of NS 6180 and/or apamin (**Figure 4.3.5C and D**). Combined treatment of L-NAME and NS 6180 completely prevented vasorelaxation to ACh (E_{max}: L-NAME, NS: -10.6 ± 1.9%; n = 6; P = 0.9996 compared to ADMA, NS). Whereas ACh-induced vasorelaxation persisted in the presence of L-NAME with apamin (E_{max}; L-NAME, Ap: 35.3 ± 13.8%; n = 7; P = 0.9025 compared to ADMA, Ap). The combination L-NAME, apamin and NS 6180 did not further inhibit vasorelaxation (E_{max}; L-NAME, Ap, NS: -12.1 ± 1.5%; n = 7; P = 0.6263 compared to L-NAME, NS) and was comparable to the presence of ADMA (P = 0.9994 compared to ADMA, Ap, NS).

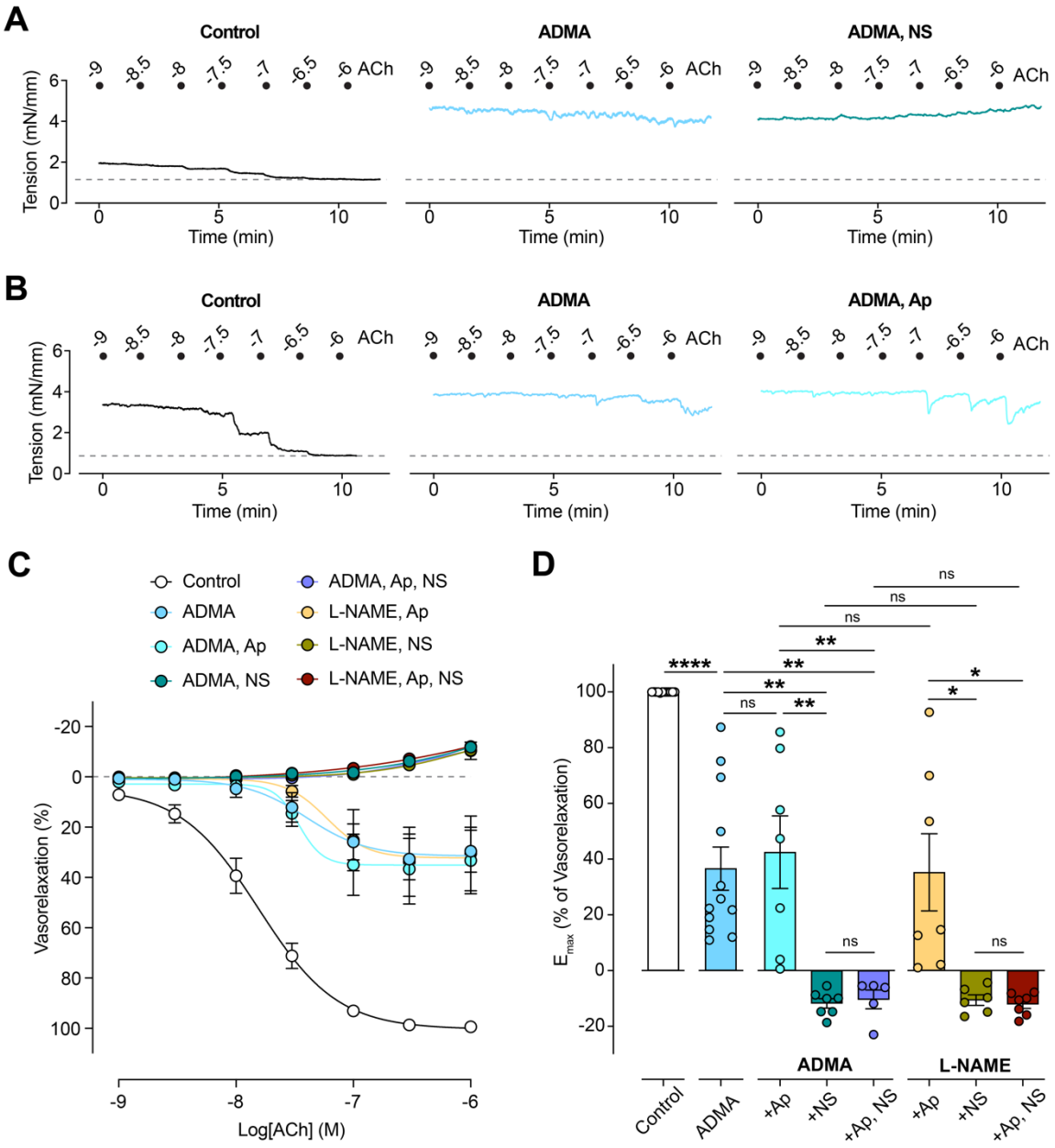


Figure 4.3.5 Nitric oxide synthase and IK_{Ca} blockade abolishes acetylcholine (ACh) vasorelaxation in intra-septal coronary arteries. A – B, Representative tension traces of ACh vasorelaxation before and after asymmetric dimethylarginine (ADMA; 300 µM) with SK_{Ca} blocker NS 6180 (NS; 1 µM; **A**) or SK_{Ca} blocker apamin (Ap; 100 nM; **B**). Dashed lines indicate baseline tension. **C,** ACh concentration-response curves for vasorelaxation before and after ADMA or L-NAME (100 µM) ± NS ± Ap. **D,** Bar graph summarising E_{max} elicited by ACh in (**C**). Data are means ± SEM; n = 5 – 12. **P* < 0.05, ***P* < 0.01, *****P* < 0.0001 using mixed-effects analysis with Dunnett's (ADMA versus Control) or Tukey's multiple comparisons tests (within ADMA and L-NAME groups) or one-way ANOVA with Sidak's multiple comparisons test (ADMA versus L-NAME groups).

4.3.3 ADMA abolishes nitric oxide-dependent vasodilation to acetylcholine in pressurised intra-septal coronary arteries

Cumulative ACh concentration-response curves were constructed in isolated coronary arteries cannulated on to glass micropipettes and intra-luminally pressurised to 80 mmHg. Concentration-response curves were conducted from myogenic tone before (Control) and after incubation with ADMA (300 μM; **Figure 4.3.6A**). ACh caused a concentration-dependent vasorelaxation which was attenuated by the addition of ADMA (E_{max}; Control: 100 ± 0.4%; ADMA: 59.3 ± 7.7%; n = 12; $P < 0.001$; **Figure 4.3.6B and C**).

In separate experiments, vasodilation to cumulative ACh was assessed in the presence of combined inhibition of EDH, with apamin (Ap; 100 nM) and NS 6180 (NS; 1 μM), and NOS with either ADMA (300 μM) or L-NAME (100 μM). The addition of apamin and NS 6180 (Ap, NS, ADMA; **Figure 4.3.7A middle panel, B and C**) further attenuated vasodilation to cumulative ACh compared to ADMA alone (**Figure 4.3.6**), almost abolished vasodilation (E_{max}; Control: 99.9 ± 0.1%; Ap, NS ADMA: 10.6 ± 3.5%; n = 7; $P < 0.0001$ compared to Control; **Figure 4.3.7A middle panel, B and C**; $P < 0.001$ compared to ADMA alone; **Figure 4.3.6**). Similarly, the presence of L-NAME with apamin and NS 6180 completely abolished ACh vasodilation (E_{max}; Ap, NS, L-NAME: -6.56 ± 3.40%; n = 6; $P < 0.0001$ compared to Control; **Figure 4.3.7A right panel, B and C**; $P < 0.0001$ compared to ADMA alone; **Figure 4.3.6**). Moreover, ADMA and L-NAME produced comparable inhibitory effects on ACh-induced vasodilation during EDH blockade ($P > 0.05$), similar to the wire myography data (**Figure 4.3.5**).

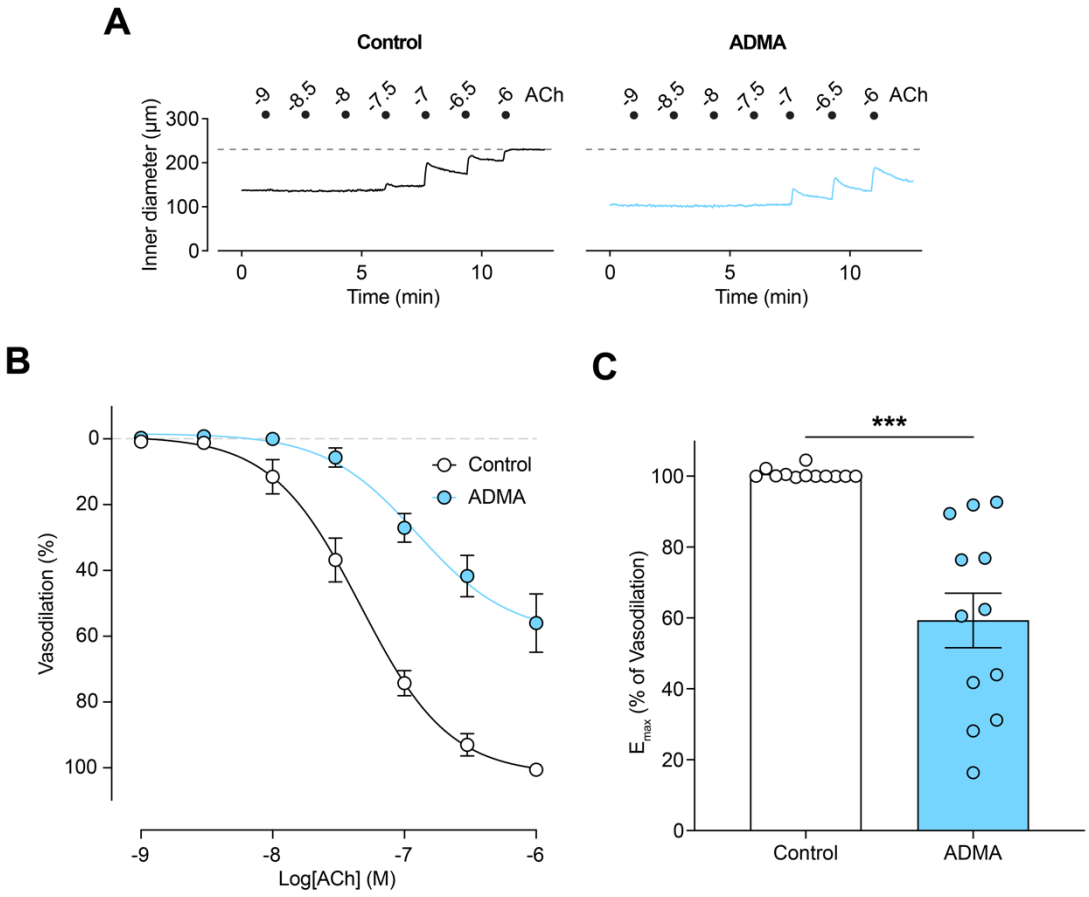


Figure 4.3.6 Asymmetric dimethylarginine (ADMA) attenuates vasodilation to acetylcholine (ACh) in pressurised intra-septal coronary arteries by inhibiting nitric oxide production. **A,** Representative diameter traces of vasodilation to cumulative ACh before (Control; Left panel) and after incubation with ADMA (300 µM; Right panel) in pressurised arteries. Dashed lines indicate passive inner diameter. **B,** ACh concentration-response curves summarising vasodilation before (Control) and after ADMA incubation. **C,** Bar graph summarising E_{max} elicited by ACh in (**B**). Data are means ± SEM; n = 12. ***$P < 0.001$ compared to Control using paired two-tailed t-test.

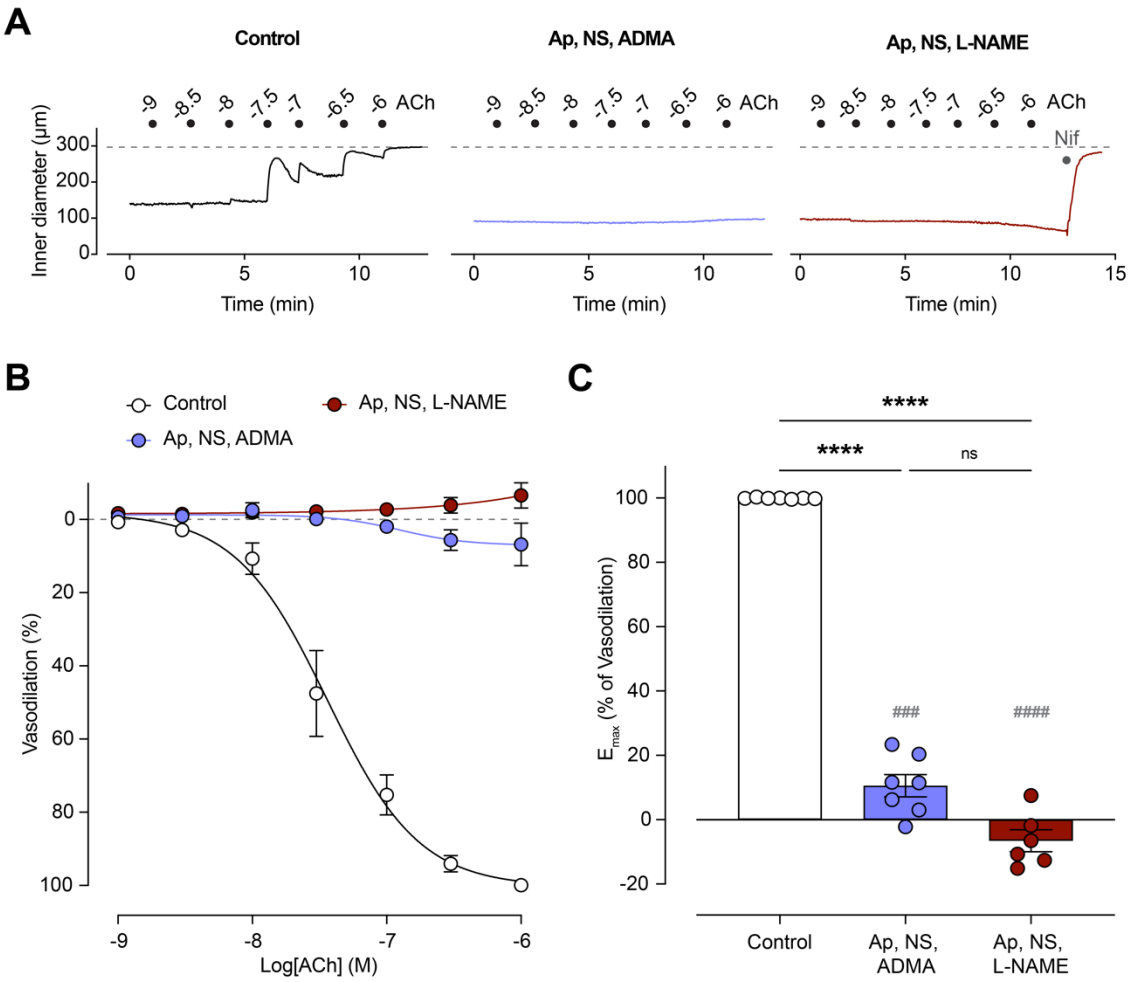


Figure 4.3.7 Nitric oxide synthase and endothelium-dependent hyperpolarization (EDH) blockade prevents vasodilation in pressurised intra-septal coronary arteries. A, Representative diameter traces of vasodilation to cumulative acetylcholine (ACh) before (Control, Left panel) and after incubation with apamin (Ap; 100 nM), NS 6180 (NS; 1 µM) and asymmetric dimethylarginine (ADMA; 300 µM; Middle panel) and Ap, NS and L-NAME (100 µM; Right panel) in pressurised arteries. Nifedipine (Nif; 1µM). Dashed lines indicate passive inner diameter. **B,** ACh concentration-response curves summarising vasodilation before (Control) and after Ap, NS ± ADMA or L-NAME incubation. **C,** Bar graph summarising E_{max} elicited by ACh in (**B**). Data are means ± SEM; n = 6 – 7. $^{****}P < 0.0001$ compared to Control using mixed-effects analysis with Tukey's multiple comparison test. $^{###}P < 0.001$ and $^{####}P < 0.0001$ versus ADMA alone (**Figure 4.3.6**) using mixed-effects analysis with Tukey's multiple comparison test.

4.4 DISCUSSION

This chapter aimed to characterise the functional effects of NOS inhibition, by the endogenous dimethylarginine, ADMA, and the block of SK_{Ca} and IK_{Ca} channels (EDH) on vasoreactivity in myogenically active rat intra-septal coronary arteries mounted under both isometric and isobaric conditions. The findings in this study support the hypothesis that ADMA increases myogenic tone of intra-septal coronary arteries and partially support the hypothesis that ADMA attenuates vasorelaxation/-dilation to ACh. However, the data here do not support the hypothesis that both SK_{Ca} and IK_{Ca} channels are involved in EDH in intra-septal coronary arteries.

The present study examined and compared the effects of NOS inhibition by ADMA (300 μM) to the widely used synthetic NOS inhibitor, L-NAME on myogenic tone and vasorelaxation/-dilation in isolated intra-septal coronary arteries. This concentration of ADMA was selected as previous studies in myogenically active cerebral arteries and arterioles reported that 300 μM ADMA enhanced myogenic tone *ex vivo* and *in vivo* (Faraci et al., 1995, Segarra et al., 1999). Furthermore, it allows for direct comparisons of the inhibitory effects of ADMA between the mesenteric and coronary microvasculature in this thesis. When mounted under both isometric and isobaric conditions, intra-septal coronary arteries developed spontaneous contraction (myogenic tone). This observation is similar to those made by Nyborg and Mikkelsen in the wire myograph, where they reported the importance of extracellular Ca^{2+} in maintaining basal tone in coronary arteries as the removal of extracellular Ca^{2+} or the addition of L-type VDCC blocker, nifedipine, abolished myogenic contraction (Nyborg and Mikkelsen, 1987). Myogenic tone was significantly increased following incubation with ADMA (300 μM). This is the first report to our knowledge that specifically studied the *ex vivo* effects of ADMA on myogenic tone in the coronary microvasculature (Ng et al., 2024). Subsequent inhibition of IK_{Ca} or SK_{Ca}

channel, by NS 6180 or apamin respectively, and in combination, did not further potentiate myogenic tone in intra-septal coronary arteries. Furthermore, the augmentation in myogenic tone induced by ADMA was comparable to L-NAME in this study, suggesting the contribution of basal NO release, but not EDH, in modulating myogenic tone in the coronary microvasculature.

As aforementioned, the involvement of NO in the regulation of the myogenic response and vascular reactivity can vary between vascular beds and with vessel diameter. Focusing on the coronary circulation, the findings presented here support the evidence that NO plays an imperative role in myogenic responses. Chemical inhibition (with L-NAME at the concentration used in this study) or mechanical disruptions on NO production (endothelium removal) evoked contraction or increased myogenic tone in rat septal coronary arteries under isometric tension (Graves et al., 2000). Similarly, NOS inhibition by L-NNA enhanced myogenic tone in pressurised rat intramural and septal coronary arteries (Szekeres et al., 2004, Garcia and Bund, 1998).

These findings from isolated arteries are also replicated in *ex vivo* whole heart preparations and *in vivo* studies across species. Using the Langendorff heart model, perfusion with L-NAME (100 μM) or methylene blue – an inhibitor for a downstream target of NO, soluble guanylate cyclase, reduced basal coronary flow in the rats (Avontuur et al., 1997). Similar observations were also reported in isolated hearts from rabbit (Pohl et al., 1994) and guinea pig (Kostic and Schrader, 1992) during NOS inhibition. In *in vivo* canine models, L-NMMA caused a dose-dependent vasoconstriction in epicardial coronary arteries (Chu et al., 1991). While Jones et al. (1995) reported similar findings using the same model, they only observed vasoconstriction in coronary arteries (diameter ≥100 μm), but not in arterioles (diameter <100 μm), in the presence

of L-NAME, suggesting possible species variations in the dependence on NO and alternative mechanisms that may govern tone in smaller vessels.

The contribution of NO in modulating basal tone is also translated to humans. Lefroy et al. (1993) observed a reduction in distal epicardial coronary artery diameter, but not in proximal segments, in patients following L-NMMA. Subsequent studies have attempted to further investigate the effects of NOS inhibition on basal tone and dissect this by vessel diameter size. In healthy subjects with angiographically (near-)normal coronary arteries, L-NMMA infusion reduced both proximal and distal epicardial coronary artery diameter, increasing arterial pressure (Quyyumi et al., 1995). Similar observations were reported by Quyyumi et al. (1997) and Nishikawa and Ogawa (1997) in healthy subjects and patients with coronary atherosclerosis, where L-NMMA reduced epicardial coronary artery diameter and blood flow, and increased coronary resistance.

While the current study did not discern the magnitude of NO in modulating myogenic tone according to artery diameter or segment (proximal versus distal), arterial segments (inner diameter: 170 – 330 μm at 80 mmHg, prior to myogenic tone) were isolated from various regions throughout the length of the intra-septal coronary artery. The data presented here clearly indicates that NOS inhibition negatively impacts coronary myogenic response as incubation with either ADMA or L-NAME consistently enhanced myogenic tone in intra-septal coronary arteries under isometric and isobaric conditions. Future investigations should further explore the possible relationship between vessel diameter, myogenic tone and basal NO release. Together with the literature, the data presented here i) confirms the basal release of NO and its importance in regulating myogenic responses in the coronary microvasculature, and

ii) supports a role of the endogenous dimethylarginine, ADMA, in disrupting myogenic response by enhancing coronary artery tone and resistance.

The contributions of NO and EDH (SK_{Ca} and IK_{Ca} channels) in agonist-induced vasodilation of intra-septal coronary arteries were also investigated in the present study. In myogenically active coronary arteries, ACh evoked concentration-dependent vasorelaxation/-dilation, which was significantly attenuated following incubation with 300 μM ADMA. Contrary to the findings in mesenteric resistance arteries presented in **Chapter 3**, ADMA completely abolished NO-dependent vasorelaxation/-dilation in intra-septal coronary arteries, as ADMA-resistant vasorelaxation/-dilation was prevented by the block of EDH. Our data indicate equal contribution of NO (~50%) and EDH (~50%) in ACh-evoked vasorelaxation/-dilation in intra-septal coronary arteries. Moreover, inhibition of NOS and EDH unmasked the vasoconstrictor effects of ACh at higher concentrations (0.3 – 1 μM). This observation is previously reported in patients with vasospastic angina (Okumura et al., 1988, Kugiyama et al., 1996), microvascular angina (Mohri et al., 1998, Sun et al., 2002, Ong et al., 2012) and hypertension (Treasure et al., 1992), all with angiographically (near-)normal coronary arteries. While not examined here, the vasoconstriction to ACh is likely due to the expression of muscarinic receptors in coronary vascular smooth muscle cells (Ren et al., 1993). Therefore, the combined loss of NO and EDH vasodilation is likely to be the cause for the vasoconstrictive effects in the coronary microcirculation of patients undergoing ACh infusion. Together, these findings indicate that ADMA exerts more potent inhibitory effects in the coronary microcirculation than in mesenteric vascular bed, and its effects are comparable to those by L-NAME. Finally, in separate experiments, our group showed that NO itself contributes to EDH in intra-septal coronary arteries as NOS inhibition by both L-NAME and ADMA attenuated hyperpolarization and vasorelaxation (Ng et al., 2024).

While it is plausible that the disparity in the inhibitory effects by ADMA between coronary and mesenteric vascular beds could be due to differences in ADMA uptake via the CAT transport system. This was not explored, and therefore cannot be discounted in the current study and should be investigated further. We hypothesised this discrepancy in the inhibitory effects of ADMA is due to the lower capacity of coronary arteries to metabolise ADMA, as metabolism by DDAH represents a major route of ADMA clearance (approximately 80 – 90%) (Achan et al., 2003) and DDAH expression appears to display tissue specific patterns (Leiper et al., 1999, Hu et al., 2009). This will be explored further in **Chapter 5**.

Our observations following ADMA are in agreement with the findings using methylarginine L-NMMA, and synthetic NOS inhibitors. Chataigneau et al. (1999) reported NOS inhibition with L-NNA significantly stunted but did not block ACh vasorelaxation in mouse coronary arteries under isometric tension. While the authors did not examine the effects of K_{Ca} channel blockade in their studies, the addition of indomethacin, inhibitor of cyclooxygenase-associated vasorelaxation, did not prevent L-NNA-resistant vasorelaxation, suggesting the involvement of alternative pathways in coronary vasorelaxation. Subsequent studies with control and spontaneous hypertensive rats observed similar blunted effects on vasorelaxation in rat left descending (Vazquez-Perez et al., 2001) and septal coronary arteries (Couto et al., 2015) following L-NAME incubation.

The effects of NOS inhibition are also reported in *ex vivo* whole heart models and *in vivo* studies. Perfusion of NOS inhibitors has prevented the increase in coronary flow induced by hyperaemia or ACh, and in some cases the latter induced further reduction in flow (vasoconstriction) in whole heart preparations (Pohl et al., 1994, Kostic and Schrader, 1992).

In canine models, ACh evoked vasodilation and increased coronary flow were significantly reduced following L-NMMA and L-NAME infusion (Chu et al., 1991, Jones et al., 1995, Richard et al., 1991). Likewise, ACh produced vasodilation in both proximal and epicardial coronary arteries, increased coronary blood flow and reduced vascular resistance in a concentration dependent manner in healthy subjects and patients, which was blunted following L-NMMA infusion (Lefroy et al., 1993, Quyyumi et al., 1995, Quyyumi et al., 1997). Finally, comparable to our findings, NOS inhibition did not fully abolish the reduction in coronary vascular resistance and augmentation in flow by ACh in humans (Lefroy et al., 1993, Quyyumi et al., 1995), suggesting additional NO-independent pathways were involved for the vasodilatory actions of ACh, such as EDH.

Feletou and Vanhoutte (1988) observed that VSM hyperpolarization to ACh occurred in endothelium-intact canine left anterior ascending coronary arteries, and using 'sandwich' bioassay, found that an EDH factor (EDHF) was released to hyperpolarize denuded coronary artery. This demonstrated that both NO and hyperpolarization contribute to ACh vasorelaxation, indicating the importance of an intact endothelium and suggesting the notion of parallel mechanisms in agonist-induced vasorelaxation. In subsequent *ex vivo* animal studies during NOS inhibition, the residual NO-independent vasorelaxation in epicardial coronary arteries was abolished by high K^+, scavengers for K^+, non-selective K_{Ca} channel blockers, or the combination of apamin and charybdotoxin – SK_{Ca} and non-selective BK_{Ca} and IK_{Ca} channel blockers respectively, (Vazquez-Perez et al., 2001, Beny and Schaad, 2000, Kaw and Hecker, 1999). Furthermore, L-NMMA attenuated ACh-induced vasodilation in canine left anterior descending coronary arteries *in vivo*, which was subsequently abolished by infusion of high K^+ (Nishikawa et al., 1999).

Likewise in human isolated coronary arteries, both L-NAME and high K^+ significantly attenuated vasodilation in pressurised right atrial appendage intramuscular resistance coronary arteries, and subsequent addition of apamin or charybdotoxin further attenuated vasodilation and hyperpolarization (Miura et al., 1999). Similarly, the presence of apamin and charybdotoxin with a NO scavenger significantly reduced ACh vasorelaxation in human left anterior descending coronary arteries (Batenburg et al., 2004). Therefore, these data confirm the parallel actions of NO and EDH/K^+ in agonist-induced vasodilation is also translated to humans. Together with the literature, the findings here indicate the importance of the synergistic actions of EDH/K^+ and NO in vasorelaxation/-dilation in coronary arteries.

Interestingly, in contrast to other vascular beds (e.g. mesenteric resistance arteries) and previous literature, we reveal that in the absence of NO, IK_{Ca} channels solely underpin the EDH vasodilatory responses in rat intra-septal coronary arteries as NS 6180 prevented ADMA-resistant vasorelaxation to ACh during NOS inhibition. Conversely, the addition of apamin, SK_{Ca} channel blocker, in the presence of ADMA had no effects on residual vasorelaxation. Subsequent addition of NS 6180 abolished the residual relaxation, further supporting the sole involvement of IK_{Ca} channels in EDH. These observations were also replicated in the presence of L-NAME. Additionally, in separate experiments with simultaneous isometric tension and membrane potential recordings, our group confirmed that NS 6180 abolished both residual hyperpolarization and vasorelaxation to ACh in the presence of ADMA (Ng et al., 2024). These findings suggest possible variation in EDH mechanisms between vascular beds.

It is unclear why IK_{Ca} channels appear to be solely underpin EDH vasorelaxation in the coronary microvasculature. A possible explanation for this observation is the absence SK_{Ca} channels, or the presence of non-functional/uncoupled channels in the coronary

microvasculature. However, while the current study did not explore the expression of K_{Ca} expression, this seems unlikely as previous rodent and human studies have reported both IK_{Ca} and SK_{Ca} expression in the coronary endothelium. Climent et al. (2014) reported endothelial expression of both IK_{Ca} and SK_{Ca} channels in rat left anterior descending coronary arteries, and Liu et al. (2015) reported comparable expression in human right atrial appendage arterioles. Furthermore, TRAM 34 and apamin were needed to abolish vasodilation and hyperpolarization induced by IK_{Ca}/SK_{ca} channel activators in rat Langendorff heart model (Mishra et al., 2013) and in pressurised human right atrial appendage coronary arterioles (Liu et al., 2015). Alternatively, the expression of SK_{Ca} channels in the coronary microcirculation could be lower or more diffused. As such, SK_{Ca} channels may not algin with M_3 muscarinic receptors and/or the associated rise in Ca^{2+} and second messengers, resulting in the lack of contribution of SK_{Ca} channels in EDH vasodilation to ACh.

Another possible explanation could be the activation of SK_{Ca} requires or is aided by the presence of NO as the current study examined the effects of K_{Ca} channels in the absence of NO, where NOS activity was blocked by ADMA. Previous studies in rat fundus smooth muscles showed that apamin attenuated relaxation by the NO donor, sodium nitroprusside (Geeson et al., 2002), suggesting a possible interplay between NO and SK_{Ca} channels. In NO-intact arteries (without L-NNA), the absence of SK_{Ca} channels attenuated ACh vasorelaxation, an observation that was lost under NOS inhibition with L-NNA, and this NO-dependent effect was not present in carotid arteries lacking IK_{Ca} channels (Brahler et al., 2009). In separate studies, immunostaining showed co-localisation of eNOS and SK_{Ca} in the endothelium of retinal arteries (Simonsen et al., 2019). Furthermore, NOS blockade by L-NAME or ADMA reduced ACh-induced hyperpolarization in intra-septal coronary arteries (Ng et al., 2024). Therefore, during ACh stimulation, the presence of NOS inhibitors may disturb the possible

interactions between NO and SK_{Ca} channels, which may be in close vicinity of each other, by blocking NO synthesis. Nevertheless, these hypotheses require further investigation to unravel the vasodilatory mechanisms in the coronary microcirculation.

The findings presented here in intra-septal coronary arteries are significant as they support the notion of and provide mechanistic insights into how elevated ADMA levels can result in endothelial dysfunction, as observed in many cardiovascular diseases including non-obstructive coronary artery diseases. Comparable to the clinical presentations, the combination of elevated ADMA levels and EDH blockade in this study unmasked the vasoconstrictor effects of ACh in intra-septal coronary arteries, suggesting that disruption of both vasodilatory pathways (seen in endothelial dysfunction) could be involved in coronary vasospasm seen in patients with microvascular angina and ANOCA. Moreover, we observed a more potent inhibitory effect of ADMA on NO synthesis in the coronary microvasculature compared to mesenteric resistance arteries, suggesting that although the mechanism of action (NOS inhibition) is alike across vascular beds, the magnitude of inhibition exerted by ADMA can vary, likely due to the presence of modulatory mechanisms (e.g. DDAH metabolism). Finally, in contrast to other vascular beds, we reveal that IK_{Ca} channel underpins EDH dilatory response during NOS inhibition.

4.5 CONCLUSION

This chapter aimed to examine the effects of NOS inhibition by endogenous dimethylarginine, ADMA, and the involvement of IK_{Ca} and SK_{Ca} channels in EDH, in myogenically active intra-septal coronary arteries using wire and pressure myography. The findings (**Figure 4.5.1**) presented here support the hypotheses that ADMA: i) enhances myogenic tone – suggesting the basal release of NO and its modulatory actions on myogenic responses; and ii) disrupts NO-dependent vasodilation to the endothelium-dependent vasodilator, ACh. In contrast to our findings in mesenteric resistance arteries, ADMA completely abolished NO-dependent vasodilation in intra-septal coronary arteries. We hypothesised this is due to differences in DDAH activity, which will be explored further in subsequent chapter (**Chapter 5**). Surprisingly, in the absence of NO, we reveal that IK_{Ca} channels underpin EDH vasorelaxation to ACh in coronary arteries.

The data presented here provide valuable insights into the mechanisms by which endothelium disruptions and elevated ADMA levels, as seen in cardiovascular disease, can result in coronary vascular dysfunction (enhanced myogenic tone and block of vasodilation).

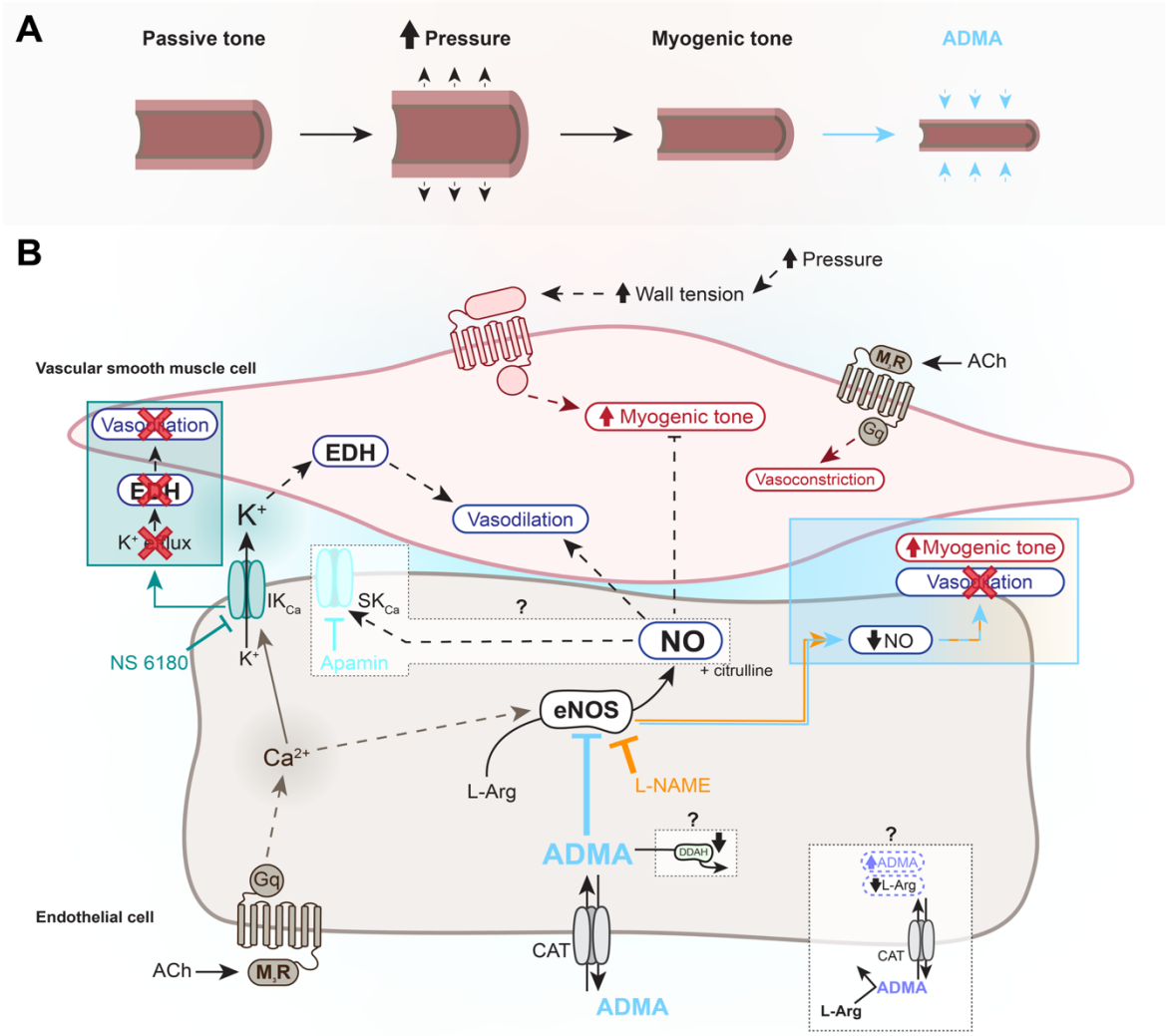


Figure 4.5.1 Summary of Chapter 4 – Nitric oxide (NO) and intermediate conductance Ca^{2+}-activated K^+ (IK_{Ca}) channel modulates the vasoreactivity of intra-septal coronary arteries. A, Diagram representation of the development of myogenic tone (MT) in intra-septal coronary arteries and the effects of asymmetric dimethylarginine (ADMA) on MT. **B,** ADMA prevents NO-dependent vasodilation to the M_3 muscarinic receptor (M_3R) agonist acetylcholine (ACh), and the ADMA-resistant (endothelium dependent hyperpolarization; EDH) vasodilation was abolished by the IK_{Ca} channel blocker, NS 6180. The addition of small K_{Ca} (SK_{Ca}) channel blocker, apamin, alone failed to prevent ADMA-resistant vasodilation and did not potentiate the inhibitory effects in the presence of ADMA and NS 6180. We hypothesise (dotted box) the stronger effects of ADMA in coronary arteries, vs mesenteric arteries, is due to a difference in DDAH. Dashed arrows represent simplified signalling pathways. Overall effects are summarised in blue/orange (for ADMA and L-NAME), and green (for NS 6180) boxes. eNOS = endothelial NO synthase; CAT = Cationic amino acid transporter; L-Arg = L-arginine.

CHAPTER FIVE

INVESTIGATING THE ROLE OF DIMETHYLARGININE DIMETHYLHYDROLASE 1 IN THE MESENTRIC AND CORONARY MICROCIRCULATION

5.1 INTRODUCTION

The renal excretion together with the metabolism by DDAH play crucial roles in the elimination of methylarginines *in vivo*. As aforementioned, the main route of SDMA elimination is via urinary excretion whereas 80 – 90% of ADMA and L-NMMA are metabolised intracellularly to L-citrulline and (di-)methylamine by DDAH (Ogawa et al., 1987a, Achan et al., 2003). As a result, DDAH activity can significantly impact not only the intracellular concentrations of ADMA, but also the plasma concentration, and thus NO bioavailability and vascular function potentially to a systemic level.

Dimethylarginine dimethylaminohydrolases were first identified and purified from rat kidney samples (Ogawa et al., 1987a), subsequent studies identified two isoforms of DDAH, DDAH1 and DDAH2, with approximately 62% degree of amino acid sequence conservation (Leiper et al., 1999). Furthermore, each DDAH isoform is highly conserved (>95%) across species including humans and rodents (Leiper et al., 1999), therefore, making rodents a suitable model to investigate the DDAH activity. Although DDAH1 and DDAH2 are widely expressed throughout the body, initial studies have reported tissue specific expression that somewhat correlate with NOS expression, where DDAH1 is more likely to co-localise with neuronal NOS, and is highly expressed in the kidneys and liver, and DDAH2 expression correlated with eNOS (Leiper et al., 1999). Therefore, previous literature postulated that DDAH2 would play a greater role in ADMA metabolism in the cardiovascular system. However, the contribution of DDAH2 in ADMA metabolism and vascular function has been controversial. While the initial *in vitro* study reported the metabolic activity of recombinant DDAH2 (Leiper et al., 1999), subsequent studies failed to detect ADMA metabolism by DDAH2 *in vitro* and *in vivo* (Altmann et al., 2012, Wang et al., 2007).

In contrast, researchers are in agreement of the critical role of DDAH1 in modulating ADMA concentration. While significant uptake and DDAH1-mediated metabolism of ADMA occurs in the kidneys and liver (Nijveldt et al., 2003), ADMA is produced ubiquitously in all cell types and can be imported or exported into cells. Therefore, the ability of vascular cells to modulate intracellular ADMA levels is crucial in balancing eNOS inhibition to ensure normal vascular function. In endothelial cell cultures and human saphenous veins, incubation with ADMA reduced L-NMMA metabolism, measured by the formation of radio-labelled L-citrulline (MacAllister et al., 1994). In separate experiments, incubation with L-NMMA alone increased intracellular ADMA levels (MacAllister et al., 1994), demonstrating both L-NMMA and ADMA are subjected to and compete for endogenous DDAH1 metabolism. Similarly, Ito et al. (1999) reported the expression of DDAH1 in cultured human umbilical vein endothelial cells using Western blots, and showed an increase in oxidative stress in endothelial cells in culture and *in vivo* reduced DDAH1 activity, but not expression, in the endothelial cells and the kidney, liver and aorta.

Using a weak DDAH1 inhibitor S-2-amino-4(3methylguanidino)butanoic acid (4124W; IC_{50} = ~416 μM), MacAllister et al. (1996) showed that the metabolism of L-NMMA to L-citrulline in rat liver homogenates, cultured endothelial cells and purified DDAH1 was reduced compared to controls. Furthermore, the addition of 4124W caused the accumulation of ADMA in human endothelial cells, enhanced PE-induced contraction in a dose-dependent manner in isolated aortic rings, and reversed endothelium-dependent vasorelaxation in human saphenous arteries *ex vivo* (MacAllister et al., 1996). Subsequent studies using the more potent DDAH1 selective inhibitor L-257 (N^G-(2-methoxyethyl) arginine; IC_{50} = <25 μM) produced comparable observations in pulmonary arterial endothelial cells, where they showed DDAH1 inhibition augmented ADMA levels and diminished NO generation (Leiper et al., 2007).

Together, these findings demonstrate the continuous turnover of ADMA and L-NMMA and the importance of DDAH1 in maintaining endothelial cell function under physiological conditions by ensuring intracellular ADMA levels are regulated to allow NO production.

Additionally, recent clinical studies have explored the associations of genetic variations in DDAH1 to the cardiovascular risk factors and the development of cardiovascular diseases. A recent genome-wide association analysis combining three population-based cohort studies showed that carriers of one or more of the minor alleles were associated with higher plasma ADMA levels (Luneburg et al., 2014). In type 2 diabetes patients, plasma ADMA levels showed DDAH1 allelic preference, which was associated with an enhanced risk of major adverse cardiovascular events, such as cardiovascular-related deaths, stroke and myocardial infarction (Lu et al., 2011, Abhary et al., 2010). Furthermore, Amir et al. (2018) reported higher levels of plasma ADMA in patients with coronary artery disease, and identified DDAH1 genotypes that were more prevalent in coronary artery disease (>2-fold increase risk), which were correlated with elevated plasma ADMA concentrations. While the authors of these studies did not directly examine the functional impact of the DDAH1 polymorphisms, the observation of enhanced ADMA levels indicates a loss of DDAH1 activity and supports the role of DDAH1 in cardiovascular complications.

In addition to the importance of DDAH1 in ADMA metabolism and as such the regulation of NOS activity, most studies have only examined the effects DDAH1 in endothelial cell models and in the macrocirculation (e.g. *ex vivo* aortic rings). Therefore, due to the importance of the microcirculation in the regulation of tissue perfusion and vascular resistance, it is crucial that we further our understanding in the contribution of DDAH1 in the microvasculature, particularly in the coronary resistance arteries. Using a combination of wire and pressure

myography techniques and the recently developed DDAH1 selective inhibitor L-257 (Rossiter et al., 2005), this chapter investigated the effects of DDAH1 inhibition on the: i) endothelium-dependent vasoreactivity in non-myogenically active mesenteric resistance arteries in the presence of ADMA; and ii) myogenic response (tone) in myogenically active intra-septal coronary arteries. Furthermore, using immunohistochemistry, the expression of DDAH1 was examined to explore the possibility of differential expression pattern between the mesenteric and coronary vascular beds, which might explain the findings in the previous chapters.

5.1.1 Aims and hypotheses

We hypothesised that:

i) DDAH1 would prevent NOS inhibition by ADMA, leading to incomplete block of vasorelaxation/-dilation by ACh in mesenteric resistance arteries (**Chapter 3**).

ii) Inhibiting DDAH1 in myogenically active intra-septal coronary arteries would increase myogenic tone.

iii) The differences in NOS inhibition by ADMA between mesenteric (**Chapter 3**) and coronary (**Chapter 4**) resistances arteries are due to the expression of DDAH1.

This chapter aims to:

i) Investigate the role of DDAH1 in modulating the action of ADMA in mesenteric resistance arteries.

ii) Characterise the effects of DDAH1 on myogenic tone in intra-septal coronary arteries.

iii) Compare the expression of DDAH1 between the mesenteric and coronary vascular beds and cell types.

5.2 MATERIALS AND METHODS

5.2.1 Wire myography

Rat mesenteric and intra-septal coronary arteries were prepared for wire myography as described in **Chapters 2.1** and **2.2**. Arteries were normalised to a resting tension equivalent to that generated at 90% of the inner diameter of the vessel at 70 mmHg (mesenteric) or 80 mmHg (coronary). Following equilibration, only arteries that relaxed >95% to ACh (0.001 – 1 μM) from stable PE constriction (mesenteric) or from stable myogenic tone (coronary) were used for further experiments.

5.2.2 Pressure myography

Mesenteric arteries were prepared for pressure myography as described in **Chapters 2.1** and **2.3**. Arteries were cannulated onto glass micropipettes and intra-luminally pressurised to 70 mmHg. Following equilibration, only arteries displayed robust vasoconstriction and that relaxed >95% to ACh (0.001 – 1 μM) were used for subsequent experiments.

5.2.3 Immunohistochemistry and imaging

Mesenteric and intra-septal coronary arteries were mounted in a wire myograph and prepared for immunohistochemistry as described in **Chapter 2.4**. Rabbit polyclonal anti-human DDAH1 primary antibody (1:500 dilution, PA5-52278, Invitrogen, USA) was used to stain for DDAH1. Goat polyclonal anti-rabbit IgG secondary antibody (A-11034, 1:1,000 dilution, Invitrogen, USA) and nuclear dye Hoechst 33342 (H3570, Invitrogen, USA) were used as described in **Chapter 2.4**. Arteries were imaged and analysed as described in **Chapter 2.4**. See **Table 2.6.2**. for more details of the antibodies used.

5.2.4 Western blotting

Rat kidney and liver samples were prepared for western blotting as described in **Chapter 2.5**. Rabbit polyclonal anti-human DDAH1 primary antibody (1:500 dilution, PA5-52278, Invitrogen, USA) and mouse monoclonal β-actin primary antibody (1:15,000 dilution, AC-15, ab6276, Abcam, UK). IRDye 800CW donkey anti-mouse (925-32212, Li-Cor Biosciences, USA) and IRDye 680RD donkey anti-rabbit (925-68073, Li-Cor Biosciences, USA) IgG secondary antibodies (at 1:15,000 dilution). Membrane was imaged at 700 and 800 wavelengths as described in **Chapter 2.5**. See **Table 2.6.2** for more details of the antibodies used.

5.2.5 Inhibitors

The following inhibitors were used to inhibit their respective targets: apamin (Ap, 100 nM) to inhibit SK_{Ca} channels, NS 6180 (NS, 1 μM) to inhibit IK_{Ca} channels, N^G,N^G-Dimethylarginine dihydrochloride (ADMA, 300 μM) to inhibit NOS, and N^G-(2-methoxyethyl) arginine (L-257; 100 μM) to inhibit DDAH1. See **Table 2.6.1** for more details.

5.3 RESULTS

5.3.1 DDAH1 prevents endothelial nitric oxide synthase inhibition by ADMA in mesenteric arteries

To investigate the modulatory role of DDAH1 on the inhibitory effects of ADMA on ACh vasorelaxation in mesenteric arteries, cumulative ACh concentration-response curves were constructed before and during EDH blockade by apamin and NS 6180 (Ap, NS) and NOS inhibition by ADMA in the presence and absence of DDAH1-selective inhibitor, L-257.

Similar to **Figure 3.3.2**, inhibition of SK_{Ca} and IK_{Ca} channels by apamin (100 nM) and NS 6180 (1 μM) respectively attenuated ACh-induced vasorelaxation (E_{max}; Control: 99.2 ± 0.2%; Ap NS: 95.3 ± 0.8%; n = 7; $P < 0.05$; **Figure 5.3.1B and C**), which was enhanced in the presence of 300 μM ADMA (E_{max}; Ap, NS, ADMA: 69.8 ± 7.3%; n = 7; $P < 0.05$ compared to Control and Ap, NS; **Figure 5.3.1A middle panel, B and C**). Residual ACh-induced vasorelaxation during ADMA and EDH blockade was further suppressed by the subsequent addition of 100 μM L-257 for 60 minutes (E_{max}; Ap, NS, ADMA, L-257: 30.8 ± 5.1%; n = 7; $P < 0.01$ compared to Ap, NS, ADMA and $P < 0.0001$ compared to Control and Ap, NS; **Figure 5.3.1A right panel, B and C**). Incubation of L-257 for 60 min was selected and used in subsequent experiments as this incubation time further suppressed ACh-induced vasorelaxation (E_{max}; Ap, NS, ADMA L-257 (30 min): 45.9 ± 4.3%; Ap, NS, ADMA, L-257 (60 min): 29.2 ± 5.7%; n = 6; $P < 0.05$; **Figure 5.3.2**). Extending L-257 incubation to 90 min in the presence of ADMA and inhibition of EDH did not further suppress vasorelaxation to ACh (E_{max}; Ap, NS, ADMA (90 min): 31.2 ± 6.0%; n = 6; $P = 0.9544$ compared to Ap, NS, ADMA, L-257 (60 min; **Figure 5.3.2**).

In separate experiments, mesenteric arteries were cannulated on to glass micropipettes of a pressure myography chamber to study the effects of DDAH1 inhibition in pressurised mesenteric arteries. The addition of L-257 (60 min), in the presence of EDH blockade and ADMA, further suppressed vasodilation to ACh (E_{max}; Ap, NS, ADMA: 77.9 ± 4.3%; Ap, NS, ADMA, L-257: 65.0 ± 4.7%; n = 10; $P < 0.01$; **Figure 5.3.3**).

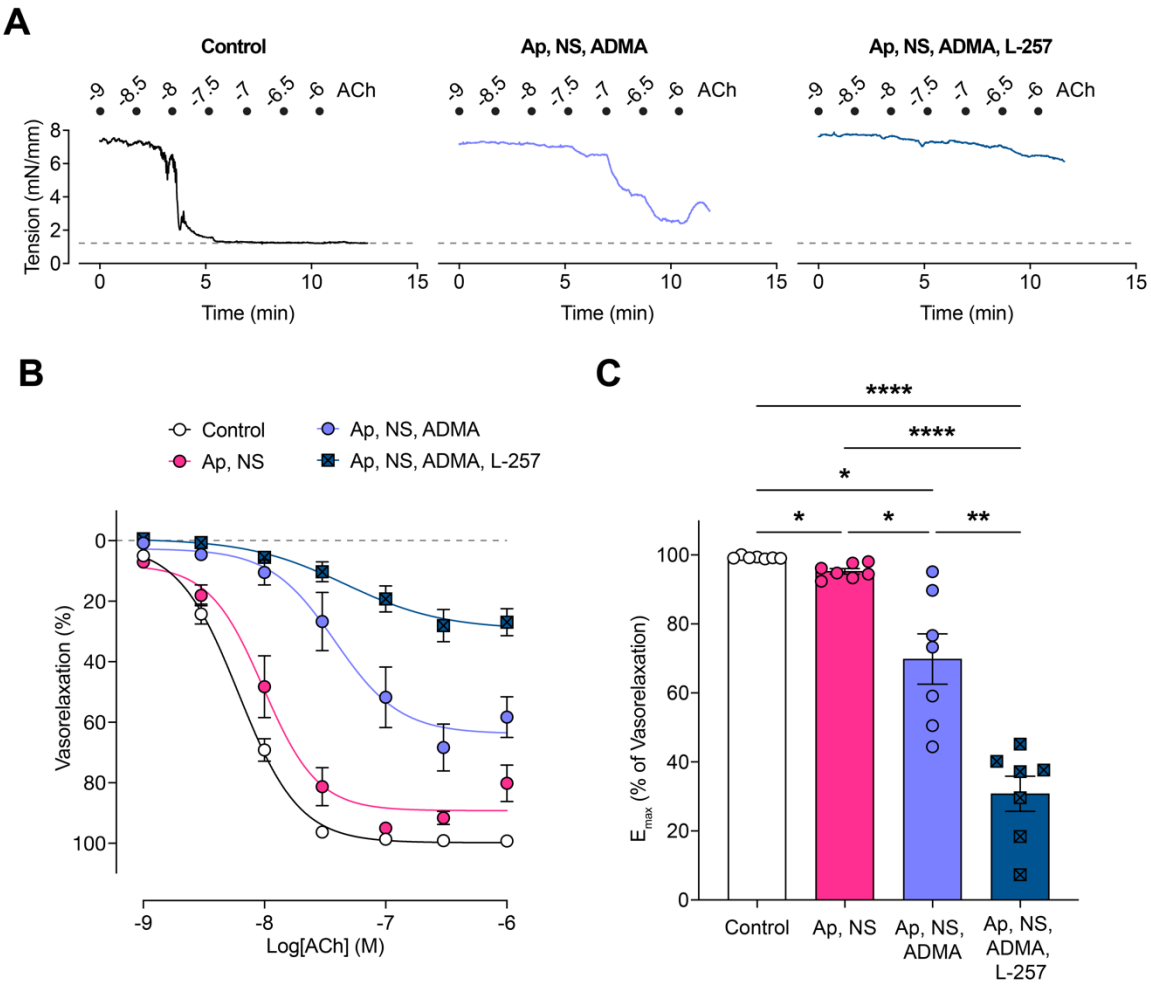


Figure 5.3.1 Inhibition of dimethylarginine dimethylaminohydrolase 1 (DDAH1) by L-257 further attenuates persistent acetylcholine (ACh) vasorelaxation in mesenteric arteries in the presence of asymmetric dimethylarginine (ADMA) and endothelium-dependent hyperpolarization (EDH) blockade. A, Representative tension traces of vasorelaxation to cumulative ACh in phenylephrine (α_1-adrenoreceptor agonist) pre-constricted mesenteric arteries under isometric tension before (Control; Left panel) and after incubation of apamin (Ap; 100 nM), NS 6180 (NS; 1 µM), and ADMA (300 µM; Middle panel), and the addition of DDAH1 inhibitor, L-257, for 60 min (100 µM; Right panel). Dashed lines indicate baseline tension. **B,** ACh concentration-response curves summarising vasorelaxation in the absence and presence of Ap, NS ± ADMA ± L-257. **C,** Bar graph summarising E_{max} evoked by ACh in (**B**). Data are means ± SEM; n = 7. **P* < 0.05, ***P* < 0.01, *****P* < 0.0001 using one-way ANOVA with Tukey's multiple comparisons test.

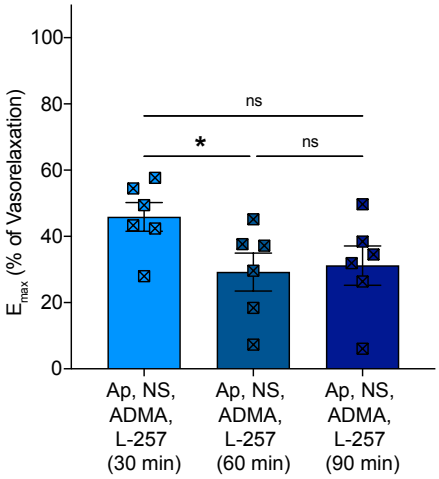


Figure 5.3.2 Time-dependent effects of dimethylarginine dimethylaminohydrolase 1 (DDAH1) selective inhibitor, L-257, incubation on percentage of maximum vasorelaxation (E_{max}). Bar graph summarising E_{max} elicited by acetylcholine (ACh) during endothelium-dependent hyperpolarization (EDH) blockade, by apamin (Ap; 100 nM) and NS 6180 (NS; 1 μM), nitric oxide synthase inhibition, by asymmetrical dimethylarginine (ADMA; 300 μM) and DDAH1 inhibition, by L-257 (100 μM; for 30, 60 or 90 min) in phenylephrine (α_1-adrenoreceptor agonist) pre-constricted mesenteric arteries. Data are means ± SEM; n = 6. *$P < 0.05$ using one-way ANOVA with Tukey's multiple comparisons test.

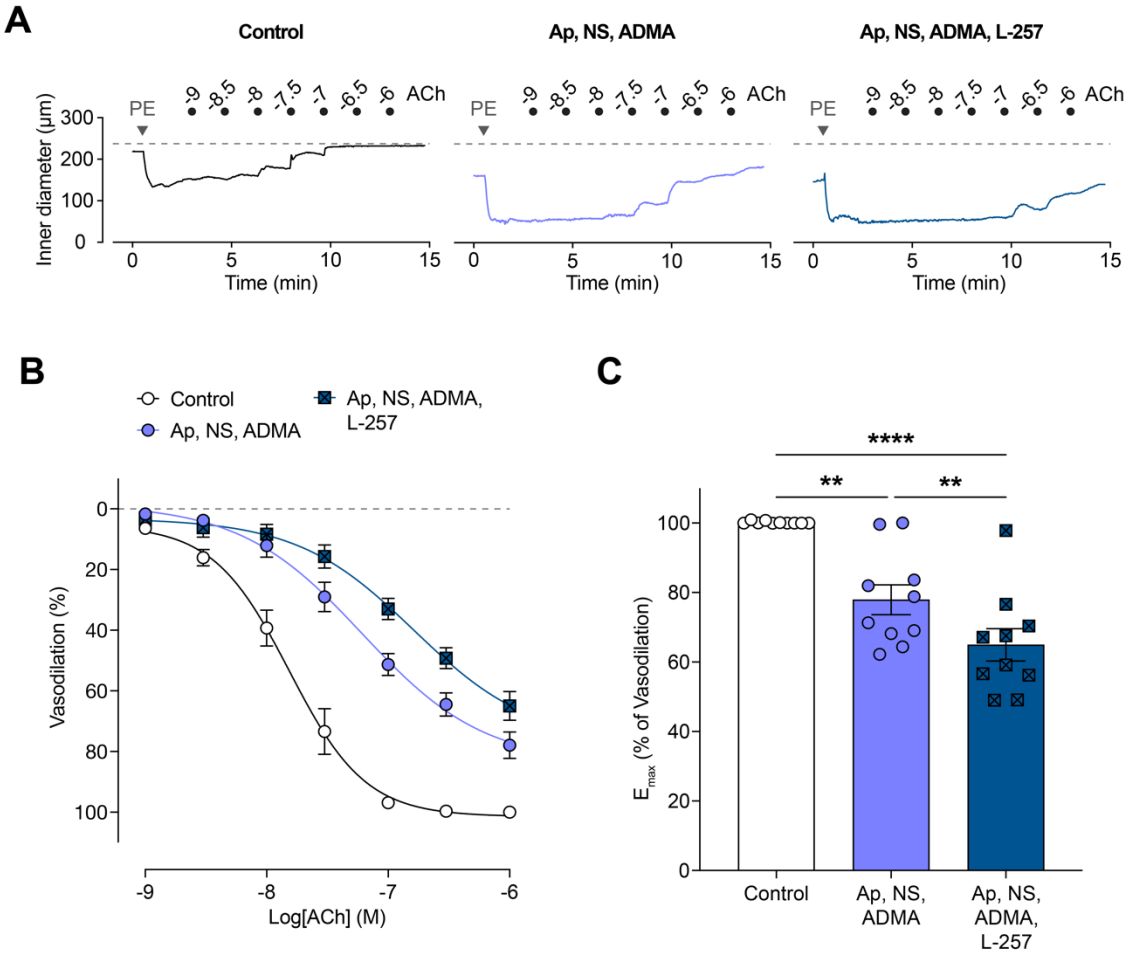


Figure 5.3.3 Dimethylarginine dimethylaminohydrolase 1 (DDAH1) inhibition by L-257 further suppresses vasodilation to acetylcholine (ACh) in pressurised mesenteric arteries in the presence of asymmetric dimethylarginine (ADMA) and endothelium-dependent hyperpolarization (EDH) blockade. A, Representative diameter traces of vasodilation to cumulative ACh in phenylephrine (α_1-adrenoreceptor agonist; PE) pre-constricted pressurised mesenteric arteries in the absence (Control; Left panel) and presence of apamin (Ap; 100 nM), NS 6180 (NS; 1 µM) and ADMA (300 µM; Middle panel), and the addition of DDAH1 inhibitor, L-257 (100 µM; Right panel) for 60 min. Dashed lines indicate passive inner diameter. **B,** Cumulative concentration-response curves in the absence (Control) and presence of Ap, NS, ADMA ± L-257. **C,** Bar graph summarising the E_{max} evoked by ACh in (**B**). Data are means ± SEM; n = 10. $^{**}P < 0.01$, $^{****}P < 0.0001$ using one-way ANOVA with Tukey's multiple comparisons test.

5.3.2 DDAH1 inhibition augments myogenic tone in intra-septal coronary arteries under isometric tension

To investigate whether increasing endogenous ADMA would augment myogenic tone (MT) in intra-septal coronary arteries, arteries mounted in a wire myograph were studied before and during DDAH1 inhibition by L-257 or during NOS blockade by L-NAME.

Under isometric tension, myogenic tone in intra-septal coronary arteries increased in the presence of DDAH1-selective inhibitor, L-257 (100 μM) compared to Control (Control: 1.49 ± 0.29 mN/mm; L-257: 2.38 ± 0.32 mN/mm; n = 5; $P < 0.01$; **Figure 5.3.4**). The addition of L-NAME (100 μM) further enhanced myogenic tone (3.22 ± 0.40 mM/mm; n = 5; $P < 0.01$ compared to Control and $P < 0.05$ compared to L-257). Representative traces before (left panel) and after L-257 (middle panel) and L-NAME (right panel) are shown in **Figure 5.3.4A**.

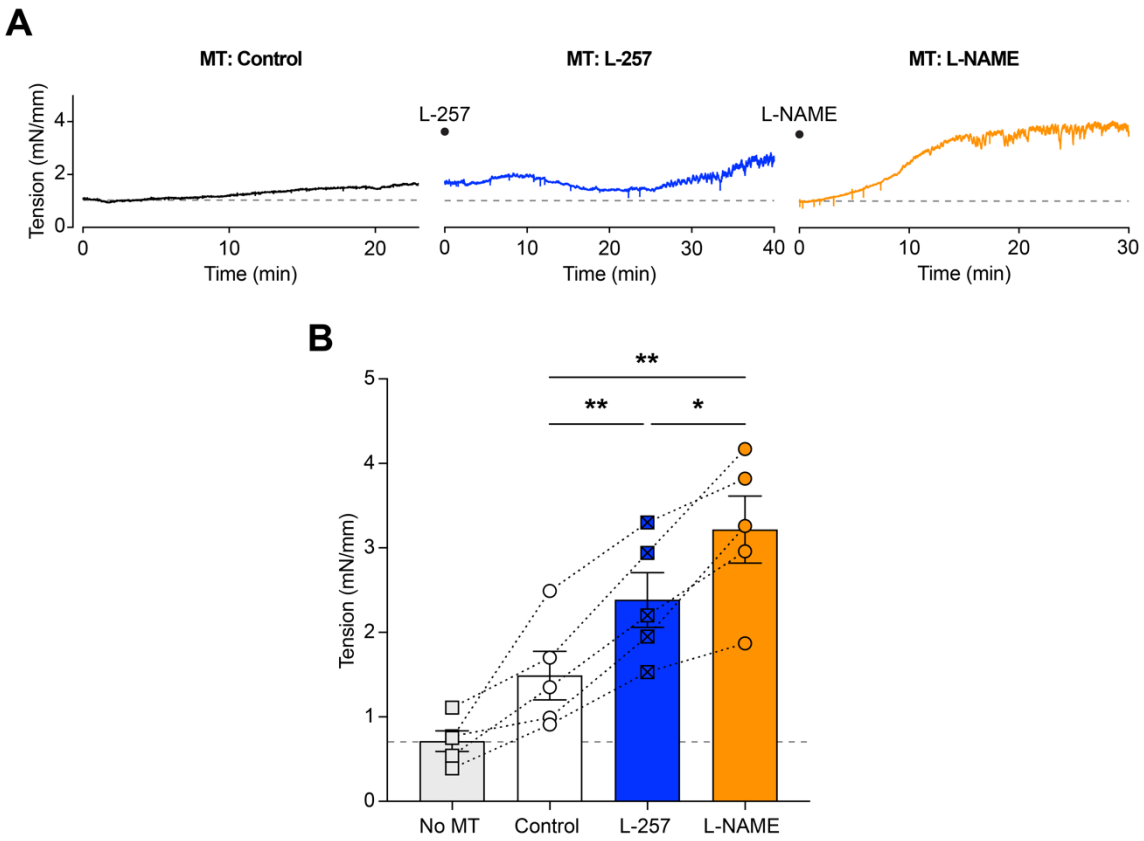


Figure 5.3.4 Inhibition of dimethylarginine dimethylaminohydrolase 1 (DDAH1) by L-257 increases myogenic tone in intra-septal coronary artery under isometric tension. A, Representative tension traces before (Control; Left panel) and after incubation with DDAH1 inhibitor, L-257 (100 µM; Middle panel) or synthetic endothelial nitric oxide synthase inhibitor, L-NAME (100 µM; Right panel). Dashed lines indicate baseline tension. **B,** Bar graph summarising the tension, before and after the development of myogenic tone, in the absence (Control) and presence of L-257 or L-NAME. Dashed line indicates mean baseline tension. Data are means ± SEM; n = 5. **P* < 0.05 and ***P* < 0.01 using one-way ANOVA with Tukey's multiple comparisons test.

5.3.3 DDAH1 expression is greater in the endothelium of mesenteric arteries compared to intra-septal coronary arteries

The differential results using ADMA with and without L-257 in the mesenteric and coronary vascular beds prompted an investigation in the expression of DDAH1 in mesenteric resistance and intra-septal coronary arteries using immunohistochemistry.

Immunohistochemistry indicated the presence of DDAH1 in both mesenteric (**Figure 5.3.5A top row**) and coronary (**Figure 5.3.5A bottom row**) resistance arteries. Interestingly, the expression of DDAH1 was markedly greater in the endothelium and perivascular nerves of mesenteric arteries (Fluorescence Intensity; Endothelium: 63.1 ± 13.1 A.U.; Nerves: 17.7 ± 3.1 A.U.; n = 7) compared to intra-septal coronary arteries (Fluorescence Intensity; Endothelium: 12.10 ± 2.20 A.U.; Nerves: 4.86 ± 0.91 A.U.; n = 6; $P < 0.01$; **Figure 5.3.5B left and right panels**). In contrast, DDAH1 expression was low in the vascular smooth muscle of both vascular beds (Fluorescence Intensity; Mesenteric: 5.26 ± 0.83 A.U.; Coronary: 3.45 ± 0.78 A.U.; n = 6; $P > 0.05$; **Figure 5.3.5B middle panel**). Furthermore, within the respective vascular beds, the endothelium exhibited the greatest expression of DDAH1 compared to other vascular tissue layers ($P < 0.05$ and $P < 0.01$ compared to mesenteric and coronary endothelium; **Figure 5.3.5B**). Images shown are representative of n = 7 (mesenteric) and 6 (coronary).

Antibody specificity was examined with western blotting and immunohistochemistry. DDAH1 bands (34 kDa) and no non-specific bands were detected in both kidney (Kid) and liver (Liv), where DDAH1 is highly expressed (n = 4; **Figure 5.3.6**). β-actin (42 kDa) was used as loading control. Negative control immunohistochemical images are shown in **Figure 5.3.7** and are representative of n = 3.

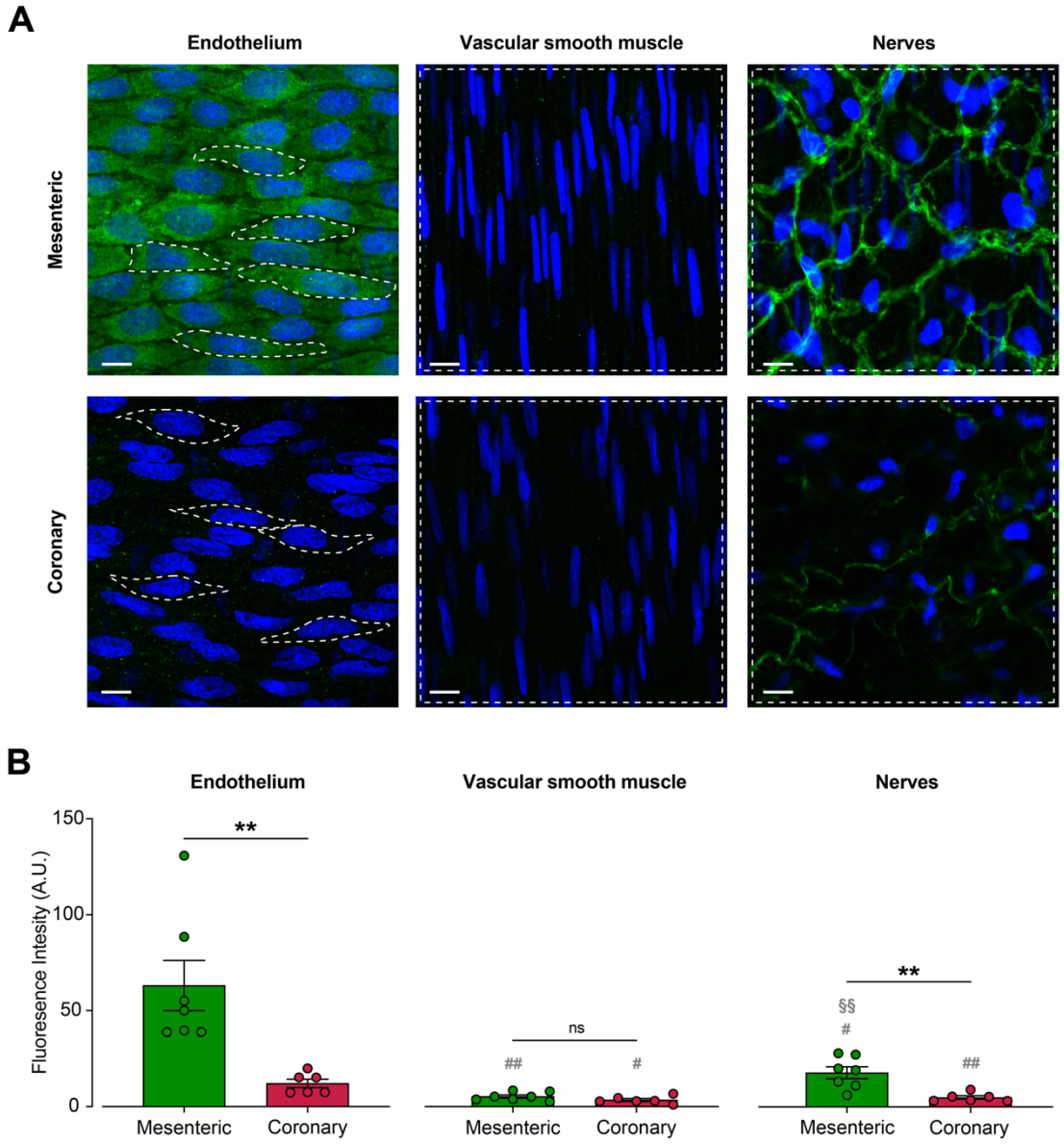


Figure 5.3.5 Expression of dimethylarginine dimethylaminohydrolase 1 (DDAH1) is greater in mesenteric compared to intra-septal coronary artery endothelium. A, Representative immunohistochemistry images labelling DDAH1 (green) in the endothelium (Left panels), vascular smooth muscles (Middle panels) and perivascular nerves (Right panels) of mesenteric arteries (Top row) and in intra-septal coronary arteries (Bottom row). Nuclei labelled blue. Scale bar = 10 μm. **B**, Bar graph summarising DDAH1 fluorescence intensity, expressed as arbitrary unit (A.U.), from the dashed regions indicated in (**A**). Data are means ± SEM; n = 6 – 7. $^{**}P < 0.01$ using unpaired two-tailed t-tests. $^{\#}P < 0.05$ and $^{\#\#}P < 0.01$ compared to endothelium in respective groups and $^{\S\S}P < 0.01$ compared to vascular smooth muscle using one-way ANOVA with Tukey's multiple comparisons test.

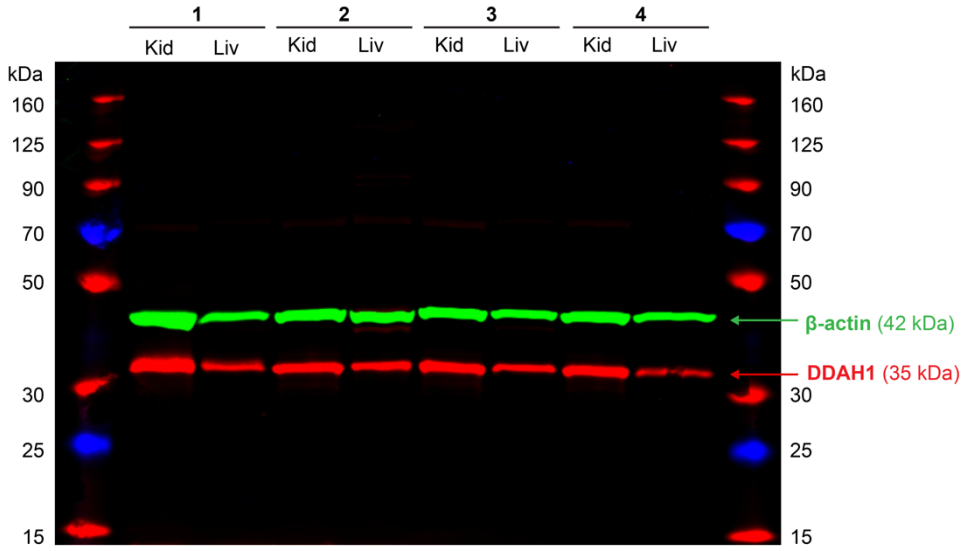


Figure 5.3.6 Expression of dimethylarginine dimethylaminohydrolase 1 (DDAH1) in rat kidney and liver. Western blot showing DDAH1 expression (35 kDa) in kidney (Kid) and liver (Liv). β-actin (42 kDa) was used as loading control. n = 4.

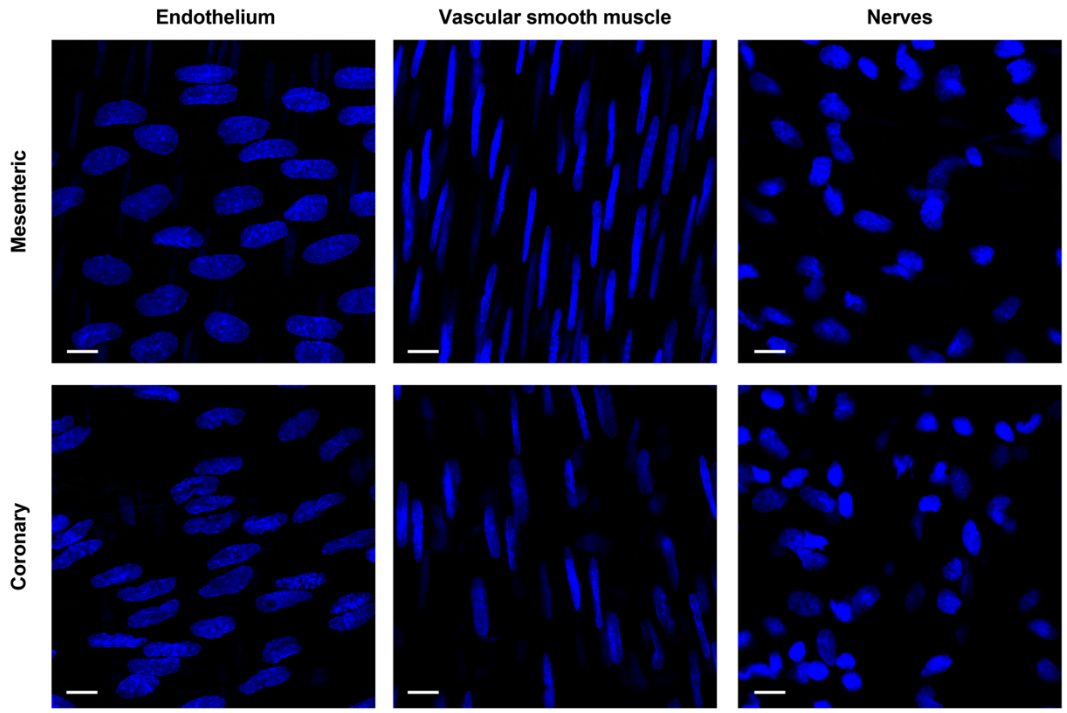


Figure 5.3.7 Primary antibody negative control images. Representative immunohistochemistry images in the absence of (dimethylarginine dimethylaminohydrolase 1) DDAH1 antibody in mesenteric (Top row) and intra-septal coronary (Bottom row) arteries. Endothelium (Left panels), vascular smooth muscle (Middle panels) and Nerves (Right panels). Nuclei labelled with Hoechst 33342 (blue). n = 3. Scale bar = 10 μm.

5.4 DISCUSSION

This chapter aimed to investigate the modulatory role of DDAH1 on NOS inhibition by ADMA in isolated rat mesenteric and intra-septal coronary resistance arteries mounted under isometric and isobaric conditions. The findings here support the hypotheses that DDAH1 prevents NOS inhibition by ADMA under physiological conditions, particularly in mesenteric arteries. An action of DDAH1 in coronary arteries could be unmasked by showing a slow augmentation of myogenic tone, mimicking that observed by adding exogenous ADMA. Moreover, immunohistochemistry data support the hypothesis that DDAH1 expression is greater in mesenteric compared to coronary vascular beds, which appears to explain the differences in NOS inhibition by ADMA.

To examine the modulatory effects of DDAH1 on NOS inhibition by ADMA in mesenteric resistance arteries mounted under isometric and isobaric conditions, the present study utilised the recently developed DDAH1 selective inhibitor, L-257 (N^G-(2-methoxyethyl) arginine). Crystallography studies revealed that L-257 occupies the active site of DDAH1, overlapping with the reaction product of ADMA metabolism, L-citrulline (Leiper et al., 2007). The specificity of L-257 for DDAH1 is further supported by site specific mutation of DDAH1 at glycine-129 (in close proximity to the catalytic region) to threonine (present in DDAH2), which prevented the binding of and inhibition by L-257 (Nandi et al., 2012). Additionally, L-257 abolished DDAH1 activity in tissue lysates, stimulated an elevation in ADMA levels and diminished NO production in endothelial cells and aortic rings in culture (Leiper et al., 2007), but had no effects on NO production in macrophages which only expressed DDAH2 (Nandi et al., 2012).

In mesenteric resistance arteries mounted under isometric and isobaric conditions, the addition of L-257 (100 μM) further inhibited ADMA-resistant ACh vasorelaxation/-dilation during EDH block, indicating the continuous turnover of ADMA and the role of DDAH1 in ADMA metabolism to protect NOS activity. Although limited studies have specifically examined the functional impact of DDAH1 inhibition using DDAH1 inhibitors in mesenteric resistance arteries, this observation aligns with the literature on the modulatory action on ADMA by DDAH1. Incubation with 100 μM L-257 disrupted NO signalling in aortic rings resulting in augmented PE-induced vasocontraction and attenuated vasorelaxation to ACh (Leiper et al., 2007). Although Leiper et al. did not examine the effects of DDAH1 inhibition on the vasodilatory responses to ACh in mesenteric arteries, the authors reported the progressive enhancement in PE-induced vasocontraction in second order (300 – 600 μm) mesenteric arteries during DDAH1 inhibition (Leiper et al., 2007), suggesting that similar modulatory mechanism is present in the mesenteric microvasculature. This is supported by the data presented in this chapter where DDAH1 inhibition further attenuated ACh vasodilatory responses in third-order mesenteric arteries in the presence of ADMA.

Comparable inhibitory effects were also reported in genetically modified animal models. In heterozygous DDAH1-deficient ($DDAH1^{+/-}$) mice, reduced DDAH1 activity blunted ACh vasorelaxation in aortic rings *ex vivo* and raised arterial blood pressure and systemic vascular resistance *in vivo* (Leiper et al., 2007). Subsequent studies using the LoxP/Cre approach generated endothelial specific homozygous DDAH1 knockouts reported similar vascular dysfunction to Leiper et al., with attenuations in NO synthesis and vasorelaxation in response to ACh in aortic segments, and rises in plasma ADMA levels in $DDAH1^{-/-}$ mice (Hu et al., 2009). On the other hand, overexpression of DDAH1 enhanced enzyme activity and reduced ADMA levels, leading to lower blood pressure and systemic vascular resistance compared to

wildtype (Dayoub et al., 2003). In mesenteric arteries, DDAH1 overexpression rescued endothelium-dependent vasorelaxation in obese mouse models compared to controls (Powers and Gefter, 2012). Similarly, DDAH1 overexpression reduced ADMA levels and protected against angiotensin-induced endothelial dysfunction by restoring vasorelaxation to ACh in mesenteric arteries (Kopaliani et al., 2021). However, in contrast to our data, another study showed that silencing DDAH1 had little to no effects on ACh vasorelaxation in mesenteric resistance arteries *ex vivo* despite a modest increase in plasma ADMA levels (Wang et al., 2007). However, the lack of inhibition on vasorelaxation may be due to only <40% silencing of DDAH1 (Wang et al., 2007). Therefore, the residual (>60%) intact DDAH1 expression and activity following gene silencing may still be sufficient for normal ADMA turnover, supported by a minute increase in ADMA levels, which are 50 – 80% lower when compared to concentrations observed in DDAH1 knockout animal models (Leiper et al., 2007, Hu et al., 2009, Hu et al., 2011). Together with the literature, the findings here support the crucial role of DDAH1 in ADMA metabolism in the mesenteric microvasculature, and how disruptions to DDAH1 activity may contribute to endothelial dysfunction due to the accumulation of ADMA.

While DDAH1 inhibition by L-257 (100 μM) in the presence of ADMA further attenuated vasorelaxation/-dilation in mesenteric resistance arteries, vasodilatory responses to ACh persisted. One could hypothesise that the residual responses could be due to the modulatory actions by other DDAH isoform, DDAH2, which was not investigated in the current study. However, unlike its counterpart, the involvement of DDAH2 in ADMA metabolism has been a matter of debate and recent studies revealed that DDAH2 cannot metabolise ADMA. Hu et al. (2011) demonstrated that global DDAH1 deletion completely abolished DDAH activity, leading to the accumulation of ADMA. Although the authors did not report the DDAH activity in mesenteric or the coronary microvasculature specifically, in conventionally known

DDAH2 rich tissues, such as the lungs, DDAH activity was undetectable following DDAH1 deletion, despite intact DDAH2 expression (Hu et al., 2011). This is comparable to the observations in tissues expressing only DDAH2, such as the thyroid glands, which did not exhibit any DDAH activity, measured by the formation of L-citrulline following incubation with ADMA (Altmann et al., 2012). Similarly, DDAH2 gene silencing failed to increase plasma ADMA concentration despite a ~85% reduction in DDAH2 expression (Wang et al., 2007).

Additionally, the absence of DDAH1 also reduced nitrite/nitrate levels to ACh in aortic and mesenteric resistance arterial segments, and DDAH1$^{-/-}$ mice exhibited elevated blood pressure (Hu et al., 2011), further support the functional role of DDAH1 in the vasculature and the ability of endogenous ADMA to disrupt vascular reactivity. Moreover, using a combination of *in silico* and *in vitro* approaches and genetically modified cell and animal models, Ragavan et al. (2023) compared the effects of DDAH1 and DDAH2 in ADMA metabolism and reported several lines of evidence that supported the hypothesis that DDAH2 is incapable to metabolise ADMA: i) molecular docking and modelling experiments indicated that, in contrast to DDAH1, ADMA do not interact with the active site of DDAH2; ii) recombinant DDAH2 and overexpression of DDAH2 failed to convert ADMA to L-citrulline, indicating a lack of DDAH activity; and iii) unlike DDAH1 manipulation, knockdown or knockout of DDAH2 failed to disrupt DDAH activity in cell and mouse models (Ragavan et al., 2023). Together, these findings suggest that DDAH1 is the main regulator of methylarginine metabolism, and DDAH2 is not involved or its role in ADMA/L-NMMA metabolism is negligible. Therefore, it is unlikely that DDAH2 contribute to the residual effects observed in the present study, and raises questions regarding the functions of DDAH2 *in vivo*, which warrants further investigations.

Interestingly, researchers have proposed a role of intracellular alanine-glyoxylate aminotransferase 2 (AGTX2) in the metabolism of methylarginines, indicating an additional route of ADMA clearance (Rodionov et al., 2014). Although the current study did not examine the expression of AGTX2, it has been reported that AGTX2 is primarily expressed in the liver and kidneys (Rodionov et al., 2014). Therefore, based on the current knowledge, it is unlikely to contribute to the residual vasodilatory responses to ACh in our preparations. However, AGTX2 is likely to play a role ADMA metabolism *in vivo* as AGTX2 disruption increased plasma ADMA concentrations and produced a hypertensive phenotype in mouse model (Caplin et al., 2012). Therefore, future studies should examine the expression and the possible role of AGTX2 specifically in the vasculature.

We hypothesised the residual vasodilatory response is due to competition with L-arginine and other arginine derivatives, such as methylarginines, resulting in incomplete inhibition of DDAH1. As a homologue L-arginine (Rossiter et al., 2005), L-257 would compete with ADMA and L-arginine for cell entry via the CAT-1 transporter system, which acts as the first site of competition. Once inside (endothelial) cells, L-257, a reversible competitive DDAH1 inhibitor, competes with ADMA for DDAH1 binding. In an environment where ADMA levels are high, such as in this study, DDAH1 may preferentially bind to ADMA (K_d: 4.27 μM) and/or ADMA may displace L-257 (K_i: 13 μM) from the active site of DDAH1 due to a (~3 fold) higher affinity of ADMA for DDAH1 (Ragavan et al., 2023, Murphy et al., 2016). Furthermore, when ADMA was substituted with the synthetic NOS inhibitor, L-NAME, vasodilatory responses to ACh were abolished (Ng et al., 2024). Therefore, it is likely that in the presence of apamin, NS 6180, ADMA and L-257, NO synthesis was still intact. To confirm this hypothesis, future investigations should examine the effects of L-257 under a range of ADMA concentrations and vice versa in cell and intact artery models. Nevertheless, the data presented here in the

mesenteric resistance arteries support the role of DDAH1 in modulating the inhibitory actions of ADMA in the mesenteric microcirculation.

In contrast to the mesenteric microcirculation, ADMA abolished NO-dependent vasorelaxation/-dilation in myogenically active intra-septal coronary arteries (**Chapter 4**). Therefore, the effects of DDAH1 inhibition in the presence of ADMA on ACh vasodilatory response was not studied. The present study is the first to our knowledge to investigate whether DDAH1 inhibition with L-257, thus raising endogenous ADMA levels, enhances myogenic tone in the rat coronary microcirculation. Previous studies utilised genetic ablation of DDAH1 to examine its modulatory effects on blood pressure in a systems level (*in vivo*) or in the macrocirculation (using *ex vivo* aortic rings). In intra-septal coronary arteries mounted under isometric tension, the addition of L-257 (100 μM) increased myogenic tone by 60%, indicating the expression and the modulatory function of DDAH1 in the coronary microcirculation, and more importantly a continuous turnover of ADMA. While the intracellular ADMA concentrations were not measured in the current study, conclusions can be drawn from the literature reporting that chemical (by L-257 at concentration used in this study) and genetic disruptions to DDAH1 activity led to ADMA accumulation, impaired vascular homeostasis and augmented blood pressure and vascular resistance (Leiper et al., 2007, Hu et al., 2009, Hu et al., 2011). Therefore, one could hypothesise that L-257 indirectly augments myogenic tone through DDAH1 inhibition, leading to the accumulation of ADMA within intra-septal coronary arteries. Nevertheless, the augmentation in intracellular ADMA concentration by DDAH1 inhibition/L-257 should be measured in future experiments.

The observation that inhibition of DDAH1 augments coronary myogenic tone is significant as the involvement and importance of ADMA in cardiovascular disease have been questioned due

to the plasma concentrations of ADMA and L-arginine *in vivo*. As aforementioned, the physiological plasma ADMA concentrations in humans and rodents are reported to be 0.3 – 1 μM (Teerlink et al., 2009). This can typically increase by as much as 10-fold in diseases, although higher plasma ADMA concentrations (3 – 15 μM) have been observed in pathological conditions (Vallance et al., 1992a, Böger, 2003). While plasma ADMA concentration is a useful indicator for cardiovascular disease, intracellular ADMA concentration may be more relevant as: i) ADMA inhibits (endothelial) NOS expressed in vascular endothelial cells; and ii) the expression of DDAH1 will modulate the intracellular concentration of ADMA in various vascular beds, as shown in the present study (Ng et al., 2024), despite a relatively constant circulating plasma concentration. Although limited studies have measured the intracellular ADMA levels, it is estimated that the concentration of ADMA is 10 – 20-fold higher intracellularly than in the plasma (Teerlink et al., 2009). Therefore, this puts ADMA levels slightly above/close to the estimated K_i for eNOS (~1 μM) under physiological conditions and manifold higher during pathophysiology. While this supports an ability of ADMA to inhibit eNOS, the plasma and intracellular concentrations of L-arginine are much higher at ≥100 μM and millimolar concentrations respectively (Jeserich et al., 1992, Teerlink et al., 2002, Davids and Teerlink, 2013), which are significantly above the K_m of eNOS (~3 μM) for L-arginine (Cardounel et al., 2007). Although ADMA would competitively inhibit eNOS, thus raising the K_m for L-arginine, L-arginine would in theory outcompete and saturates eNOS due to the high ratio of L-arginine to ADMA intracellularly. However, this does not appear to be the case as NO production is subjected to the availability of extracellular L-arginine despite the high concentration intracellularly (MacKenzie and Wadsworth, 2003, Zani and Bohlen, 2005). Therefore, other mechanisms are likely to contribute to this complex observation, which is widely termed as the “L-arginine paradox”.

Furthermore, in line with our observations regarding DDAH1, Ding et al. (2010) reported a loss-of-function polymorphism in the DDAH1 promoter region, which diminished the expression and activity of DDAH1 *in vitro* and *in vivo*, and was associated with increased risk in coronary heart disease and stroke. Similarly, Valkonen and colleagues identified numerous polymorphisms of DDAH1 which were associated with elevated plasma ADMA levels, and 6-fold and >50-fold increase in the occurrences of hypertension and coronary heart disease respectively compared to non-carriers (Valkonen et al., 2005). Together, the preliminary data presented here support the notions that: i) endogenous ADMA is capable of augmenting myogenic tone in the coronary microvasculature; ii) DDAH1 activity is crucial for vascular homeostasis; and iii) disturbances to ADMA turnover, such as with reduced DDAH1 activity, could alter the myogenic response and tone, promoting vasoreactivity and the development of coronary microvascular dysfunction.

Due to the differences in NOS inhibition by ADMA between the mesenteric and coronary vascular beds observed in the previous chapters, and the established role of DDAH1 in ADMA metabolism, the expression of DDAH1 in mesenteric resistance and intra-septal coronary arteries were examined and compared for the first-time using immunohistochemistry. Existing studies have mainly utilised Western blotting techniques to examine DDAH1 levels in tissue lysates, such as the heart and kidney (Leiper et al., 1999, Leiper et al., 2007, Hu et al., 2009), but not the microvasculature. Therefore, it is important to investigate whether the same modulatory mechanism is present in the microcirculation, particularly in the coronary microvasculature due to the more potent inhibitory actions of ADMA. The isolated arterial preparations and immunohistochemical techniques performed in this study offer a better resolution and insights as they allow the visualisation and semi-quantitative comparison of DDAH1 expression between cell types and vascular beds.

The specificity of DDAH1 primary antibody was confirmed by the absence of non-specific bands in Western blot with rat tissues (e.g. kidneys and liver) known to highly express DDAH1, and the lack of immunofluorescent signal in primary antibody negative control. Immunohistochemical staining revealed the presence of DDAH1 in both mesenteric resistance and intra-septal coronary arteries. The observations of DDAH1 expression in the coronary microvasculature are in line with previous reports using canine myocardial slices (Chen et al., 2005). Comparisons between arterial layers (vascular cell types) revealed that the expression of DDAH1 was the greatest in the endothelium in both vascular beds, indicating the vascular endothelium is a critical site for the metabolism of methylarginines. This is somewhat unsurprising as eNOS, essential for NO synthesis, is a target of ADMA and is highly expressed in the vascular endothelium. Thus, the presence of high levels of DDAH1 in the vascular endothelium offers a tight regulation on ADMA levels at the site of NO production to ensure vascular homeostasis. The importance of endothelial DDAH1 is in agreement with previous findings by Hu et al. (2009), where endothelial specific DDAH1 knockout mice showed little to no DDAH1 expression and reduced NO production in aortic rings *ex vivo*. Therefore, one could postulate that disruptions to the endothelium and/or alterations in DDAH1 expression or activity would lead to ADMA accumulation, resulting in endothelial dysfunction.

Interestingly, we revealed that DDAH1 expression is >5-fold lower in the endothelium of intra-septal coronary arteries compared to the mesenteric endothelium. This finding is significant as it highlights for the first time the variations in the metabolism of ADMA, and other methylarginines, by DDAH1 between vascular beds. Therefore, susceptibility to NOS inhibition by ADMA may vary depending on vascular beds. Furthermore, the lower metabolic capacity for ADMA in intra-septal coronary arteries, as suggested by the lower expression,

would favour a more effective inhibition of NOS. These hypotheses are supported by our observations in the previous chapters where NO-dependent vasodilatory responses to ACh were abolished by 300 μM ADMA in coronary resistance arteries (**Chapter 4**), but not in small mesenteric arteries (**Chapter 3**). This is noteworthy as the coronary microvasculature may have a greater susceptibility to endothelial dysfunction associated with ADMA due to the lower DDAH1 expression, and thus at a higher risk for developing microvascular dysfunction (e.g. increased vasoreactivity), leading to microvascular angina and ANOCA.

The findings presented here in mesenteric resistance and intra-septal coronary arteries showcase the importance of DDAH1 in the metabolism of ADMA to maintain normal vascular function, and how disruptions to DDAH1 activity and variation in expression levels can enhance vasoreactivity and susceptibility to ADMA-associated endothelial dysfunction. As such, augmenting DDAH1 expression and/or activity, thus restoring/increasing ADMA metabolism, in cardiovascular disease could be a possible therapeutic strategy to counter the rise of ADMA levels. Interestingly, studies have shown that DDAH1 expression can be regulated by farnesoid X receptors (FXRs) as the FXR response element sits upstream of the gene for DDAH1, and activation of FXRs *in vivo* increased DDAH1 expression in the liver and reduced plasma ADMA levels (Hu et al., 2006). The ability of FXRs to modulate DDAH1 expression and plasma ADMA levels indicate a possible association between FXR and vascular function. While the expression of FXRs has been reported in the kidneys and liver (Forman et al., 1995), established sites of DDAH1 expression and ADMA metabolism, it is unclear whether FXRs are expressed in the vasculature and its activation can modulate DDAH1 gene expression and ADMA concentrations. Therefore, this link between FXRs, DDAH1 and ADMA warrants further investigations as it could be a potential therapeutic option to manage ADMA levels and improve NO bioavailability in cardiovascular vascular diseases.

5.5 CONCLUSION

This chapter investigated the role of DDAH1 on NOS inhibition by ADMA in isolated rat mesenteric and intra-septal coronary resistance arteries using wire and pressure myography. The findings (**Figure 5.5.1**) presented here support the hypotheses that: i) DDAH1 prevents NOS inhibition by ADMA; ii) inhibition of DDAH1 augments myogenic tone in myogenically active intra-septal coronary arteries; and iii) expression of DDAH1 differs in mesenteric and coronary microvasculature.

The functional data support the continuous turnover of ADMA under physiological conditions and the crucial role of DDAH1 in ADMA metabolism and maintaining vascular homeostasis as L-257 enhanced the NOS inhibition by ADMA in mesenteric resistance arteries and augmented myogenic tone in intra-septal coronary arteries. Furthermore, immunohistochemical staining indicated the vascular endothelium is a major site of ADMA metabolism and revealed a low expression of DDAH1 in the coronary endothelium, which may translate to a greater susceptibility to vascular dysfunction associated with ADMA in the coronary microvasculature.

The observations made here provide valuable preliminary insights into the importance of DDAH1 in maintaining normal vascular function as disruptions to DDAH1 activity negatively impacted vascular reactivity. Therefore, enhancing DDAH1 expression and/or activity may be beneficial in cardiovascular diseases due to its interaction with ADMA.

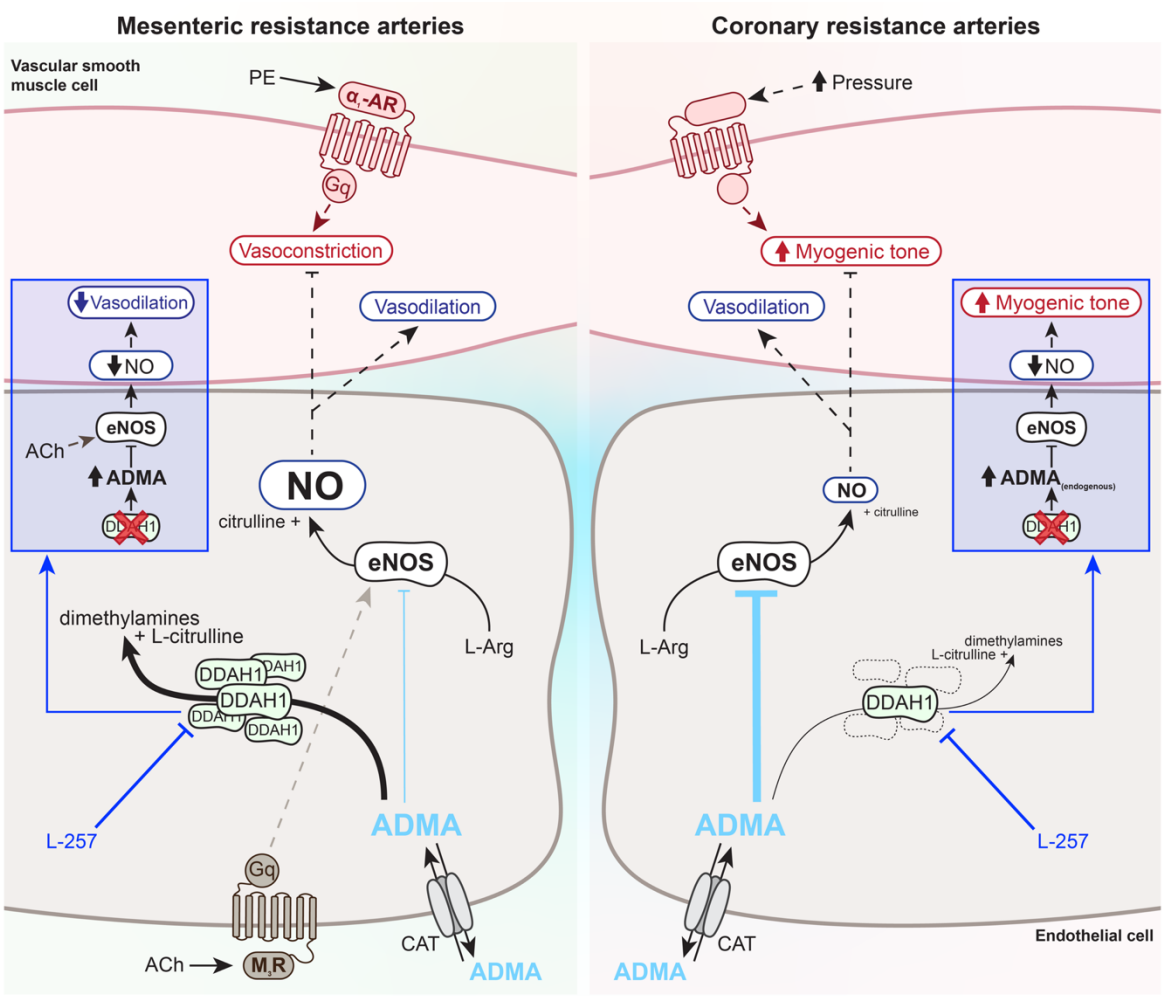


Figure 5.5.1 Summary of Chapter 5 – Dimethylarginine dimethylaminohydrolases 1 (DDAH1) expression is greater in mesenteric versus coronary resistance arteries and prevents endothelial nitric oxide (NO) synthase (eNOS) inhibition by asymmetric dimethylarginine (ADMA). Immunostaining revealed that DDAH1 expression is greater in mesenteric versus coronary resistance arteries. In phenylephrine (α_1-adrenoreceptor (α_1-AR) agonist; PE) pre-constricted mesenteric arteries, DDAH1 inhibition by selective DDAH1 inhibitor, L-257, further suppressed acetylcholine (ACh; M_3 muscarinic receptor (M_3R) agonist) vasodilation in the presence of ADMA and endothelium-dependent hyperpolarization inhibition, indicating that DDAH1 modulates the effects of ADMA. In myogenically active intra-septal coronary arteries, the lower DDAH1 expression supports our findings of more potent inhibitory effects of ADMA. L-257 increased myogenic tone in intra-septal coronary arteries, indicating a continuous turnover of ADMA and the ability of endogenous ADMA to modulate myogenic tone. Dashed arrows represent simplified signalling pathways. Overall effects of DDAH1 inhibition by L-257 are summarised in blue boxes. CAT = Cationic amino acid transporter; L-Arg = L-arginine.

CHAPTER SIX

INVESTIGATING THE EFFECTS OF L-ARGININE SUPPLEMENATION IN ADMA-MEDIATED ENDOTHELIAL DYSFUNCTION

6.1 INTRODUCTION

Since the confirmation of NO as endothelium dependent relaxing factor by Palmer et al. (1987) in porcine aortic endothelial cells, subsequent studies have investigated the origin of NO. Follow up studies in cultured vascular endothelial cells showed that the addition of L-arginine in arginine-free medium enhanced agonist-induced NO production, an effect that was absent using D-arginine (Palmer et al., 1988b). Using cascade superfusion bioassays where tissues were superfused by the effluent from stimulated endothelial cells, Palmer et al. (1988b) showed that the increase in endothelial cell NO synthesis by L-arginine evoked vasorelaxation in pre-contracted rabbit endothelium-free aortic strips. Furthermore, Gold et al. reported the importance of endogenous L-arginine and cGMP for vasodilation in bovine pulmonary arterial segments as the depletion of L-arginine correlated with a concomitant decrease in cGMP levels and an absence of vasorelaxation *ex vivo*, which were rescued by pre-incubation with exogenous L-arginine (Gold et al., 1990).

Previous research has investigated the use of NO donors to directly raise NO levels in patients with cardiovascular disease. Indeed, ACh-induced and spontaneous coronary vasospasm in patients during ACh provocation testing was reversed with NO donors such as isosorbide dinitrate and nitroglycerin (Okumura et al., 1988, Treasure et al., 1992, Mohri et al., 1998, Sun et al., 2002, Ong et al., 2012), supporting the use of nitrates in coronary vascular dysfunction. However, long-term use of nitrates to generate NO may be associated to excessive NO supplementation resulting in undesirable side effects, such as nitrosative stress and lower tolerance (Godo et al., 2021). Therefore, there is a need for alternative and/or additional approaches to rescue/protect NO signalling.

Due to the importance of L-arginine in NO synthesis, and thus in endothelium-dependent vasodilation, one can hypothesise that in endothelial dysfunction, as observed in many cardiovascular diseases, where NO generation and levels are compromised, raising intracellular and plasma levels of L-arginine could be an effective method to enhance NO synthesis and overcome the disruptions of vascular reactivity. This sparked interests in investigating the effects of L-arginine supplementation in *ex vivo* and *in vivo* animal studies. Palmer et al. (1988a) showed the addition of L-arginine reversed the attenuation in ACh-induced vasorelaxation in *ex vivo* rabbit aortic rings in the presence of endothelial dysfunction induced by L-NMMA. Similarly, the administration of L-arginine normalised the reduced ACh-induced vasodilation in cremaster arterioles during NOS inhibition by L-NMMA and L-NNA (Kaley et al., 1992). While the concentration of methylarginines was not measured, in experimental hypercholesterolaemic animal models, infusion of L-arginine or twelve-week oral treatment preserved vasorelaxation to ACh in aortic rings *ex vivo* (Cooke et al., 1991, Böger et al., 1995). Similarly, studies in non-human primates showed that long-term (six months) oral administration of L-arginine improved the cholesterol-mediated attenuation of ACh vasorelaxation and raised plasma nitrite and cGMP levels compared to controls (Dhawan et al., 2005). Together, these findings from animal studies support the capacity of exogenous L-arginine to reverse experimental endothelial dysfunction.

Surprisingly, despite the association of elevated levels of ADMA in many cardiovascular diseases, the direct effects of L-arginine supplementation on ADMA-induced endothelial dysfunction in the microvasculature have not been examined. This is particularly relevant in the coronary microcirculation as disturbances to coronary vascular function would disruption vascular homeostasis, altering coronary blood flow to the heart and promoting microvascular dysfunction, as occurs in microvascular angina and heart failure. Moreover, clinical studies

examining the effects of L-arginine administration in patients with cardiovascular disease tend to be of small sample sizes and reported mixed results (**Table 6.4.1**) despite promising data from animal studies. As such, it is essential that we further our understanding of the relationship between L-arginine, ADMA and vascular reactivity to enable the development of therapeutic treatments for patients with cardiovascular disease. This chapter investigated whether L-arginine supplementation can: i) rescue vasodilatory responses to ACh in mesenteric and coronary resistance arteries in the presence of ADMA, DDAH1 inhibition and EDH blockade; and ii) reverse ADMA-mediated increase in myogenic tone in myogenically active intra-septal coronary arteries.

6.1.1 Aims and hypotheses

We hypothesised that L-arginine supplementation would:

i) Rescue vasorelaxation and vasodilation to acetylcholine (ACh) in mesenteric and intra-septal coronary arteries in the presence of ADMA and block of endothelium-dependent hyperpolarization (EDH).

ii) Reverse the increase in myogenic tone to ADMA in myogenically active intra-septal coronary arteries.

The aims of this chapter were to:

i) Investigate whether L-arginine can rescue vasorelaxation/-dilation to ACh in mesenteric arteries in the presence of ADMA, EDH and DDAH1 inhibition.

ii) Examine whether L-arginine can reverse ADMA-induced myogenic tone in intra-septal coronary arteries.

iii) Assess whether L-arginine can rescue vasodilation to ACh in intra-septal coronary arteries in the presence of ADMA.

6.2 MATERIALS AND METHODS

6.2.1 Wire myography

Rat mesenteric and intra-septal coronary arteries were prepared for wire myography as described in **Chapters 2.1** and **2.2**. Arteries were normalised to a resting tension equivalent to that generated at 90% of the inner diameter of the vessel at 70 mmHg (mesenteric) and 80 mmHg (coronary). Following equilibration, only arteries that exhibited robust vasoconstriction to PE (mesenteric) or developed myogenic tone (coronary) and relaxed >95% to ACh (0.001 – 1 μM) were used for further experiments.

6.2.2 Pressure myography

Rat mesenteric and intra-septal coronary arteries were prepared for pressure myography as described in in **Chapters 2.1** and **2.3**. Arteries were cannulated onto glass micropipettes and intra-luminally pressurised to 70 mmHg (mesenteric) and 80 mmHg (coronary). Following equilibration, only arteries that exhibited robust vasoconstriction to PE (mesenteric) or developed myogenic tone (coronary) and relaxed >95% to ACh (0.001 – 1 μM) were used for subsequent experiments.

6.2.3 Drugs and inhibitors

The following drugs and inhibitors were used in this chapter: apamin (Ap, 100 nM) to inhibit SK_{Ca} channels, NS 6180 (NS, 1 μM) or TRAM 34 (TR, 1 μM) to inhibit IK_{Ca} channels, and N^G,N^G-dimethylarginine dihydrochloride (ADMA, 300 μM) and synthetic inhibitor, N_ω-Nitro-L-arginine methyl ester hydrochloride (L-NAME) to inhibit NOS. L-arginine (1 and 10 mM) to rescue vaso-relaxation and -dilation, or its inactive enantiomer, D-arginine (1 mM). See **Table 2.6.1** for more details.

6.3 RESULTS

6.3.1 L-arginine, but not D-arginine, rescues vasorelaxation and vasodilation in mesenteric arteries

To assess whether exogenous L-arginine can rescue vasorelaxation and vasodilation to ACh during ADMA, EDH and DDAH1 blockade in mesenteric arteries, arteries were incubated with L-arginine (1 mM) for 1 hour alongside the respective inhibitors for NOS, EDH and DDAH1.

In mesenteric arteries under isometric tension, the addition of L-arginine rescued vasorelaxation to cumulative ACh during inhibition of NOS and EDH, and even in the presence of a DDAH1 inhibitor, L-257 (**Figure 6.3.1C**). Representative traces for each condition are shown in **Figure 6.3.1A and B**. In the presence of L-arginine, E_{max}, as a percentage of maximum vasorelaxation, evoked by ACh was not different between the treatment groups (Control: 99.08 ± 0.52%; Ap, NS, ADMA, L-Arg: 95.30 ± 1.30%; Ap, NS, ADMA, L-257, L-Arg: 93.84 ± 1.77%; n = 7; $P > 0.05$; **Figure 6.3.1D**).

To confirm the effects of L-arginine, the inactive enantiomer, D-arginine was used (**Figure 6.3.2**). Simultaneous SK_{Ca} and IK_{Ca} channel blockade, with apamin (Ap, 100 nM) and TRAM 34 (TR, 1 μM), and NOS inhibition by ADMA (300 μM) attenuated vasorelaxation to ACh (E_{max}: Control: 99.48 ± 0.27%; Ap, TR, ADMA: 85.53 ± 4.43%; n = 11; $P < 0.05$; **Figure 6.3.2A, D and E**). The addition of L-arginine (1 mM) rescued vasorelaxation to ACh (E_{max}: Ap, TR, ADMA, L-Arg: 96.88 ± 0.98%; n = 10; $P < 0.05$ compared to Ap, TR, ADMA; **Figure 6.3.2B, D and E**). In contrast to L-arginine, blunted vasorelaxation to ACh persisted in the presence of 1 mM D-arginine (E_{max}: Ap, TR, ADMA, D-Arg: 87.27 ± 1.75%; n = 6; $P < 0.01$ compared to Control and Ap, TR, ADMA, L-Arg; **Figure 6.3.2C, D and E**).

The effects of L-arginine were also examined in pressurised mesenteric arteries. The addition of L-arginine (1 mM) again rescued ACh-vasodilation in the presence of apamin, NS 6180 and ADMA (E_{max}: Ap, NS, ADMA: 51.71 ± 8.74%; Ap, NS, ADMA, L-Arg: 91.25 ± 5.62%; n = 6–7; $P < 0.01$; **Figure 6.3.3**). In separate experiments, the presence of L-257 did not affect the reversal with L-Arg (E_{max}: Ap, NS, ADMA, L-257: 64.96 ± 4.65%; Ap, NS, ADMA, L-257, L-Arg: 99.97 ± 1.70%; n = 10; $P < 0.0001$; **Figure 6.3.4**). Representative diameter traces are shown in **Figure 6.3.3A** (for Ap, NS, ADMA) and **Figure 6.3.4A** (for Ap, NS, ADMA, L-257).

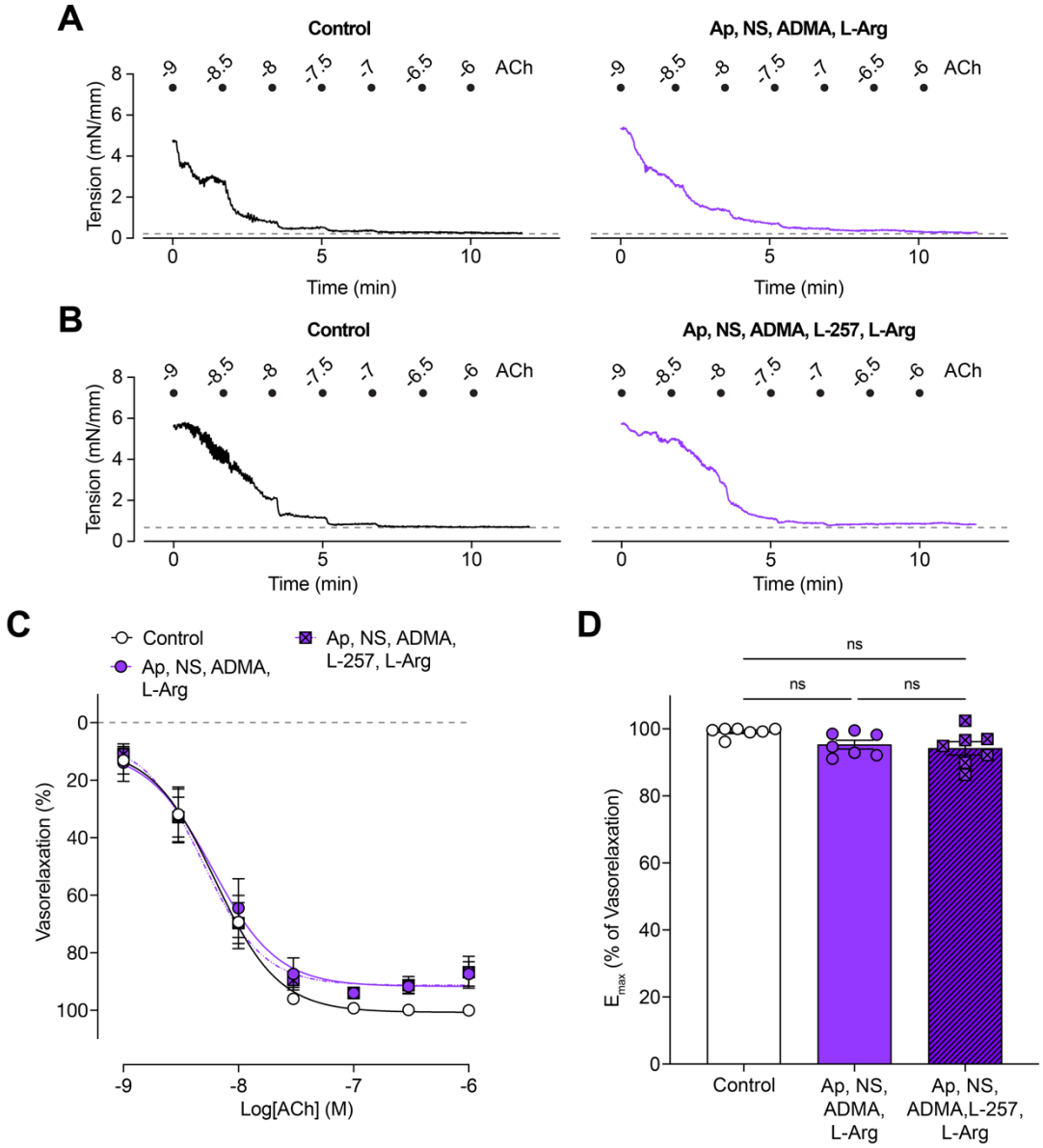


Figure 6.3.1 L-arginine (L-Arg) restores acetylcholine (ACh) vasorelaxation in the presence of asymmetric dimethylarginine (ADMA), endothelium-dependent hyperpolarization and dimethylarginine dimethylaminohydrolase 1 (DDAH1) inhibition in mesenteric arteries. **A – B,** Representative tension traces to cumulative ACh in the absence (Control) and presence of apamin (Ap; 100 nM), NS 6180 (NS; 1 μM), ADMA (300 μM) and L-Arg (1 mM; **A**) and DDAH1 inhibitor, L-257 (100 nM; **B**) in phenylephrine (α_1-adrenoreceptor agonist) pre-constricted mesenteric arteries under isometric tension. Dashed line indicates baseline tension. **C,** Concentration-response curves summarising ACh vasorelaxation in Ap, NS, ADMA ± L-257 ± L-Arg-treated mesenteric arteries. **D,** Bar graph summarising the E_{max} evoked by ACh in (**C**). Data are means ± SEM; n = 7. Analysed using one-way ANOVA with Tukey's multiple comparisons test.

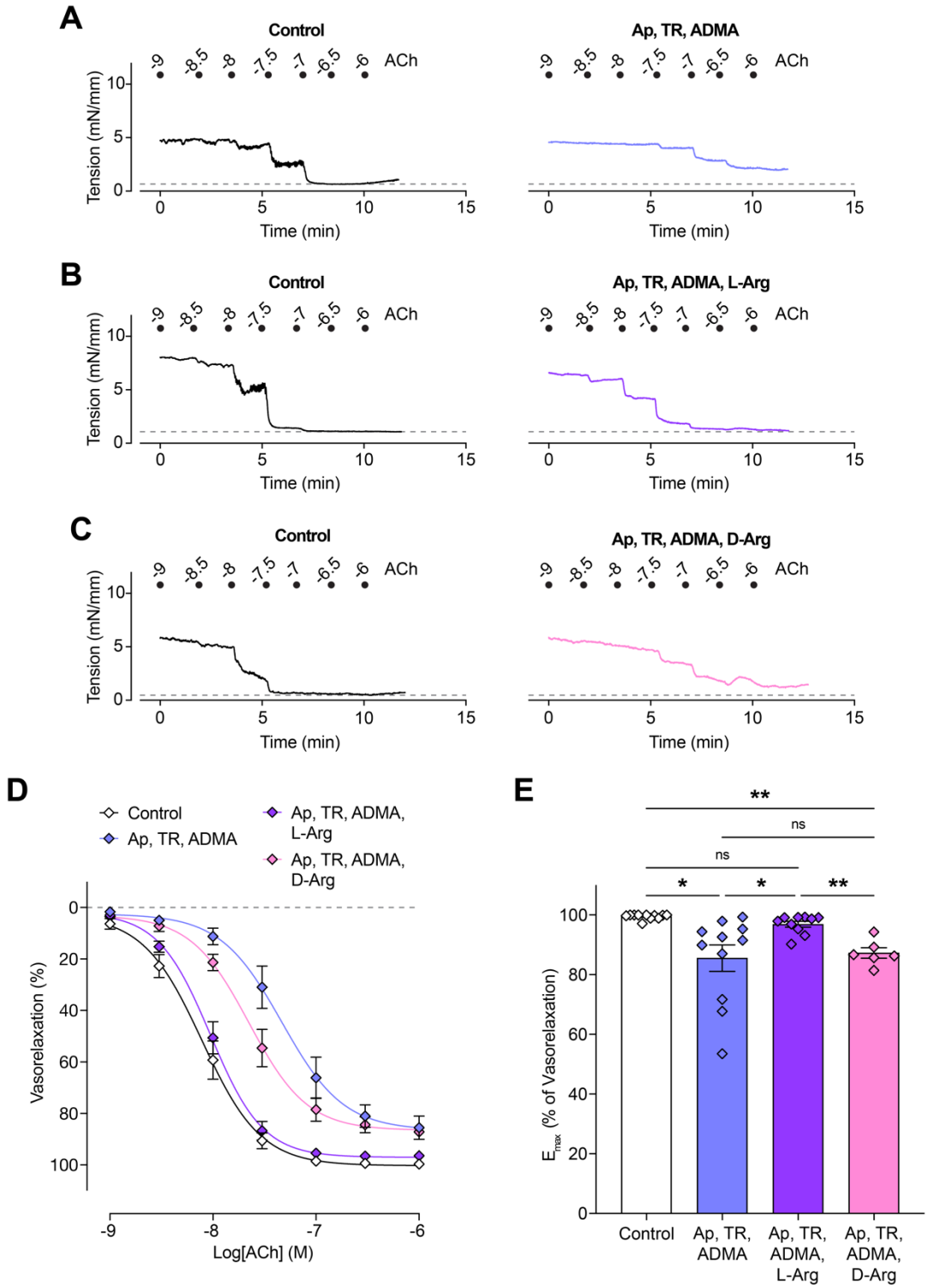


Figure 6.3.2 D-arginine is unable to restore vasorelaxation to acetylcholine (ACh) in the presence of asymmetric dimethylarginine (ADMA) and endothelium-dependent hyperpolarization blockade in mesenteric arteries. A – C, Representative tension traces for vasorelaxation to cumulative ACh in the absence (Control, Left panels) and presence of apamin (Ap, 100 nM), TRAM 34 (TR, 1 μM) and ADMA (300 μM; **A**, Right panel), and the addition of L-arginine (L-Arg, 1 mM; **B**, Right

panel) or D-arginine (D-Arg, 1 mM; **C**, Right panel). **D,** ACh concentration-response curves in the absence (Control) and the presence of Ap, TR, ADMA, ± L-Arg or D-Arg. **E,** Bar graph summarising the E_{max} evoked by ACh in (**D**). Data are means ± SEM; n = 6 – 11. *****$P < 0.05$, ******$P < 0.01$ using mixed-effects analysis with Tukey's multiple comparisons test.

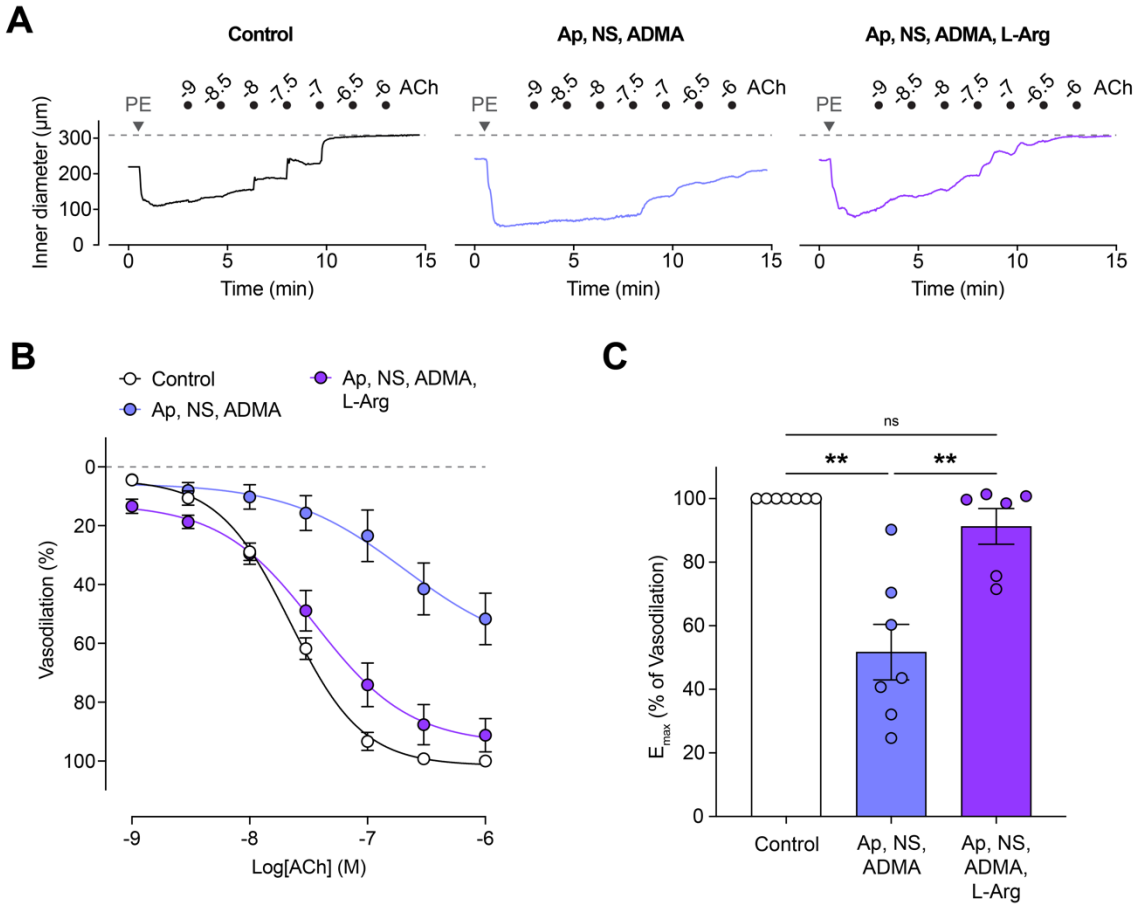


Figure 6.3.3 L-arginine rescues vasodilation to acetylcholine (ACh) in pressurised mesenteric arteries in the presence of asymmetric dimethylarginine (ADMA) and endothelium-dependent hyperpolarization blockade. A, Representative diameter traces for vasodilation to cumulative ACh before (Control; Left panel) and after incubation with apamin (Ap; 100 nM), NS 6180 (NS; 1 µM) and ADMA (300 µM; Middle panel), and the addition of L-arginine (L-Arg; 1 mM; Right panel) in phenylephrine (α_1-adrenoreceptor agonist; PE) pre-constricted pressurised mesenteric arteries. Dashed line indicates passive inner diameter. **B,** Concentration-response curves summarising ACh-vasodilation in pressurised mesenteric arteries before (Control) and after Ap, NS, ADMA ± L-Arg. **C,** Bar graph summarising the E_{max} elicited by ACh in (**B**). Data are means ± SEM; n = 6 – 7. $^{**}P < 0.01$ using mixed-effects analysis with Tukey's multiple comparisons test.

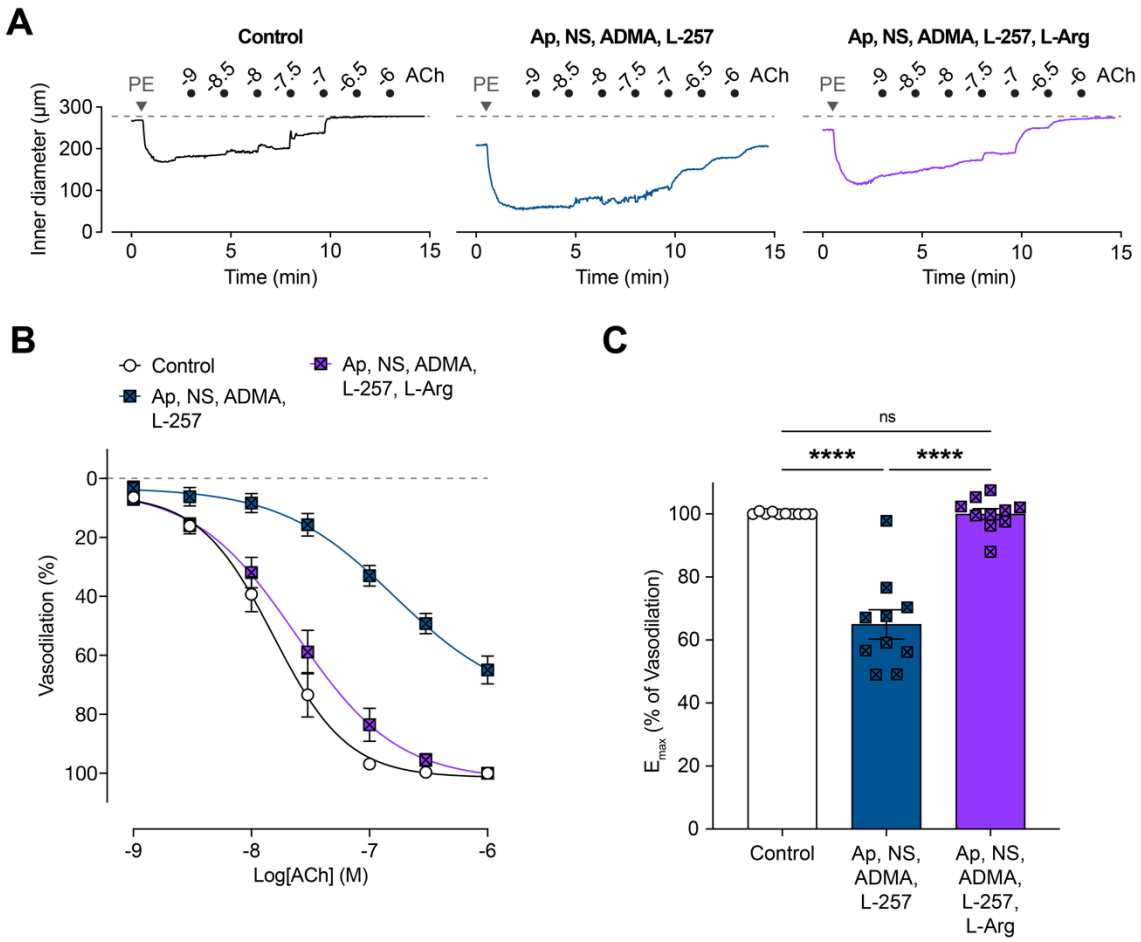


Figure 6.3.4 L-arginine rescues vasodilation to acetylcholine (ACh) in pressurised mesenteric arteries even during dimethylarginine dimethylaminohydrolase 1 (DDAH1), nitric oxide synthase and endothelium-dependent hyperpolarization blockade. A, Representative diameter traces for vasodilation to cumulative ACh before (Control; Left panel) and after incubation with apamin (Ap, 100 nM), NS 6180 (NS; 1 µM), asymmetric dimethylarginine (ADMA; 300 µM) and DDAH1 inhibitor, L-257 (100 µM; Middle panel), and the addition of L-arginine (L-Arg; 1 mM; Right panel) in phenylephrine (α_1-adrenoreceptor agonist; PE) pre-constricted pressurised mesenteric arteries. Dashed line indicates passive inner diameter. **B,** Concentration-response curves summarising ACh-vasodilation in pressurised mesenteric arteries before and after Ap, NS, ADMA, L-257 ± L-Arg. **C,** Bar graph summarising the E_{max} elicited by ACh in (**B**). Data are means ± SEM; n = 10. ****$P < 0.0001$ using one-way ANOVA with Tukey's multiple comparisons test.

6.3.2 L-arginine reverses ADMA-induced myogenic tone to basal levels in intra-septal coronary arteries

The effects of L-arginine on myogenic tone in intra-septal coronary arteries were first examined in arteries under isometric tension. Representative tension traces are show in **Figure 6.3.5A**. The addition of 1 mM L-arginine did not alter control myogenic tone (Control: 2.07 ± 0.34 mN/mm; + 1 mM L-Arg: 1.86 ± 0.34 mN/mm; n = 7; **Figure 6.3.5A and B left panels**). In contrast, the addition of 10 mM L-Arg lowered myogenic tone (1.39 ± 0.24 mN/mm; n =7; $P < 0.05$). In the presence of ADMA (300 μM), 1 mM L-Arg reversed myogenic tone back to basal (Control; **Figure 6.3.5B left panel**) myogenic tone (ADMA: 3.29 ± 0.27 mN/mm; + 1 mM L-Arg: 2.17 ± 0.30 mN/mm; n = 7; $P < 0.05$ compared to ADMA; **Figure 6.3.5A and B middle panels**). Increasing L-arginine concentration to 10 mM in the presence of ADMA further reduced myogenic tone (1.48 ± 0.20 mN/mm; n = 7; $P < 0.01$ compared to ADMA + 1 mM L-Arg; $P < 0.001$ compared to ADMA). In comparison, both L-arginine concentrations failed to reverse the myogenic tone induced by the synthetic NOS inhibitor, 100 μM L-NAME (L-NAME: 3.17 ± 0.18 mN/mm; + 1 mM L-Arg: 3.09 ± 0.16 mN/mm; + 10 mM L-Arg: 2.89 ± 0.17 mN/mm; n = 7; **Figure 6.3.5A and B right panels**).

In separate experiments, intra-septal coronary arteries were cannulated onto glass micropipettes and the effects of 1 and 10 mM L-arginine on myogenic tone were studied. Representative diameter traces are shown in **Figure 6.3.6A**. Both concentrations of L-arginine reversed ADMA augmented myogenic tone to basal values (Control), as a percentage of maximum vasoconstriction, (Control: 38.71 ± 2.02%; ADMA: 59.09 ± 2.36%; $P < 0.0001$ compared to Control; + 1 mM L-Arg: 45.54 ± 3.03%; $P < 0.01$ compared to ADMA; + 10 mM L-Arg: 39.57 ± 1.74%; $P < 0.0001$ compared to ADMA; n = 7; **Figure 6.3.6B**).

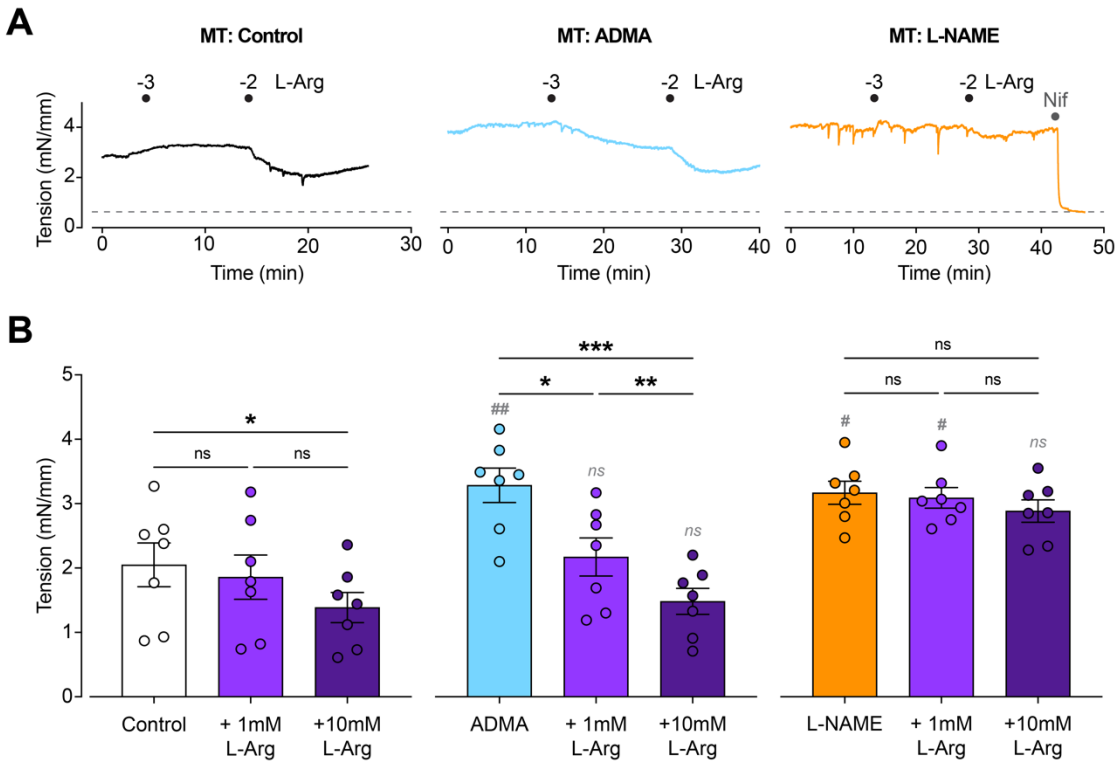


Figure 6.3.5 L-Arginine (1 mM) reverses asymmetric dimethylarginine (ADMA)-induced myogenic tone but not control myogenic tone in intra-septal coronary arteries under isometric tension. A, Representative tension traces from control myogenic tone (MT; Left panel), MT in the presence of ADMA (300 µM; Middle panel) or L-NAME (100 µM; Right panel) to 1 and 10 mM L-arginine (L-Arg) in intra-septal coronary arteries under isometric tension. Nifedipine (Nif; 1 µM) was added at the end of experiment to abolish tone. Dashed lines indicate baseline tension. **B,** Summary of the effects of L-Arg on MT in the absence (Left panel), presence of ADMA (Middle panel) or L-NAME (Right panel). Data are means ± SEM; n = 7. *$P < 0.05$, **$P < 0.01$, ***$P < 0.001$ within treatment group using one-way ANOVA with Tukey's multiple comparisons test. $^{\#}P < 0.05$, $^{\#\#}P < 0.01$ compared to Control myogenic tone using one-way ANOVA with Dunnett's multiple comparisons test.

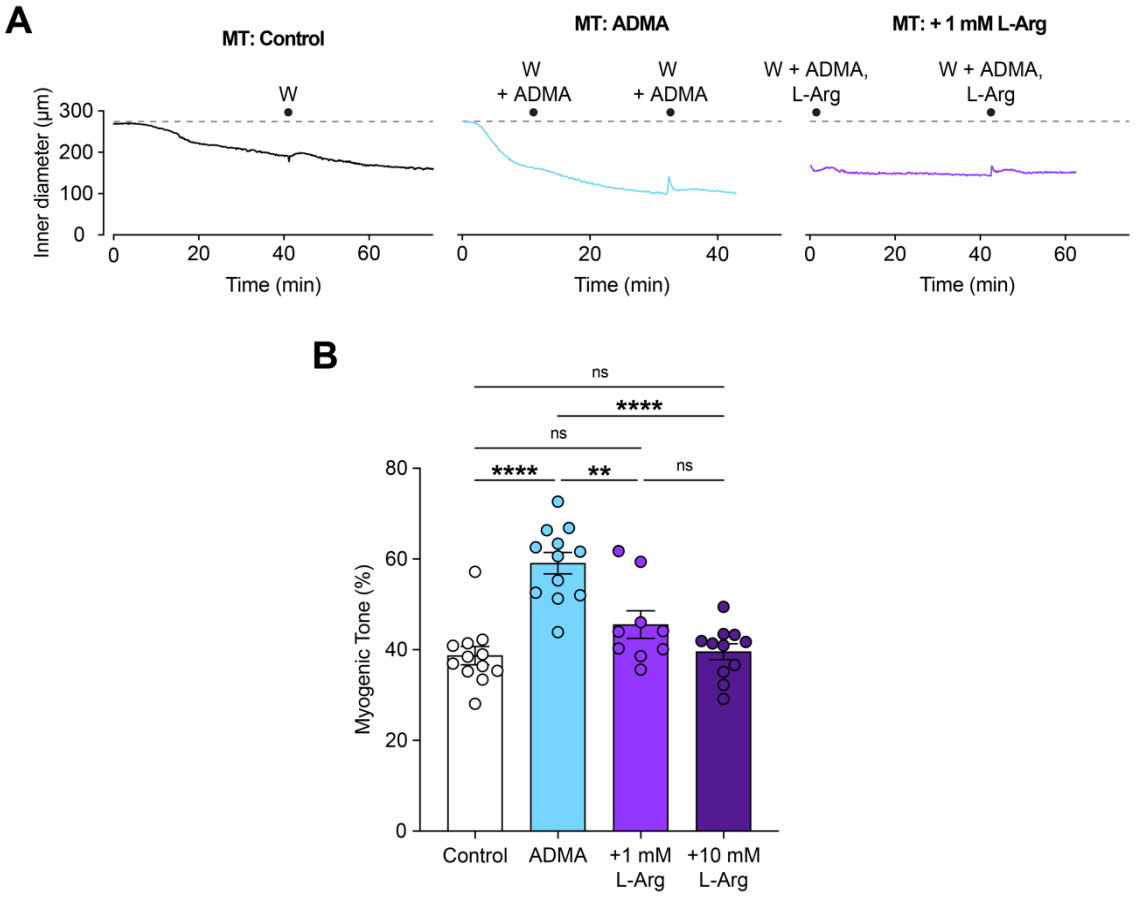


Figure 6.3.6 L-Arginine reverses asymmetric dimethylarginine (ADMA)-induced vasoconstriction in pressurised intra-septal coronary arteries. A, Representative diameter traces for myogenic tone (MT) in Control (Left panel) and in the presence of ADMA (300 µM; Middle panel) and L-arginine (L-Arg, 1 mM; Right panel) in myogenically active pressurised intra-septal coronary arteries. Dashed line indicates passive inner diameter. **B,** Bar graph summarising myogenic tone, as a percentage of maximum vasoconstriction, in pressurised coronary arteries in the absence (Control) and the presence of ADMA ± L-arginine (L-Arg; 1 or 10 mM). Data are means ± SEM; n = 9 – 12. $^{**}P < 0.01$, $^{****}P < 0.0001$ using on-way ANOVA with Tukey's multiple comparisons test.

6.3.3 L-arginine rescues vasodilation in pressurised intra-septal coronary arteries in the presence of ADMA

The effect of L-arginine on vasodilation to cumulative ACh was examined in pressurised intra-septal coronary arteries in the presence of ADMA. Representative diameter traces are shown in **Figure 6.3.7A**. In the presence of 300 μM ADMA, 1 h incubation of L-arginine, at both 1 and 10 mM, rescued vasodilation to ACh (E_{max}: ADMA: 59.29 ± 7.71%; + 1 mM L-Arg: 99.51 ± 1.42%; $P < 0.05$; + 10 mM L-Arg: 98.10 ± 2.46%; $P < 0.01$; n = 8 – 12; **Figure 6.3.7B**).

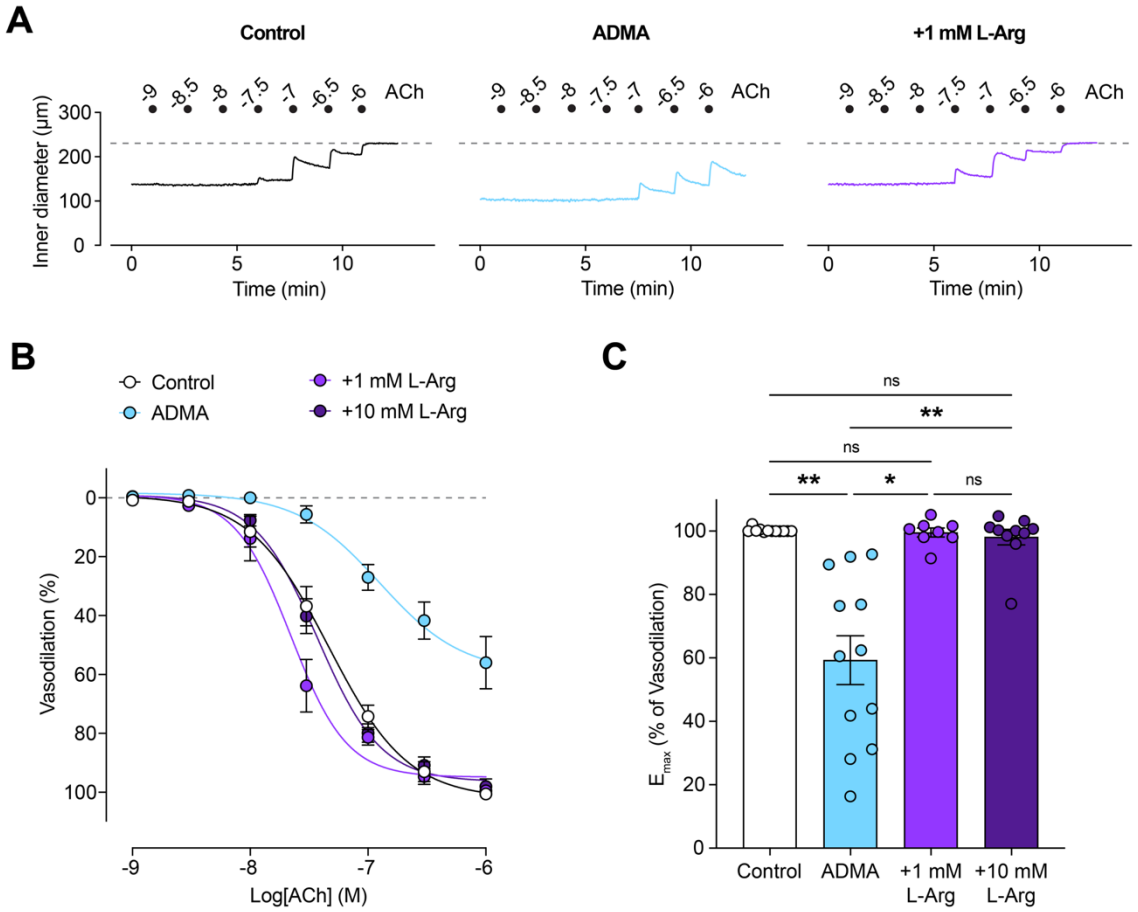


Figure 6.3.7 L-arginine (1 mM) rescued vasodilation to acetylcholine (ACh) in pressurised intra-septal coronary arteries in the presence of asymmetric dimethylarginine (ADMA). **A,** Representative diameter traces for vasodilation to cumulative ACh in the absence (Control; Right panel) and presence of ADMA (300 µM; Middle panel) and L-arginine (L-Arg; 1 mM; Right panel) in pressurised myogenically active intra-septal coronary arteries. Dashed line indicates passive inner diameter. **B,** Concentration-response curves for ACh-vasodilation in Control, ADMA and in the addition of L-Arg (1 or 10 mM). **C,** Bar graph summarising the E_{max}, as percentage of maximum vasodilation, evoked by ACh in (**B**). Data are means ± SEM; n = 9 – 12. **P* < 0.05, ***P* < 0.01 using mixed-effects analysis with Tukey's multiple comparisons test.

6.4 DISCUSSION

The experiments in this chapter investigated, for the first time, whether L-arginine supplementation can reverse endothelial dysfunction induced by ADMA in mesenteric and coronary resistance arteries mounted under either isometric or isobaric conditions. The findings presented here support the hypotheses that the administration of L-arginine can rescue endothelium-dependent vasorelaxation/-dilation to ACh in mesenteric resistance and intra-septal coronary arteries, and can reverse the increase in myogenic tone induced by ADMA in myogenically active intra-septal coronary arteries.

To examine the effects of L-arginine supplementation on endothelium-dependent vasorelaxation/-dilation in the presence of NOS inhibition by ADMA, EDH inhibition by apamin and NS 6180 or TRAM 34, and DDAH1 inhibition by L-257 (endothelial dysfunction), third-order mesenteric resistance arteries were studied using wire and pressure myography. Similarly in myogenically active intra-septal coronary arteries, the effects of exogenous L-arginine on endothelium-dependent vasodilatory responses and on myogenic tone in the presence of ADMA were examined. The concentrations of L-arginine were selected as previous studies in aorta and skeletal muscle arterioles (Kaley et al., 1992, Frew et al., 1993, Leiper et al., 2007, Al-Zobaidy et al., 2010) and in myogenically active cerebral arteries and arterioles (Faraci et al., 1995, Segarra et al., 1999) reported that 1 or 10 mM L-arginine reversed the effects of NOS and DDAH1 inhibition by methylarginines and L-257 respectively at concentrations used in the current study.

In mesenteric resistance arteries mounted under both isometric and isobaric conditions, the inhibitory effects of ADMA alone and combined with L-257 on ACh-induced vasorelaxation/-dilation were prevented by 1 mM L-arginine. In contrast, the reversal in the vasodilatory

responses to ACh was absent in arteries treated with D-arginine, which is not a substrate for NOS or a precursor for NO synthesis (Palmer et al., 1988b, Palmer et al., 1988a). Similarly in pressurised intra-septal coronary arteries, the addition of 1 mM L-arginine was sufficient to rescue NO-dependent vasodilation to ACh in the presence of ADMA as increasing the concentration did not potentiate the beneficial effects of L-arginine supplementation. The salutary effects of L-arginine are consistent with previous cell and animal studies in NOS inhibition by methylarginines and in microvascular dysfunction. Infusion of L-arginine reversed the blunted flow- and ACh-mediated vasodilation in the presence of L-NMMA back to control levels in canine epicardial coronary arteries *in vivo* (Chu et al., 1991). More recent studies examined directly the effect of ADMA and exogenous L-arginine showing that co-incubation of L-arginine could reverse the inhibitory effects of ADMA on NO synthesis in culture endothelial cells (Böger et al., 2000). Furthermore, and similar to the findings here, L-arginine, but not D-arginine, reversed the inhibitory effects of ADMA on ACh-induced vasorelaxation in canine circumflex coronary arteries *ex vivo* (Cable et al., 2009).

Due to the difficulties and limitations of current *in vivo* technologies for assessing the diameter of the coronary microvasculature at high resolution, limited clinicals studies have examined the direct effects of L-arginine supplementations on the coronary microcirculation. Those studies that have attempted to investigate the effects of L-arginine in the coronary microvasculature either used other peripheral (micro-)vascular beds and/or coronary blood flow as a proxy for diameter measurements. Furthermore, most of these studies failed to measure and report the plasma and intracellular concentrations of ADMA in healthy and diseased subjects. Nevertheless, the beneficial effects of L-arginine observed here is consistent with the limited clinical studies (summarised in **Table 6.4.1**) examining L-arginine

supplementation in patients with cardiovascular disease and risk factors, including conditions that are now known to be associated with elevated plasma ADMA levels.

Focusing on the coronary microvasculature, in both hypercholesterolaemic patients and patients undergone cardiac transplantation, L-arginine infusion reversed the blunted coronary blood flow increase to ACh (Drexler et al., 1991, Drexler et al., 1994). Dubois-Rande et al. (1992) reported L-arginine infusion attenuated vasoconstriction in left anterior descending coronary arteries to ACh, where vasoconstriction indicates endothelial dysfunction, and improved increase in coronary blood flow to ACh in patients with hypercholesterolaemia and atherosclerosis. Comparable with our findings, intra-coronary infusion of L-arginine significantly augmented vasodilation to ACh in epicardial coronary arteries in patients with microvascular angina, which was absent in health subjects (Egashira et al., 1996). Moreover in a double-blind randomised clinical trial, long-term (six-months) oral L-arginine supplementation (3 g ter in die; t.i.d) enhanced increases in coronary blood flow to ACh compared with placebo in patients with coronary heart disease and minimal diameter stenosis (Lerman et al., 1998). While the authors of these studies did not measure the plasma ADMA concentration, subsequent studies observed elevated plasma ADMA levels in patients with hypercholesterolaemia and microvascular angina (Böger et al., 1998, Chen et al., 2002, Lu et al., 2017), suggesting an association between increased ADMA and the development of microvascular dysfunction. Indeed, although the direct effects of L-arginine in the coronary vasculature was not assessed, Piatti et al. reported that plasma ADMA concentrations were higher in patients with microvascular angina (~0.7 μM) compared to control (~0.4 μM), and showed that L-arginine infusion normalised NO production and enhanced forearm blood flow (Piatti et al., 2003). Therefore, due to the close interaction between L-arginine and ADMA with NOS, it is reasonable to suggest that the beneficial effect of L-arginine supplementation is due

to L-arginine outcompeting ADMA, a suggestion which is supported by the findings in this chapter.

As mentioned, the beneficial effect of L-arginine has been questioned because not all clinical studies observed a beneficial effect with L-arginine supplementation. Blum et al. (2000) reported that one-month oral L-arginine supplementation (3 g t.i.d) in patients with coronary artery disease failed to enhance either NO production or basal/hyperaemia-mediated blood flow in brachial arteries despite an increase in plasma L-arginine levels. Similarly, while two weeks oral L-arginine (5 g t.i.d) increased L-arginine plasma concentration, there was no change in vasodilation to ACh in brachial arteries in males with stable angina (Walker et al., 2001). Finally, Chin-Dusting et al. (1996) reported that four-week oral L-arginine treatment failed to restore endothelial function assessed by forearms blood flow in patients with severe heart failure.

The lack of therapeutic effects following oral L-arginine supplementation may reflect a combination of factors: i) the bioavailability of L-arginine would influence the ability of exogenous L-arginine to raise plasma and intracellular concentrations. The average bioavailability of oral L-arginine is estimated to be ~20%, with a range from 5 – 50% (Tangphao et al., 1999). Such large variability may help explain the discrepancy in the therapeutic effect of oral L-arginine in clinical studies; ii) long-term (six months) oral L-arginine treatments did improve coronary vascular function (Lerman et al., 1998) compared to shorter term exposure (≤ four weeks). This suggests that the treatment period may impact on the effectiveness of L-arginine supplementation; and iii) as demonstrated in **Chapter 5**, the endothelial metabolic enzyme DDAH1 plays a crucial role in modulating intracellular concentration of ADMA, which will be reflected in the plasma. Despite the crucial importance

of DDAH1 in determining cellular ADMA levels, and as such regulating NO synthesis, clinical studies have not considered the possibility of individual variability of DDAH1 activity in trial design and in the interpretation of patient outcomes; and iv) as L-arginine competes with ADMA for NOS binding, the intracellular and plasma ADMA concentrations will play a significant role in determining the outcome of L-arginine supplementation.

The latter hypothesis is supported by the differential observations reported by several studies which measured plasma ADMA levels. In patients with microvascular angina, Palloshi et al. (2004) reported that plasma ADMA concentration to be ~0.64 μM, with plasma L-arginine concentration increased to ~72 μM (L-Arg/ADMA ratio = ~113) following oral supplementations of L-arginine for four weeks (2 g t.i.d), which was associated with enhanced forearm blood flow. Similarly, in patients with hypercholesterolaemia (plasma ADMA concentration = 3.5 μM), Sydow et al. (2003) reported a comparable increase in plasma L-arginine concentration with oral supplementation, an increase that was accompanied by enhanced flow-mediated vasodilation in the radial artery. Whereas, in patients where oral L-arginine failed to produce an effect, despite an increase in plasma L-arginine levels to ~117 μM, Walker et al. (2001) reported that the plasma ADMA concentration was 5.6 μM (L-Arg/ADMA ratio = ~21). Therefore, it is plausible that despite the increase in plasma L-arginine, the intracellular, and thus plasma, pools of L-arginine are unable to outcompete ADMA at multiple points in the L-arginine/ADMA/NO cascade (e.g. cell entry and NOS binding) due to the high intracellular and plasma ADMA levels. This may also explain the failure of oral L-arginine to enhance NO synthesis and improve vascular function observed in the studies described above. As such, ADMA concentration is likely to be one of the main culprits for the lack of positive therapeutic effect with L-arginine supplementation. Furthermore, it highlights the importance of monitoring patient ADMA levels in the design of

treatment protocols involving of L-arginine supplementation. Thus, it is essential to measure the intracellular and/or plasma concentrations of ADMA in future *in vivo* animal and clinical studies.

While this was outside the scope of the current study, intracellular L-arginine level is modulated by arginase in cells. Berkowitz et al. (2003) showed aged-associated increase in endothelial arginase expression in aorta of old Wistar rats, and arginase inhibition with BEC ((S)-(2-boronoethyl)-l-Cysteine-HCl) augmented vasorelaxation to L-arginine in PE pre-constricted aortic rings, which was previously absent. Furthermore, intravenous infusion of ADMA in Wistar rats increase mean arterial pressure and systemic vascular resistance and was potentiated with prior infusion of arginase (Richir et al., 2009), indicating a role of arginase in the vascular dysfunction. Thus, it is likely that L-arginine through (oral) supplementation would be metabolised by plasma and intracellular arginases, limiting the intracellular effects of L-arginine. Hence, in addition to the low and varied oral bioavailability of L-arginine (Tangphao et al., 1999), this may explain the lack of therapeutic effects with L-arginine. Therefore, the involvement of arginase should be probed *ex vivo* in intra-septal coronary arteries with BEC in the presence of ADMA and L-arginine to examine whether arginase inhibition augments the effects of 1 mM L-arginine or produces the same effect as 1 mM at lower L-arginine concentrations.

Together with the literature described, data presented in this chapter is significant in: i) confirming the competitive reversible nature of NOS inhibition with ADMA, indicated by L-arginine reversal; and ii) supporting the therapeutic use of L-arginine supplementation as a means to reverse microvascular endothelial dysfunction due to elevated ADMA levels, as

1 mM L-arginine successfully restored vasodilation to ACh during inhibition of NOS and of DDAH1.

In separate experiments, the effect of L-arginine supplementation (1 and 10 mM) on myogenic tone during NOS inhibition by ADMA were examined in isometric and isobaric intra-septal coronary arteries. One millimolar L-arginine was shown to be sufficient to reverse the augmented tone with ADMA, returning myogenic tone to basal levels but not abolishing the basal (control) myogenic tone. Although L-arginine at higher concentration (10 mM) also reversed ADMA-induced enhanced myogenic tone, this concentration also reduced myogenic tone under control conditions. In contrast to ADMA, L-arginine (1 and 10 mM) failed to rescue NOS inhibition by L-NAME, presumably reflecting higher affinity binding to NOS. The L-arginine reversable effect of ADMA is comparable to previous reports in the cerebral microcirculation, where the addition of (1 mM) L-arginine prevented the augmented tone with ADMA (Faraci et al., 1995, Segarra et al., 1999).

Although previous studies have not directly examined the effect of L-arginine on the extent ADMA influences basal coronary microvascular tone, several studies that examined the effects of L-arginine supplementation in the presence of exogenous L-NMMA or on basal myogenic tone. L-arginine infusion reversed the L-NMMA enhanced myogenic tone in epicardial canine coronary arteries to basal levels (Chu et al., 1991). While in humans, L-arginine supplementation prevented an increase in myogenic tone in epicardial coronary arteries and in coronary vascular resistance with L-NMMA, restoring coronary blood flow in both atherosclerotic and healthy subjects (Quyyumi et al., 1997). Overall, this indicates the reversibility of methylarginines in an *in vivo* setting.

Although plasma ADMA concentrations were not measured, a similar beneficial effect with L-arginine supplementation was observed in patients. Intra-coronary infusion of L-arginine caused a small but significant increase in basal coronary blood flow in hypercholesterolaemic patients (Dubois-Rande et al., 1992). In patients with coronary artery disease but angiographically normal arteries experiencing stable angina, infusion of L-arginine, but not D-arginine, caused vasodilation in the left anterior descending and circumflex coronary arteries (Tousoulis et al., 1999). L-arginine infusion also enhanced forearm blood flow and reduced blood pressure, associated with increase NO production and cGMP levels, in patients with microvascular angina (Piatti et al., 2003). Similar enhancement in NO and cGMP levels, and reduction in peripheral vascular resistance were observed in type 2 diabetic patients after one-month oral L-arginine (3 g t.i.d), changes that were absent in placebo control subjects (Piatti et al., 2001). Additionally, a recent study by Lauer and colleagues indicates that L-arginine (infusion) preferentially dilates stenotic arterial segments of the left anterior descending coronary artery compared to pre- and post-stenotic regions and to control arteries in patients with chronic stable angina (Lauer et al., 2008). L-arginine-mediated vasodilation correlated with an increase in coronary blood flow, which was not associated with D-arginine. Overall, these observations are consistent with our data where although 1 mM L-arginine did not alter basal myogenic tone, it did reverse ADMA-mediated vasoconstriction. However, we also show that at a higher concentration, L-arginine can disrupt vascular homeostasis as it reduced basal myogenic tone.

We show in the coronary microvasculature that (1 mM) L-arginine supplementation is effective in reversing augmented myogenic tone with ADMA, but without disrupting normal vascular function (basal myogenic tone). This supports the use of L-arginine in addressing microvascular dysfunction. While NO synthesis was not examined directly in the current study,

the most reasonable explanation of the salutary effects of L-arginine supplementation is due to L-arginine outcompeting ADMA for NOS binding. Further investigation is needed to confirm this hypothesis *ex vivo* and *in vivo*. Nevertheless, data presented here provide preliminary but crucial insights into the possible mechanism by which L-arginine can rescue endothelial function in patients with cardiovascular diseases and risk factors that are known to associate with raised levels of ADMA. Conversely, at higher concentrations, L-arginine may also depress coronary myogenic tone, which may compromise autoregulation. Therefore, caution is required in determining an appropriate concentration of L-arginine to ensure a beneficial effect whilst not impacting physiological function. As such, further investigation should elucidate the relationship between L-arginine and ADMA, and determine the optimal ratio for these two compounds to enable L-arginine effectively to outcompete ADMA. This is likely to be dependent on intracellular, and thus plasma, ADMA concentrations, highlighting the importance of ADMA measurements.

Table 6.4.1 Summary table of the mentioned studies in Chapter 6.4 that examined the effects of L-arginine supplementation in patients with cardiovascular disease. L-Arg = L-arginine; ADMA = asymmetric dimethylarginine; HC = Hypercholesterolaemia; AS = Atherosclerosis; MVA = Microvascular angina; T2DM; Type 2 Diabetes Mellitus; CAD = coronary artery disease; HF = Heart failure; t.i.d = ter in die (three times a day); PAD = Peripheral artery disease; HTN = Hypertension; – = Data not measured/reported. Values expressed as mean ± SEM.

Studies	Patients (sample size)	Route of administration	Dosage of L-Arg	Plasma [L-Arg] (μM)		Plasma [ADMA] (μM)
				Before	After	
Drexler et al. (1991)	HC (n = 15)	Intra-coronary infusion	160 μmol/min (20 min)	–	–	–
Dubois-Rande et al. (1992)	HC, AS (n = 13)		25 mg/min	–	~1000	–
Drexler et al. (1994)	HC (n = 18)		10 mg/kg (15 min)	–	–	–
Egashira et al. (1996)	MVA (n = 16)		50 mg/min (10 min)	–	–	–
Tousoulis et al. (1999)	T2DM (n = 23)		50 and 150 μmol/min	–	–	–

Studies	Patients (sample size)	Route of administration	Dosage of L-Arg	Plasma [L-Arg] (μM)		Plasma [ADMA] (μM)
				Before	After	
Lauer et al. (2008)	CAD, MVA (n = 24)	Intra-coronary infusion	150 μmol/min (10 min)	–	–	–
Böger et al. (1998)	HC (n = 16)	Intravenous infusion	10 mg/kg	52.4 ± 5.4	4843.9 ± 233.5	2.2 ± 0.2
Piatti et al. (2003)	MVA (n = 23)		125 mg/min (120 min)	–	–	0.70 ± 0.06
Chin-Dusting et al. (1996)	HF (n = 27)	Oral	20 g; daily (1 month)	–	–	–
Lerman et al. (1998)	CAD (n = 26)		3 g; t.i.d (6 months)	83 ± 19	112 ± 11	–
Blum et al. (2000)	CAD (n = 30)		3 g; t.i.d (1 month)	70 ± 17	130 ± 53	–

Studies	Patients (sample size)	Route of administration	Dosage of L-Arg	Plasma [L-Arg] (μM)		Plasma [ADMA] (μM)
				Before	After	
Piatti et al. (2001)	T2DM (n = 22)	Oral	3 g; t.i.d (1 month)	–	–	–
Walker et al. (2001)	Stable Angina (n = 40)		5 g; t.i.d; (2 weeks)	80 ± 2	117 ± 4	5.6 ± 0.3
Sydow et al. (2003)	PAD, HC (n = 27)		8 g; t.i.d (8 weeks)	47 ± 7	71 ± 13	3.1 ± 0.4
Palloshi et al. (2004)	MVA, HTN (n = 13)		2 g; t.i.d (4 weeks)	54 ± 17.4	71.7 ± 19.7	0.64 ± 0.13

6.5 CONCLUSION

This chapter investigated effects of L-arginine supplementation in endothelial dysfunction by elevated ADMA levels in isolated rat mesenteric and intra-septal coronary resistance arteries using wire and pressure myography. The findings (**Figure 6.5.1**) presented here support the hypotheses that L-arginine supplementation: i) rescues vasorelaxation/-dilation to ACh in the mesenteric and coronary microvasculature in the presence of endothelial dysfunction by ADMA, DDAH1 inhibition and endothelium-dependent hyperpolarization blockade; and ii) reverses the enhanced myogenic tone by elevated levels of ADMA in myogenically active intra-septal coronary arteries.

The observations made here provide valuable preliminary insights into the possible mechanism involved in the beneficials effects of L-arginine seen in patients with coronary artery disease and microvascular dysfunction. Therefore, supporting the clinical use of L-arginine supplementation. Furthermore, it highlights the importance of plasma and intracellular ADMA concentration measurements in subsequent *in vivo* animal and clinical studies examining the therapeutic effects of L-arginine.

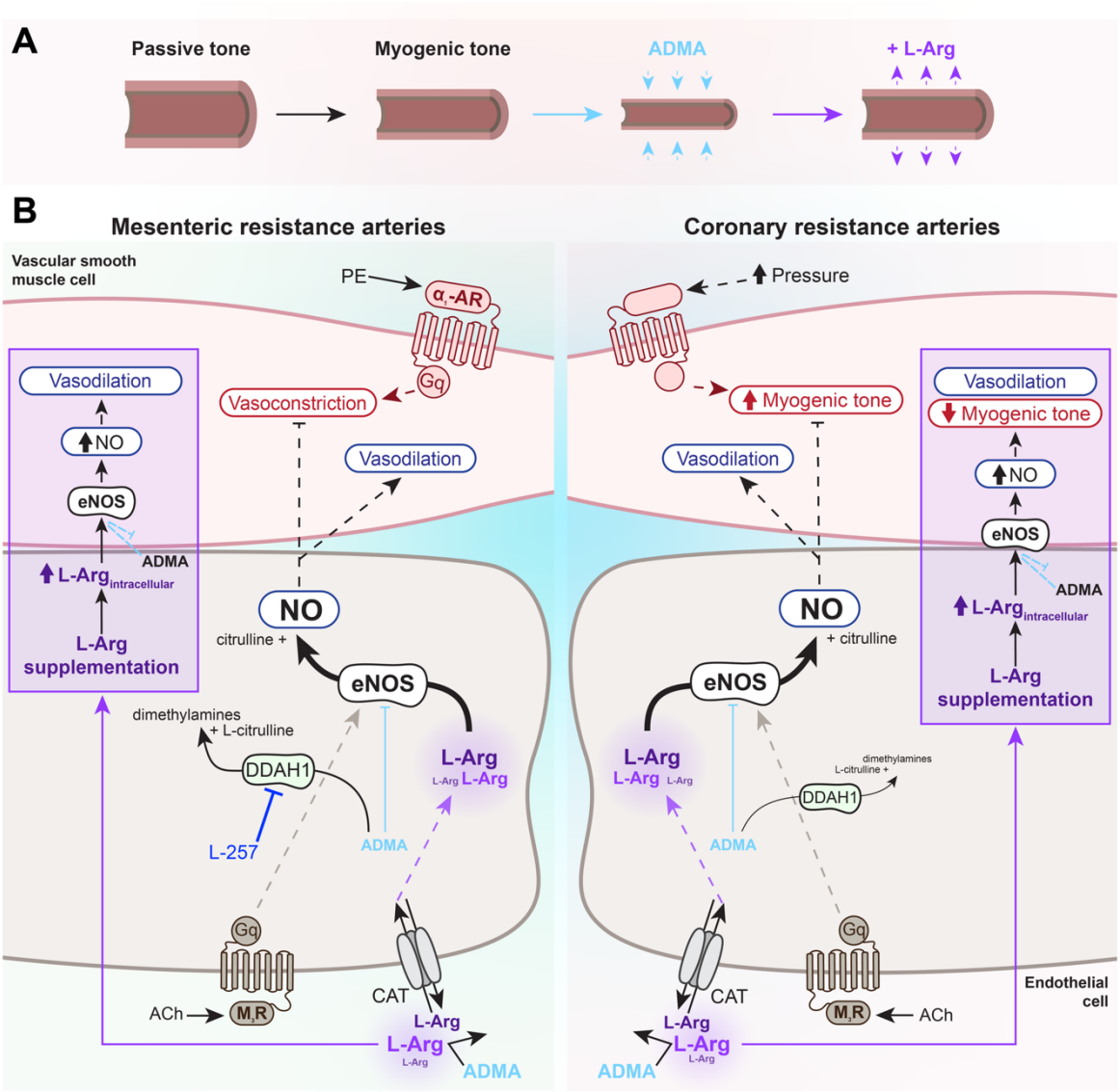


Figure 6.5.1 Summary of Chapter 6 – L-arginine (L-Arg) supplementation reverses the endothelial nitric oxide (NO) synthase (eNOS) inhibition by asymmetric dimethylarginine (ADMA). A, Diagram representation of the effects of ADMA ± L-Arg on myogenic tone (MT) in myogenically active intra-septal coronary arteries. **B,** L-Arg supplementation rescues NO-dependent vasodilation to acetylcholine (ACh; M_3 muscarinic receptor (M_3R) agonist) in phenylephrine (PE; selective α_1-adrenergic receptor (α_1-AR) agonist) pre-constricted mesenteric resistance arteries in the presence of ADMA, endothelium-dependent hyperpolarization inhibition and dimethylarginine dimethylaminohydrolases 1 (DDAH1) blockade by L-257. L-Arg reverses ADMA-induced augmented tone, but not basal myogenic tone, and rescued ACh vasodilation in intra-septal coronary arteries in the presence of ADMA. Dashed arrows represent simplified signalling pathways. Overall effects are summarised in purple boxes. CAT = Cationic amino acid transporter.

CHAPTER SEVEN

INVESTIGATING THE EFFECTS OF ADMA ON INTRACELLULAR Ca^{2+} IN THE CORONARY MICROCIRCULATION

7.1 INTRODUCTION

As observed in previous chapters, NOS inhibition with ADMA enhanced myogenic tone, and in separate experiments, our group showed that ADMA increased depolarising spikes in vascular smooth muscle of intra-septal coronary arteries (Ng et al., 2024). Furthermore, previous studies have reported that NO can modulate T-type VDCC activity and is associated with vasoconstriction in myogenically active cerebral and coronary arteries, and in non-myogenic mesenteric resistance arteries (Harraz et al., 2014, Smith et al., 2020), suggesting this modulation is likely to be present across vascular beds. Due to the importance of intracellular Ca^{2+} in myogenic tone and the ability of NO to modulate T-type VDCC activity, and as such Ca^{2+} influx into vascular smooth muscle, ADMA is likely to enhance vasoconstriction by increasing VSMC Ca^{2+} activity.

As mentioned in **Chapter 1.1.2**, endothelial cells often protrude through the fenestrations present in the internal elastic lamina and make contact with neighbouring vascular smooth muscle (Moore and Ruska, 1957). The prevalence of these protrusions, known as myoendothelial junctions (MEJs) and myoendothelial gap junctions (MEGJs) present in these protrusions, increases as the diameter of mesenteric arteries decreases (Sandow and Hill, 2000) suggesting a possible predominant influence microvasculature. Subsequent studies showed that MEGJs allow bidirectional transmission of electrochemical signals, such as hyperpolarization and Ca^{2+}, between vascular smooth muscle and endothelial cells (Beny and Pacicca, 1994, Yashiro and Duling, 2000). The transfer of signals allows for tight modulation on vascular tone and therefore vascular resistance (Dora et al., 1997, Mather et al., 2005), a phenomenon known as myoendothelial feedback. This feedback mechanism is supported by the findings in previous chapters where NOS inhibition with ADMA enhanced PE-induced vasoconstriction in mesenteric resistance arteries (**Chapter 3**) and myogenic tone in intra-septal coronary arteries

(**Chapter 4**). As such any increased VSMC Ca^{2+} with ADMA is likely to signal to neighbouring endothelial cells and increase intracellular endothelial cell Ca^{2+} (EC Ca^{2+}) as part of myoendothelial feedback.

Despite the importance of intracellular Ca^{2+} in myogenic tone and vasoconstriction and the coupling between VSMCs and endothelial cells, limited studies have investigated Ca^{2+} signalling and myoendothelial feedback in intact coronary resistance arteries under myogenic tone. Due to the enhancement on myogenic tone and depolarising spikes with ADMA, this chapter investigated the effects of ADMA on VSMC and EC Ca^{2+} in myogenically active intra-septal coronary arteries using a combination of Ca^{2+}-sensitive fluorescent indicators and wire and pressure myography.

7.1.1 Aims and hypotheses

We hypothesised that:

i) The augmented myogenic tone with ADMA in intra-septal coronary arteries is associated with increases in intracellular Ca^{2+} events in VSMCs.

ii) ADMA would increase Ca^{2+} events in endothelial cells of coronary arteries.

The aims of this chapter were to investigate the effects of ADMA on:

i) Vascular smooth muscle cell Ca^{2+} in intra-septal coronary arteries under isometric tension.

ii) Endothelial cell Ca^{2+} in intra-septal coronary arteries under isobaric condition.

7.2 MATERIALS AND METHODS

7.2.1 Wire myography

Rat intra-septal coronary arteries were prepared for wire myography as described in **Chapters 2.1** and **2.2**. Arteries were normalised to a resting tension equivalent to that generated at 90% of the inner diameter of the vessel at 80 mmHg. Following equilibration, arteries were left to develop myogenic tone. Only arteries that developed myogenic tone and relaxed >95% to ACh (0.001 – 1 μM) were used for further experiments.

7.2.2 Wire myography calcium imaging

Vascular smooth muscle cells of intra-septal coronary arteries were loaded with Ca^{2+}-sensitive fluorescent indicator, CalBryte 520 AM (2.5 μM; 2550971, AA Bioquest, USA) at 30°C until a clear signal was detected, as described in **Chapter 2.2.6**. See **Table 2.6.3** for more details of the fluorescent indicator used.

7.2.3 Pressure myography

Intra-septal coronary arteries were prepared for pressure myography as described in **Chapters 2.1** and **2.3**. Arteries were cannulated and secured on to glass micropipettes using nylon sutures, and intra-luminally pressurised to 80 mmHg. Following equilibration, arteries were left to develop myogenic tone. Only arteries with myogenic tone and relaxed >95% to ACh (0.001 – 1 μM) were used for subsequent experiments.

7.2.4 Pressure myography calcium imaging

Endothelial cells of intra-septal coronary arteries were selectively loaded with Ca^{2+}-sensitive indicator, Oregon Green BAPTA-1 AM (OGB-1, 10 μM; O6807, Invitrogen, USA) through the

lumen using a peristaltic pump at 30°C, until a clear signal was detected, as described in **Chapter 2.3.6**. See **Table 2.6.3** for more details of the fluorescent indicator used.

7.2.5 Inhibitors

N^G,N^G-dimethylarginine dihydrochloride (ADMA, 300 μM) was used to inhibit NOS. See **Table 2.6.1** for more details.

7.3 RESULTS

7.3.1 Augmented myogenic tone with ADMA in intra-septal coronary arteries is associated with an increase in VSMC Ca^{2+} flashes

To determine the effect of ADMA on intracellular Ca^{2+} in vascular smooth muscle, intra-septal arteries were mounted in a confocal wire myography chamber for simultaneous isometric tension and intracellular Ca^{2+} recordings. Vascular smooth muscle cells of coronary arteries were loaded with the Ca^{2+}-sensitive fluorescent indicator, CalBryte 520 AM (2.5 μM). Representative image of VSMCs loaded with CalBryte 520 AM is shown in **Figure 7.3.1A top panel**.

During myogenic tone (Control), coronary arteries developed isometric tension of 1.95 ± 0.30 mN/mm, which was associated with VSMC Ca^{2+} flashes at 0.93 ± 0.11 Hz (n = 7; **Figure 7.3.1B and C**). Simultaneous tension and Ca^{2+} recordings revealed ADMA (300 μM) increased both myogenic tone (3.25 ± 0.30 mN/mm; n = 7; $P < 0.01$; **Figure 7.3.1C**) and the frequency of Ca^{2+} flashes in VSMCs (1.08 ± 0.11 Hz; n = 7; $P < 0.05$; **Figure 7.3.1B**). Representative fluorescence intensity (F/F_0) traces of VSM Ca^{2+} flashes of the analysed regions are shown in **Figure 7.3.1A**.

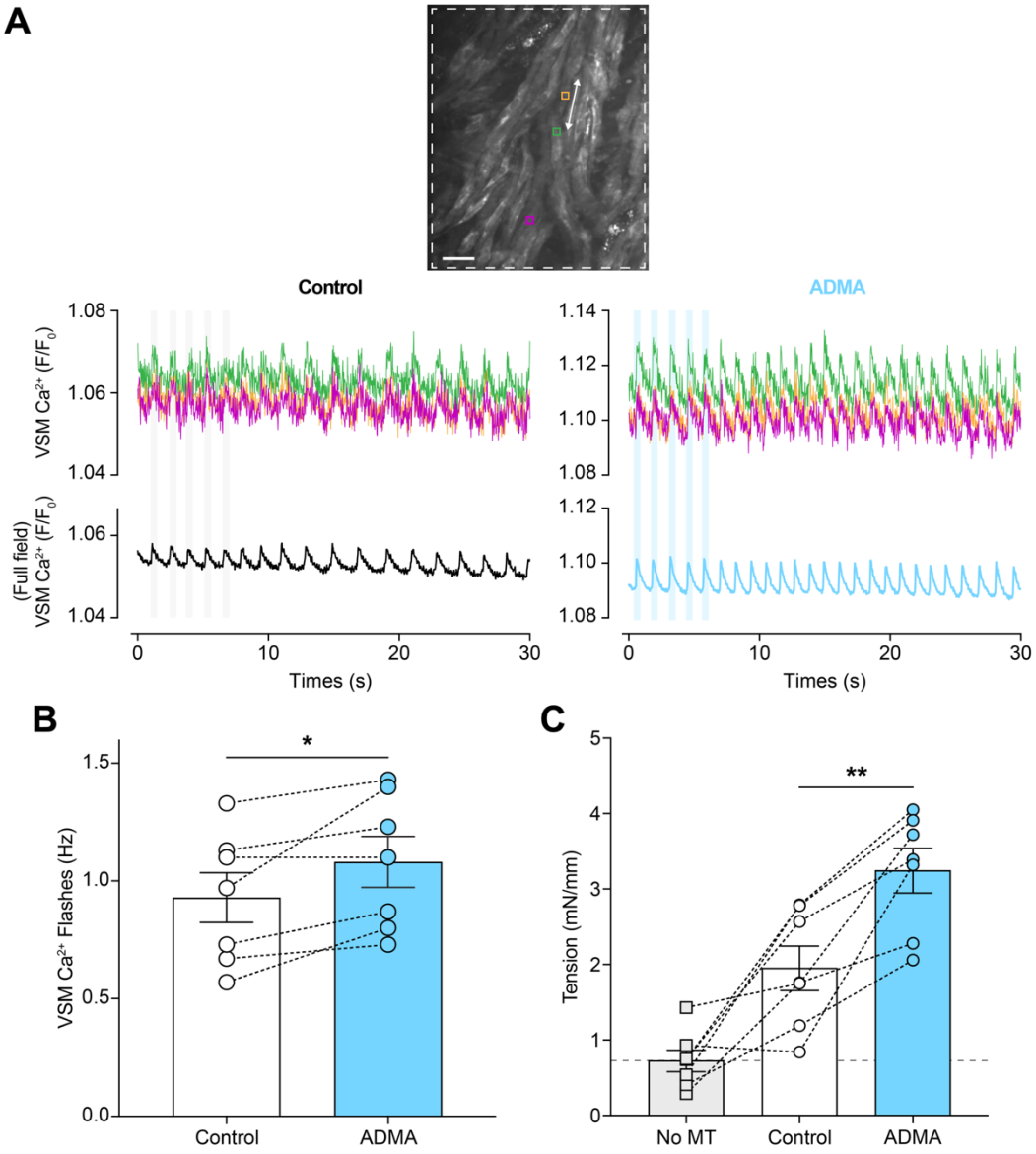


Figure 7.3.1 Asymmetric dimethylarginine (ADMA) increases the frequency of vascular smooth muscle cell (VSMC) Ca^{2+} flashes and myogenic tone (MT) in intra-septal coronary arteries. **A,** Representative image of VSMCs loaded with Ca^{2+}-sensitive fluorescent indicator, CalBryte 520 AM (2.5 µM; Top panel). Arrow indicates VSMC. Scale bar = 20 µm. Representative fluorescence intensity (F/F_0) traces of VSM Ca^{2+} flashes of the analysed regions in arteries (Top panel: Coloured squares (individual VSMC) = Top traces; White dashed square (full field) = Bottom traces) during MT (Control; Left) and after 300 µM ADMA (Right). **B – C**, Bar graphs summarising the frequency of VSMC Ca^{2+} flashes in Hz (**B**) and tension in mN/mm (**C**) in coronary arteries before (No MT) and following the development of MT (Control) and after ADMA. Dashed line indicates the mean baseline tension in (**C**). Data are means ± SEM; n = 7. **P* < 0.05, ***P* < 0.01 using paired two-tailed t-test.

7.3.2 ADMA increases EC Ca^{2+} events in pressurised intra-septal coronary arteries

To examine the effect of ADMA on EC Ca^{2+}, intra-septal coronary arteries were cannulated onto micropipettes in a confocal pressure myography chamber and intra-luminally pressurised. Endothelial cells were selectively loaded with Ca^{2+}-sensitive fluorescent indicator, Oregon Green BAPTA-1 AM (OGB-1; 10 μM), through the artery lumen. Representative fluorescent image of endothelial cells loaded with OGB-1 is shown in **Figure 7.3.2A top panel**.

During myogenic tone (Control), 24.67 ± 4.30% of endothelial cells exhibited intracellular Ca^{2+} events, with a frequency of 0.48 ± 0.07 events/min/cell (n = 5; **Figure 7.3.2B and C**). Asymmetric dimethylarginine (300 μM) increased both the percentage of endothelial cells with intracellular Ca^{2+} events (71.56 ± 6.51%; n = 5; $P < 0.01$; **Figure 7.3.2B**) and the frequency of Ca^{2+} events (2.11 ± 0.31 events/min/cell; n = 5; $P < 0.01$; **Figure 7.3.2C**). Representative traces for Control and ADMA are shown in **Figure 7.3.2A top and middle traces**. Arrowheads indicate intracellular Ca^{2+} events. Acetylcholine (100 – 1 μM) was added at the end of the experiment to confirm the health of endothelial cells in intra-coronary arteries. The concentration of ACh used was determined by the lowest ACh concentration that caused maximum vasodilation during the assessment of vascular reactivity. Acetylcholine evoked Ca^{2+} events, and at a higher frequency, in all endothelial cells in field of view (**Figure 7.3.2A bottom trace and B**).

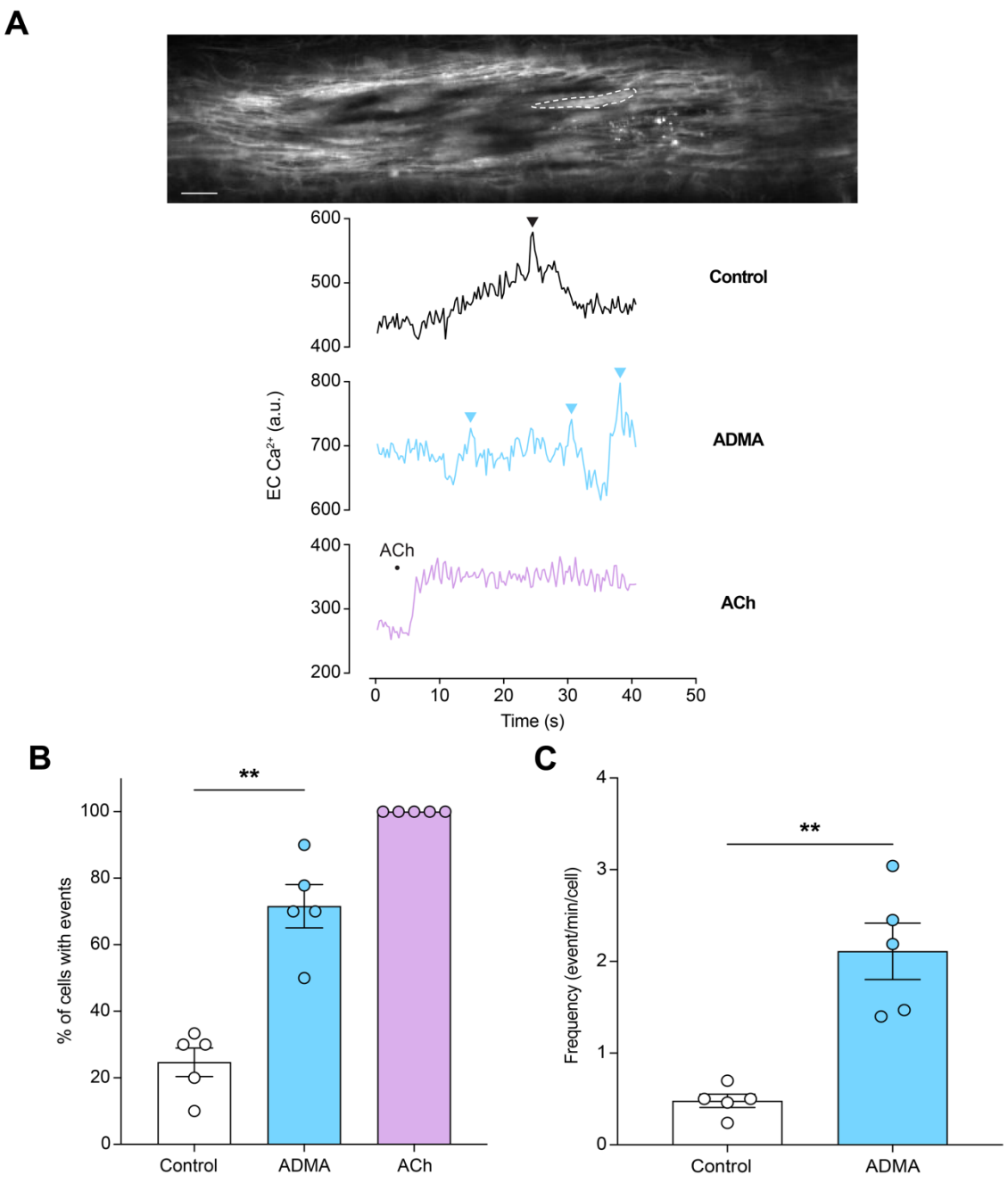


Figure 7.3.2 Asymmetric dimethylarginine (ADMA) increases endothelial cell (EC) Ca^{2+} events in pressurised intra-septal coronary arteries. A, Representative image of endothelial cells loaded with Ca^{2+}-sensitive fluorescent indicator, Oregon Green BAPTA-1 AM (10 μM; Top panel) and fluorescence intensity (arbitrary units; a.u.) traces of the analysed cell (dashed region) during myogenic tone (Control; Black trace), after the addition of ADMA (300 μM; Blue trace) and acetylcholine (ACh; Pink trace). Arrowheads indicate intracellular Ca^{2+} events. Scale bar = 20 μm. **B – C,** Bar graphs summarising the percentage of endothelial cells with Ca^{2+} events (**B**) and the frequency of Ca^{2+} events (**C**) in Control, after ADMA and ACh. Data are means ± SEM; n = 5. *$P < 0.01$ using paired two-tailed t-test.

7.4 DISCUSSION

The experiments in this chapter investigated the effects of NOS inhibition by ADMA on VSMC and EC Ca^{2+} signalling in myogenically active intra-septal coronary arteries. The findings presented here support the hypotheses that ADMA increases intracellular Ca^{2+} events in both vascular smooth muscle and endothelial cells of coronary resistance arteries.

To examine the effects of ADMA on VSMC Ca^{2+} events in the coronary microvasculature, VSMCs of intra-septal coronary arteries mounted under isometric tension were loaded with a Ca^{2+}-sensitive indicator, CalBryte 520 AM. Our group previously used CalBryte 520 AM to study VSMC Ca^{2+} in mesenteric and coronary resistance arteries (Smith et al., 2020, Lin et al., 2023, Ng et al., 2024). Here we show that under myogenic tone coronary VSMCs generates synchronous Ca^{2+} flashes at a frequency comparable to previous studies (Dora et al., 2022), and similar to the frequency of depolarising spikes in VSMCs of myogenically active coronary arteries (Ng et al., 2024). Furthermore, the augmented vasoconstriction, and depolarising spikes, with L-NAME and ADMA (Smith et al., 2020, Ng et al., 2024), are associated with increased VSMC Ca^{2+} flashes of matching frequency. These findings suggest that NO normally suppresses VSMC Ca^{2+} flashes, giving rise to depolarising spikes and subsequent VSMC contraction/vasoconstriction. Therefore, blocking NO synthesis with ADMA reduces this suppression on Ca^{2+} events, leading to augmented coronary vascular tone.

While the current study did not examine the signalling pathways contributing to these observations, the augmented VSMC Ca^{2+} flashes and depolarising spikes with NOS inhibition are dependent on Ca^{2+} influx and T-type VDCCs ($Ca_v3.x$). Previous studies from our group showed that T-type VDCC blocker, NNC 55-0396 (NNC) abolished the depolarising spikes induced by L-NAME and reduced vasoconstriction in intra-septal coronary arteries under

isometric tension (Smith et al., 2020). The enhanced depolarising spikes in vascular smooth muscle and vasoconstriction with L-NAME and ADMA were also observed in non-myogenic mesenteric resistance arteries upon PE stimulation, and were abolished by blocking T-type VDCCs (Smith et al., 2020, Ng et al., 2024). This contribution of T-type VDCC in vasospasm was first observed by McNeish et al. in rat middle cerebral arteries using simultaneous membrane potential and tension recordings. L-NAME evoked depolarising spikes and vasoconstriction in cerebral arteries were both abolished by selective T-type VDCC inhibitors, mibefradil and NNC (McNeish et al., 2010). Furthermore, NNC did not affect membrane potential or tension during basal myogenic tone, indicating a specific contribution of T-type VDCC in the development of vasospasm in the absence of NO. Comparable findings have also been reported in pressurised middle cerebral arteries and in isolated cerebral VSMCs (Howitt et al., 2013, Harraz et al., 2014). Interestingly, in the rat cerebral circulation, the contribution of T-type VDCCs seems to be inversely proportional to artery diameter as the mibefradil- and NNC-sensitive component in myogenic tone increases as cerebral artery diameter decreases (Kuo et al., 2010). Therefore, the involvement of T-type VDCC and associated VSMC depolarising spikes are likely to be features of vasospasm in the microcirculation with the loss of NO synthesis.

While the precise mechanism by which NO regulate T-type VDCC activity in the coronary microcirculation remains to be elucidated, NO activates the conversion of GTP to cGMP via soluble guanylyl cyclase (sGC) in VSMCs. Therefore, it is likely that this signalling cascade is involved in the modulation of T-type VDCC. Studies in cerebral and mesenteric resistance arteries using NO donors; sodium nitroprusside, SNAP (*S*-Nitroso-*N*-acetyl-DL-penicillamine) and SNOG (*S*-nitrosoglutathione), cGMP and inhibitor of sGC (ODQ) reported comparable suppression on T-type VDCC current (Harraz et al., 2014, Smith et al., 2020). Furthermore,

direct sGC activation with Bay 41-2272 in the presence of L-NAME prevented depolarising spikes and vasospasm, re-establishing vasomotion in PE-contracted mesenteric arteries (Smith et al., 2020). Therefore, these findings support the involvement of the NO-sGC-cGMP signalling in the microcirculation. Additionally, Howitt et al. (2013) observed that L-NAME increased T-type VDCC ($Ca_v3.1$) expression/trafficking to the membrane in isolated cerebral VSMCs. As such, recruitment of $Ca_v3.1$ may in part be involved in this modulation by NO, although the mechanism by which this occurs and its relevance in the coronary microcirculation remains to be investigated.

Interestingly, this modulation on T-type VDCC with NO has been reported to be both cGMP-dependent and -independent in the brain. In rat reticular thalamic neurons (expressing $Ca_v3.2$ and $Ca_v3.3$), Joksovic et al. (2007) reported the inhibition of T-type current with cGMP analogue, 8-Br-cGMP, suggesting the contribution of cGMP in modulating T-type VDCC activity. This inhibition was potentiated by *S*-nitrosothiols (e.g. SNOG and SNAP), which when added alone were sensitive to *N*-ethylmaleimide (NEM; thiol modifier/blocker) but not to ODQ, indicating a possible cGMP-independent effect of NO/*S*-nitrosothiols on T-type current. The lack of requirement of intracellular second messengers with *S*-nitrosothiols is supported by the comparable inhibition measured in outside-out patch clamp experiments (Joksovic et al., 2007), suggesting a direct effect of NO on T-type VDCC activity. These findings suggest the presence of both cGMP-dependent and -independent modulation on T-type VDCC current in reticular thalamic neurons. Lee et al. (2013) also observed comparable cGMP-independent T-type inhibition with SNOG in dorsal root ganglia (expressing $Ca_V3.2$), which was abolished with NEM and site-specific mutagenesis of cysteine residues in T-type VDCC. This indicates the possible involvement of *S*-nitrosylation of T-type channel cysteine residues in the modulation by NO/*S*-nitrosothiols. Therefore, the regulation on T-type VDCC

by NO (and NO donors) through cGMP-dependent and/or *S*-nitrosylation mechanisms may depend on the tissue, cell type and receptor subtypes. In addition to clear contribution of T-type VDCC in the generation of depolarising spikes and associated vasospasm, this warrants further research as T-type VDCC modulation may act as a therapeutic target for endothelial microvascular dysfunction.

In separate experiments, endothelial cells of pressurised intra-septal coronary arteries were loaded with a Ca^{2+}-sensitive indicator, OGB-1, by luminal perfusion as previous described (Kansui et al., 2008), to investigate the effects of ADMA on EC Ca^{2+}. In the absence of agonist stimulation, spontaneous Ca^{2+} events were observed in coronary endothelial cells under myogenic tone. Asymmetric dimethylarginine increased the frequency of and the percentage of endothelial cells with Ca^{2+} events. This is, to our knowledge, the first demonstration of spontaneous EC Ca^{2+} events in pressurised intra-septal coronary arteries under myogenic tone and with ADMA. As ADMA has no known direct effects on intracellular Ca^{2+}, the enhanced EC Ca^{2+} events are likely in response to the effects of ADMA in vascular smooth muscle. As shown in the wire myography experiments, intra-septal coronary arteries generate VSMC Ca^{2+} flashes under myogenic tone, which increased with ADMA. Therefore, we hypothesise the enhanced Ca^{2+} activity in VSMCs is likely to signal to neighbouring endothelial cells via MEGJs as part of myoendothelial feedback. While the presence of MEGJs is probable, due to previous observations in porcine coronary arterial strips (Beny and Pacicca, 1994), this would need to be confirmed in rat intra-septal coronary arteries in future investigations. Furthermore, the increase in EC Ca^{2+} events could be caused by direct extracellular Ca^{2+} influx through store-operated or voltage-dependent Ca^{2+} channels. Although the latter does not seem likely as endothelial cells are considered to be “non-excitable”, this would still need to be ruled out to confirm the enhanced EC Ca^{2+} events are due to myoendothelial coupling.

Previous studies in porcine coronary arterial strips showed that vasoconstrictors directly act on vascular smooth muscle to increase intracellular Ca^{2+} also indirectly enhance EC Ca^{2+}, an effect that was absent when vasoconstrictors were added to cultured endothelial cells alone (Budel et al., 2001). Similarly in pressurised hamster cheek pouch arterioles, the increase in VSMC Ca^{2+} by PE and high K^+ was followed by an increase in EC Ca^{2+}, which preceded vasoconstriction (Dora et al., 1997). Moreover, comparable to our findings in mesenteric and coronary resistance arteries with ADMA in **Chapters 3** and **4**, L-NAME augmented vasoconstriction in these pressurised arterioles (Dora et al., 1997). This suggests that the rise in EC Ca^{2+} upon vasoconstrictor/vascular smooth muscle stimulation leads to NO synthesis, supporting the concept of myoendothelial feedback in modulating vascular tone and resistance. In mesenteric arterial strips, simultaneous VSMC and EC Ca^{2+} imaging showed that EC Ca^{2+} events upon vascular smooth muscle stimulation were reduced by PLC and IP_3 receptor inhibitors, and palmitoleic acid – a gap junction uncoupler (Lamboley et al., 2005). Similar reduction in EC Ca^{2+} events were also reported with gap junction uncoupler and intraluminal delivery of PLC inhibitor in pressurised mesenteric resistance arteries (Kansui et al., 2008) and cremaster arterioles (Bagher et al., 2012), indicating the movement of IP_3 from vascular smooth muscle into endothelial cells in myoendothelial feedback. In porcine coronary arterial strips, Francis et al. (2016) show that basal EC Ca^{2+} events were attenuated with inhibitors of IP_3 receptors, PLC or cyclopiazonic acid – sarcoendoplasmic reticulum Ca^{2+}-ATPase (SERCA) to deplete internal ER Ca^{2+} stores. Moreover, simultaneous Ca^{2+} and NO imaging in pinned porcine coronary arterial strips showed that NO synthesis (rise in NO fluorescence) corresponded to increases in EC Ca^{2+} signal in a spatiotemporal manner, and L-NNA augmented vasoconstriction in coronary arteries under isometric tension (Francis et al., 2016). These

findings support the coupling between vascular smooth muscle and endothelial cells, and the involvement of Ca^{2+}, IP_3 and heterocellular gap junctions in EC Ca^{2+} events.

Together with our findings in previous chapters, we showed, for the first time to our knowledge, that in pressurised intra-septal coronary arteries under myogenic tone, vascular smooth muscle generates synchronous Ca^{2+} flashes that might then spread to endothelial cells to generate EC Ca^{2+} events. While it was not studied here, the coupling between vascular smooth muscle and endothelial cells is likely to be dependent on both Ca^{2+} and IP_3 signalling via MEGJ and should be further investigated. The rise in EC Ca^{2+} would then have the potential to stimulate NO synthesis, leading to myoendothelial feedback, limiting myogenic tone and vascular resistance at physiological conditions. Asymmetric dimethylarginine augmented myogenic tone, and depolarising spikes (Ng et al., 2024), are associated with enhanced VSMC Ca^{2+} flashes of similar frequency. The enhanced VSMC Ca^{2+} is likely to increase the activation of the vascular smooth muscle contractile machinery, leading to augment vasoconstriction/myogenic tone. Furthermore, ADMA also increased EC Ca^{2+} events, likely as a result of myoendothelial feedback and warrant further investigation.

7.5 CONCLUSION

This chapter investigated, for the first time, the effects of ADMA on vascular smooth muscle and endothelial cell Ca^{+} events in isolated myogenically active intra-septal coronary arteries using Ca^{2+}sensitive fluorescent indicators, and wire and pressure myography. The findings (**Figure 7.5.1**) presented here support the hypotheses that the augmented tone with ADMA is associated with increased VSM Ca^{2+} and EC Ca^{2+} events in the coronary microvasculature, the latter is likely due to the spread of Ca^{2+} and IP_3 from vascular smooth muscle via MEGJs.

The observations made here provide preliminary insights into the myoendothelial feedback mechanism in intra-septal coronary arteries under myogenic tone and how ADMA disrupts intracellular Ca^{2+} signalling leading to coronary vasospasm.

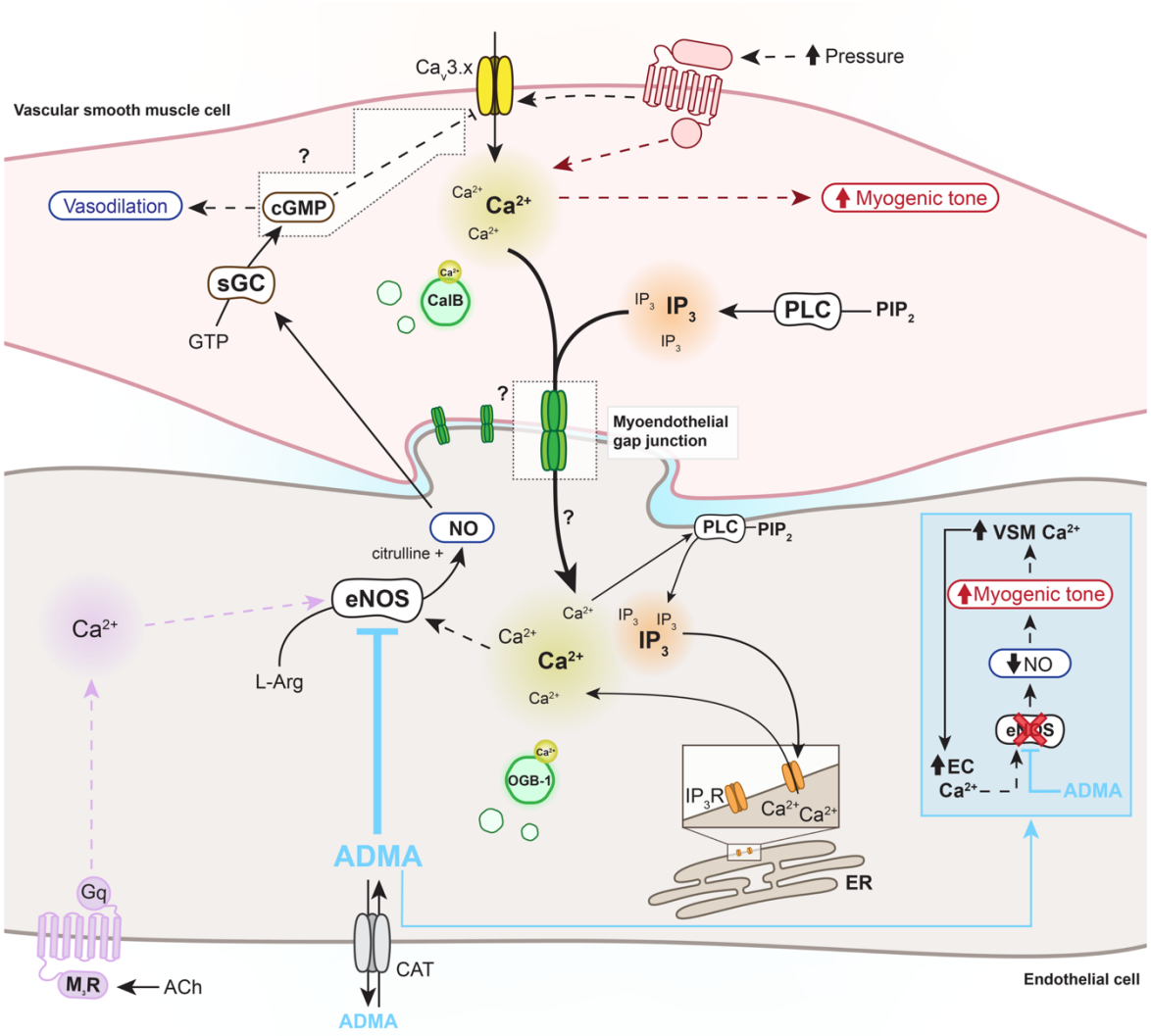


Figure 7.5.1 Summary findings of Chapter 7 – Asymmetric dimethylarginine (ADMA) increases intracellular Ca^{2+} events in vascular smooth muscle (VSM) and endothelial cells (EC) of coronary resistance arteries. Endothelial nitric oxide (NO) synthase (eNOS) inhibition by ADMA increases tone in myogenically active intra-septal coronary arteries is associated with increases in intracellular Ca^{2+} events in both coronary VSM and EC. We hypothesise (dotted boxes) that this is due to Ca^{2+} influx through T-type voltage dependent Ca^{2+} channels ($Ca_v3.x$) into the VSM, which subsequently diffuses to the neighbouring EC via myoendothelial gap junctions. ACh = Acetylcholine; CAT = Cationic amino acid transporter; CalB = CalBryte 520 AM; cGMP = Cyclic guanosine monophosphate; GTP = Guanosine triphosphate; ER = Endoplasmic reticulum; IP_3R = inositol 1,4,5-trisphosphate (IP_3) receptor; L-Arg = L-arginine; M_3R = M_3 muscarinic receptor; OGB-1= Oregon Green BAPTA-1 AM; PLC = Phospholipase C; PIP_2 = Phosphatidylinositol 4,5-bisphosphate; sGC = Soluble guanylyl cyclase. Dashed arrows represent simplified pathways. Summary effect of ADMA is in blue box.

CHAPTER EIGHT

SUMMARY AND FUTURE DIRECTIONS

The main aim of this thesis was to examine the effects of NOS inhibition with the endogenous methylarginine, ADMA, on vascular reactivity in the coronary and mesenteric microcirculation. The most significant findings of the research presented here involve the ability of ADMA to cause endothelial dysfunction, which has previously been questioned. This results in the inhibition of NO-dependent vasodilation and vasospasm. Furthermore, by examining the effects of ADMA and its modulation in mesenteric resistance and intra-septal coronary arteries, we reveal a difference in the expression of the ADMA metabolising enzyme, DDAH1, suggesting the metabolism and inhibitory actions of ADMA may vary in different parts of the circulation. This may translate to a greater susceptibility to vascular dysfunction in the coronary microvasculature, and predispose to the development of coronary microvascular disease.

In non-myogenic mesenteric resistance arteries (**Chapter 3**), ADMA promoted vascular dysfunction by enhancing vasoreactivity to PE (vasospasm) and attenuating NO-dependent vasodilation during EDH inhibition. This contrasts with L-NAME which abolished vasodilation to ACh (Ng et al., 2024), suggesting that NO synthesis is still intact. In myogenically active intra-septal coronary arteries (**Chapter 4**), ADMA enhanced myogenic tone to levels comparable to L-NAME, supporting the importance of NO synthesis in the modulation of myogenic tone but also suggesting higher basal NO synthesis than the mesenteric arteries. Contrary to mesenteric arteries, ADMA abolished NO-dependent vasodilation to ACh in coronary resistance arteries, supporting a more effective inhibition on (endothelial) NOS with ADMA. Immunohistochemistry for DDAH1 revealed the endothelium as the main site of ADMA metabolism and a significantly lower expression of DDAH1 in the coronary microvasculature compared to mesenteric arteries (**Chapter 5**). Furthermore, inhibition of DDAH1 with L-257 further attenuated ACh vasodilation in mesenteric arteries

and augmented myogenic tone in intra-septal coronary arteries. Together, the functional and immunostaining data presented here are consistent with a continuous turnover of ADMA with DDAH1 limiting intracellular accumulation of ADMA to levels that are normally insufficient to disrupt NO synthesis.

Due to the crucial role of DDAH1 in modulating intracellular ADMA levels, strategies to restore and/or augment DDAH1 expression and activity may be beneficial in microvascular dysfunction. While there are no known direct activators of DDAH1, limited studies have reported a role for farnesoid X receptors (FXRs), a nuclear receptor, in the modulation of DDAH1 expression. Hu et al. (2006) reported that the FXR response element is located upstream of DDAH1, and the activation of FXRs with a synthetic activator, GW4064, enhanced DDAH1 expression in the liver and reduced plasma ADMA levels in *in vivo* rodent models. Furthermore, in a small study in patients with coronary heart disease, oral administration of ursodeoxycholic acid (UDCA), an activator of FXR and a component of bile, improved endothelium-dependent vasodilation in brachial arteries (Sinisalo et al., 1999). Similar improvements in post-ischaemia forearm blood flow were observed in a small double-blind, randomised, placebo-controlled, crossover trial in patients with chronic heart failure following oral UDCA (von Haehling et al., 2012), indicating a link between FXR and vascular reactivity. Furthermore, He et al. (2006) reported the functional expression of FXRs in pulmonary artery endothelial cells as FXR stimulation reduced endothelin-1 expression. However, it is unclear whether FXRs are expressed in the coronary endothelium and its activation can modulate DDAH1 gene expression and enzyme activity. Future studies should first confirm the expression of FXRs in the coronary endothelium with immunohistochemistry as previously described (He et al., 2006). Subsequent experiments with FXR selective agonists (e.g. UDCA and GW4064) and antagonist (DY268) would confirm whether FXRs are functional and can

modulate the expression of DDAH1 in coronary endothelial cells using DDAH1 antibodies described here. If this modulation is present, studies could also examine whether FXR stimulation can modify coronary microvascular function and overcome or attenuate the effects of L-257 and/or ADMA using wire and pressure myography. As such, this link between FXRs, DDAH1 and ADMA and the availability of FXR specific agonists, that are well tolerated *in vivo* (Sinisalo et al., 1999, von Haehling et al., 2012), makes FXR a promising therapeutic target to modulate DDAH1 expression and ADMA levels in cardiovascular disease.

Chapter 4 reveals that IK_{Ca} channels alone underpins EDH vasodilation to ACh in intra-septal coronary arteries, which differs from other vascular beds. While the expression of K_{Ca} channels was not examined in the current study, this is unlikely to be due to the absence of SK_{Ca} channels as previous studies reported the expression and function of SK_{Ca} channels in the rat coronary microcirculation (Mishra et al., 2013, Climent et al., 2014). Nevertheless, the expression of K_{Ca} channels in intra-septal coronary arteries should be confirmed using anti-K_{Ca}3.1 (IK_{Ca}) and anti-K_{Ca}2.3 (SK_{Ca}) antibodies to clarify this discrepancy. Moreover, Brahler et al. (2009) reported that doxycycline-induced knockdown of SK_{Ca} channel inhibited ACh vasorelaxation in NO-intact (without L-NNA) PE pre-constricted mouse carotid arteries. However, during NOS inhibition with L-NNA, which attenuated vasorelaxation, the additional block of SK_{Ca} channels failed to potentiate the inhibition on ACh vasorelaxation. In contrast, the inhibition on ACh vasorelaxation was augmented in arteries lacking IK_{Ca} channels independent of the presence of NO (Brahler et al., 2009). These findings suggest the possibility that SK_{Ca} channel activity requires or is aided by NO, and may explain our observations in the absence on NO synthesis. To investigate this, simultaneous membrane potential and isometric tension recordings in intra-septal coronary arteries with SK_{Ca} and IK_{Ca} channels activator SKA-31 or NS 309 in the presence and absence of NS 6180 would assess whether SK_{Ca} channels are

functional. The same approach could also be used to probe whether NO opens/modulates SK_{Ca} channel with NO donors, such as SNAP, in the presence and absence of apamin. Furthermore, co-immunostaining for SK_{Ca} and eNOS may provide insights as to possible protein co-localisation.

The findings in **Chapter 6** support the use of (1 mM) L-arginine in addressing coronary microvascular dysfunction without disrupting normal vascular function and ACh vasodilation. Conversely, we showed that L-arginine at higher concentrations may disrupt normal vascular homeostasis by depressing basal coronary myogenic tone, compromising autoregulation. While the excessive vasodilation may translate into increased blood flow, the ability to direct/control blood flow would be compromised, resulting in flow-metabolic mismatch. Furthermore, the excessive flow and compromised autoregulation may increase vascular resistance and pressure in the microcirculation, resulting in turbulent flow and paradoxically predisposing to endothelial dysfunction and damage to the vessel wall. Therefore, it is crucial to understand the optimal ratio of L-arginine to ADMA, particularly their intracellular concentrations, to ensure L-arginine supplementation can effectively outcompete ADMA.

A limitation of this study, and similarly in most animal and clinical studies, is the lack of intracellular ADMA and L-arginine measurements following NOS and DDAH1 inhibition, and L-arginine supplementation. This is mostly due to the lack of a method in harvesting coronary microvascular endothelial cells for intracellular measurements. Due to the intracellular modulatory mechanisms (e.g. DDAH1 and arginase), the plasma concentration may not accurately represent the intracellular environment. Future studies could employ wire and pressure myography techniques and/or *in vitro* coronary microvascular endothelial cell models in tandem with liquid chromatography-mass spectrometry and/or ELISA to measure the

intracellular ADMA and L-arginine concentrations following ADMA, L-257 and/or L-arginine treatments. This would allow for: i) estimations of intracellular ADMA concentration that causes microvascular endothelial dysfunction; ii) estimations of L-arginine/ADMA ratio for L-arginine to effectively reverse the actions of ADMA whilst accounting for intracellular modulation; and iii) intracellular ADMA measurements following L-257, to confirm the enhanced coronary myogenic tone is a direct consequence of ADMA accumulation. Furthermore, chronic infusion of L-257 would allow for the *in vivo* effects of DDAH1 and ADMA in the coronary microcirculation to be examined using wire and pressure myography.

Chapter 7 provides preliminary insights into the effects of elevated ADMA levels on intracellular Ca^{2+} signalling in the coronary microvasculature. A limitation of the current study is the use of low magnification, therefore, small, localised EC Ca^{2+} events may have been missed. Experiments at higher magnification would allow for more detailed examination of intracellular events. Nevertheless, basal VSMC and EC Ca^{2+} were observed under myogenic tone and were increased with ADMA. Although the precise mechanism remains to be elucidated, the basal and ADMA-augmented EC Ca^{2+} events might be due to myoendothelial feedback. To confirm this, the current experiments should be repeated in the presence of gap junction inhibitors or antibodies for connexins, components of MEGJs, described in pressurised mesenteric arteries (Mather et al., 2005, Kansui et al., 2008). The use of arterial midplane imaging (Bagher et al., 2012) would allow for simultaneous VSM and EC Ca^{2+} imaging in adjacent cells, providing more evidence into the VSMC-EC coupling. Furthermore, experiments with PLC and IP_3 receptor inhibitors (e.g. U-73122 and xestospongin C respectively) would further delineate the signalling from VSMCs to endothelial cells. Intraluminal delivery of PLC inhibitors, previously described Kansui et al. (2008) and Bagher

et al. (2012), would confine PLC inhibition to endothelial cells and likely to overcome the disruption to myogenic tone previously reported in cerebral arteries (Jarajapu and Knot, 2002).

Moreover, the functional effects of EC Ca^{2+} signals should be examined, as they most likely contribute to basal NO synthesis. The use of NO-sensitive fluorescent indicator (e.g. DAR-4M AM) previously described by Francis et al. (2016) in pinned coronary arterial segments would overcome the difficulty in directly measure NO levels, a short half-life of sub-seconds (Liu et al., 1998). Our group has recently optimised DAR-4M AM in pressurised arteries (Wallis et al., 2023). Therefore, concomitant EC Ca^{2+} and NO imaging in intact arteries may provide more direct evidence as to whether: i) the basal EC Ca^{2+} events lead to NO synthesis; and ii) ADMA causes coronary endothelial dysfunction by abolishing NO synthesis.

Additionally, it should be noted that the experiments in this thesis were only conducted using tissue from male Wistar rats to limit inter-sex variability. Therefore, the observations reported here should be repeated using female rats to confirm the translatability of the inhibitory effects of ADMA in the coronary microcirculation. Using non-invasive PET (positron emission tomography) imaging, Murthy et al. (2014) reported that coronary microvascular dysfunction was highly prevalent in suspected patients with coronary artery disease (n = 1,218) regardless of sex, women (54%) and men (51%), and is a strong predictor of cardiovascular-related adverse events. Similarly, almost half of female patients with ANOCA in the WISE study presented with reduced CFR (Reis et al., 2001). Although some studies with coronary angiography reported that women are five-times more likely to present with angiographically normal arteries compared to age-matched male subjects (Sullivan et al., 1994). These observations indicate the clinical importance of coronary microvascular dysfunction and ANOCA in both populations. Interestingly in animal models, Huang et al. (1997) reported a

gender difference in myogenic response, where pressure-induced vasoconstriction was significantly less in gracilis muscle arterioles of female rats compared to males. Furthermore, NOS inhibition with L-NNA or ovariectomy produced a larger reduction in arteriolar diameter of female rats, which the latter was reversed by oestrogen supplementation (Huang et al., 1997). Although Skarsgard et al. (1997) reported no sex difference in basal myogenic tone in middle cerebral arteries, L-NAME evoked greater augmentation in myogenic tone in female arteries at higher pressures, indicating a possible greater contribution of NO in modulating myogenic tone. Conversely, myogenic tone in male spiral modiolar artery were more sensitive to NOS inhibition with L-NNA compared to females (Reimann et al., 2011). These findings suggest a possible gender and vascular bed differences in the modulation of myogenic tone. Therefore, the magnitude of inhibition with elevated ADMA levels may differ in the coronary microcirculation in females and warrant further investigation in sex- and age-matched studies. This is of particularly importance as women are reported to have poorer prognosis and higher cardiovascular-related mortality rates. Moreover, to confirm the clinical translatability of the observations made here, the present study should be repeated *ex vivo* using human coronary microvessels. Future investigations should match these functional studies to the patient data (e.g. plasma (and intracellular) ADMA and L-arginine concentrations) to elucidate the potential casual role for ADMA in coronary endothelial dysfunction.

In summary (**Figure 8.1**), this thesis demonstrates the ability of ADMA in causing endothelial dysfunction in the coronary microcirculation, thus supporting the clinical relevance of elevated ADMA levels in cardiovascular disease (e.g. microvascular angina). In intra-septal coronary arteries, ADMA exerts a greater inhibition on NOS, likely due to the lower expression of DDAH1 compared to mesenteric resistance arteries. This inter-vascular bed variation in DDAH1 expression is likely to translate to differences in the susceptibility to ADMA-mediated

endothelial dysfunction between vascular beds. Therefore, strategies to enhance DDAH1 expression and/or activity may be a promising therapeutic avenue to counteract the elevated intracellular ADMA levels. Furthermore, this thesis reveals that IK_{Ca} channel alone underpins EDH vasodilation to ACh in coronary resistance arteries, but further investigation is needed to confirm this observation. In addition, our findings support the use of L-arginine supplementation as a mean to reverse coronary microvascular dysfunction. Finally, VSMC and EC Ca^{2+} events were observed under myogenic tone, which were increased with ADMA. The EC Ca^{2+} events are likely due to myoendothelial feedback. We hope the findings in this thesis and the future work described will further our understanding in the L-arginine/ADMA/DDAH1/NO cascade in the coronary and mesenteric microcirculation. Ultimately, leading to the development of new therapeutic strategies to improve patients' prognosis.

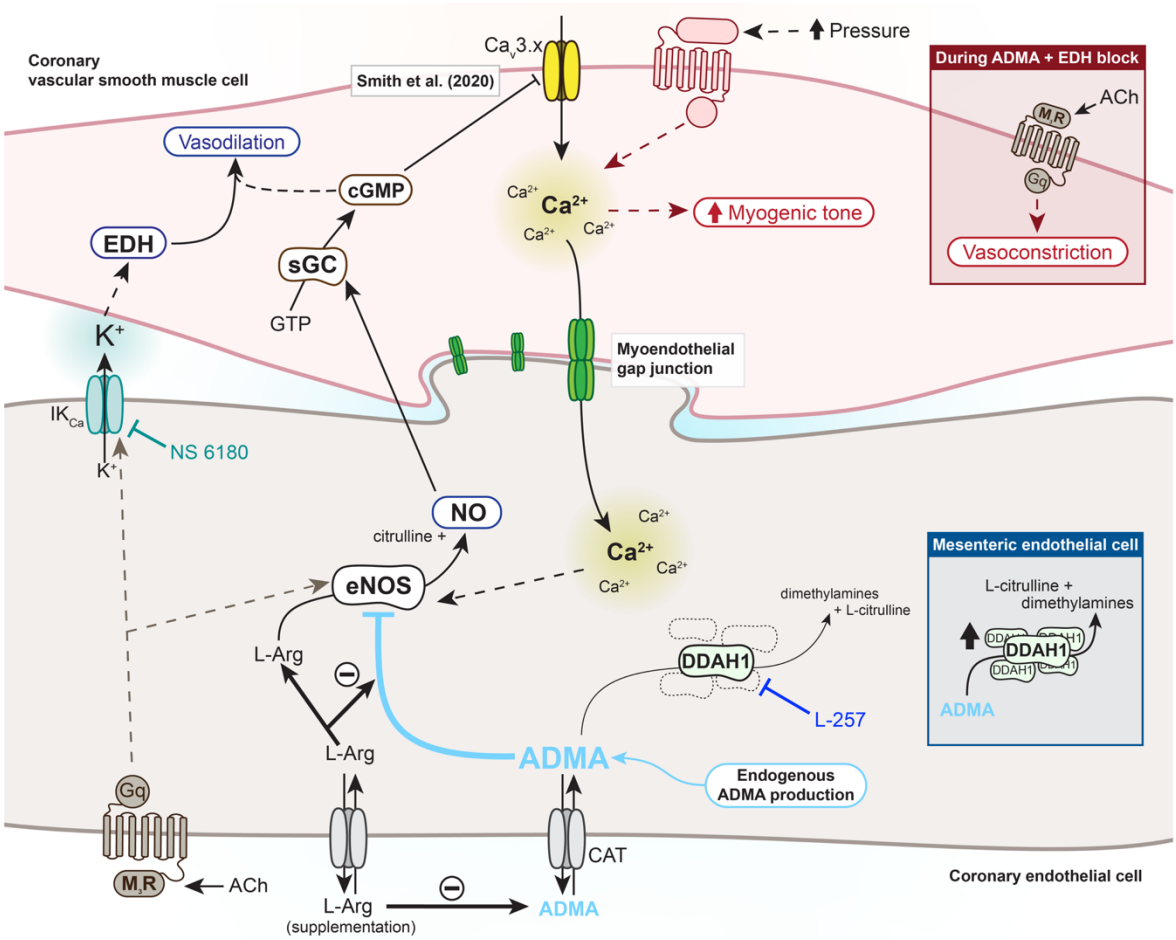


Figure 8.1 Summary of thesis findings. Asymmetric dimethylarginine (ADMA) augments coronary myogenic tone (MT) by inhibiting endothelial nitric oxide (NO) synthase (eNOS), resulting in the loss of inhibition on T-type voltage-dependent Ca^{2+} channel ($Ca_v3.x$; Smith et al. 2020). ADMA exerts more potent eNOS inhibition in intra-septal coronary arteries, which is associated with lower expression of dimethylarginine dimethylaminohydrolase 1 (DDAH1) compared to mesenteric resistance arteries (Blue inset). Selective DDAH1 inhibitor (L-257) enhanced MT by disrupting turnover of endogenous ADMA. Intermediate conductance Ca^{2+}-activated K^+ (IK_{Ca}) channels underpin endothelium-dependent hyperpolarization (EDH) in intra-septal coronary arteries, blocked by NS 6180 (IK_{Ca} channel inhibitor). Upon ADMA and IK_{Ca} block, acetylcholine (ACh) elicits coronary vasoconstriction by activating M_3 muscarinic receptor (M_3R) on vascular smooth muscle cells (VSMCs; Red inset). L-arginine (L-Arg) restores basal MT and ACh vasodilation by outcompeting ADMA for eNOS binding and access to cationic amino acid transporter (CAT). Basal MT is associated with VSMC Ca^{2+} and endothelial cell Ca^{2+} events, where the latter via myoendothelial feedback. Augmented MT with ADMA is associated with increased VSM and EC Ca^{2+} events.

CHAPTER NINE

REFERENCES

ABBASI, F., ASAGMI, T., COOKE, J. P., LAMENDOLA, C., MCLAUGHLIN, T., REAVEN, G. M., STUEHLINGER, M. & TSAO, P. S. 2001. Plasma concentrations of asymmetric dimethylarginine are increased in patients with type 2 diabetes mellitus. *Am J Cardiol,* 88**,** 1201-3.

ABHARY, S., BURDON, K. P., KUOT, A., JAVADIYAN, S., WHITING, M. J., KASMERIDIS, N., PETROVSKY, N. & CRAIG, J. E. 2010. Sequence variation in DDAH1 and DDAH2 genes is strongly and additively associated with serum ADMA concentrations in individuals with type 2 diabetes. *PLoS One,* 5**,** e9462.

ACHAN, V., BROADHEAD, M., MALAKI, M., WHITLEY, G., LEIPER, J., MACALLISTER, R. & VALLANCE, P. 2003. Asymmetric dimethylarginine causes hypertension and cardiac dysfunction in humans and is actively metabolized by dimethylarginine dimethylaminohydrolase. *Arterioscler Thromb Vasc Biol,* 23**,** 1455-9.

ADEAGBO, A. S. & TRIGGLE, C. R. 1993. Interactions of nitric oxide synthase inhibitors and dexamethasone with alpha-adrenoceptor-mediated responses in rat aorta. *Br J Pharmacol,* 109**,** 495-501.

AL-ZOBAIDY, M. J., CRAIG, J. & MARTIN, W. 2010. Differential sensitivity of basal and acetylcholine-induced activity of nitric oxide to blockade by asymmetric dimethylarginine in the rat aorta. *Br J Pharmacol,* 160**,** 1476-83.

ALTMANN, K. S., HAVEMEYER, A., BEITZ, E. & CLEMENT, B. 2012. Dimethylarginine-Dimethylaminohydrolase-2 (DDAH-2) Does Not Metabolize Methylarginines. *ChemBioChem,* 13**,** 2599-2604.

AMIR, M., HASSANEIN, S. I., ABDEL RAHMAN, M. F. & GAD, M. Z. 2018. AGXT2 and DDAH-1 genetic variants are highly correlated with serum ADMA and SDMA levels and with incidence of coronary artery disease in Egyptians. *Mol Biol Rep,* 45**,** 2411-2419.

ANTHONY, S., LEIPER, J. & VALLANCE, P. 2005. Endogenous production of nitric oxide synthase inhibitors. *Vasc Med,* 10 Suppl 1**,** S3-9.

ANTONIADES, C., SHIRODARIA, C., LEESON, P., ANTONOPOULOS, A., WARRICK, N., VAN-ASSCHE, T., CUNNINGTON, C., TOUSOULIS, D., PILLAI, R., RATNATUNGA, C., STEFANADIS, C. & CHANNON, K. M. 2009. Association of plasma asymmetrical dimethylarginine (ADMA) with elevated vascular superoxide production and endothelial nitric oxide synthase uncoupling: implications for endothelial function in human atherosclerosis. *Eur Heart J,* 30**,** 1142-50.

ARNOLD, W. P., MITTAL, C. K., KATSUKI, S. & MURAD, F. 1977. Nitric oxide activates guanylate cyclase and increases guanosine 3':5'-cyclic monophosphate levels in various tissue preparations. *Proc Natl Acad Sci U S A,* 74**,** 3203-7.

AVONTUUR, J. A., BRUINING, H. A. & INCE, C. 1997. Nitric oxide causes dysfunction of coronary autoregulation in endotoxemic rats. *Cardiovasc Res,* 35**,** 368-76.

AYDIN, F., ROSENBLUM, W. I. & POVLISHOCK, J. T. 1991. Myoendothelial junctions in human brain arterioles. *Stroke,* 22**,** 1592-7.

BAGHER, P., BELEZNAI, T., KANSUI, Y., MITCHELL, R., GARLAND, C. J. & DORA, K. A. 2012. Low intravascular pressure activates endothelial cell TRPV4 channels, local Ca2+ events, and IKCa channels, reducing arteriolar tone. *Proc Natl Acad Sci U S A,* 109**,** 18174-9.

BATENBURG, W. W., GARRELDS, I. M., VAN KATS, J. P., SAXENA, P. R. & DANSER, A. H. 2004. Mediators of bradykinin-induced vasorelaxation in human coronary microarteries. *Hypertension,* 43**,** 488-92.

BAYLISS, W. M. 1902. On the local reactions of the arterial wall to changes of internal pressure. *J Physiol,* 28**,** 220-31.

BELTRAME, J. F., CREA, F., KASKI, J. C., OGAWA, H., ONG, P., SECHTEM, U., SHIMOKAWA, H., BAIREY MERZ, C. N. & CORONARY VASOMOTION DISORDERS INTERNATIONAL STUDY, G. 2016. The Who, What, Why, When, How and Where of Vasospastic Angina. *Circ J,* 80**,** 289-98.

BENY, J. L. & PACICCA, C. 1994. Bidirectional electrical communication between smooth muscle and endothelial cells in the pig coronary artery. *Am J Physiol,* 266**,** H1465-72.

BENY, J. L. & SCHAAD, O. 2000. An evaluation of potassium ions as endothelium-derived hyperpolarizing factor in porcine coronary arteries. *Br J Pharmacol,* 131**,** 965-73.

BERKOWITZ, D. E., WHITE, R., LI, D., MINHAS, K. M., CERNETICH, A., KIM, S., BURKE, S., SHOUKAS, A. A., NYHAN, D., CHAMPION, H. C. & HARE, J. M. 2003. Arginase reciprocally regulates nitric oxide synthase activity and contributes to endothelial dysfunction in aging blood vessels. *Circulation,* 108**,** 2000-6.

BLUM, A., HATHAWAY, L., MINCEMOYER, R., SCHENKE, W. H., KIRBY, M., CSAKO, G., WACLAWIW, M. A., PANZA, J. A. & CANNON, R. O., 3RD 2000. Oral L-arginine in patients with coronary artery disease on medical management. *Circulation,* 101**,** 2160-4.

BöGER, R. H. 2003. Association of asymmetric dimethylarginine and endothelial dysfunction. *Clin Chem Lab Med,* 41**,** 1467-72.

BöGER, R. H., BODE-BöGER, S. M., MUGGE, A., KIENKE, S., BRANDES, R., DWENGER, A. & FROLICH, J. C. 1995. Supplementation of hypercholesterolaemic rabbits with L-arginine reduces the vascular release of superoxide anions and restores NO production. *Atherosclerosis,* 117**,** 273-84.

BöGER, R. H., BODE-BöGER, S. M., SZUBA, A., TSAO, P. S., CHAN, J. R., TANGPHAO, O., BLASCHKE, T. F. & COOKE, J. P. 1998. Asymmetric dimethylarginine (ADMA):

a novel risk factor for endothelial dysfunction: its role in hypercholesterolemia. *Circulation,* 98**,** 1842-7.

BöGER, R. H., BODE-BöGER, S. M., THIELE, W., JUNKER, W., ALEXANDER, K. & FROLICH, J. C. 1997. Biochemical evidence for impaired nitric oxide synthesis in patients with peripheral arterial occlusive disease. *Circulation,* 95**,** 2068-74.

BöGER, R. H., BODE-BöGER, S. M., TSAO, P. S., LIN, P. S., CHAN, J. R. & COOKE, J. P. 2000. An endogenous inhibitor of nitric oxide synthase regulates endothelial adhesiveness for monocytes. *Journal of the American College of Cardiology,* 36**,** 2287-2295.

BOLTON, T. B., LANG, R. J. & TAKEWAKI, T. 1984. Mechanisms of action of noradrenaline and carbachol on smooth muscle of guinea-pig anterior mesenteric artery. *J Physiol,* 351**,** 549-72.

BRAHLER, S., KAISTHA, A., SCHMIDT, V. J., WOLFLE, S. E., BUSCH, C., KAISTHA, B. P., KACIK, M., HASENAU, A. L., GRGIC, I., SI, H., BOND, C. T., ADELMAN, J. P., WULFF, H., DE WIT, C., HOYER, J. & KOHLER, R. 2009. Genetic deficit of SK3 and IK1 channels disrupts the endothelium-derived hyperpolarizing factor vasodilator pathway and causes hypertension. *Circulation,* 119**,** 2323-32.

BROZOVICH, F. V., NICHOLSON, C. J., DEGEN, C. V., GAO, Y. Z., AGGARWAL, M. & MORGAN, K. G. 2016. Mechanisms of Vascular Smooth Muscle Contraction and the Basis for Pharmacologic Treatment of Smooth Muscle Disorders. *Pharmacol Rev,* 68**,** 476-532.

BUDEL, S., SCHUSTER, A., STERGIOPOULOS, N., MEISTER, J. J. & BENY, J. L. 2001. Role of smooth muscle cells on endothelial cell cytosolic free calcium in porcine coronary arteries. *Am J Physiol Heart Circ Physiol,* 281**,** H1156-62.

BURG, M., GRANTHAM, J., ABRAMOW, M. & ORLOFF, J. 1966. Preparation and study of fragments of single rabbit nephrons. *Am J Physiol,* 210**,** 1293-8.

CABLE, D. G., CELOTTO, A. C., EVORA, P. R. & SCHAFF, H. V. 2009. Asymmetric dimethylarginine endogenous inhibition of nitric oxide synthase causes differential vasculature effects. *Med Sci Monit,* 15**,** BR248-53.

CAMICI, P. G. & CREA, F. 2007. Coronary microvascular dysfunction. *N Engl J Med,* 356**,** 830-40.

CAPLIN, B., WANG, Z., SLAVIERO, A., TOMLINSON, J., DOWSETT, L., DELAHAYE, M., SALAMA, A., INTERNATIONAL CONSORTIUM FOR BLOOD PRESSURE GENOME-WIDE ASSOCIATION, S., WHEELER, D. C. & LEIPER, J. 2012. Alanine-glyoxylate aminotransferase-2 metabolizes endogenous methylarginines, regulates NO, and controls blood pressure. *Arterioscler Thromb Vasc Biol,* 32**,** 2892-900.

CARDOUNEL, A. J., CUI, H., SAMOUILOV, A., JOHNSON, W., KEARNS, P., TSAI, A. L., BERKA, V. & ZWEIER, J. L. 2007. Evidence for the pathophysiological role of endogenous methylarginines in regulation of endothelial NO production and vascular function. *J Biol Chem,* 282**,** 879-87.

CHATAIGNEAU, T., FELETOU, M., HUANG, P. L., FISHMAN, M. C., DUHAULT, J. & VANHOUTTE, P. M. 1999. Acetylcholine-induced relaxation in blood vessels from endothelial nitric oxide synthase knockout mice. *Br J Pharmacol,* 126**,** 219-26.

CHEN, G., SUZUKI, H. & WESTON, A. H. 1988. Acetylcholine releases endothelium-derived hyperpolarizing factor and EDRF from rat blood vessels. *Br J Pharmacol,* 95**,** 1165-74.

CHEN, J. W., HSU, N. W., WU, T. C., LIN, S. J. & CHANG, M. S. 2002. Long-term angiotensin-converting enzyme inhibition reduces plasma asymmetric dimethylarginine and improves endothelial nitric oxide bioavailability and coronary microvascular function in patients with syndrome X. *Am J Cardiol,* 90**,** 974-82.

CHEN, Y., LI, Y., ZHANG, P., TRAVERSE, J. H., HOU, M., XU, X., KIMOTO, M. & BACHE, R. J. 2005. Dimethylarginine dimethylaminohydrolase and endothelial dysfunction in failing hearts. *Am J Physiol Heart Circ Physiol,* 289**,** H2212-9.

CHIN-DUSTING, J. P., KAYE, D. M., LEFKOVITS, J., WONG, J., BERGIN, P. & JENNINGS, G. L. 1996. Dietary supplementation with L-arginine fails to restore endothelial function in forearm resistance arteries of patients with severe heart failure. *J Am Coll Cardiol,* 27**,** 1207-13.

CHU, A., CHAMBERS, D. E., LIN, C. C., KUEHL, W. D., PALMER, R. M., MONCADA, S. & COBB, F. R. 1991. Effects of inhibition of nitric oxide formation on basal vasomotion and endothelium-dependent responses of the coronary arteries in awake dogs. *J Clin Invest,* 87**,** 1964-8.

CLIMENT, B., MORENO, L., MARTINEZ, P., CONTRERAS, C., SANCHEZ, A., PEREZ-VIZCAINO, F., GARCIA-SACRISTAN, A., RIVERA, L. & PRIETO, D. 2014. Upregulation of SK3 and IK1 channels contributes to the enhanced endothelial calcium signaling and the preserved coronary relaxation in obese Zucker rats. *PLoS One,* 9**,** e109432.

COOKE, J. P., ANDON, N. A., GIRERD, X. J., HIRSCH, A. T. & CREAGER, M. A. 1991. Arginine restores cholinergic relaxation of hypercholesterolemic rabbit thoracic aorta. *Circulation,* 83**,** 1057-62.

COUTO, G. K., BRITTO, L. R., MILL, J. G. & ROSSONI, L. V. 2015. Enhanced nitric oxide bioavailability in coronary arteries prevents the onset of heart failure in rats with myocardial infarction. *J Mol Cell Cardiol,* 86**,** 110-20.

CRANE, G. J., GALLAGHER, N., DORA, K. A. & GARLAND, C. J. 2003. Small- and intermediate-conductance calcium-activated K+ channels provide different facets of

endothelium-dependent hyperpolarization in rat mesenteric artery. *J Physiol,* 553**,** 183-9.

DAVIDS, M. & TEERLINK, T. 2013. Plasma concentrations of arginine and asymmetric dimethylarginine do not reflect their intracellular concentrations in peripheral blood mononuclear cells. *Metabolism,* 62**,** 1455-61.

DAYOUB, H., ACHAN, V., ADIMOOLAM, S., JACOBI, J., STUEHLINGER, M. C., WANG, B.-Y., TSAO, P. S., KIMOTO, M., VALLANCE, P., PATTERSON, A. J. & COOKE, J. P. 2003. Dimethylarginine Dimethylaminohydrolase Regulates Nitric Oxide Synthesis. *Circulation,* 108**,** 3042-3047.

DE GENNARO COLONNA, V., BONOMO, S., FERRARIO, P., BIANCHI, M., BERTI, M., GUAZZI, M., MANFREDI, B., MULLER, E. E., BERTI, F. & ROSSONI, G. 2007. Asymmetric dimethylarginine (ADMA) induces vascular endothelium impairment and aggravates post-ischemic ventricular dysfunction in rats. *Eur J Pharmacol,* 557**,** 178-85.

DHAWAN, V., HANDU, S. S., NAIN, C. K. & GANGULY, N. K. 2005. Chronic L-arginine supplementation improves endothelial cell vasoactive functions in hypercholesterolemic and atherosclerotic monkeys. *Mol Cell Biochem,* 269**,** 1-11.

DING, H., WU, B., WANG, H., LU, Z., YAN, J., WANG, X., SHAFFER, J. R., HUI, R. & WANG, D. W. 2010. A novel loss-of-function DDAH1 promoter polymorphism is associated with increased susceptibility to thrombosis stroke and coronary heart disease. *Circ Res,* 106**,** 1145-52.

DORA, K. A., DOYLE, M. P. & DULING, B. R. 1997. Elevation of intracellular calcium in smooth muscle causes endothelial cell generation of NO in arterioles. *Proc Natl Acad Sci U S A,* 94**,** 6529-34.

DORA, K. A., LIN, J., BORYSOVA, L., BELEZNAI, T., TAGGART, M., ASCIONE, R. & GARLAND, C. 2022. Signaling and structures underpinning conducted vasodilation in human and porcine intramyocardial coronary arteries. *Front Cardiovasc Med,* 9**,** 980628.

DREXLER, H., FISCHELL, T. A., PINTO, F. J., CHENZBRAUN, A., BOTAS, J., COOKE, J. P. & ALDERMAN, E. L. 1994. Effect of L-arginine on coronary endothelial function in cardiac transplant recipients. Relation to vessel wall morphology. *Circulation,* 89**,** 1615-23.

DREXLER, H., ZEIHER, A. M., MEINZER, K. & JUST, H. 1991. Correction of endothelial dysfunction in coronary microcirculation of hypercholesterolaemic patients by L-arginine. *Lancet,* 338**,** 1546-50.

DUBOIS-RANDE, J. L., ZELINSKY, R., ROUDOT, F., CHABRIER, P. E., CASTAIGNE, A., GESCHWIND, H. & ADNOT, S. 1992. Effects of infusion of L-arginine into the left anterior descending coronary artery on acetylcholine-induced vasoconstriction of human atheromatous coronary arteries. *Am J Cardiol,* 70**,** 1269-75.

DULING, B. R., GORE, R. W., DACEY, R. G., JR. & DAMON, D. N. 1981. Methods for isolation, cannulation, and in vitro study of single microvessels. *Am J Physiol,* 241**,** H108-116.

EDWARDS, G., DORA, K. A., GARDENER, M. J., GARLAND, C. J. & WESTON, A. H. 1998. K+ is an endothelium-derived hyperpolarizing factor in rat arteries. *Nature,* 396**,** 269-72.

EGASHIRA, K., HIROOKA, Y., KUGA, T., MOHRI, M. & TAKESHITA, A. 1996. Effects of L-arginine supplementation on endothelium-dependent coronary vasodilation in patients with angina pectoris and normal coronary arteriograms. *Circulation,* 94**,** 130-4.

EGASHIRA, K., INOU, T., HIROOKA, Y., YAMADA, A., URABE, Y. & TAKESHITA, A. 1993. Evidence of impaired endothelium-dependent coronary vasodilatation in patients with angina pectoris and normal coronary angiograms. *N Engl J Med,* 328**,** 1659-64.

EL ASSAR, M., ANGULO, J., SANTOS-RUIZ, M., RUIZ DE ADANA, J. C., PINDADO, M. L., SANCHEZ-FERRER, A., HERNANDEZ, A. & RODRIGUEZ-MANAS, L. 2016. Asymmetric dimethylarginine (ADMA) elevation and arginase up-regulation contribute to endothelial dysfunction related to insulin resistance in rats and morbidly obese humans. *J Physiol,* 594**,** 3045-60.

FAN, N. C., TSAI, C. M., HSU, C. N., HUANG, L. T. & TAIN, Y. L. 2013. N-acetylcysteine prevents hypertension via regulation of the ADMA-DDAH pathway in young spontaneously hypertensive rats. *Biomed Res Int,* 2013**,** 696317.

FARACI, F. M., BRIAN, J. E., JR. & HEISTAD, D. D. 1995. Response of cerebral blood vessels to an endogenous inhibitor of nitric oxide synthase. *Am J Physiol,* 269**,** H1522-7.

FELETOU, M. & VANHOUTTE, P. M. 1988. Endothelium-dependent hyperpolarization of canine coronary smooth muscle. *Br J Pharmacol,* 93**,** 515-24.

FENG, Q., LU, X., FORTIN, A. J., PETTERSSON, A., HEDNER, T., KLINE, R. L. & ARNOLD, J. M. 1998. Elevation of an endogenous inhibitor of nitric oxide synthesis in experimental congestive heart failure. *Cardiovasc Res,* 37**,** 667-75.

FORMAN, B. M., GOODE, E., CHEN, J., ORO, A. E., BRADLEY, D. J., PERLMANN, T., NOONAN, D. J., BURKA, L. T., MCMORRIS, T., LAMPH, W. W., EVANS, R. M. & WEINBERGER, C. 1995. Identification of a nuclear receptor that is activated by farnesol metabolites. *Cell,* 81**,** 687-93.

FRANCIS, M., WALDRUP, J. R., QIAN, X., SOLODUSHKO, V., MERIWETHER, J. & TAYLOR, M. S. 2016. Functional Tuning of Intrinsic Endothelial Ca2+ Dynamics in Swine Coronary Arteries. *Circ Res,* 118**,** 1078-90.

FREW, J. D., PAISLEY, K. & MARTIN, W. 1993. Selective inhibition of basal but not agonist-stimulated activity of nitric oxide in rat aorta by NG-monomethyl-L-arginine. *Br J Pharmacol,* 110**,** 1003-8.

FULTON, D., GRATTON, J. P., MCCABE, T. J., FONTANA, J., FUJIO, Y., WALSH, K., FRANKE, T. F., PAPAPETROPOULOS, A. & SESSA, W. C. 1999. Regulation of endothelium-derived nitric oxide production by the protein kinase Akt. *Nature,* 399**,** 597-601.

FURCHGOTT, R. F. & ZAWADZKI, J. V. 1980. The obligatory role of endothelial cells in the relaxation of arterial smooth muscle by acetylcholine. *Nature,* 288**,** 373-376.

GARCIA, S. R. & BUND, S. J. 1998. Nitric oxide modulation of coronary artery myogenic tone in spontaneously hypertensive and Wistar-Kyoto rats. *Clin Sci (Lond),* 94**,** 225-9.

GARDINER, S. M., KEMP, P. A., BENNETT, T., PALMER, R. M. & MONCADA, S. 1993. Regional and cardiac haemodynamic effects of NG, NG,dimethyl-L-arginine and their reversibility by vasodilators in conscious rats. *Br J Pharmacol,* 110**,** 1457-64.

GARLAND, C. J., HILEY, C. R. & DORA, K. A. 2011. EDHF: spreading the influence of the endothelium. *Br J Pharmacol,* 164**,** 839-52.

GARLAND, C. J. & MCPHERSON, G. A. 1992. Evidence that nitric oxide does not mediate the hyperpolarization and relaxation to acetylcholine in the rat small mesenteric artery. *Br J Pharmacol,* 105**,** 429-35.

GEESON, J., LARSSON, K., HOURANI, S. M. & TOMS, N. J. 2002. Sodium nitroprusside-induced rat fundus relaxation is ryanodine-sensitive and involves L-type Ca2+ channel

and small conductance Ca(2+)-sensitive K+ channel components. *Auton Autacoid Pharmacol,* 22**,** 297-301.

GODO, S., TAKAHASHI, J., YASUDA, S. & SHIMOKAWA, H. 2021. Endothelium in Coronary Macrovascular and Microvascular Diseases. *J Cardiovasc Pharmacol,* 78**,** S19-S29.

GOLD, M. E., WOOD, K. S., BYRNS, R. E., BUGA, G. M. & IGNARRO, L. J. 1990. L-arginine-dependent vascular smooth muscle relaxation and cGMP formation. *Am J Physiol,* 259**,** H1813-21.

GRAVES, J. E., GREENWOOD, I. A. & LARGE, W. A. 2000. Tonic regulation of vascular tone by nitric oxide and chloride ions in rat isolated small coronary arteries. *Am J Physiol Heart Circ Physiol,* 279**,** H2604-11.

HAND, M. F., HAYNES, W. G. & WEBB, D. J. 1998. Hemodialysis and L-arginine, but not D-arginine, correct renal failure-associated endothelial dysfunction. *Kidney Int,* 53**,** 1068-77.

HARRAZ, O. F., BRETT, S. E. & WELSH, D. G. 2014. Nitric oxide suppresses vascular voltage-gated T-type Ca2+ channels through cGMP/PKG signaling. *Am J Physiol Heart Circ Physiol,* 306**,** H279-85.

HE, F., LI, J., MU, Y., KURUBA, R., MA, Z., WILSON, A., ALBER, S., JIANG, Y., STEVENS, T., WATKINS, S., PITT, B., XIE, W. & LI, S. 2006. Downregulation of endothelin-1 by farnesoid X receptor in vascular endothelial cells. *Circ Res,* 98**,** 192-9.

HINTON, J. M. & LANGTON, P. D. 2003. Inhibition of EDHF by two new combinations of K+-channel inhibitors in rat isolated mesenteric arteries. *Br J Pharmacol,* 138**,** 1031-5.

HORI, T., MATSUBARA, T., ISHIBASHI, T., OZAKI, K., TSUCHIDA, K., MEZAKI, T., TANAKA, T., NASUNO, A., KUBOTA, K., NAKAMURA, Y., YAMAZOE, M., AIZAWA, Y. & NISHIO, M. 2003. Significance of asymmetric dimethylarginine

(ADMA) concentrations during coronary circulation in patients with vasospastic angina. *Circ J,* 67**,** 305-11.

HOWITT, L., KUO, I. Y., ELLIS, A., CHASTON, D. J., SHIN, H.-S., HANSEN, P. B. & HILL, C. E. 2013. Chronic deficit in nitric oxide elicits oxidative stress and augments T-type calcium-channel contribution to vascular tone of rodent arteries and arterioles. *Cardiovascular Research,* 98**,** 449-457.

HU, T., CHOUINARD, M., COX, A. L., SIPES, P., MARCELO, M., FICORILLI, J., LI, S., GAO, H., RYAN, T. P., MICHAEL, M. D. & MICHAEL, L. F. 2006. Farnesoid X receptor agonist reduces serum asymmetric dimethylarginine levels through hepatic dimethylarginine dimethylaminohydrolase-1 gene regulation. *J Biol Chem,* 281**,** 39831-8.

HU, X., ATZLER, D., XU, X., ZHANG, P., GUO, H., LU, Z., FASSETT, J., SCHWEDHELM, E., BOGER, R. H., BACHE, R. J. & CHEN, Y. 2011. Dimethylarginine dimethylaminohydrolase-1 is the critical enzyme for degrading the cardiovascular risk factor asymmetrical dimethylarginine. *Arterioscler Thromb Vasc Biol,* 31**,** 1540-6.

HU, X., XU, X., ZHU, G., ATZLER, D., KIMOTO, M., CHEN, J., SCHWEDHELM, E., LüNEBURG, N., BöGER, R. H., ZHANG, P. & CHEN, Y. 2009. Vascular endothelial-specific dimethylarginine dimethylaminohydrolase-1-deficient mice reveal that vascular endothelium plays an important role in removing asymmetric dimethylarginine. *Circulation,* 120**,** 2222-9.

HUANG, A., SUN, D., KOLLER, A. & KALEY, G. 1997. Gender difference in myogenic tone of rat arterioles is due to estrogen-induced, enhanced release of NO. *Am J Physiol,* 272**,** H1804-9.

HWA, J. J., GHIBAUDI, L., WILLIAMS, P. & CHATTERJEE, M. 1994. Comparison of acetylcholine-dependent relaxation in large and small arteries of rat mesenteric vascular bed. *Am J Physiol,* 266**,** H952-8.

ITO, A., TSAO, P. S., ADIMOOLAM, S., KIMOTO, M., OGAWA, T. & COOKE, J. P. 1999. Novel mechanism for endothelial dysfunction: dysregulation of dimethylarginine dimethylaminohydrolase. *Circulation,* 99**,** 3092-5.

JARAJAPU, Y. P. & KNOT, H. J. 2002. Role of phospholipase C in development of myogenic tone in rat posterior cerebral arteries. *Am J Physiol Heart Circ Physiol,* 283**,** H2234-8.

JESERICH, M., MUNZEL, T., JUST, H. & DREXLER, H. 1992. Reduced plasma L-arginine in hypercholesterolaemia. *Lancet,* 339**,** 561.

JOKSOVIC, P. M., DOCTOR, A., GASTON, B. & TODOROVIC, S. M. 2007. Functional regulation of T-type calcium channels by s-nitrosothiols in the rat thalamus. *J Neurophysiol,* 97**,** 2712-21.

JONES, C. J., KUO, L., DAVIS, M. J., DEFILY, D. V. & CHILIAN, W. M. 1995. Role of nitric oxide in the coronary microvascular responses to adenosine and increased metabolic demand. *Circulation,* 91**,** 1807-13.

JUONALA, M., VIIKARI, J. S., ALFTHAN, G., MARNIEMI, J., KAHONEN, M., TAITTONEN, L., LAITINEN, T. & RAITAKARI, O. T. 2007. Brachial artery flow-mediated dilation and asymmetrical dimethylarginine in the cardiovascular risk in young Finns study. *Circulation,* 116**,** 1367-73.

KALEY, G., KOLLER, A., RODENBURG, J. M., MESSINA, E. J. & WOLIN, M. S. 1992. Regulation of arteriolar tone and responses via L-arginine pathway in skeletal muscle. *Am J Physiol,* 262**,** H987-92.

KANAIDE, H., ICHIKI, T., NISHIMURA, J. & HIRANO, K. 2003. Cellular mechanism of vasoconstriction induced by angiotensin II: it remains to be determined. *Circ Res,* 93**,** 1015-7.

KANSUI, Y., GARLAND, C. J. & DORA, K. A. 2008. Enhanced spontaneous Ca2+ events in endothelial cells reflect signalling through myoendothelial gap junctions in pressurized mesenteric arteries. *Cell Calcium,* 44**,** 135-46.

KAW, S. & HECKER, M. 1999. Endothelium-derived hyperpolarizing factor, but not nitric oxide or prostacyclin release, is resistant to menadione-induced oxidative stress in the bovine coronary artery. *Naunyn Schmiedebergs Arch Pharmacol,* 359**,** 133-9.

KIELSTEIN, J. T., BOGER, R. H., BODE-BOGER, S. M., SCHAFFER, J., BARBEY, M., KOCH, K. M. & FROLICH, J. C. 1999. Asymmetric dimethylarginine plasma concentrations differ in patients with end-stage renal disease: relationship to treatment method and atherosclerotic disease. *J Am Soc Nephrol,* 10**,** 594-600.

KIELSTEIN, J. T., DONNERSTAG, F., GASPER, S., MENNE, J., KIELSTEIN, A., MARTENS-LOBENHOFFER, J., SCALERA, F., COOKE, J. P., FLISER, D. & BODE-BOGER, S. M. 2006. ADMA increases arterial stiffness and decreases cerebral blood flow in humans. *Stroke,* 37**,** 2024-9.

KNOT, H. J. & NELSON, M. T. 1998. Regulation of arterial diameter and wall [Ca2+] in cerebral arteries of rat by membrane potential and intravascular pressure. *J Physiol,* 508 (Pt 1)**,** 199-209.

KOPALIANI, I., JARZEBSKA, N., BILLOFF, S., KOLOUSCHEK, A., MARTENS-LOBENHOFFER, J., BORNSTEIN, S. R., BODE-BOGER, S. M., RAGAVAN, V. N., WEISS, N., MANGONI, A. A., DEUSSEN, A. & RODIONOV, R. N. 2021. Overexpression of dimethylarginine dimethylaminohydrolase 1 protects from

angiotensin II-induced cardiac hypertrophy and vascular remodeling. *Am J Physiol Heart Circ Physiol,* 321**,** H825-H838.

KOSTIC, M. M. & SCHRADER, J. 1992. Role of nitric oxide in reactive hyperemia of the guinea pig heart. *Circ Res,* 70**,** 208-12.

KUGIYAMA, K., YASUE, H., OKUMURA, K., OGAWA, H., FUJIMOTO, K., NAKAO, K., YOSHIMURA, M., MOTOYAMA, T., INOBE, Y. & KAWANO, H. 1996. Nitric oxide activity is deficient in spasm arteries of patients with coronary spastic angina. *Circulation,* 94**,** 266-71.

KUO, I. Y., ELLIS, A., SEYMOUR, V. A., SANDOW, S. L. & HILL, C. E. 2010. Dihydropyridine-insensitive calcium currents contribute to function of small cerebral arteries. *J Cereb Blood Flow Metab,* 30**,** 1226-39.

KUO, L., CHILIAN, W. M. & DAVIS, M. J. 1990. Coronary arteriolar myogenic response is independent of endothelium. *Circ Res,* 66**,** 860-6.

LAMBOLEY, M., PITTET, P., KOENIGSBERGER, M., SAUSER, R., BENY, J. L. & MEISTER, J. J. 2005. Evidence for signaling via gap junctions from smooth muscle to endothelial cells in rat mesenteric arteries: possible implication of a second messenger. *Cell Calcium,* 37**,** 311-20.

LANDRY, D. W., ANUBKUMAR, S. & OLIVER, J. A. 2006. Chapter 4 - Vascular Tone. *In:* ALBERT, R. K., SLUTSKY, A. S., RANIERI, V. M., TAKALA, J. & TORRES, A. (eds.) *Clinical Critical Care Medicine.* Philadelphia: Mosby.

LAUER, T., KLEINBONGARD, P., RATH, J., SCHULZ, R., KELM, M. & RASSAF, T. 2008. L-arginine preferentially dilates stenotic segments of coronary arteries thereby increasing coronary flow. *J Intern Med,* 264**,** 237-44.

LAWTON, P. F., LEE, M. D., SAUNTER, C. D., GIRKIN, J. M., MCCARRON, J. G. & WILSON, C. 2019. VasoTracker, a Low-Cost and Open Source Pressure Myograph System for Vascular Physiology. *Front Physiol,* 10**,** 99.

LEE, J., NELSON, M. T., ROSE, K. E. & TODOROVIC, S. M. 2013. Redox mechanism of S-nitrosothiol modulation of neuronal CaV3.2 T-type calcium channels. *Mol Neurobiol,* 48**,** 274-80.

LEFROY, D. C., CRAKE, T., UREN, N. G., DAVIES, G. J. & MASERI, A. 1993. Effect of inhibition of nitric oxide synthesis on epicardial coronary artery caliber and coronary blood flow in humans. *Circulation,* 88**,** 43-54.

LEIPER, J., NANDI, M., TORONDEL, B., MURRAY-RUST, J., MALAKI, M., O'HARA, B., ROSSITER, S., ANTHONY, S., MADHANI, M., SELWOOD, D., SMITH, C., WOJCIAK-STOTHARD, B., RUDIGER, A., STIDWILL, R., MCDONALD, N. Q. & VALLANCE, P. 2007. Disruption of methylarginine metabolism impairs vascular homeostasis. *Nat Med,* 13**,** 198-203.

LEIPER, J. M., SANTA MARIA, J., CHUBB, A., MACALLISTER, R. J., CHARLES, I. G., WHITLEY, G. S. & VALLANCE, P. 1999. Identification of two human dimethylarginine dimethylaminohydrolases with distinct tissue distributions and homology with microbial arginine deiminases. *Biochem J,* 343 Pt 1**,** 209-14.

LERMAN, A., BURNETT, J. C., JR., HIGANO, S. T., MCKINLEY, L. J. & HOLMES, D. R., JR. 1998. Long-term L-arginine supplementation improves small-vessel coronary endothelial function in humans. *Circulation,* 97**,** 2123-8.

LI, D., GUO, R., CHEN, Q. Q., HU, C. P. & CHEN, X. 2011. Increased plasma level of asymmetric dimethylarginine in hypertensive rats facilitates platelet aggregation: role of plasma tissue factor. *Can J Physiol Pharmacol,* 89**,** 151-8.

LI, J., ZHOU, Z., JIANG, D. J., LI, D., TAN, B., LIU, H. & LI, Y. J. 2007. Reduction of NO- and EDHF-mediated vasodilatation in hypertension: role of asymmetric dimethylarginine. *Clin Exp Hypertens,* 29**,** 489-501.

LIN, J., SCULLION, L., GARLAND, C. J. & DORA, K. 2023. Gbetagamma subunit signalling underlies neuropeptide Y-stimulated vasoconstriction in rat mesenteric and coronary arteries. *Br J Pharmacol,* 180**,** 3045-3058.

LIU, X., MILLER, M. J., JOSHI, M. S., SADOWSKA-KROWICKA, H., CLARK, D. A. & LANCASTER, J. R., JR. 1998. Diffusion-limited reaction of free nitric oxide with erythrocytes. *J Biol Chem,* 273**,** 18709-13.

LIU, Y., XIE, A., SINGH, A. K., EHSAN, A., CHOUDHARY, G., DUDLEY, S., SELLKE, F. W. & FENG, J. 2015. Inactivation of Endothelial Small/Intermediate Conductance of Calcium-Activated Potassium Channels Contributes to Coronary Arteriolar Dysfunction in Diabetic Patients. *J Am Heart Assoc,* 4**,** e002062.

LU, T. M., LEE, T. S., LIN, S. J., CHAN, W. L. & HSU, C. P. 2017. The prognostic value of asymmetric dimethylarginine in patients with cardiac syndrome X. *PLoS One,* 12**,** e0188995.

LU, T. M., LIN, S. J., LIN, M. W., HSU, C. P. & CHUNG, M. Y. 2011. The association of dimethylarginine dimethylaminohydrolase 1 gene polymorphism with type 2 diabetes: a cohort study. *Cardiovasc Diabetol,* 10**,** 16.

LUNEBURG, N., LIEB, W., ZELLER, T., CHEN, M. H., MAAS, R., CARTER, A. M., XANTHAKIS, V., GLAZER, N. L., SCHWEDHELM, E., SESHADRI, S., IKRAM, M. A., LONGSTRETH, W. T., JR., FORNAGE, M., KONIG, I. R., LOLEY, C., OJEDA, F. M., SCHILLERT, A., WANG, T. J., STICHT, H., KITTEL, A., KONIG, J., BENJAMIN, E. J., SULLIVAN, L. M., BERNGES, I., ANDERSSOHN, M., ZIEGLER, A., GIEGER, C., ILLIG, T., MEISINGER, C., WICHMANN, H. E., WILD,

P. S., SCHUNKERT, H., PSATY, B. M., WIGGINS, K. L., HECKBERT, S. R., SMITH, N., LACKNER, K., LUNETTA, K. L., BLANKENBERG, S., ERDMANN, J., MUNZEL, T., GRANT, P. J., VASAN, R. S. & BOGER, R. H. 2014. Genome-wide association study of L-arginine and dimethylarginines reveals novel metabolic pathway for symmetric dimethylarginine. *Circ Cardiovasc Genet,* 7**,** 864-72.

MACALLISTER, R. J., FICKLING, S. A., WHITLEY, G. S. & VALLANCE, P. 1994. Metabolism of methylarginines by human vasculature; implications for the regulation of nitric oxide synthesis. *Br J Pharmacol,* 112**,** 43-8.

MACALLISTER, R. J., PARRY, H., KIMOTO, M., OGAWA, T., RUSSELL, R. J., HODSON, H., WHITLEY, G. S. & VALLANCE, P. 1996. Regulation of nitric oxide synthesis by dimethylarginine dimethylaminohydrolase. *Br J Pharmacol,* 119**,** 1533-40.

MACKENZIE, A. & WADSWORTH, R. M. 2003. Extracellular L-arginine is required for optimal NO synthesis by eNOS and iNOS in the rat mesenteric artery wall. *Br J Pharmacol,* 139**,** 1487-97.

MATHER, S., DORA, K. A., SANDOW, S. L., WINTER, P. & GARLAND, C. J. 2005. Rapid endothelial cell-selective loading of connexin 40 antibody blocks endothelium-derived hyperpolarizing factor dilation in rat small mesenteric arteries. *Circ Res,* 97**,** 399-407.

MCNEISH, A. J., JIMENEZ ALTAYO, F. & GARLAND, C. J. 2010. Evidence both L-type and non-L-type voltage-dependent calcium channels contribute to cerebral artery vasospasm following loss of NO in the rat. *Vascul Pharmacol,* 53**,** 151-9.

MISHRA, R. C., BELKE, D., WULFF, H. & BRAUN, A. P. 2013. SKA-31, a novel activator of SK(Ca) and IK(Ca) channels, increases coronary flow in male and female rat hearts. *Cardiovasc Res,* 97**,** 339-48.

MISTRY, D. K. & GARLAND, C. J. 1998. Nitric oxide (NO)-induced activation of large conductance Ca2+-dependent K+ channels (BK(Ca)) in smooth muscle cells isolated from the rat mesenteric artery. *Br J Pharmacol,* 124**,** 1131-40.

MIURA, H., LIU, Y. & GUTTERMAN, D. D. 1999. Human coronary arteriolar dilation to bradykinin depends on membrane hyperpolarization: contribution of nitric oxide and Ca2+-activated K+ channels. *Circulation,* 99**,** 3132-8.

MOHRI, M., KOYANAGI, M., EGASHIRA, K., TAGAWA, H., ICHIKI, T., SHIMOKAWA, H. & TAKESHITA, A. 1998. Angina pectoris caused by coronary microvascular spasm. *Lancet,* 351**,** 1165-9.

MOORE, D. H. & RUSKA, H. 1957. The fine structure of capillaries and small arteries. *J Biophys Biochem Cytol,* 3**,** 457-62.

MOORE, P. K., AL-SWAYEH, O. A., CHONG, N. W., EVANS, R. A. & GIBSON, A. 1990. L-NG-nitro arginine (L-NOARG), a novel, L-arginine-reversible inhibitor of endothelium-dependent vasodilatation in vitro. *Br J Pharmacol,* 99**,** 408-12.

MORSE, C. J., BOERMAN, E. M., MCDONALD, M. W., PADILLA, J. & OLVER, T. D. 2022. The role of nitric oxide in flow-induced and myogenic responses in 1A, 2A, and 3A branches of the porcine middle cerebral artery. *J Appl Physiol (1985),* 133**,** 1228-1236.

MULSCH, A. & BUSSE, R. 1990. NG-nitro-L-arginine (N5-[imino(nitroamino)methyl]-L-ornithine) impairs endothelium-dependent dilations by inhibiting cytosolic nitric oxide synthesis from L-arginine. *Naunyn Schmiedebergs Arch Pharmacol,* 341**,** 143-7.

MULVANY, M. J. & AALKJAER, C. 1990. Structure and function of small arteries. *Physiol Rev,* 70**,** 921-61.

MULVANY, M. J. & HALPERN, W. 1977. Contractile properties of small arterial resistance vessels in spontaneously hypertensive and normotensive rats. *Circ Res,* 41**,** 19-26.

MURPHY, R. B., TOMMASI, S., LEWIS, B. C. & MANGONI, A. A. 2016. Inhibitors of the Hydrolytic Enzyme Dimethylarginine Dimethylaminohydrolase (DDAH): Discovery, Synthesis and Development. *Molecules,* 21**,** 615.

MURTHY, V. L., NAYA, M., TAQUETI, V. R., FOSTER, C. R., GABER, M., HAINER, J., DORBALA, S., BLANKSTEIN, R., RIMOLDI, O., CAMICI, P. G. & DI CARLI, M. F. 2014. Effects of sex on coronary microvascular dysfunction and cardiac outcomes. *Circulation,* 129**,** 2518-27.

NAGAO, T., ILLIANO, S. & VANHOUTTE, P. M. 1992. Heterogeneous distribution of endothelium-dependent relaxations resistant to NG-nitro-L-arginine in rats. *Am J Physiol,* 263**,** H1090-4.

NANDI, M., KELLY, P., TORONDEL, B., WANG, Z., STARR, A., MA, Y., CUNNINGHAM, P., STIDWILL, R. & LEIPER, J. 2012. Genetic and Pharmacological Inhibition of Dimethylarginine Dimethylaminohydrolase 1 Is Protective in Endotoxic Shock. *Arteriosclerosis, Thrombosis, and Vascular Biology,* 32**,** 2589-2597.

NG, Y. Y. H., DORA, K. A., LEMMEY, H. A. L., LIN, J., ALDEN, J., WALLIS, L., DONOVAN, L., SHORTHOSE, O., LEIPER, F. C., LEIPER, J. & GARLAND, C. J. 2024. Asymmetric Dimethylarginine Enables Depolarizing Spikes and Vasospasm in Mesenteric and Coronary Resistance Arteries. *Hypertension,* 81**,** 764-775.

NIJVELDT, R. J., TEERLINK, T., SIROEN, M. P., VAN LAMBALGEN, A. A., RAUWERDA, J. A. & VAN LEEUWEN, P. A. 2003. The liver is an important organ in the metabolism of asymmetrical dimethylarginine (ADMA). *Clin Nutr,* 22**,** 17-22.

NISHIKAWA, Y. & OGAWA, S. 1997. Importance of nitric oxide in the coronary artery at rest and during pacing in humans. *J Am Coll Cardiol,* 29**,** 85-92.

NISHIKAWA, Y., STEPP, D. W. & CHILIAN, W. M. 1999. In vivo location and mechanism of EDHF-mediated vasodilation in canine coronary microcirculation. *Am J Physiol,* 277**,** H1252-9.

NYBORG, N. C. & MIKKELSEN, E. O. 1987. Comparison of the inhibitory effects of nifedipine and nimodipine on mechanical responses of isolated rat coronary small arteries. *J Cardiovasc Pharmacol,* 9**,** 519-24.

OGAWA, T., KIMOTO, M. & SASAOKA, K. 1987a. Occurrence of a new enzyme catalyzing the direct conversion of NG,NG-dimethyl-L-arginine to L-citrulline in rats. *Biochem Biophys Res Commun,* 148**,** 671-7.

OGAWA, T., KIMOTO, M., WATANABE, H. & SASAOKA, K. 1987b. Metabolism of NG,NG- and NG,NG-dimethylarginine in rats. *Archives of Biochemistry and Biophysics,* 252**,** 526-537.

OKUMURA, K., YASUE, H., MATSUYAMA, K., GOTO, K., MIYAGI, H., OGAWA, H. & MATSUYAMA, K. 1988. Sensitivity and specificity of intracoronary injection of acetylcholine for the induction of coronary artery spasm. *J Am Coll Cardiol,* 12**,** 883-8.

OLOIZIA, B. & PAUL, R. J. 2008. Ca2+ clearance and contractility in vascular smooth muscle: evidence from gene-altered murine models. *J Mol Cell Cardiol,* 45**,** 347-62.

ONG, P., ATHANASIADIS, A., MAHRHOLDT, H., BORGULYA, G., SECHTEM, U. & KASKI, J. C. 2012. Increased coronary vasoconstrictor response to acetylcholine in women with chest pain and normal coronary arteriograms (cardiac syndrome X). *Clin Res Cardiol,* 101**,** 673-81.

PALLOSHI, A., FRAGASSO, G., PIATTI, P., MONTI, L. D., SETOLA, E., VALSECCHI, G., GALLUCCIO, E., CHIERCHIA, S. L. & MARGONATO, A. 2004. Effect of oral L-arginine on blood pressure and symptoms and endothelial function in patients with

systemic hypertension, positive exercise tests, and normal coronary arteries. *Am J Cardiol,* 93**,** 933-5.

PALMER, R. M., FERRIGE, A. G. & MONCADA, S. 1987. Nitric oxide release accounts for the biological activity of endothelium-derived relaxing factor. *Nature,* 327**,** 524-6.

PALMER, R. M., REES, D. D., ASHTON, D. S. & MONCADA, S. 1988a. L-arginine is the physiological precursor for the formation of nitric oxide in endothelium-dependent relaxation. *Biochem Biophys Res Commun,* 153**,** 1251-6.

PALMER, R. M. J., ASHTON, D. S. & MONCADA, S. 1988b. Vascular endothelial cells synthesize nitric oxide from L-arginine. *Nature,* 333**,** 664-666.

PATEL, M. R., PETERSON, E. D., DAI, D., BRENNAN, J. M., REDBERG, R. F., ANDERSON, H. V., BRINDIS, R. G. & DOUGLAS, P. S. 2010. Low diagnostic yield of elective coronary angiography. *N Engl J Med,* 362**,** 886-95.

PERTICONE, F., SCIACQUA, A., MAIO, R., PERTICONE, M., MAAS, R., BOGER, R. H., TRIPEPI, G., SESTI, G. & ZOCCALI, C. 2005. Asymmetric Dimethylarginine, L-Arginine, and Endothelial Dysfunction in Essential Hypertension. *Journal of the American College of Cardiology,* 46**,** 518-523.

PIATTI, P., FRAGASSO, G., MONTI, L. D., SETOLA, E., LUCOTTI, P., FERMO, I., PARONI, R., GALLUCCIO, E., POZZA, G., CHIERCHIA, S. & MARGONATO, A. 2003. Acute intravenous L-arginine infusion decreases endothelin-1 levels and improves endothelial function in patients with angina pectoris and normal coronary arteriograms: correlation with asymmetric dimethylarginine levels. *Circulation,* 107**,** 429-36.

PIATTI, P. M., MONTI, L. D., VALSECCHI, G., MAGNI, F., SETOLA, E., MARCHESI, F., GALLI-KIENLE, M., POZZA, G. & ALBERTI, K. G. 2001. Long-term oral L-arginine

administration improves peripheral and hepatic insulin sensitivity in type 2 diabetic patients. *Diabetes Care,* 24**,** 875-80.

PIZZARELLI, F., MAAS, R., DATTOLO, P., TRIPEPI, G., MICHELASSI, S., D'ARRIGO, G., MIETH, M., BANDINELLI, S., FERRUCCI, L. & ZOCCALI, C. 2013. Asymmetric dimethylarginine predicts survival in the elderly. *Age (Dordr),* 35**,** 2465-75.

POHL, U., LAMONTAGNE, D., BASSENGE, E. & BUSSE, R. 1994. Attenuation of coronary autoregulation in the isolated rabbit heart by endothelium derived nitric oxide. *Cardiovasc Res,* 28**,** 414-9.

POWERS, R. & GEFTER, J. 2012. OS075. Endothelial-dependent vascular function is significantly impaired in obesity and restored by overexpression of DDAH1: Evidence for the role of ADMA. *Pregnancy Hypertens,* 2**,** 218.

QUYYUMI, A. A., DAKAK, N., ANDREWS, N. P., GILLIGAN, D. M., PANZA, J. A. & CANNON, R. O., 3RD 1995. Contribution of nitric oxide to metabolic coronary vasodilation in the human heart. *Circulation,* 92**,** 320-6.

QUYYUMI, A. A., DAKAK, N., MULCAHY, D., ANDREWS, N. P., HUSAIN, S., PANZA, J. A. & CANNON, R. O., 3RD 1997. Nitric oxide activity in the atherosclerotic human coronary circulation. *J Am Coll Cardiol,* 29**,** 308-17.

RAGAVAN, V. N., NAIR, P. C., JARZEBSKA, N., ANGOM, R. S., RUTA, L., BIANCONI, E., GROTTELLI, S., TARAROVA, N. D., RYAZANSKIY, D., LENTZ, S. R., TOMMASI, S., MARTENS-LOBENHOFFER, J., SUZUKI-YAMAMOTO, T., KIMOTO, M., RUBETS, E., CHAU, S., CHEN, Y., HU, X., BERNHARDT, N., SPIETH, P. M., WEISS, N., BORNSTEIN, S. R., MUKHOPADHYAY, D., BODE-BOGER, S. M., MAAS, R., WANG, Y., MACCHIARULO, A., MANGONI, A. A., CELLINI, B. & RODIONOV, R. N. 2023. A multicentric consortium study

demonstrates that dimethylarginine dimethylaminohydrolase 2 is not a dimethylarginine dimethylaminohydrolase. *Nat Commun,* 14**,** 3392.

REES, D. D., PALMER, R. M., HODSON, H. F. & MONCADA, S. 1989. A specific inhibitor of nitric oxide formation from L-arginine attenuates endothelium-dependent relaxation. *Br J Pharmacol,* 96**,** 418-24.

REES, D. D., PALMER, R. M., SCHULZ, R., HODSON, H. F. & MONCADA, S. 1990. Characterization of three inhibitors of endothelial nitric oxide synthase in vitro and in vivo. *Br J Pharmacol,* 101**,** 746-52.

REIMANN, K., KRISHNAMOORTHY, G., WIER, W. G. & WANGEMANN, P. 2011. Gender differences in myogenic regulation along the vascular tree of the gerbil cochlea. *PLoS One,* 6**,** e25659.

REIS, S. E., HOLUBKOV, R., CONRAD SMITH, A. J., KELSEY, S. F., SHARAF, B. L., REICHEK, N., ROGERS, W. J., MERZ, C. N., SOPKO, G., PEPINE, C. J. & INVESTIGATORS, W. 2001. Coronary microvascular dysfunction is highly prevalent in women with chest pain in the absence of coronary artery disease: results from the NHLBI WISE study. *Am Heart J,* 141**,** 735-41.

REN, L. M., NAKANE, T. & CHIBA, S. 1993. Muscarinic receptor subtypes mediating vasodilation and vasoconstriction in isolated, perfused simian coronary arteries. *J Cardiovasc Pharmacol,* 22**,** 841-6.

RHODIN, J. A. 1967. The ultrastructure of mammalian arterioles and precapillary sphincters. *J Ultrastruct Res,* 18**,** 181-223.

RICHARD, V., BERDEAUX, A., LA ROCHELLE, C. D. & GIUDICELLI, J. F. 1991. Regional coronary haemodynamic effects of two inhibitors of nitric oxide synthesis in anaesthetized, open-chest dogs. *Br J Pharmacol,* 104**,** 59-64.

RICHIR, M. C., VAN LAMBALGEN, A. A., TEERLINK, T., WISSELINK, W., BLOEMENA, E., PRINS, H. A., DE VRIES, T. P. & VAN LEEUWEN, P. A. 2009. Low arginine/asymmetric dimethylarginine ratio deteriorates systemic hemodynamics and organ blood flow in a rat model. *Crit Care Med,* 37**,** 2010-7.

RODIONOV, R. N., JARZEBSKA, N., WEISS, N. & LENTZ, S. R. 2014. AGXT2: a promiscuous aminotransferase. *Trends Pharmacol Sci,* 35**,** 575-82.

RODRIGUEZ-RODRIGUEZ, R., STANKEVICIUS, E., HERRERA, M. D., OSTERGAARD, L., ANDERSEN, M. R., RUIZ-GUTIERREZ, V. & SIMONSEN, U. 2008. Oleanolic acid induces relaxation and calcium-independent release of endothelium-derived nitric oxide. *Br J Pharmacol,* 155**,** 535-46.

ROSSITER, S., SMITH, C. L., MALAKI, M., NANDI, M., GILL, H., LEIPER, J. M., VALLANCE, P. & SELWOOD, D. L. 2005. Selective Substrate-Based Inhibitors of Mammalian Dimethylarginine Dimethylaminohydrolase. *Journal of Medicinal Chemistry,* 48**,** 4670-4678.

SANDOO, A., VAN ZANTEN, J. J., METSIOS, G. S., CARROLL, D. & KITAS, G. D. 2010. The endothelium and its role in regulating vascular tone. *Open Cardiovasc Med J,* 4**,** 302-12.

SANDOW, S. L. & HILL, C. E. 2000. Incidence of myoendothelial gap junctions in the proximal and distal mesenteric arteries of the rat is suggestive of a role in endothelium-derived hyperpolarizing factor-mediated responses. *Circ Res,* 86**,** 341-6.

SANDOW, S. L., TARE, M., COLEMAN, H. A., HILL, C. E. & PARKINGTON, H. C. 2002. Involvement of myoendothelial gap junctions in the actions of endothelium-derived hyperpolarizing factor. *Circ Res,* 90**,** 1108-13.

SARA, J. D., WIDMER, R. J., MATSUZAWA, Y., LENNON, R. J., LERMAN, L. O. & LERMAN, A. 2015. Prevalence of Coronary Microvascular Dysfunction Among

Patients With Chest Pain and Nonobstructive Coronary Artery Disease. *JACC Cardiovasc Interv,* 8**,** 1445-1453.

SCHNABEL, R., BLANKENBERG, S., LUBOS, E., LACKNER, K. J., RUPPRECHT, H. J., ESPINOLA-KLEIN, C., JACHMANN, N., POST, F., PEETZ, D., BICKEL, C., CAMBIEN, F. O., TIRET, L. & MÜNZEL, T. 2005. Asymmetric Dimethylarginine and the Risk of Cardiovascular Events and Death in Patients With Coronary Artery Disease. *Circulation Research,* 97**,** e53-e59.

SCOTLAND, R. S., AHLUWALIA, A. & HOBBS, A. J. 2005. C-type natriuretic peptide in vascular physiology and disease. *Pharmacol Ther,* 105**,** 85-93.

SEGARRA, G., MEDINA, P., BALLESTER, R. M., LLUCH, P., ALDASORO, M., VILA, J. M., LLUCH, S. & PELLIGRINO, D. A. 1999. Effects of some guanidino compounds on human cerebral arteries. *Stroke,* 30**,** 2206-10; discussion 2210-11.

SEGARRA, G., MEDINA, P., VILA, J. M., CHUAN, P., DOMENECH, C., TORONDEL, B. & LLUCH, A. 2001. Inhibition of nitric oxide activity by arginine analogs in human renal arteries. *Am J Hypertens,* 14**,** 1142-8.

SELCUK, M. T., SELCUK, H., TEMIZHAN, A., MADEN, O., ULUPINAR, H., BAYSAL, E., OZEKE, O. & SASMAZ, A. 2007. Asymmetric dimethylarginine plasma concentrations and L-arginine/asymmetric dimethylarginine ratio in patients with slow coronary flow. *Coron Artery Dis,* 18**,** 545-51.

SHIMOKAWA, H., SUDA, A., TAKAHASHI, J., BERRY, C., CAMICI, P. G., CREA, F., ESCANED, J., FORD, T., YII, E., KASKI, J. C., KIYOOKA, T., MEHTA, P. K., ONG, P., OZAKI, Y., PEPINE, C., RIMOLDI, O., SAFDAR, B., SECHTEM, U., TSUJITA, K., YASUDA, S., BELTRAME, J. F. & MERZ, C. N. B. 2021. Clinical characteristics and prognosis of patients with microvascular angina: an international and prospective

cohort study by the Coronary Vasomotor Disorders International Study (COVADIS) Group. *Eur Heart J,* 42**,** 4592-4600.

SIMONSEN, U., WINTHER, A. K., OLIVAN-VIGUERA, A., COMERMA-STEFFENSEN, S., KOHLER, R. & BEK, T. 2019. Extracellular l-arginine Enhances Relaxations Induced by Opening of Calcium-Activated SKCa Channels in Porcine Retinal Arteriole. *Int J Mol Sci,* 20.

SINISALO, J., VANHANEN, H., PAJUNEN, P., VAPAATALO, H. & NIEMINEN, M. S. 1999. Ursodeoxycholic acid and endothelial-dependent, nitric oxide-independent vasodilatation of forearm resistance arteries in patients with coronary heart disease. *Br J Clin Pharmacol,* 47**,** 661-5.

SKARSGARD, P., VAN BREEMEN, C. & LAHER, I. 1997. Estrogen regulates myogenic tone in pressurized cerebral arteries by enhanced basal release of nitric oxide. *Am J Physiol,* 273**,** H2248-56.

SMITH, J. F., LEMMEY, H. A. L., BORYSOVA, L., HILEY, C. R., DORA, K. A. & GARLAND, C. J. 2020. Endothelial Nitric Oxide Suppresses Action-Potential-Like Transient Spikes and Vasospasm in Small Resistance Arteries. *Hypertension,* 76**,** 785-794.

STANKEVICIUS, E., DALSGAARD, T., KROIGAARD, C., BECK, L., BOEDTKJER, E., MISFELDT, M. W., NIELSEN, G., SCHJORRING, O., HUGHES, A. & SIMONSEN, U. 2011. Opening of small and intermediate calcium-activated potassium channels induces relaxation mainly mediated by nitric-oxide release in large arteries and endothelium-derived hyperpolarizing factor in small arteries from rat. *J Pharmacol Exp Ther,* 339**,** 842-50.

STROBAEK, D., BROWN, D. T., JENKINS, D. P., CHEN, Y. J., COLEMAN, N., ANDO, Y., CHIU, P., JORGENSEN, S., DEMNITZ, J., WULFF, H. & CHRISTOPHERSEN, P.

2013. NS6180, a new K(Ca) 3.1 channel inhibitor prevents T-cell activation and inflammation in a rat model of inflammatory bowel disease. *Br J Pharmacol,* 168**,** 432-44.

STROBEL, J., MIETH, M., ENDRESS, B., AUGE, D., KONIG, J., FROMM, M. F. & MAAS, R. 2012. Interaction of the cardiovascular risk marker asymmetric dimethylarginine (ADMA) with the human cationic amino acid transporter 1 (CAT1). *J Mol Cell Cardiol,* 53**,** 392-400.

SULLIVAN, A. K., HOLDRIGHT, D. R., WRIGHT, C. A., SPARROW, J. L., CUNNINGHAM, D. & FOX, K. M. 1994. Chest pain in women: clinical, investigative, and prognostic features. *BMJ,* 308**,** 883-6.

SUN, H., MOHRI, M., SHIMOKAWA, H., USUI, M., URAKAMI, L. & TAKESHITA, A. 2002. Coronary microvascular spasm causes myocardial ischemia in patients with vasospastic angina. *J Am Coll Cardiol,* 39**,** 847-51.

SURDACKI, A., NOWICKI, M., SANDMANN, J., TSIKAS, D., BOEGER, R. H., BODE-BOEGER, S. M., KRUSZELNICKA-KWIATKOWSKA, O., KOKOT, F., DUBIEL, J. S. & FROELICH, J. C. 1999. Reduced urinary excretion of nitric oxide metabolites and increased plasma levels of asymmetric dimethylarginine in men with essential hypertension. *J Cardiovasc Pharmacol,* 33**,** 652-8.

SVERDLOV, A. L., NGO, D. T., CHAN, W. P., CHIRKOV, Y. Y. & HOROWITZ, J. D. 2014. Aging of the nitric oxide system: are we as old as our NO? *J Am Heart Assoc,* 3.

SYDOW, K., SCHWEDHELM, E., ARAKAWA, N., BODE-BOGER, S. M., TSIKAS, D., HORNIG, B., FROLICH, J. C. & BOGER, R. H. 2003. ADMA and oxidative stress are responsible for endothelial dysfunction in hyperhomocyst(e)inemia: effects of L-arginine and B vitamins. *Cardiovasc Res,* 57**,** 244-52.

SZEKERES, M., NADASY, G. L., KALEY, G. & KOLLER, A. 2004. Nitric oxide and prostaglandins modulate pressure-induced myogenic responses of intramural coronary arterioles. *J Cardiovasc Pharmacol,* 43**,** 242-9.

TANGPHAO, O., GROSSMANN, M., CHALON, S., HOFFMAN, B. B. & BLASCHKE, T. F. 1999. Pharmacokinetics of intravenous and oral L-arginine in normal volunteers. *Br J Clin Pharmacol,* 47**,** 261-6.

TAYLOR, M. S., BONEV, A. D., GROSS, T. P., ECKMAN, D. M., BRAYDEN, J. E., BOND, C. T., ADELMAN, J. P. & NELSON, M. T. 2003. Altered expression of small-conductance Ca2+-activated K+ (SK3) channels modulates arterial tone and blood pressure. *Circ Res,* 93**,** 124-31.

TEERLINK, T., LUO, Z., PALM, F. & WILCOX, C. S. 2009. Cellular ADMA: regulation and action. *Pharmacol Res,* 60**,** 448-60.

TEERLINK, T., NIJVELDT, R. J., DE JONG, S. & VAN LEEUWEN, P. A. 2002. Determination of arginine, asymmetric dimethylarginine, and symmetric dimethylarginine in human plasma and other biological samples by high-performance liquid chromatography. *Anal Biochem,* 303**,** 131-7.

TEWARY, S. K., ZHENG, Y. G. & HO, M. C. 2019. Protein arginine methyltransferases: insights into the enzyme structure and mechanism at the atomic level. *Cell Mol Life Sci,* 76**,** 2917-2932.

TOTH, J., RACZ, A., KAMINSKI, P. M., WOLIN, M. S., BAGI, Z. & KOLLER, A. 2007. Asymmetrical Dimethylarginine Inhibits Shear Stress–Induced Nitric Oxide Release and Dilation and Elicits Superoxide-Mediated Increase in Arteriolar Tone. *Hypertension,* 49**,** 563-568.

TOUSOULIS, D., TENTOLOURIS, C., CRAKE, T., KATSIMAGLIS, G., STEFANADIS, C., TOUTOUZAS, P. & DAVIES, G. J. 1999. Effects of L- and D-arginine on the basal

tone of human diseased coronary arteries and their responses to substance P. *Heart,* 81**,** 505-11.

TREASURE, C. B., MANOUKIAN, S. V., KLEIN, J. L., VITA, J. A., NABEL, E. G., RENWICK, G. H., SELWYN, A. P., ALEXANDER, R. W. & GANZ, P. 1992. Epicardial coronary artery responses to acetylcholine are impaired in hypertensive patients. *Circ Res,* 71**,** 776-81.

VALKONEN, V. P., TUOMAINEN, T. P. & LAAKSONEN, R. 2005. DDAH gene and cardiovascular risk. *Vasc Med,* 10 Suppl 1**,** S45-8.

VALLANCE, P., LEONE, A., CALVER, A., COLLIER, J. & MONCADA, S. 1992a. Accumulation of an endogenous inhibitor of nitric oxide synthesis in chronic renal failure. *Lancet,* 339**,** 572-5.

VALLANCE, P., LEONE, A., CALVER, A., COLLIER, J. & MONCADA, S. 1992b. Endogenous dimethylarginine as an inhibitor of nitric oxide synthesis. *J Cardiovasc Pharmacol,* 20 Suppl 12**,** S60-2.

VAZQUEZ-PEREZ, S., NAVARRO-CID, J., DE LAS HERAS, N., CEDIEL, E., SANZ-ROSA, D., RUILOPE, L. M., CACHOFEIRO, V. & LAHERA, V. 2001. Relevance of endothelium-derived hyperpolarizing factor in the effects of hypertension on rat coronary relaxations. *J Hypertens,* 19**,** 539-45.

VON HAEHLING, S., SCHEFOLD, J. C., JANKOWSKA, E. A., SPRINGER, J., VAZIR, A., KALRA, P. R., SANDEK, A., FAULER, G., STOJAKOVIC, T., TRAUNER, M., PONIKOWSKI, P., VOLK, H. D., DOEHNER, W., COATS, A. J., POOLE-WILSON, P. A. & ANKER, S. D. 2012. Ursodeoxycholic acid in patients with chronic heart failure: a double-blind, randomized, placebo-controlled, crossover trial. *J Am Coll Cardiol,* 59**,** 585-92.

WALDRON, G. & GARLAND, C. 1994a. Effects of potassium channel blockers on L-NAME insensitive relaxations in rat small mesenteric artery. *Can. J. Physiol. Pharmacol.,* 72**,** 115.

WALDRON, G. J. & GARLAND, C. J. 1994b. Contribution of both nitric oxide and a change in membrane potential to acetylcholine-induced relaxation in the rat small mesenteric artery. *Br J Pharmacol,* 112**,** 831-6.

WALKER, H. A., MCGING, E., FISHER, I., BOGER, R. H., BODE-BOGER, S. M., JACKSON, G., RITTER, J. M. & CHOWIENCZYK, P. J. 2001. Endothelium-dependent vasodilation is independent of the plasma L-arginine/ADMA ratio in men with stable angina: lack of effect of oral L-arginine on endothelial function, oxidative stress and exercise performance. *J Am Coll Cardiol,* 38**,** 499-505.

WALLIS, L., DONOVAN, L., JOHNSTON, A., PHILLIPS, L. C., LIN, J., GARLAND, C. J. & DORA, K. A. 2023. Tracking endothelium-dependent NO release in pressurized arteries. *Front Physiol,* 14**,** 1108943.

WANG, D., GILL, P. S., CHABRASHVILI, T., ONOZATO, M. L., RAGGIO, J., MENDONCA, M., DENNEHY, K., LI, M., MODLINGER, P., LEIPER, J., VALLANCE, P., ADLER, O., LEONE, A., TOJO, A., WELCH, W. J. & WILCOX, C. S. 2007. Isoform-Specific Regulation by N^G,N^G-Dimethylarginine Dimethylaminohydrolase of Rat Serum Asymmetric Dimethylarginine and Vascular Endothelium-Derived Relaxing Factor/NO. *Circulation Research,* 101**,** 627-635.

XAVIER, F. E., BLANCO-RIVERO, J., SASTRE, E., CARACUEL, L., CALLEJO, M. & BALFAGON, G. 2014. Tranilast increases vasodilator response to acetylcholine in rat mesenteric resistance arteries through increased EDHF participation. *PLoS One,* 9**,** e100356.

YAMAMOTO, Y., IMAEDA, K. & SUZUKI, H. 1999. Endothelium-dependent hyperpolarization and intercellular electrical coupling in guinea-pig mesenteric arterioles. *J Physiol,* 514 (Pt 2)**,** 505-13.

YASHIRO, Y. & DULING, B. R. 2000. Integrated Ca(2+) signaling between smooth muscle and endothelium of resistance vessels. *Circ Res,* 87**,** 1048-54.

ZANI, B. G. & BOHLEN, H. G. 2005. Transport of extracellular l-arginine via cationic amino acid transporter is required during in vivo endothelial nitric oxide production. *Am J Physiol Heart Circ Physiol,* 289**,** H1381-90.

ZHARIKOV, S. I. & BLOCK, E. R. 1998. Characterization of L-arginine uptake by plasma membrane vesicles isolated from cultured pulmonary artery endothelial cells. *Biochim Biophys Acta,* 1369**,** 173-83.